DOE/MC/23274-2941
(DE91001008)

FOSSIL

Development of Internal Reforming Carbonate Fuel Cell Stack Technology

Final Report

M. Farooque

October 1990

Work Performed Under Contract No.: DE-AC21-87MC23274

For
U.S. Department of Energy
Office of Fossil Energy
Morgantown Energy Technology Center
Morgantown, West Virginia

By
Energy Research Corporation
Danbury, Connecticut

DISCLAIMER

Printed in the United States of America, Office of Scientific and Technical Information, Oak Ridge, Tennessee

DOE/MC/23274--2941

DE91 002008

Development of Internal Reforming Carbonate Fuel Cell Stack Technology

Final Report

M. Farooque

Work Performed Under Contract No.: DE-AC21-87MC23274

For
U.S. Department of Energy
Office of Fossil Energy
Morgantown Energy Technology Center
P.O. Box 880
Morgantown, West Virginia 26507-0880

By
Energy Research Corporation
3 Great Pasture Road
Danbury, Connecticut 06813

October 1990

ACKNOWLEDGEMENT

Numerous ERC employee have contributed to this report. The principal contributors include: R. Bernard, R. Chamberlin, H. Carr, J. Fan, M. Farooque, S. Gionfriddo, D. Kelley, H. Maru, J. Martin, D. Patel, P. Patel, A. Skok, G. Steinfeld, L. Richards, C. Yuh, S. Viswanathan

Interactions and guidance of DOE Technical Representative Dr. Mark Williams and his predecessor Jim Copley are also acknowledged.

TABLE OF CONTENTS

TABLE OF CONTENTS CONT'D

TABLE OF CONTENTS CONT'D

TABLE OF CONTENTS CONT'D

LIST OF FIGURES

LIST OF FIGURES CONT'D

LIST OF FIGURES CONT'D

LIST OF FIGURES CONT'D

LIST OF FIGURES CONT'D

LIST OF TABLES

LIST OF TABLES CONT'D

LIST OF ABBREVIATIONS

100-MW Class	100-400 MW Size Dual fuel -- natural gas and/or coal-gas CFC Power Plants
AC	Alternating Current
AFBC	Atmospheric Fluidized Bed Combustion
AB-X-Y AF-X-Y AS-X-Y	ERC's Stack Identification Convention A = Atmospheric, F = Full Size, S = Subscale, B=Bench-Scale X = kW Rating, Y = Serial Number
AG	Advanced Gasket
ASF	Amperes per Square Foot
BBU	Building Block Unit of ERC's Full Size Stack (60 cells, 20 kW)
BGL	British Gas Lurgi
BOL	Beginning of Life
CCC	Corrugated Current Collector
CFB	Circulating Fluid Bed Power Plant
CFC	Carbonate Fuel Cell
CGCFC	Coal-Gas Carbonate Fuel Cell
C-H-O Diagram	Carbon-Hydrogen-Oxygen Diagram
DAS	Data Acquisition System
DC	Direct Current
DFC	Direct Fuel Cell
DIR	Direct Internal Reforming
DOE-X	Stack Built and Tested in DOE/METC Program X = Serial Number
EDS	Energy Dispersive Spectroscopy
EOL	End-of-Life
EP	End Plate
EPA	Environmental Protection Agency
EPRI	Electric Power Research Institute (Palo Alto, CA)
ERC	Energy Research Corporation
FOB	Freight on Board Basis
FD	Fluor Daniel
Full/Tall Size Stack	100-kW Size CFC Stack ~ 230 cells (4-ft)
G-Force	Gravitational Force
IGCC	Integrated Gasification Combined Cycles Power Plant
IIR	Indirect Internal Reforming
IOU	Investor-Owned Utilities
IVD	Ion Vapor Deposition
KRW	Kellogg Rust Westinghouse
MHC	Manifold Horizontal Clamp
MOL	Middle of Life
MVC	Manifold Vertical Clamp

LIST OF ABBREVIATIONS (cont'd)

MW-Class	2-10 MW size natural gas/CFC Power Plant
NG	Natural Gas
NGCFC	Natural Gas Carbonate Fuel Cell
OSHA	Occupational Safety and Health Administration
PC	Pulverized Coal
PFBC	Pressurized Fluidized Bed Combustion Power Plant
PG&E	Pacific Gas & Electric Company (San Francisco, CA)
PM	Process Monitoring System
ppmv	Parts Per Million, Volume Basis
Rg	Gasket Electrical Resistance
RU	Reforming Unit
Rw	Wet Seal Electrical Resistance
SRNG	Simulated Reformed Natural Gas
System 6C	Integrated Natural Gas-Based MW-Class (Type A) Power Plant
TAG	Technical Assesment Guide (EPRI Special Report)
UAG	Utility Advisory Group

EXECUTIVE SUMMARY

This final report summarizes the work performed under the U.S. Department of Energy Morgantown Energy Technology Center (DOE/METC) Contract No. DE-AC21-87MC23274 for the February 1988 through September 1990 period. Activities under this contract focused on the development of a coal-fueled carbonate fuel cell system design and the stack technology consistent with the system design. The overall contract effort was divided into three phases. The first phase, completed in January 1988, provided carbonate fuel cell component scale-up from the $1ft^2$ size to the commercial $4ft^2$ size. The second phase of the program provided the coal-fueled carbonate fuel cell system (CGCFC) conceptual design and carried out initial research and development needs of the CGCFC system. The final phase of the program emphasized stack height scale-up and improvement of stack life. This effort was cost-shared by Electric Power Research Institute, Pacific Gas and Electric Company, and ERC's corporate funds. The results of the second and third phases are included in this report.

Program activities under Phases 2 and 3 were designed to address several key development areas to prepare the carbonate fuel cell system, particularly the coal-fueled CFC power plant, for commercialization in late 1990's. The issues addressed include:

- Coal-Gas Related Considerations
- Cell and Stack Technology Improvement
- Carbonate Fuel Cell Stack Design Development
- Stack Tests for Design Verification
- Full-Size Stack Design
- Test Facility Development
- Carbonate Fuel Cell Stack Cost Assessment
- Coal-Fueled Carbonate Fuel Cell System Design

All the major program objectives in each of the topical areas were successfully achieved. This report is organized along the above-mentioned topical areas. The key achievements in each of these areas are summarized below.

Coal-Gas Related Considerations

Operation of carbonate fuel cell on coal-gas requires the consideration of appropriate soot suppression as well as the effects of water gas shift equilibrium, fuel and oxidant utilizations in the cell, fuel and oxidant concentrations, and trace impurities. Fundamental and practical data were generated on these issues.

The effect of moisture on soot suppression and cell performance was investigated. Approximately 2mV performance loss was measured experimentally for each percentage point increase in steam content. This information will be utilized for optimization of power plant subsystems.

Bench-scale cells were operated with continuous addition of 1ppmv H_2S in fuel and 0.1ppmv HCl in oxidant, both singly and in combination. It was concluded from tests up to 3000 hours that performance and life are unaffected by this level of impurities. Post-test analysis verified this observation.

Cell and Stack Technology Improvement

Significant advancement of the cell and stack technology was achieved. An improved matrix was successfully evaluated in single cells and then in stacks showing approximately 10% reduction in cell resistance and at least 50% improvement in matrix gas seal efficiency.

Several manifold gasket designs were identified which are expected to meet the seal efficiency goal of 0.2% fuel leak at 15 inches of water pressure. One of these designs also showed potential for reduction of the electrolyte migration rate by approximately an order of magnitude (Figure S-1) in out-of-cell tests. This gasket design as well as a parallel end-cell electrolyte source and sink approach (which was successfully verified in single cells), promise adequate electrolyte management to ensure 40,000 hours of useful life for a full-size stack. This approach for electrolyte management is currently being evaluated in a short stack.

An approach for achieving two-fold improvement in cathode stability was also demonstrated in single-cell accelerated tests. These improvements together project improved performance, higher fuel utilization, longer stack life, and provide a sound basis for a full-size stack design for demonstration.

Carbonate Fuel Stack Design Development

ERC selected a fuel-flexible internal reforming carbonate fuel cell stack design. This allows operation on both pipeline natural gas and various coal-derived gases with a common stack design. The basic stack design includes external manifolding, rectangular cell size, and internal reforming. The intital design (selected based on prior test experience) was improved in the program with input from mechanistic modeling and iterative stack tests. The 2ft X 2ft area stacks were utilized for the stack design evaluation testing. An overall summary of ERC's stack test in this program is presented in Table S-1. Over 14,000 hours of cummulative stack test experience, most of which at system operating conditions, was accumulated.

TABLE S-1

SUMMARY OF ERC'S PROGRAM STACK TESTS:

Over 14,000 Hours of Stack Test Experience Accumulated,
Mostly at System Operating Conditions

STACK DESCRIPTION	TEST OBJECTIVE	LIFE	PERFORMANCE		OPERATING CONDITION**	
		Hours	mV	$m\Omega \cdot cm^2$		
2kW-CLASS (5 CELLS)						
- DOE-5 (AF-2-3)	DUAL-FUEL	2100	640	690	100MW-CLASS COAL	75% FUEL UTIL.
- DOE-6 (AF-2-4)	BIPOLAR PLATE	2100	750	380	100MW-CLASS COAL	55% F, 40% O UTIL., $120 ma/cm^2$
- DOE-7 (AF-2-5)	MODULE COMPATIBILITY	800	725	390	100MW-CLASS COAL	55% F, 40% O UTIL., $120 ma/cm^2$
- DOE-10 (AF-2-6)	MANIFOLD SYSTEM DESIGN	200	672	390	100MW-CLASS COAL	72% FUEL UTIL.
- AF-2-S (STACKABILITY TEST)	RAIL DESIGN	200	720	530	100MW-CLASS COAL	CENTRAL CELLS
5kW-CLASS (11 CELLS)						
- PG&E-2 (AF-5-1)*	IIR SCALE-UP	5000	765	410	MW-CLASS TYPE-B	
5kW-CLASS (60 CELLS, $1 ft^2$)						
- EPRI-60 (AS-5-1)*	DIR HEIGHT SCALE-UP	2000	690	350	MW-CLASS TYPE-A	CENTRAL 40 CELLS
8kW-CLASS (20 CELLS)						
- DOE-8 (AF-8-1)	HEIGHT SCALE-UP	1600 (cont'd)	735	460	100MW-CLASS COAL	

*SYSTEM DESIGNATION	CURRENT mA/cm^2	FUEL COMPOSITION %							OXIDANT %				
		H_2	CO_2	CO	CH_4	N_2	H_2O	UTIL	O_2	CO_2	N_2	H_2	UTIL CO_2
LABORATORY TEST CONDITION	AS SPECIFIED	73	18				9		16	25	59		50
MW-CLASS TYPE-A	160	32			27		41	75	9	13	73	5	50
MW-CLASS TYPE-B	140				40		60	75	13	16	55	16	75
100MW-CLASS COAL	160	50	35		5	1	9	85	13	12	63	12	25

WM8960a

* Represents cost share stacks

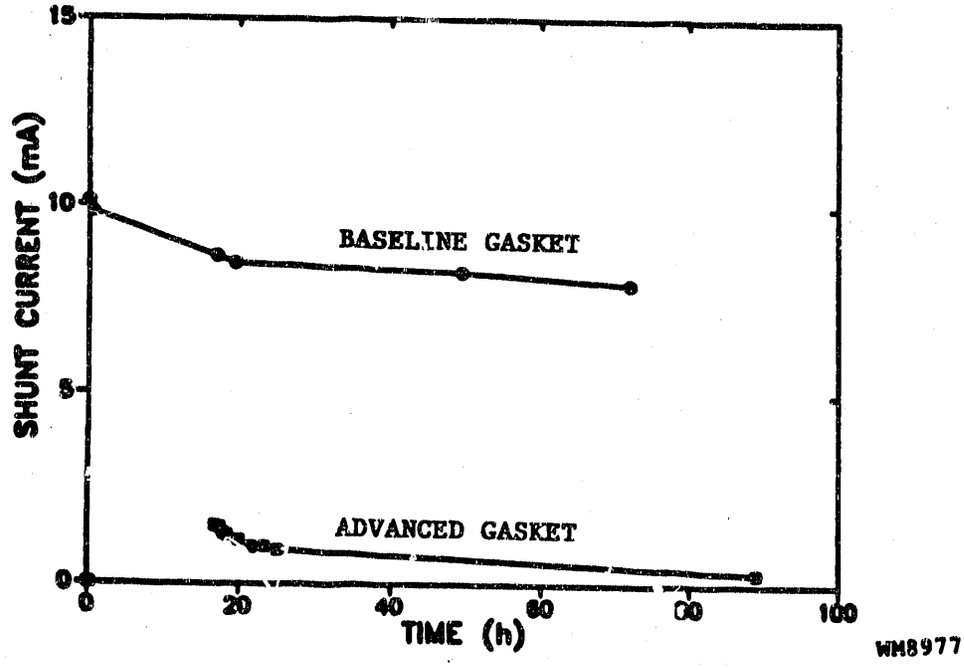

FIGURE S-1 ELECTROLYTE MIGRATION RATE CHARACTERIZATION (OUT-OF-CELL, 12-CELL SIMULATOR TEST):

Approximately an Order of Magnitude Improvement in Migration Rate Demonstrated

The thermo-mechanical behavior of the carbonate fuel cell stack was modeled and the impact of key design variables was analyzed. The results were utilized to select a mechanically sound stack design. The electrolyte loss mechanisms were investigated and quantified. An electrolyte management strategy was recommended from this effort.

As a final product, the component designs as well as the assembly approach for the stack scale-up were recommended; and the areas for further improvement, which would allow attainment of performance and cost goals, were identified.

Stack Tests For Design Verification

ERC tested seven $4ft^2$ stacks (of which five were five-cell, 2kW size) and one 60-cell $1ft^2$ stack for stack design evaluations. These tests were conducted at system operating conditions, providing operating experience with dilute fuel and oxidant at high utilizations.

The stack testing activities emphasized the development and verification of stack repeat and non-repeat hardware. The end plate, bipolar plate, and manifold retention designs were refined through several design iterations and made available for full-size stack use. The stack component designs developed in this program, except a manifold dielectric, are compatible

with mass production. Some cost reduction of stack components at a future time is desired. The stack manifold dielectric will require future developmental focus.

In the 1988-89 period, ERC tested an internal reforming stack at the MW-Class power plant (natural gas) system condition for 5000 hours. During the same time, ERC tested a 60-cell $1ft^2$ size stack, the tallest IRCFC stack tested to date, to investigate the stack height scale-up issues. ERC also tested a 20-cell, 8kW stack at coal-gas/carbonate fuel cell conditions. In addition, a 54-cell $4ft^2$ area stack, intended for natural gas system condition testing, was assembled (Figure S-2).

Attainment of performance within 7% of the coal-gas as well as natural gas power plant goals was demonstrated. Activities leading to further performance improvement were planned. Attainment of 0.5%/1000h decay rate (Table S-2) was demonstrated in an 11-cell, $4ft^2$ stack operated at natural gas conditions for 5000 hours.

TABLE S-2

DEMONSTRATED CFC DECAY RATE:

ERC has Demonstrated a Decay Rate
of 0.5%/1000h in an 11-Cell Stack.

TEST VEHICLE	HOUR	DECAY RATE mV/1000h
Single Cell	10,000	5
Stack w/$1ft^2$ Cells (DOE-2, 4-Cell, 1 ft^2)	3,000	3
Stack w/$4ft^2$ Cells (PG&E-2, 11-Cell, 4 ft^2)	5,000	3

Full-Size Stack Design

The stack to be used in a pilot demonstration of the simplified natural gas power plant design (MW-Class Type B System) has been designed. Both the direct and the indirect internal reforming features (DIR/IIR) have been incorporated to allow stable operation on pipeline natural gas. A 232-cell single stack using $4ft^2$ area cells with a reforming unit every six cells has been selected. An exploded assembly drawing of the stack is shown in Figure S-3.

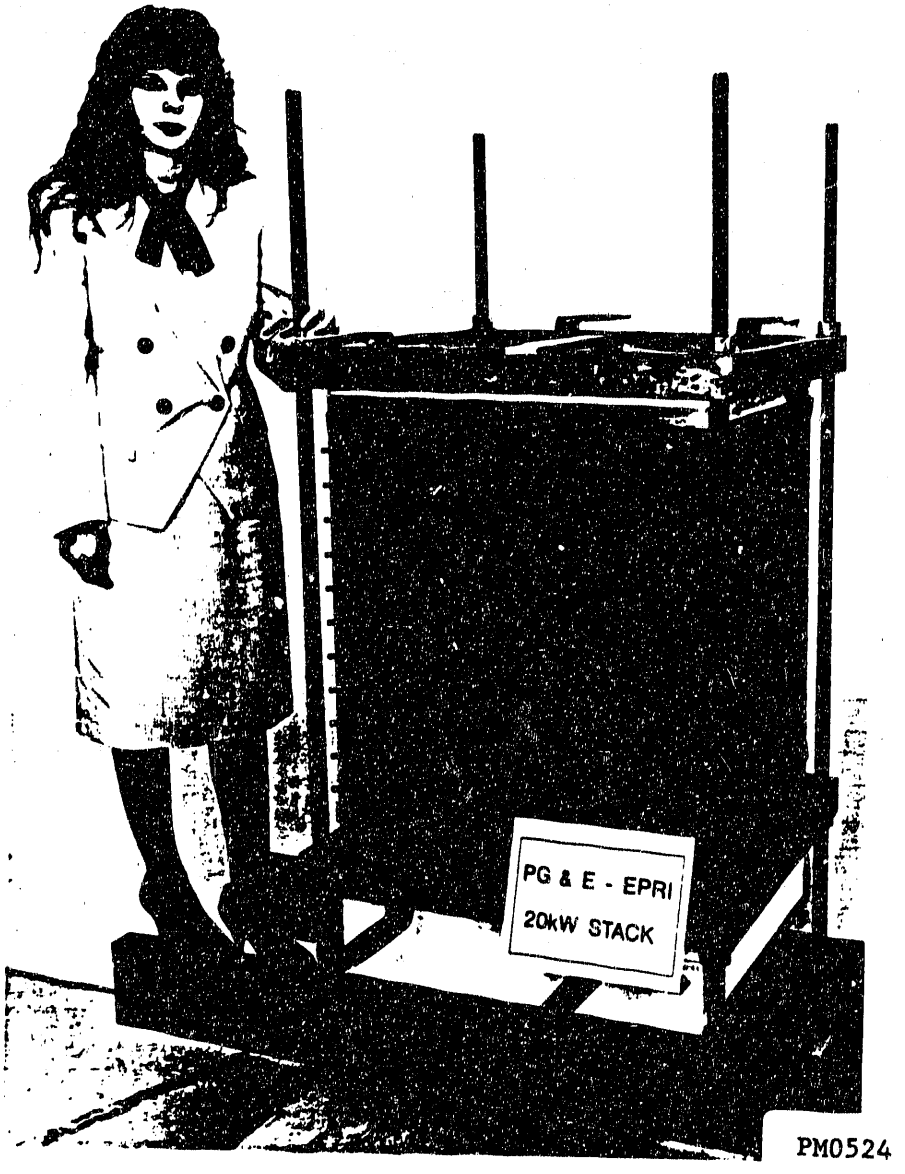

FIGURE S-2 **ASSEMBLY PHOTOGRAPH OF A 20kW*, 4FT² AREA, DUAL-FUEL STACK:**

Tallest 4ft² Area Stack Built at ERC to Date; Evaluation of Electrolyte Migration Mitigation Approaches Planned

* Cost-Share Stack

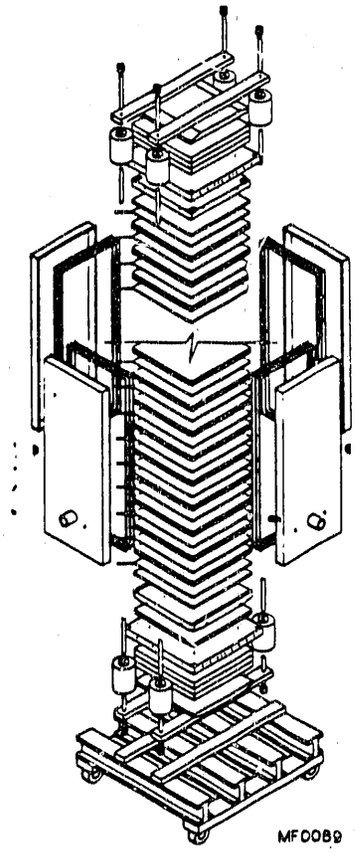

FIGURE S-3 FULL-HEIGHT STACK ASSEMBLY DRAWING:

This 232-Cell (4ft^2 Cell Area; 39 Reforming Units) Stack will be Tested at MW-Class (Type B) System Integrated Mode

The power plant demonstration site is at Pacific Gas and Electric Company's Research and Development Facility in San Ramon, California. The stack will be manufactured and pretested at Energy Research Corporation's Danbury facility. The stack will be truck transported from Energy Research Corporation to PG&E's San Ramon test site. The carbonate fuel cell transportation logistics related to packaging, environmental, and shock and vibration controls have been established. Proven cell and the auxiliary hardware designs (already qualified in multiple short stack tests) have been incorporated in the stack design. The indirect internal reformer selected has also been prequalified in two short stacks.

Test Facility Development

The capability in terms of coal system gases and contaminants simulation and reliability of existing test facilities was greatly improved. A new flexible facility was designed and fabricated to test taller stacks in the size range of 8 to 32 kW. A photograph of this facility is shown in Figure S-4. This

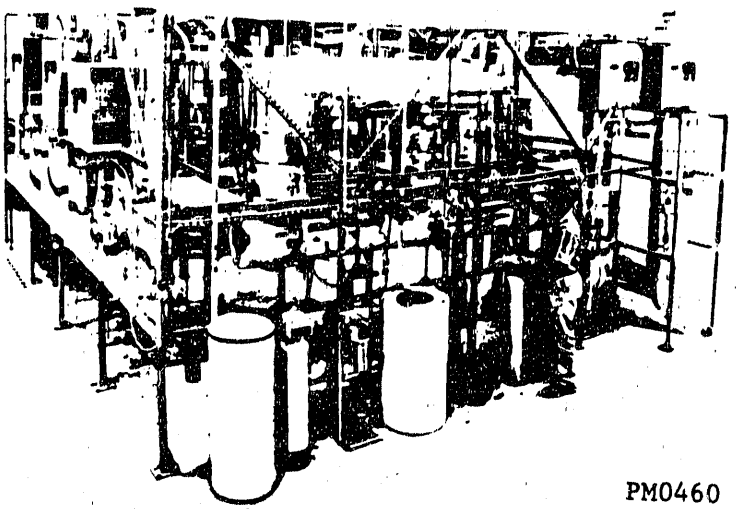

PM0460

Facility Includes All
Required Process Equipment

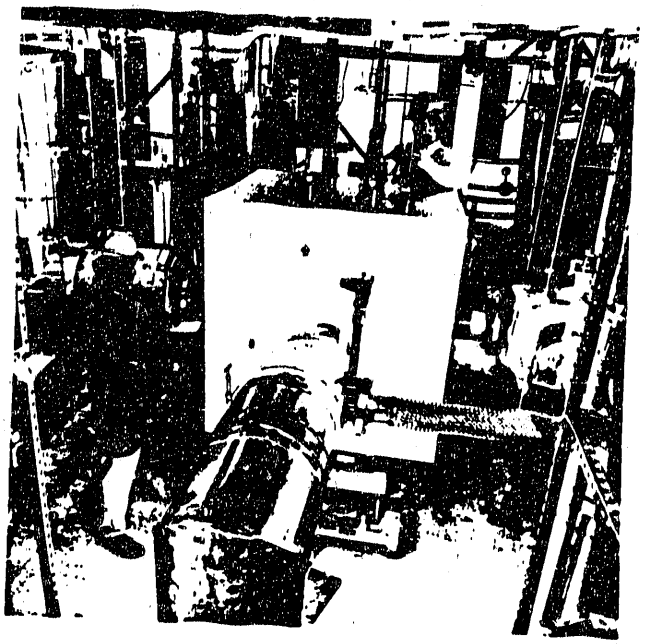

PM0470

Facility Operation Check-out In
Progress Using a 60-Cell Stack
Simulator

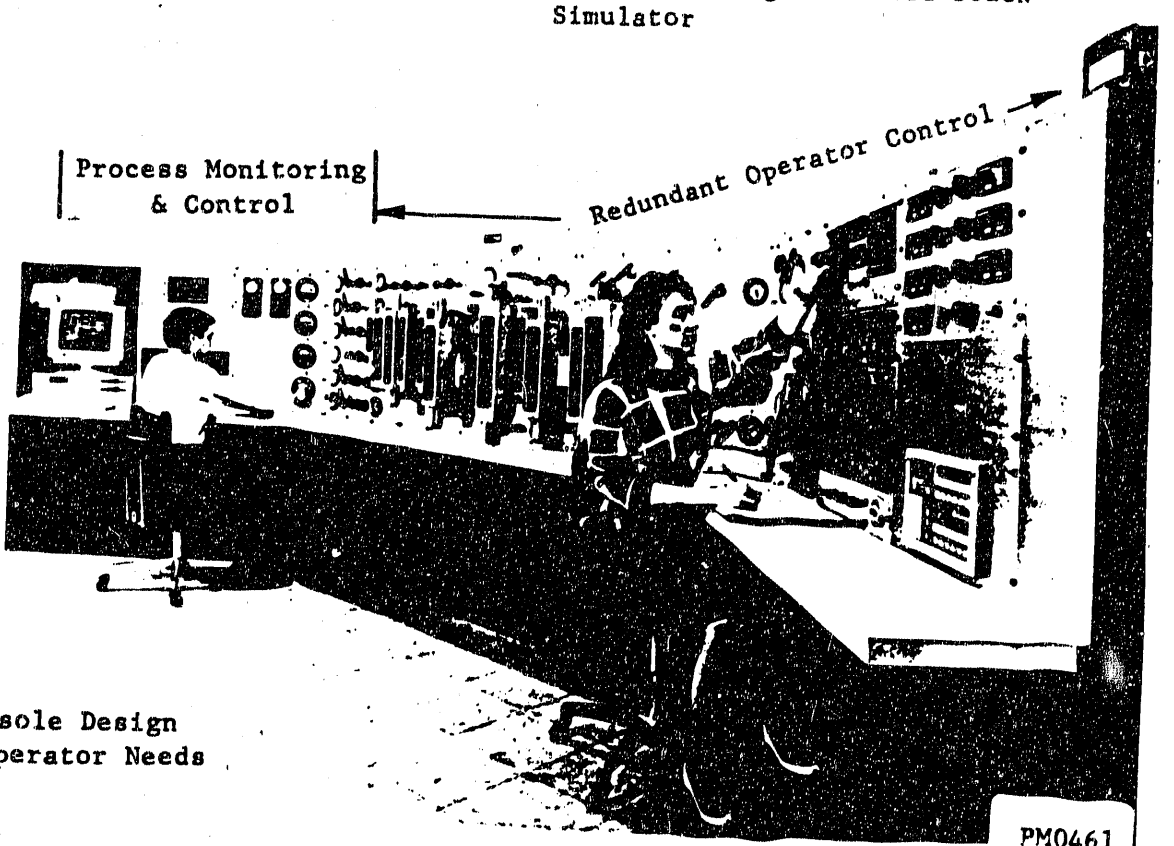

PM0461

Control Console Design
Minimizes Operator Needs

FIGURE S-4 ERC'S 8 to 32kW STACK TEST FACILITY:

This Facility is Fully Operational

facility can simulate gas compositions for different type natural gas as well as coal-gas power plants. Capability for future pressurization was also incorporated. Provision was made for hot recirculation of cathode gases and regenerative heat exchangers, thus providing experience towards power plant system operation.

Carbonate Fuel Cell Stack Cost Assessment

A detailed materials and manufacturing cost estimate of the carbonate fuel cell stack was developed. This cost estimate was arrived at through defining components manufacturing processes, establishing a conceptual design for a fully equipped and staffed manufacturing plant, and obtaining materials cost quotes from vendors. A computer cost model was developed and utilized to evaluate various design concepts and stack cost sensitivities to cell size (4 ft^2 to 16 ft^2), production volume scenarios (400, 800, and 1600 MW per year), and other production parameters.

The findings of this study show (Figure S-5) that the carbonate fuel cell costs are sensitive to production volume, manufacturing equipment capacity, especially the Ni-plating line speeds and widths, and to cell size at the larger production volume (1600 MW) only. The carbonate fuel cell cost was found to be materials cost driven, which contributes over 60% of the final cost. The bipolar plate material alone contributes 45%

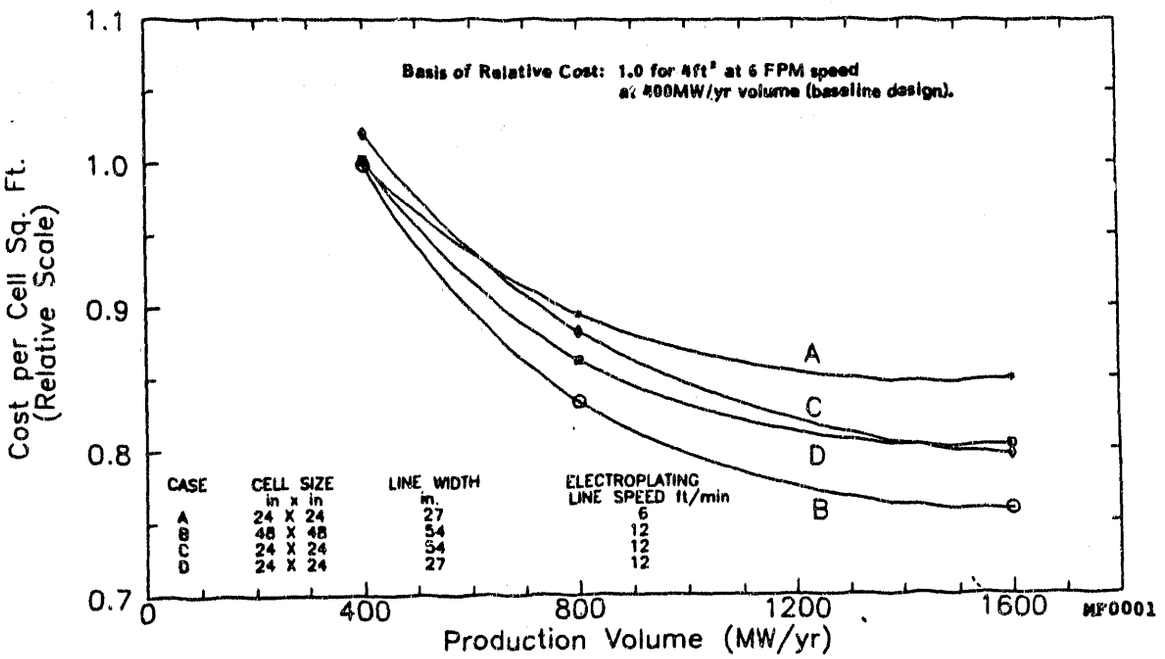

FIGURE S-5 EFFECT OF VARIABLES ON STACK COST:

At 400MW/yr Rate, the 4ft^2 Stack Cost is Quite Similar to the Larger Size Stacks (16 ft^2)

of the material cost, and thus provides the best opportunity for cost reduction. A significant materials credit, over 20% of the initial stack cost, appears to be feasible by recovering material contents of a used carbonate fuel cell stack in the form of specialty steel.

Coal-Fueled Carbonate Fuel Cell System Design

ERC identified economically attractive and technically feasible coal-fueled carbonate fuel cell power plant (CGCFC) configurations. An artist's conceptual view of a power plant developed in this program is shown in Figure S-6. The CGCFC power plant designs using available gasifier types (entrained, fluidized, and moving beds) and cleanup systems (cold and hot), and ERC's dual-fuel carbonate fuel cell provide efficiencies approaching 50% (HHV coal), and have very low environmental emissions and market responsive cost-of-electricity.

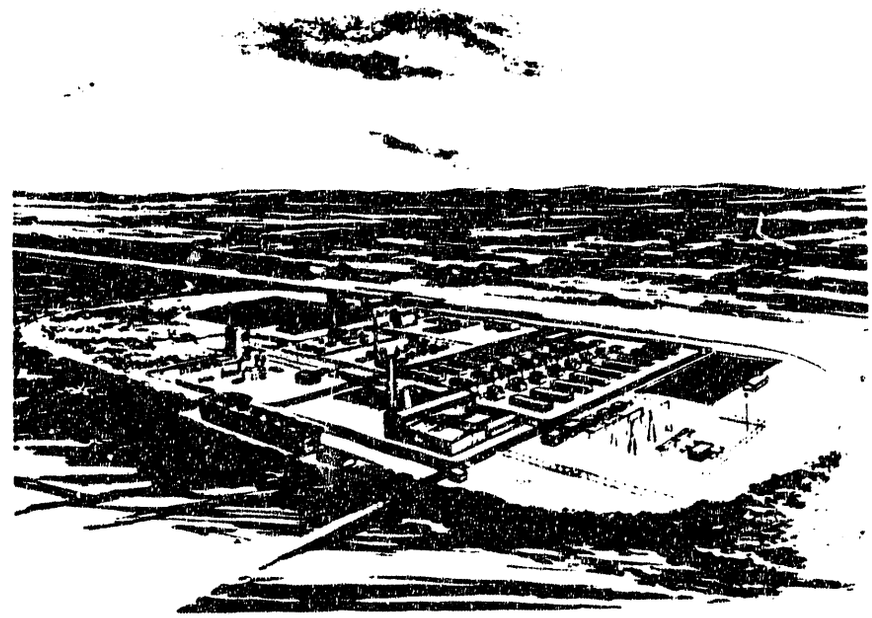

PM0538

FIGURE S-6 ARTISTS RENDERING OF A TYPICAL 200MW CGCFC POWER PLANT:

Offering High Efficiency and Low Emissions at Competitive COE

When compared with both the present day and emerging alternate coal technologies, the CFC shows an energy conversion efficiency advantage of better than 15% and acid rain precursor (NO_x and SO_x) emission reduction by an order of magnitude over the nearest competition, and yet cost-competitive cost-of-electricity. In addition, many other benefits such as cost-effectiveness in small sizes, high part-load efficiency, better power quality, and modularity, make the CGCFC a very attractive power generation option of the future.

Thus ERC has defined viable carbonate fuel cell power plant systems and also demonstrated excellent progress in preparing the carbonate fuel cell technology for commercialization. Approaches for resolving key issues have been defined and subsequently verified in subscale stack. Demonstration of life and full-size stack operations are the next two important milestones towards successful commercialization. The technology is ready for demonstration of a full-size stack (which appears to be the pacing subsystem for commercialization). Demonstration of a full-size stack in a natural gas system operation mode at a utility test site, and endurance testing of subscale stacks are planned next.

1.0 INTRODUCTION

Energy Research Corporation (ERC) is developing the highly efficient, environmentally clean, and economically attractive coal-gas as well as natural gas fueled carbonate fuel cell power plants. The carbonate fuel cell (CFC) stack is the heart of these power plant systems. ERC has been active in developing this key subsystem technology since 1976.

The CFC developmental activities of the early years (1976-80) [1-1] concentrated on cell active component development and single cell testing. The stack development activities were initiated in the early eighties. From the very beginning, ERC recognized the fuel flexibility, system simplification, and improved overall system efficiency benefits of the internal reforming CFC stacks; as such, in the early 1980's ERC initiated in-house work on internal reforming stack development. The internal reforming stack design is quite versatile in the choice of fuels including coal-gas, hydrogen, carbon monoxide, methane and higher hydrocarbons. In 1984 ERC tested the world's first internal reforming stack [1-2].

Activities during the 1985-86 period emphasized internal reforming stack component specifications development, fabrication of the components to meet these specifications, and performance verification of these components [1-3], culminating in a successful 3000-hour, 4-cell, 1ft^2 size stack test. Subsequently, under the current program, initiated in 1987, the cell components were scaled up to the 4ft^2 size in 1987-88. During the 1988 and 1989 period, ERC focused on developing stack repeat and non-repeat hardware and utilized the 2kW, 4ft^2 size stack as the design evaluation tool. Stack height scale-up and improvement of cell technology were also carried out during this period.

ERC has developed a common stack design for both of natural gas and coal-gas systems. The stack can run on either pipeline natural gas or any type of coal gasifier gas, or hydrocarbon fuels such as methanol, without requiring stack design changes. This fuel-flexible capability opens up many highly sought options. For example, a "phased power plant construction" based on fuel-flexible CFC will allow utilities to match demand growth closely and defer capital layout. The fuel-flexible CFC will also improve power plant availability by providing backup for both the coal gasifier and the cleanup subsystems. The higher stack volume production resulting from a multi-fuel market reduces stack cost. Also, the stack technology can be demonstrated and refined using natural gas first, thus leading to a lower overall development cost for coal-gas application.

Since 1986, ERC (in collaboration with Fluor-Daniel) has been very active in defining the CFC power plant conceptual designs and identifying the CFC operating parameters. ERC has focused on developing a simple all-electric MW-Class natural gas-fueled power plant and an integrated 100MW-Class (includes bottoming cycle) dual-fuel, operable on natural gas or coal-gas, power plant for utility applications. To date, several design iterations on MW-Class plants have been conducted. From these studies, two types of power plant designs have evolved: (a) an

"Integrated" design [1-4, 1-5], (b) a "Simplified" design. Detailed designs of these systems are planned in the future. During the 1988-89 period, in the current program, ERC has evaluated the 100MW-Class coal-fueled CFC power plant designs and identified plant configurations projecting very attractive efficiencies [1-6, 1-7], competitive economics, and very low environment emissions.

The present program was built on the successes of previous efforts and was designed to prepare the carbonate fuel cell for demonstration. The program was organized in three phases and was cost-shared by Electric Power Research Institute, Pacific Gas and Electric Company, and ERC corporate funds. In the first phase (April 1987 - January 1988), carbonate fuel cell components were successfully scaled-up from the pilot size (1 ft^2) to the large size (4 ft^2) (Tasks 1 through 4). Details of these efforts were discussed previously. The second phase of the program (February 1988 - December 1989), focused on the definition of the coal-fueled carbonate fuel cell power plant system (Tasks 5 through 7) and meeting the stack research needs for height scale-up and resolve coal-gas related issues (Tasks 8 through 12). The third phase of the program (February 1990 - September 1990), emphasized stack height scale-up and improvement in stack and cell technology (Tasks 13 through 15). The Tasks 5 through 15 are:

Task 5 CGMCFC System Design

Task 6 Comparison with Competing Systems

Task 7 System Analysis Topical Report

Task 8 Stack Design and CDR Definitions

Task 9 Test Facility Upgrade and Construction

Task 10 Technology Development

Task 11 Materials and Manufacturing Cost Assessment

Task 12 Update Design Control Document

Task 13 Technology Improvements

Task 14 Full-Size Stack

Task 15 Complementary Technology Activities

The results of the activities in Tasks 5 through 15 are presented in this report. The report has been organized along the following topical issues which were addressed in this program:

- Coal-Gas Related Carbonate Fuel Cell Considerations
- Cell and Stack Technology Improvement
- Carbonate Fuel Cell Stack Design Development
- Stack Test for Design Verification
- Full-Size Stack Design
- Test Facility Development
- Carbonate Fuel Cell Stack Cost Assessment
- Coal-Fueled Carbonate Fuel Cell Power Plant Design and Comparative Assessment

The relationship between the program tasks and the topical sections of the report is presented in Table 1.1. A listing of all cell tests performed under this program is presented in Table 1.2, also cross-referenced to the specific tasks of the program. The table is organized according to bench-scale cell tests (7in. X 7in. size) and stack tests. In addition, there were, in some tasks, a variety of out-of-cell tests. These are not listed in the table, but are referred to directly in the individual sections of the report.

TABLE 1.1

RELATIONSHIP OF REPORT SECTIONS WITH PROGRAM TASKS:

The Report Reflects Logical Organization of Topical Area Addressed in Various Tasks

Final Report Sections	Program Task
1.0 Introduction	
2.0 Coal-Gas Related CFC Considerations	10
3.0 Cell and Stack Technology Improvement	13
4.0 CFC Stack Design Development	8, 10
5.0 Stack Tests for Design Verification	10, 13, 15
6.0 Full-Size Stack Design	12, 14
7.0 Test Facility Development	9
8.0 Carbonate Fuel Cell Cost Assessment	11
9.0 Coal-Fueled CFC Power Plant Designs and Comparative Assessment	5, 6, 7

TABLE 1.2

SUMMARY OF CELL TESTS PERFORMED UNDER THE PROGRAM ACTIVITIES:

A Total of 59 Single Cells, One 0.1kW, Five 2kW, Two 5kW, and One 8kW Stacks Were Tested

7-Inch by 7-Inch Cell Tests

CELL #	OBJECTIVE	PROGRAM TASK
7-146	Fuel Performance Study	10
7-164	Fuel Performance, Fuel Stability	10
7-165	Ni Plating Evaluation	10
7-167	CCC Protrusion	10
7-170	Stack DOE-6 Design Evaluation	10
7-171	CCC Pattern Evaluation	10
7-172	CCC Pattern Evaluation	10
7-173	CCC Pattern Evaluation	10
7-174	CCC Pattern Evaluation	10
7-182	Fuel Performance, Fuel Stability	10
7-187	Contaminant Study	10
7-193	Contaminant Study	10
7-194	Oxidant Performance	10
7-196	Thick Anode	10
7-198	CCC Pattern Evaluation	10
7-199	CCC Pattern Evaluation	10
7-200	Contaminant Study	10
7-201	Contaminant Study; Effect of Fuel Moisture	10
7-203	Stack DOE-7 Design Evaluation	10
7-203	Oxidant Performance	10
7-205	CCC Pattern Evaluation (Internal Reforming)	10
7-206	Cathode Additive (Supress NiO Dissolution)	10
7-207	Alternate Electrolyte	10
7-212	Contaminant Study	10
7-216	CCC Pattern Evaluation	10
7-217	CCC Pattern Evaluation	10
7-219	Contaminant Study	10
7-220	CCC Pattern Evaluation	10
7-222	Cathode Additive (Supress NiO Dissolution)	10
7-223	Evaluate Stack DOE-10 Protrusion	10
7-225	Cathode Additive (Supress NiO Dissolution)	10
7-226	CCC Height Evaluation	10
7-229	CCC Height Evaluation	10
7-230	Electrolyte Additive	10
7-231	CCC Pattern Evalualtion	10
7-234	CCC Pattern Evaluation	10
7-235	CCC Pattern Evaluation	10
7-236	CCC Pattern Evaluation	10
7-237	Electrolyte Additive; Alternate Matrix	13
7-239	CCC Pattern Evaluation	13
7-241	Alternate Matrix	13

TABLE 1.2 (continued)

CELL ID	OBJECTIVE	PROGRAM TASK
7-242	Thick Matrix with Additive	13
7-243	Alternate Matrix	13
7-244	Thick Anode and Thick Cathode	13
7-245	Thick Anode	13
7-247	Thick Cathode	13
7-249	Alternate Electrolyte	13
7-250	Alternate Electrolyte	13
7-253	Thick Anode	13
7-255	High Back Pressure Study	13
7-256	Thick Cathode	13
7-258	Alternate Matrix	13
7-259	Alternate Matrix	13
7-260	Alternate matrix Support Method	13
7-261	Alternate Matrix Support	13
7-262	Thick Cathode	13
7-263	Alternate Matrix Support	13
7-264	Effect of OCV on Cell Shorting	13
7-265	Alternate Electrolyte	13

Stacks Tests

	STACK ID	OBJECTIVE	PROGRAM TASK
a)	0.1kW-Class	(5 cells, 0.1 ft^2)	
	AB-0.1-1	Electrolyte Migration Evaluation	13
b)	2kW-Class (5 cells, 4 ft^2)		
	DOE-5 (AF-2-3)	Dual Fuel	10
	DOE-6 (AF-2-4)	Bipolar Plate	10, 10
	DOE-7 (AF-2-5)	Module Compatibility	10, 10, 10
	DOE-10 (AF-2-6)	Manifold System Design	10, 10
	AF-2-S	Stackability, Rail Design	10, 10
c)	5kW-Class (11 cells, 4 ft^2)		
	PG&E-2* (AF-5-1)	Indirect Internal Reformer Scale-up	13
d)	5kW-Class (60 cells, 1 ft^2)		
	EPRI-60* (AS-5-1)	Direct Internal Reformer Height Scale-up	10
e)	8kW-Class (20 cells, 4 ft^2)		
	DOE-8 (AF-8-1)	Height Scale-up	13

*Cost-share stacks

Each section starts with a summary. The figures and tables are provided with primary as well as secondary titles for convenience of interpreting the thought of the visual. References for each section are provided at the end of each section.

1.1 REFERENCES

1-1a. B. Baker, et al., "Development of Molten Carbonate Fuel Cell Technology", Interim Technical Progress Report (March 1976 to January 1980), ERDA-DOE Contract Nos. E(043)1196, EY-76-AC03-1196, DE-AC03-76ET11304.

1-1b. A. Pigeaud, "Development of Molten Carbonate Fuel Cell Technology", Final Report for the Period February to December 1980, Contract No. DE-AC03-76ET11304.

1-2. L. Paetsch, et al., "Development of Molten Carbonate Fuel Cell Components", EPRI AP-5789, Research Project 1085-3, Final Report, July 1988.

1-3. L. Paetsch, et al., "Molten Carbonate Fuel Cell Development", DOE Contract No. DE-AC21-76ET11304, Final Report, April 1987.

1-4. P. Patel, "Assessment of a 6500-Btu/kWhr Heat Rate Dispersed Generator", EPRI, EM-3307, November 1983.

1-5. P. Patel, "Parametric Analysis of a 6500-Btu/kWhr Heat Rate Dispersed Generator", EPRI, EM04179, August 1985.

1-6. G. Steinfeld, et al., "MCFC Systems, Coal-Gas Based", Proceedings of the First Annual Fuel Cell Contractors Review Meeting, Editor W.J. Huber, p. 140, May 1989.

1-7. M. Farooque, et al., "Assessment of Coal Gasification/Carbonate Fuel Cell Power Plants", Topical Report (to be published), under Contract No. DE-AC21-87MC23274, June 1990.

2.0 COAL-GAS RELATED CARBONATE FUEL CELL CONSIDERATIONS

Operation of carbonate fuel cells on coal-gas requires the consideration of: appropriate soot suppression, effect of water-gas shift equilibrium, fuel and oxidant utilizations in the cell, and effect of trace impurities. Fundamental and practical data were generated on these issues.

Data were generated on the effect of moisture on soot suppression and cell performance. An approximately 2mV performance loss was measured for each percentage point increase in steam content. This information will be utilized for optimization of power plant subsystems.

Bench-scale cells were operated with the continuous addition of 1ppmv H_2S in fuel and 0.1ppmv HCl in oxidant, both singly and in combination. It was concluded from tests of up to 3000 hours that performance and life are unaffected by this level of impurities. Post-test analysis verified this observation.

2.1 INTRODUCTION

Energy Research Corporation has developed a carbonate fuel cell (CFC) capable of operating on either natural gas or a variety of coal-gases. An effort was therefore devoted to coal-gas and natural gas related issues and differences between the two fuels. The composition of coal-gas differs from natural gas, primarily in having a large amount of CO and varying amounts of moisture. In the fuel cell system, spent fuel is blended with oxidant gases and recycled with fresh air to manage the heat load in the cell. Oxidant composition and per pass utilization thus depend on the overall utilization of fresh air. Variations in performance arising from these changes were investigated experimentally and theoretically (using a performance model developed at ERC).

Coal-gas streams are expected to have trace impurities. The effects of two of these, namely H_2S and HCl, singly and in combination, on cell performance and stability were also assessed in single-cell tests. The rationale and results of these tests are discussed in this section.

2.2 EFFECT OF MOISTURE ON FUEL STABILITY AND PERFORMANCE

The presence of moisture in the fuel has two implications for carbonate fuel cell (CFC) operation. Moisture is necessary to suppress the formation of elemental carbon (soot) but is also a diluent in the fuel, depressing fuel activity and thus lowering the cell performance. The latter effect was evaluated for a typical oxygen-blown fluidized bed coal-gas in a bench-scale CFC. Figure 2.1 illustrates the resulting 1.8mV decrease in performance for each percentage point increase in fuel water content. The observed performance losses at various moisture levels were compared with those calculated from a carbonate fuel cell performance model developed at ERC. This model includes only thermodynamic and kinetic polarizations. At the highest water content (corresponding to the most stable resulting fuel composition), the deviation between observed and model performance becomes much larger. This suggests a possible mass transfer limitation (diffusional loss) with the larger amount of water. These results suggest that the level

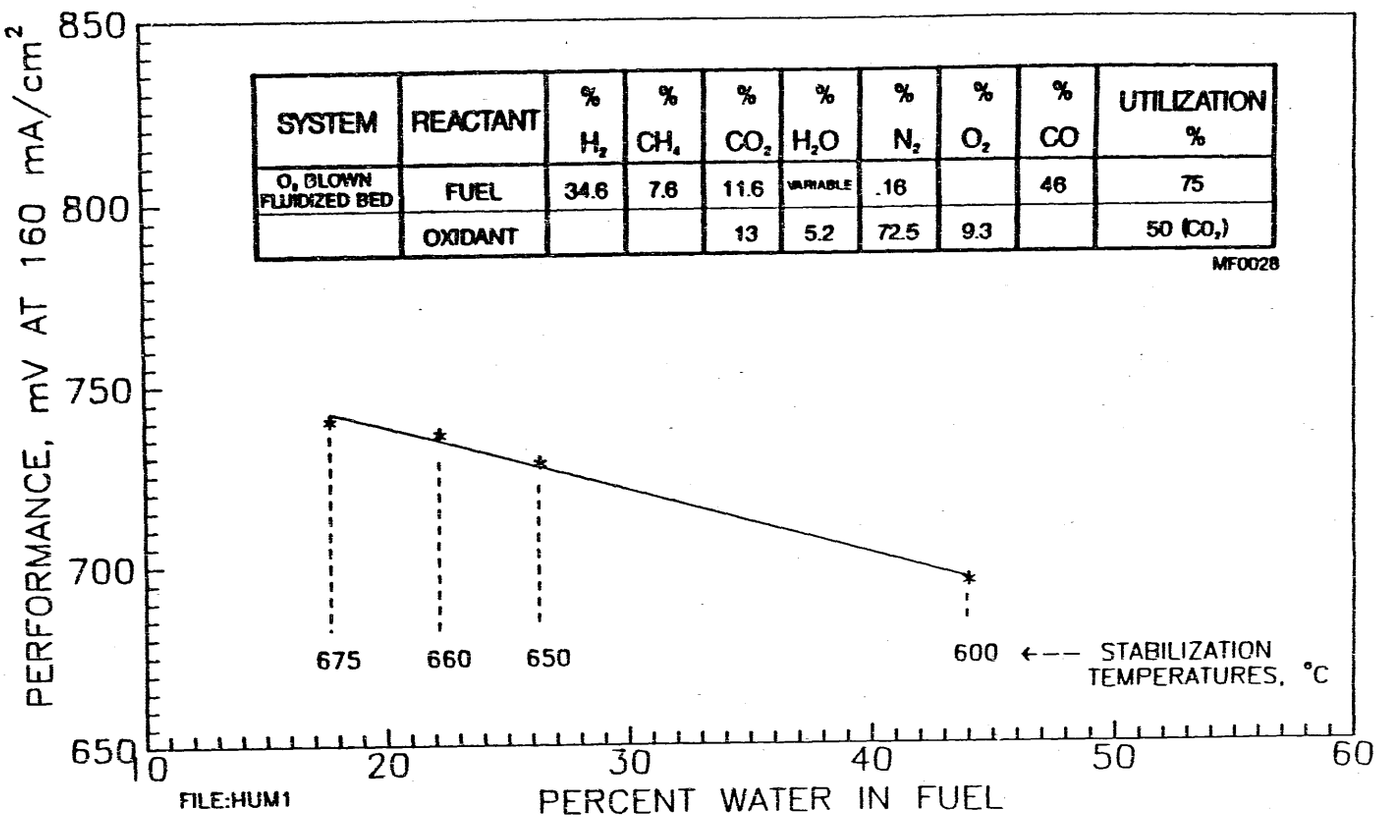

FIGURE 2.1 EFFECT OF HUMIDITY ON PERFORMANCE:

1.8mV Loss in Performance Per Percent H_2O Increase

of water vapor in the fuel should be maintained at the minimum needed to assure its stability with respect to carbon deposition and to optimize cell performance.

The amount of water required to stabilize a coal-gas fuel can be estimated using available thermodynamic information. A thermodynamically stable coal-gas composition for carbonate fuel cell operation using an entrained bed oxygen-blown coal-gas as an example is shown in Figure 2.2 in a C-H-O diagram constructed from literature data [2-1]. Depicted are the carbon-forming region and the thermodynamically stable region. The isotherms represent temperatures at which the corresponding gas composition will be stabilized with respect to soot formation at equilibrium. The points shown represent an oxygen-blown fuel as produced and the same fuel with additional water to stabilize it at 650°C (925°K). It is evident that significant water addition may be required to stabilize the fuels as received from the gasifier after cleanup. Previous ERC experience [2-2] has shown that soot formation may be kinetically limited at certain instances where it is thermodynamically possible. An experimental program was undertaken to test the stability of coal-gas mixtures at inlet piping conditions where soot formation is most likely to occur. Typical coal-gas mixtures were (a) an oxygen-blown fluidized bed, (b) an air-blown fluidized bed, and (c) an oxygen-blown entrained bed. The gas compositions on a dry basis are provided in Table 2.1. The steam-to-carbon ratio of these gases was varied to correspond to various stabilization temperatures and their stability temperatures up to 650°C were experimentally studied. The results are shown plotted on a C-H-O diagram in Figure 2.3, giving an indication of the critical moisture content of each gas to guard against carbon deposition. In general, the gases deposited soot at different stabilization temperatures, with the oxygen-blown entrained bed mixture being somewhat less stable than the others.

TABLE 2.1

GAS-COMPOSITIONS USED IN THIS STUDY (DRY BASIS):

Steam-to-Carbon Ratios Varied to Achieve Desired Stabilization Temperatures

	Percentage Composition				
Gasifier	H_2	CH_4	CO	CO_2	N_2
Fluidized Bed Oxygen-Blown	34.6	7.6	46.0	11.6	0.2
Fluidized Bed Air-Blown	17.4	0.9	19.0	10.9	51.8
Moving Bed Oxygen-Blown	28.7	7.3	54.0	6.2	3.8
Entrained Bed Oxygen-Blown	36.2	0.2	49.9	11.6	2.1
SRNG (unshifted)	80			20	

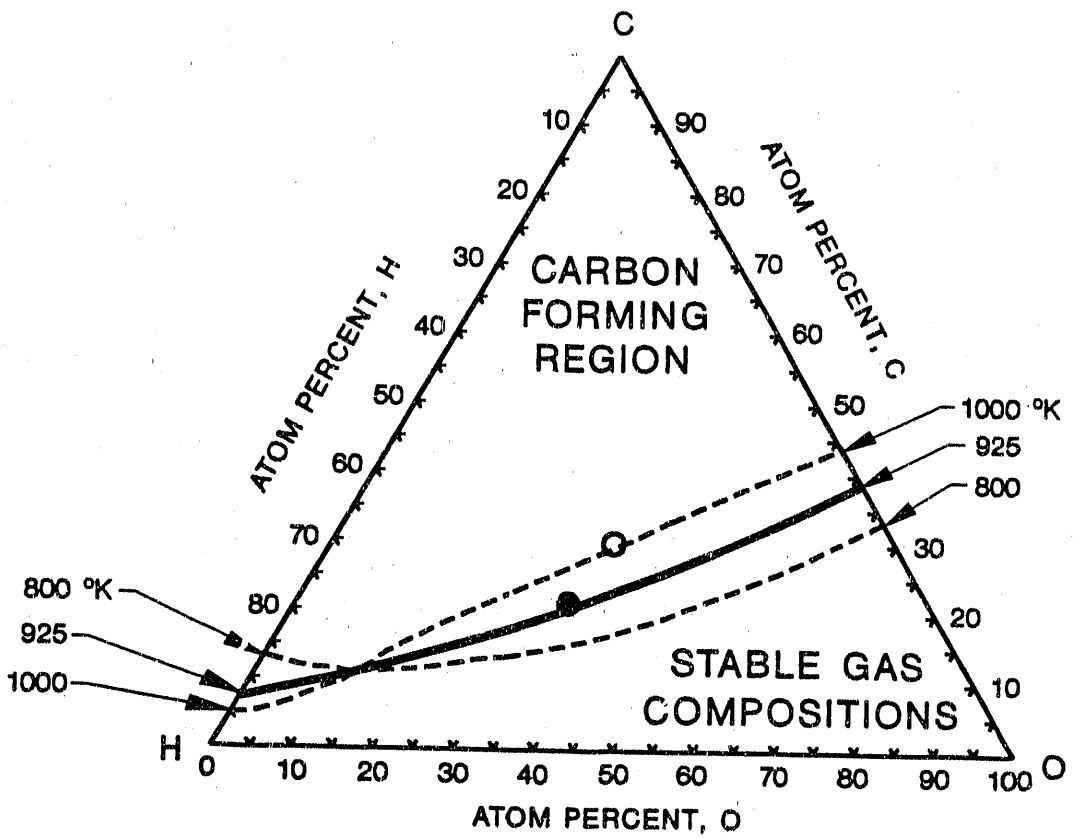

FUEL COMPOSITION	% H_2	% CH_4	% CO_2	% H_2O	% N_2/Ar	% CO
O - AS PRODUCED	36.2	0.2	11.5	0.3	2.0	49.8
● - STABILIZED	29.0	0.2	9.2	20.0	1.6	39.9

WM9009

FIGURE 2.2 C-H-O DIAGRAM FOR ENTRAINED BED OXYGEN-BLOWN FUEL:

Water Must Be Added to Stabilize Fuel at Working Temperature.

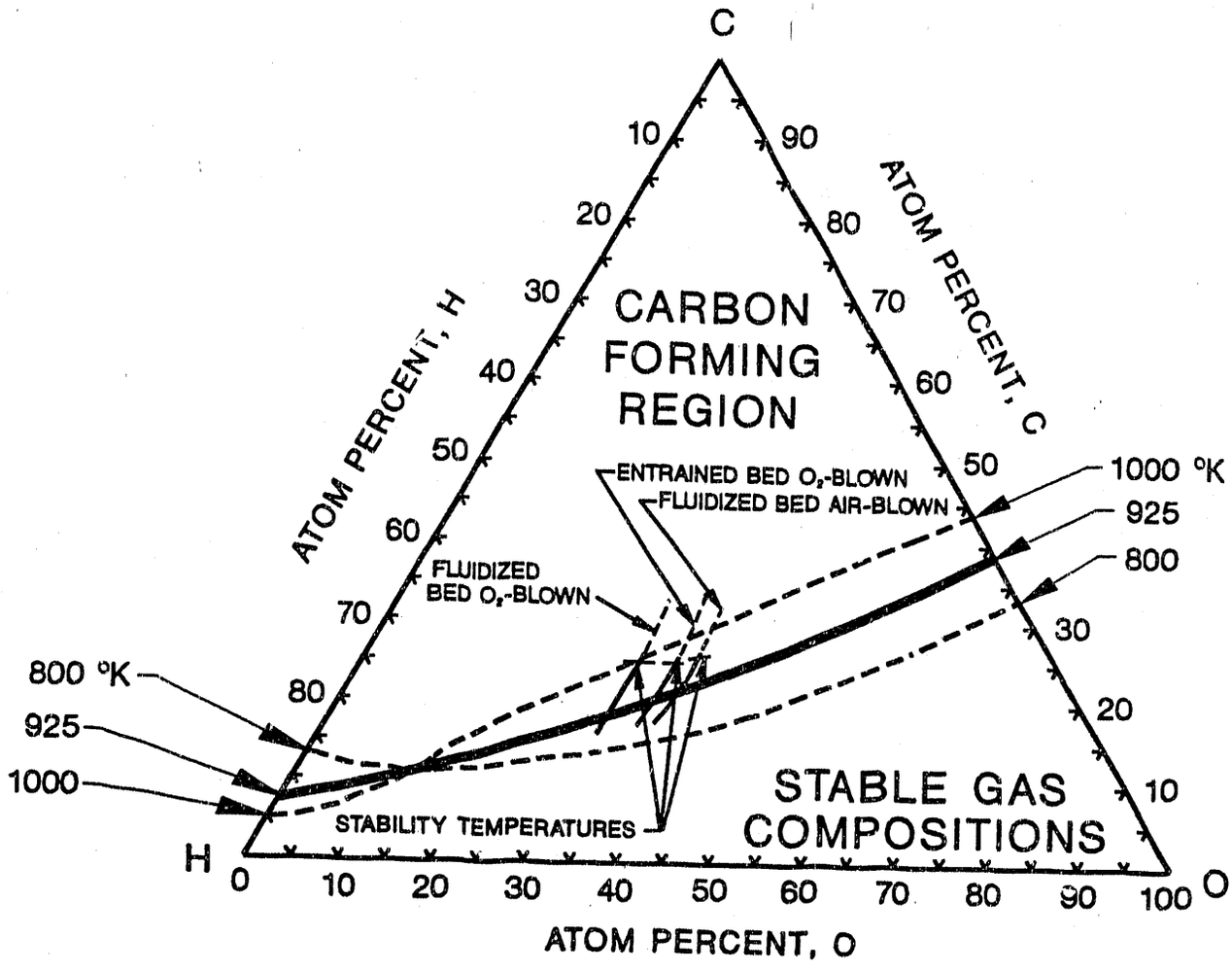

WM9062

FIGURE 2.3 EXPERIMENTALLY OBSERVED STABILITY OF FUEL GASES AT INLET PIPING CONDITIONS (UP TO 650°C):

Entrained Bed Oxygen-Blown Fuel Appears to be More Unstable than Others.

2.3 PERFORMANCE ISSUES

The coal-gas utilization in a carbonate fuel cell may have an impact on the overall system performance. Coal-gas fuels contain varying amounts of their fuel value in the form of carbon monoxide. This CO must participate in the water-gas shift reaction and come to an equilibrium in the cell to yield the maximum possible hydrogen needed for cell performance. The overall fuel utilization affects the cell performance, as does the overall oxidant utilization. In the latter case, the actual composition and per pass utilization of the oxidant depend on the overall fresh air utilization. These factors were investigated singly and in combination and compared with the operation on simulated reformed natural gas fuel.

2.3.1 Effect of CO Content in Fuel

To study the impact of the CO content of the fuel on the cell performance, a cell was operated on a simulated coal fuel and on an "equivalent" fuel with the completely preshifted composition. Both the fuel gas mixtures were stabilized against soot formation at 650°C. Stabilization was established by calculating the equilibrium position of the fuel composition on a C-H-O diagram as described in Section 2.2 and illustrated in Figure 2.2. The comparison of cell performances in Figure 2.4 shows that the performance was identical for the fuels. The electrochemical performance of the carbonate fuel cell, therefore, depends on the equivalent fuel and is not affected by the presence of CO as such, implying that the water-gas shift reaction is essentially at equilibrium in the fuel cell. It also means that for coal-gas simulation purposes, it is satisfactory to feed a more economical coal-gas equivalent, rather than the actual carbon monoxide-containing mixture.

2.3.2 Utilization Effects

The performance of a carbonate fuel cell depends strongly on the composition of the fuel gas and on its utilization. In a carbonate fuel cell, the oxidant stream is recycled. The cathode inlet composition and per pass utilization thus depend on the overall utilization of fresh air. As the overall oxidant utilization increases, the increased CO_2 provides a favorable effect on cell performance, while the lower O_2 content results in a negative effect. The effects of changes in utilization in the fuel and in the oxidant were investigated.

The effect of fuel utilization on cell performance was investigated using a fluidized bed oxygen-blown gas. Results are shown in Figure 2.5. As expected, there was a decrease in performance when fuel utilization increased from 60% to 80%. This decrease amounts to 1.9 mV for each percentage point. The effect is linear, with no evidence of diffusion limitation at utilizations approaching 80%.

In the recycled oxidant stream of the carbonate fuel cell, the cathode inlet composition and utilization for a given fuel depend on the overall utilization of fresh air. As this overall utilization increases, the increasing CO_2 content provides a favorable effect, while the decreasing O_2 content results in a negative effect. The relationship between cell

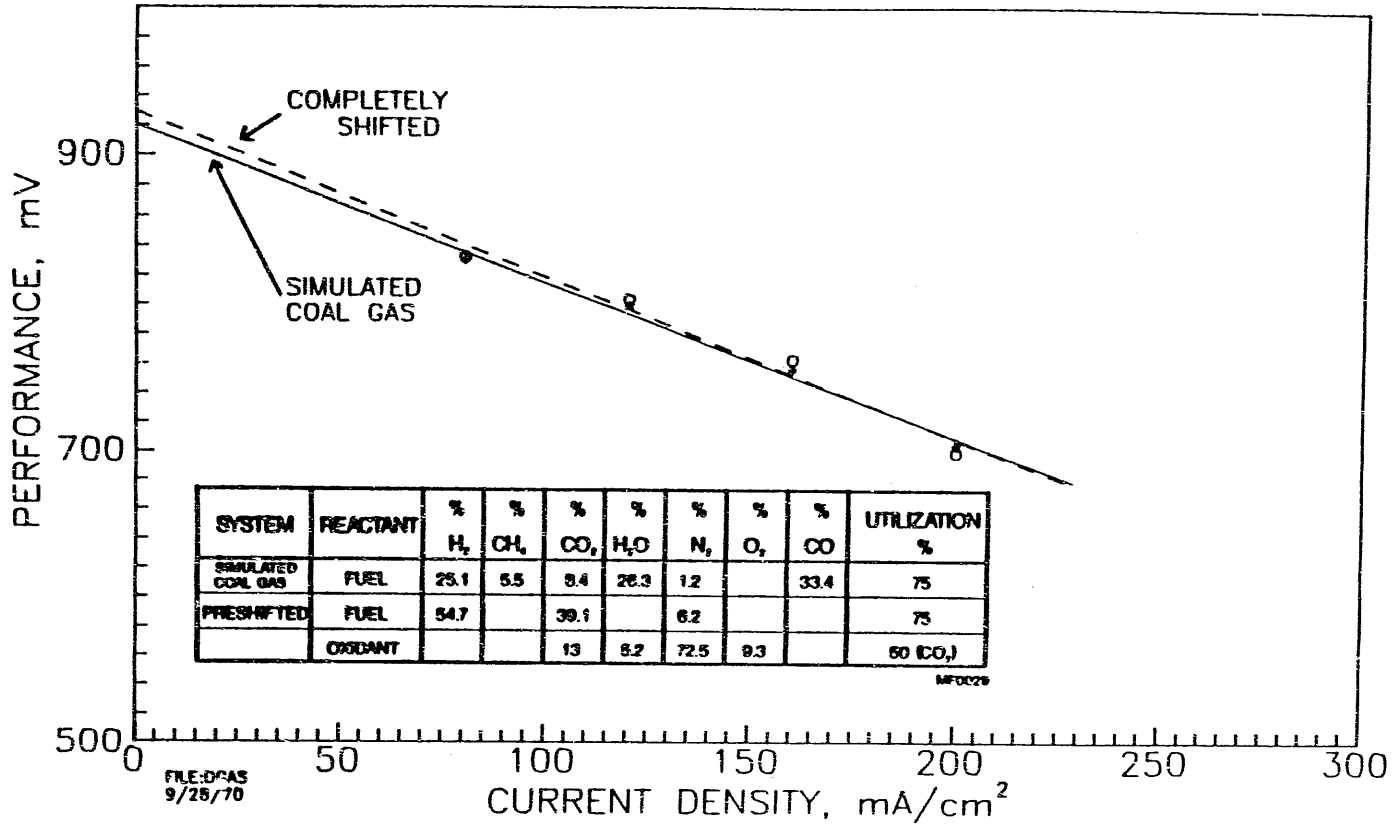

SYSTEM	REACTANT	% H_2	% CH_4	% CO_2	% H_2O	% N_2	% O_2	% CO	UTILIZATION %
SIMULATED COAL GAS	FUEL	25.1	5.5	8.4	26.3	1.2		33.4	75
PRESHIFTED	FUEL	54.7		39.1		6.2			75
	OXIDANT			13	5.2	72.5	9.3		50 (CO_2)

MF0029

FIGURE 2.4 PERFORMANCE OF CARBONATE FUEL CELL AS COAL-GAS:

Electrochemical Performance of Carbonate Fuel Cell Depends on Equivalent Fuel and is not Affected by CO Content

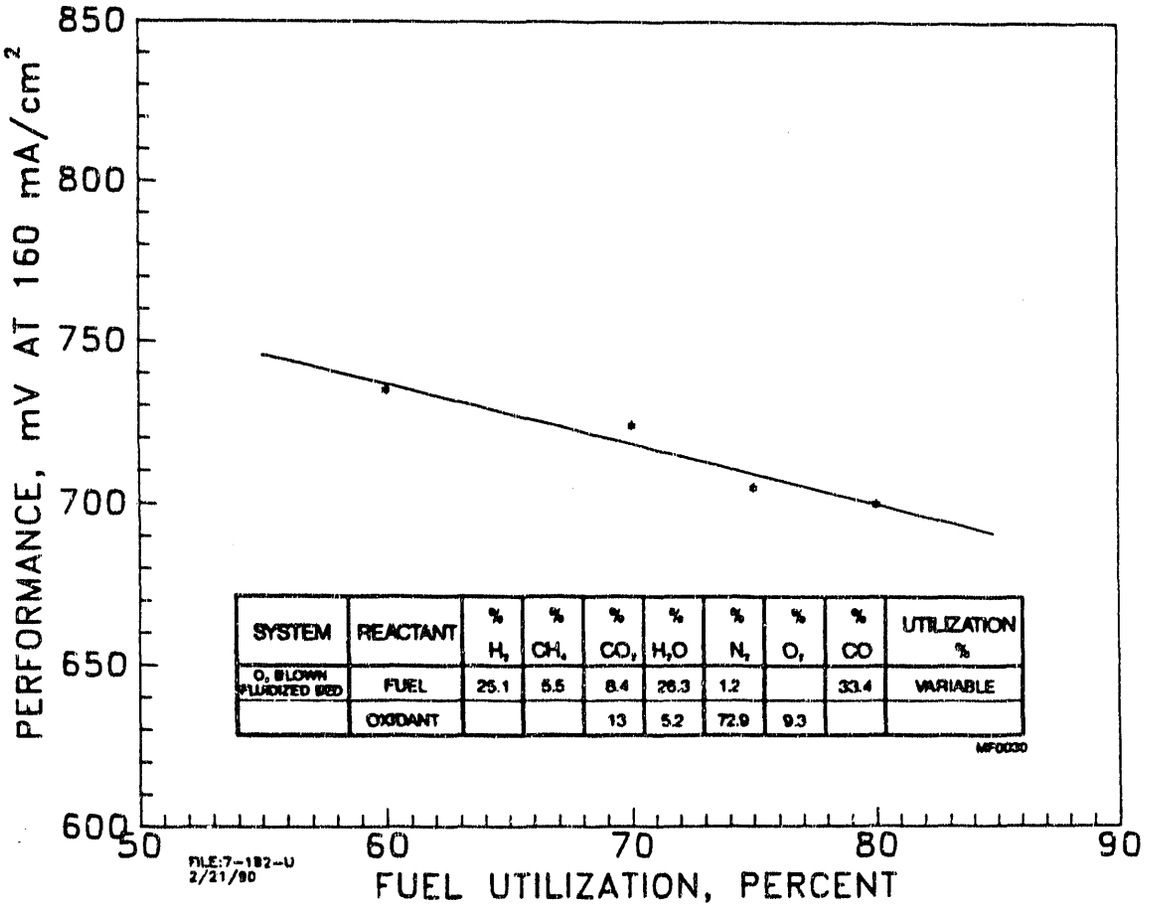

SYSTEM	REACTANT	% H_2	% CH_4	% CO_2	% H_2O	% N_2	% O_2	% CO	UTILIZATION %
O_2 BLOWN FLUIDIZED BED	FUEL	25.1	5.5	8.4	26.3	1.2		33.4	VARIABLE
	OXIDANT			13	5.2	72.9	9.3		

FIGURE 2.5 EFFECT OF UTILIZATION OF FUEL GAS ON PERFORMANCE:

Loss of 1.9 mV for Each Percentage Increase in Fuel Utilization

performance and increase in overall oxygen utilization was estimated using the ERC cell performance model for two coal-gas fuels: (i) oxygen-blown fluidized bed and (ii) oxygen-blown entrained bed. Water was added to both fuels to stabilize them with respect to soot formation at 650°C. Stabilization was established by calculating the equilibrium position of the fuel composition on a C-H-O diagram as described in Section 2.2 and illustrated in Figure 2.2. In this study, the fuel composition and utilization were held constant while the oxidant composition used corresponded to different overall air utilization cases. As anticipated, there was a slight increase in performance with increasing oxygen utilization, as shown in Figure 2.6. A carbonate fuel cell performance model developed at ERC predicts a similar trend.

The combined effect of fuel and oxidant compositions on carbonate fuel cell performance was investigated. The effects of changes in fuel and in oxidant compositions on carbonate fuel cell performances, both singly and in combination, were investigated both experimentally and by using a cell performance model. The gas mixtures used in this study were: oxygen-blown fluidized bed; air-blown fluidized bed; oxygen-blown moving bed; oxygen-blown entrained bed; simulated reformed natural gas. Table 2.1 lists the gas compositions on a dry basis. The fuel gas compositions were stabilized to 650°C with respect to soot formation as described above.

Figure 2.7 shows the results in comparison with the reformed natural gas operation case. The first section of the figure, "coal fuel loss", gives the effect of fuel independent of oxidant. For these investigations the oxidant composition was held constant while the fuel composition was varied. There is a loss in performance with coal-derived fuel compared with SRNG. The two experimental results agree reasonably well with the calculated values. To study the effect of coal system oxidant, the fuel composition was held constant and the oxidant composition as calculated by the model was used for computation of the performance and for obtaining the experimental values. Again, the experimental results are in reasonable agreement with those estimated by the performance model. There is a slight gain in performance for the coal-gas cases compared with SRNG. The final section of the figure shows the net effect. In general, there are small net losses predicted for the oxygen-blown systems compared with natural gas, with a slight net gain calculated for the one air-blown system.

2.4 CONTAMINANT ISSUES

The carbonate fuel cell developed by ERC is capable of operating on either natural gas or coal-gas. In both cases, there are impurities present in the gas streams which need to be removed. Coal-gases in particular may contain a number of trace level contaminants as residual content from the clean-up subsystem which may affect the operation of the CFC. These include sulfur species, halides, ammonia, and heavy metals. Two important contaminants were chosen for study in this program at levels considered to be safe from previous studies [2-2, 2-5, 2-6, 2-7]. As a representative contaminant in the fuel gas, H_2S at a level of 1 ppmv was chosen. HCl was chosen as a representative halide to be added to the oxidant stream at a level of 0.1 ppmv.

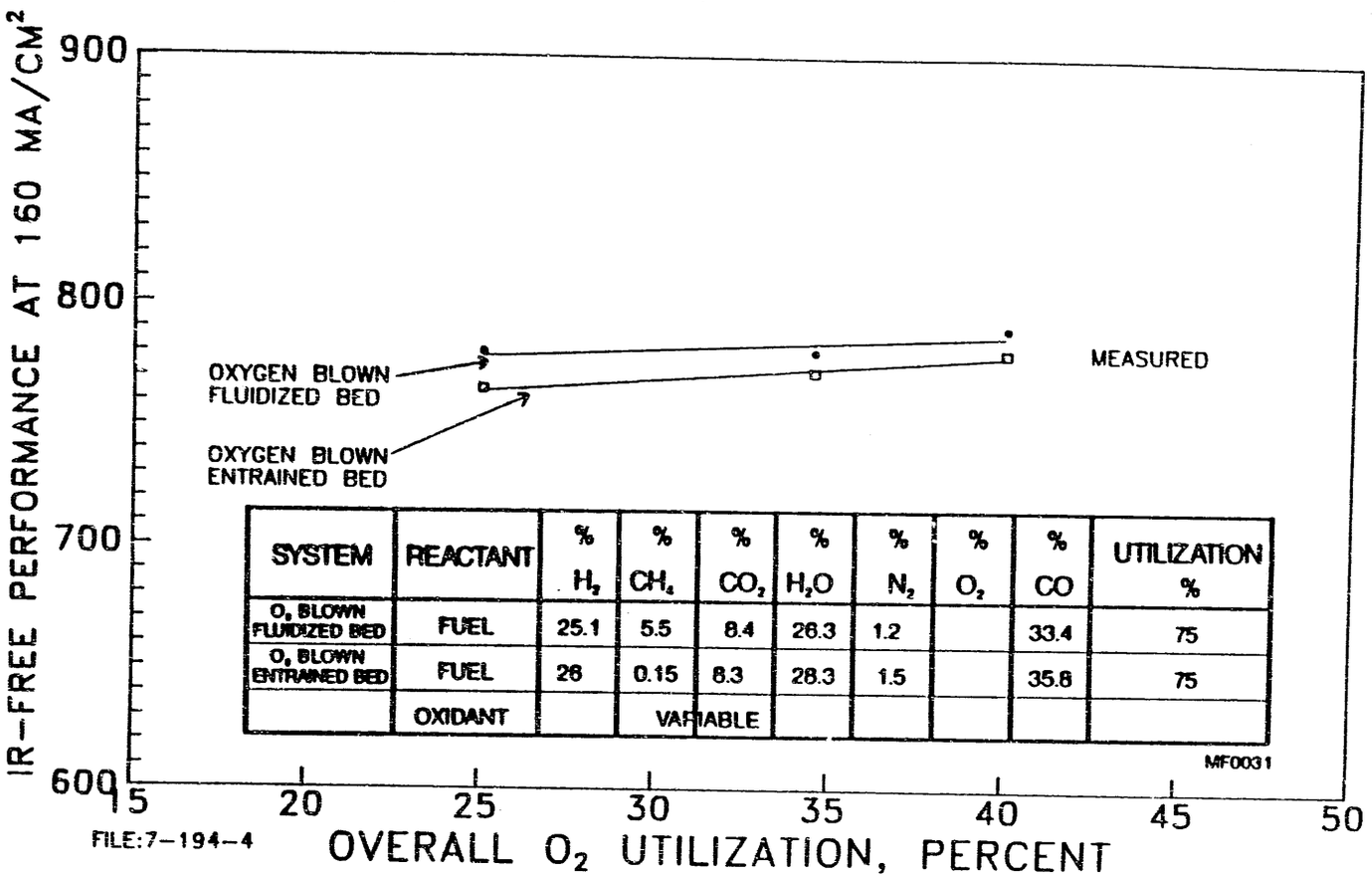

SYSTEM	REACTANT	% H_2	% CH_4	% CO_2	% H_2O	% N_2	% O_2	% CO	UTILIZATION %
O_2 BLOWN FLUIDIZED BED	FUEL	25.1	5.5	8.4	26.3	1.2		33.4	75
O_2 BLOWN ENTRAINED BED	FUEL	26	0.15	8.3	28.3	1.5		35.6	75
	OXIDANT		VARIABLE						

FIGURE 2.6 OBSERVED EFFECT OF INCREASED OVERALL AIR UTILIZATION:

Slight Gain in Performance Observed Due to Higher O_2 Lower CO_2 Utilization Per Pass

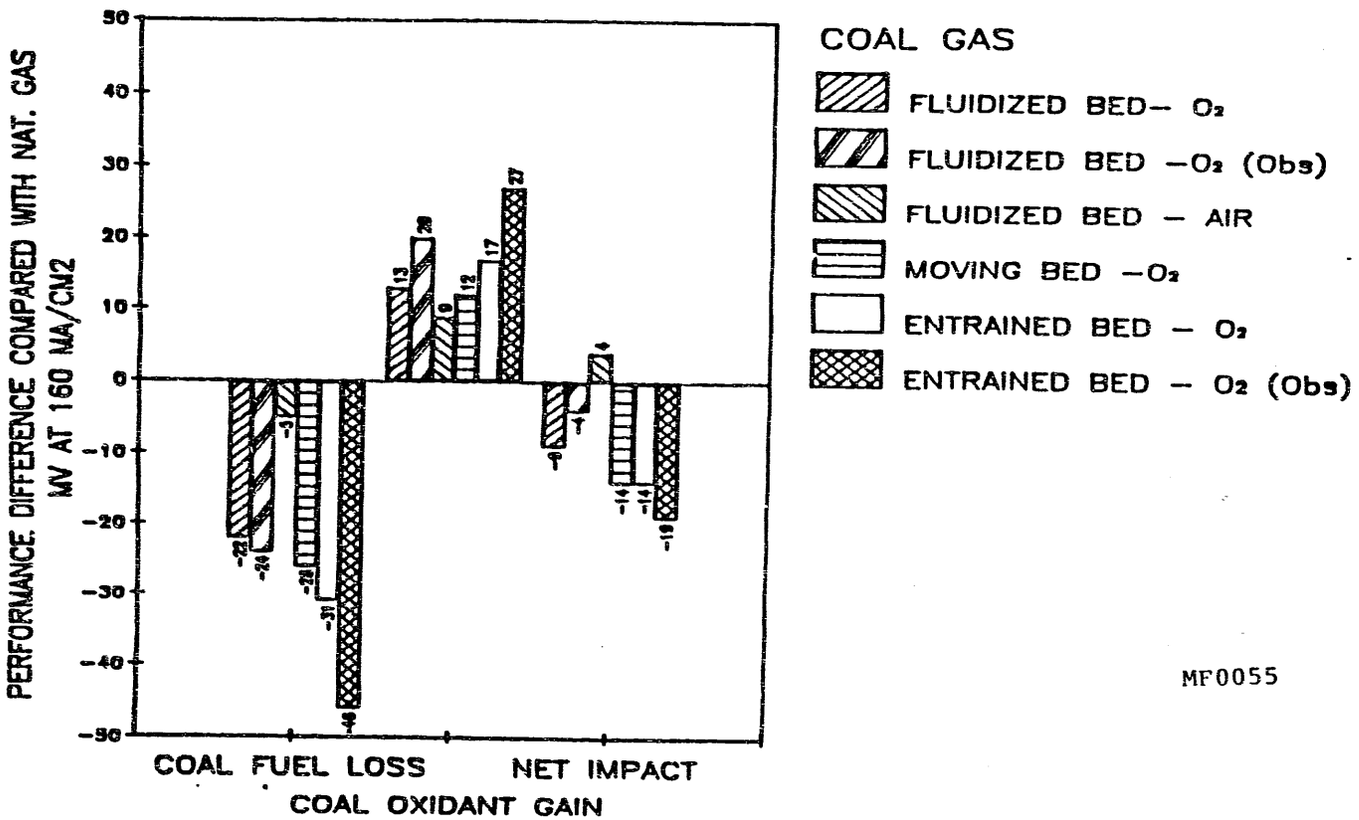

FIGURE 2.7 COAL GAS PERFORMANCE ANALYSIS:

Cell Performance in Natural Gas and Coal Gas Systems is About the Same

There are some implications for the carbonate fuel cell system of this amount (0.1 ppmv) of HCl in the oxidant. It should be recalled that, in the power plant system, partially spent fuel is burned to produce carbon dioxide, combined with make-up fresh air and sent to the cathode manifold. In addition, a portion of the partially spent oxidant will be recycled to the cathode to manage the heat balance in the stack. Using flow rates calculated for oxygen-blown fluidized bed fuel at 75% utilization and an overall oxidant utilization of 40%, the amount of HCl in the fuel which would give rise to the 0.1 ppmv in the oxidant is calculated to be 0.3 ppmv. This represents the level expected to accumulate in the recycled stream if the amount of 0.3 ppmv were introduced with the fuel gas after the clean-up system. Another implication for the fuel cell arises from the chemical reaction of the introduced chloride with the carbonate electrolyte. Replacement of carbonate anions with an equivalent amount of chloride anions would be expected to go to completion at fuel cell conditions. Since the chloride salts are more volatile than the carbonate salts at these temperatures, they could be carried away from the cell by volatilization. This would be 4% by weight of the electrolyte over the anticipated 40,000h life of the stack, assuming that all of the 0.1ppmv chloride in the oxidant replaces carbonate and then volatilizes completely without corrosive side reactions.

The contaminants were introduced to the gas streams by a permeation tube device. The schematic of the contaminant feed system is shown in Figure 2.8. A nitrogen carrier gas was introduced in a permeation tube at a rate to produce the desired concentration of contaminant. The temperature of the permeation tube was carefully controlled. The contaminant stream was introduced to the cell through a closed-end ceramic tube which had several slits for uniform mixing with the process gas. In this arrangement, the contaminant contacted only ceramic or plastic before entering the cell and did not contact any metallic surface with which it could react or adsorb on.

2.4.1 Effects of HCl

A bench-scale carbonate fuel cell was operated with the addition of 0.1 ppmv of HCl to the oxidant stream. The cell was first operated for about 500 hours on simulated reformed natural gas; then HCl was introduced. After no effect was observed on the performance for about 250 hours, the fuel gas was changed to a typical oxygen-blown fluidized bed fuel gas. The cell was operated with continuous 0.1ppmv HCl addition for an additional 1000 hours with no performance decay which could be ascribed to the HCl addition. The cell was terminated after a facility upset. Figure 2.9 displays a lifegraph of the cell.

Upon post-test, no noticeable corrosion was found in the cathode chamber. Samples were measured for chloride along the depth of each cell component by Energy Dispersive Spectroscopy (EDS). Observations were compared with those from another bench-scale cell which had run for a similar length of time and which used similar hardware. The comparison revealed chloride accumulation in the test cell, primarily on the surface, with little or no penetration into the interior of the cell components. There was no evidence of the expected stress corrosion cracking, but only normal hot corrosion.

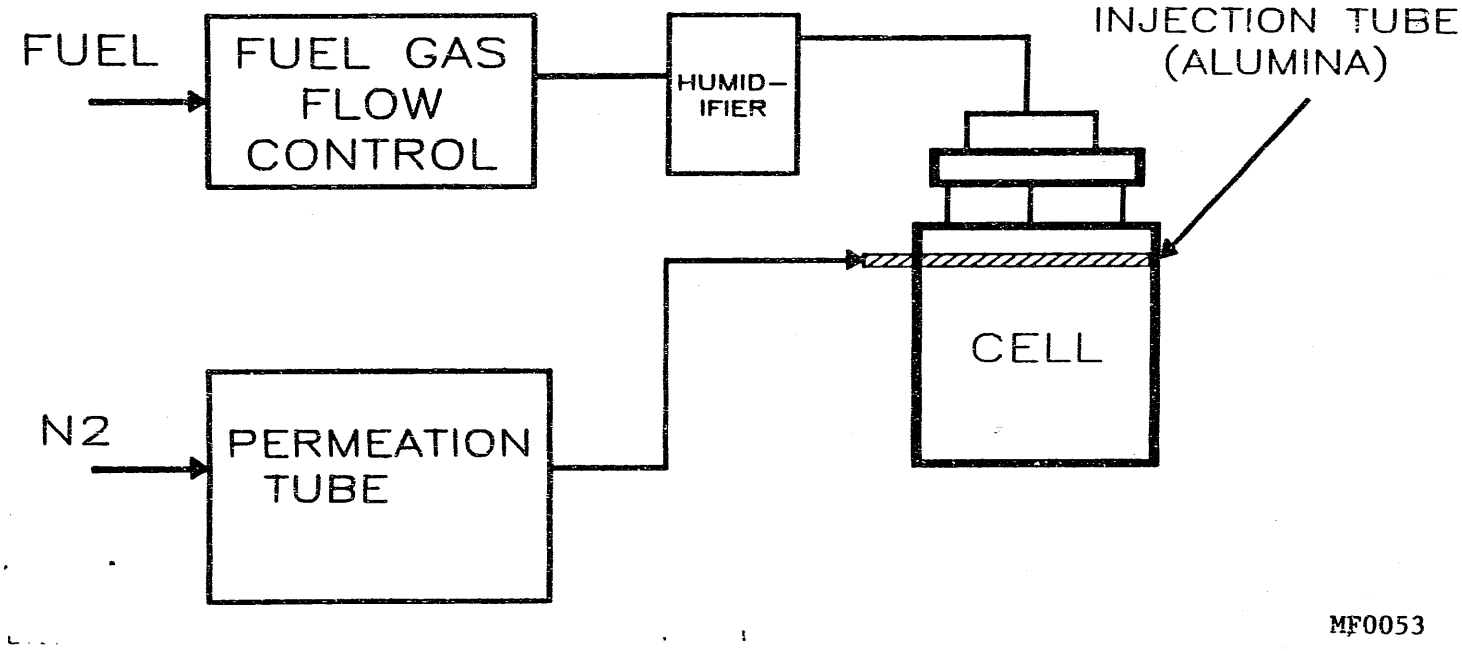

FIGURE 2.8 CONTAMINANT FUEL SYSTEM FOR BENCH-SCALE TESTS:

Contaminant Contacts Only Ceramic and Plastic Before Entering Cell

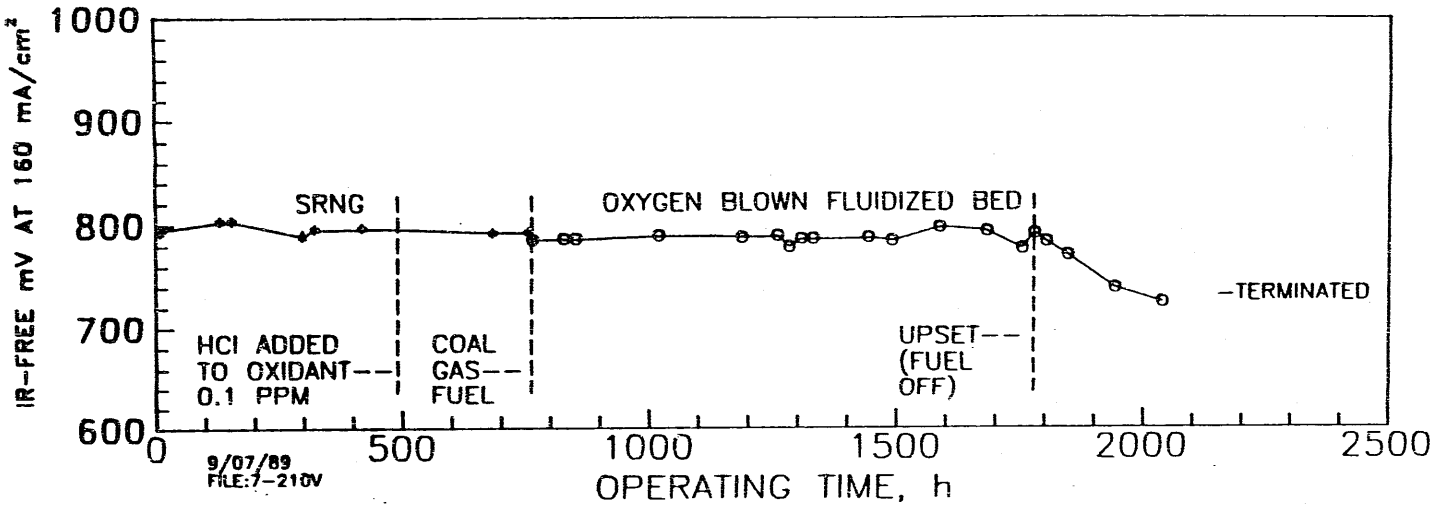

SYSTEM	REACTANT	% H_2	% CH_4	% CO_2	% H_2O	% N_2	% O_2	% CO	UTILIZATION %
O_2 BLOWN FLUIDIZED BED	FUEL	25.1	5.5	8.4	28.3	1.2		33.4	75
SRNG	FUEL	74.8		18.7	6.5				75
	OXIDANT			13	5.2	72.5	9.3		50(CO_2)

MF0032

FIGURE 2.9 LIFEGRAPH OF HCl CELL:

No Performance Decay Attributable to HCl Addition to the Oxidant Stream was Noticed

2.4.2 Effects of Sulfur

Hydrogen sulfide, H_2S, was chosen as the representative sulfur-containing chemical species occurring in a fuel gas derived from coal. This was added to the fuel via the permeation tube system at 1.0 ppmv. A cell was operated for 1250 hours, 850 hours with H_2S. A performance comparison with and without H_2S did not indicate any effect on performance. Post-test sulfur analysis on the hardware and components of the cell by EDS compared with a blank cell indicated essentially no sulfur pickup by the cell hardware.

A second cell was operated for 1600 hours (950 hours on H_2S). There was no effect on performance attributable to the H_2S until the permeation tube ruptured. At this point, a large dose of H_2S was introduced to the cell over a 20 to 60-minute period, causing a massive poisoning of the electrode. A lifegraph shown in Figure 2.10 indicates that the cell performance was regained by operating the cell on a sulfur-free fuel.

2.4.3 Effect of Combined Addition of HCl and H_2S

Investigation of the combined effects of both HCl and H_2S added to fuel cell feed gases simultaneously over a much longer time period was carried out in a bench-scale carbonaate fuel cell. HCl was added to the oxidant stream at 0.1 ppmv, while H_2S was added to the fuel at 1.0 ppmv, as before. H_2S was added after stabilizing the cell on standard gas, then on oxygen-blown fluidized bed fuel, at about 350 hours. After the cell stabilized, HCl was added at about 500 hours. A facility upset at about 1000 hours caused a drop in overall performance, but there was no change in performance which could be attributed to the presence of the contaminants. A final facility upset at about 3000 hours caused the cell to be terminated.

As mentioned above, some of the mechanistic considerations concerning the addition of H_2S were investigated. The approach to equilibrium of the water-gas shift reaction in degrees Celsius with respect to cell exhaust temperatures of 650°C was determined from effluent gas analysis. When plotted against the time from addition of H_2S (Figure 2.11) it was found to change rapidly, becoming roughly constant. At 350 hours when the cell was placed at open circuit, the water-gas shift reaction went to equilibrium, showing that the absorption of sulfur on the hardware reversed when the cell was taken off load. When again put on load at 500 hours, the internal surfaces again equilibrated with the H_2S concentration in the fuel stream. The water-gas shift approached a constant equilibrium temperature and the effluent H_2S concentration became constant by about 750 hours. Using data from Reference 2-1, an equilibrium sulfur coverage can be calculated for the estimated internal metallic area in the fuel chamber of the cell, including the Ni anode. From this, a time to saturation of 200 hours was calculated, which is in reasonable agreement with the observed 250 hours.

The overall sulfur balance based on effluent analysis indicates there should be an accumulation of ca. 0.14 g of S in the cell. This ignores desorption of the estimated equilibrium coverage of 0.13 g during open

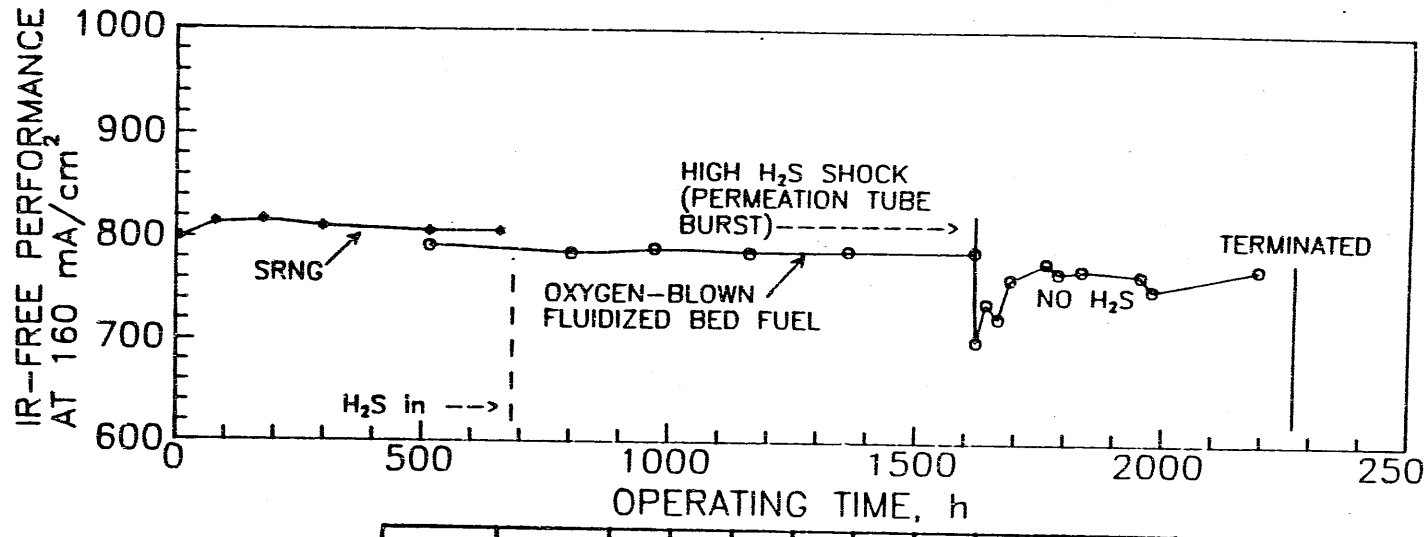

SYSTEM	REACTANT	% H_2	% CH_4	% CO_2	% H_2O	% N_2	% O_2	% CO	UTILIZATION %
O_2 BLOWN FLUIDIZED BED	FUEL	25.1	5.5	8.4	28.3	1.2		33.4	75
SRNG	FUEL	74.8		16.7	6.5				75
	OXIDANT			1.3	5.2	72.5	9.3		

MF0056

FIGURE 2.10 LIFEGRAPH OF H_2S CELL:

No Effect from 1.0ppmv H_2S,
Cell Recovered After High
H_2S Shock

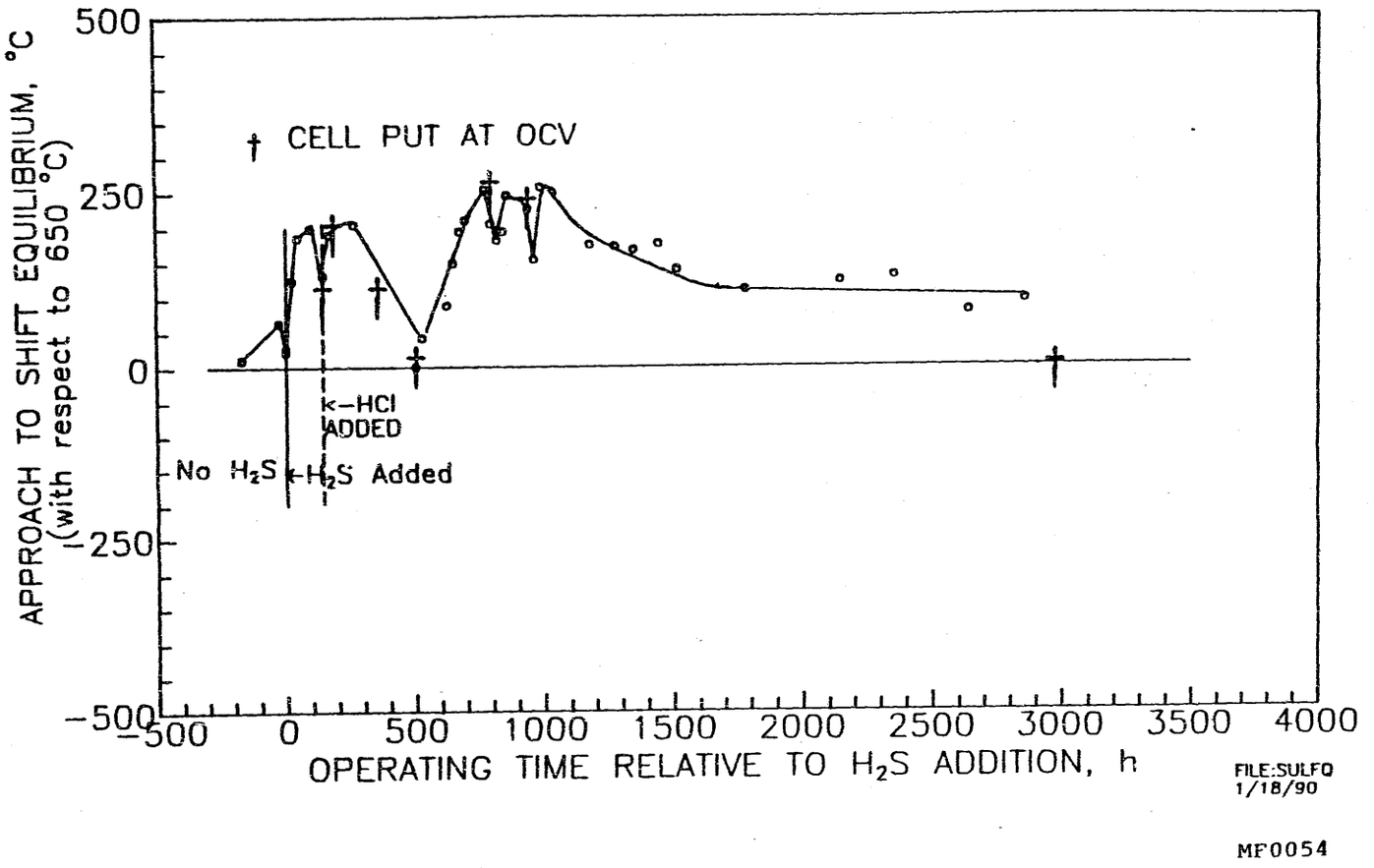

FIGURE 2.11 EFFECT OF H_2S ADDITION ON SHIFT EQUILIBRIUM:

Addition of 1ppmv H_2S Prevents Equilibration of Water Gas Shift Reaction

circuit episodes. The 'accumulated' sulfur presumably remains reacted as bulk metal sulfide or as dissolved sulfur species in the electrolyte (no SO_2 was detected in the oxidant effluent).

The post-test distribution of S and Cl in the 3000-hour bench-scale cell was measured by EDS. Some small sulfur buildup on the anode side surfaces was evident, especially at the fuel inlet, as was chloride at the oxidant inlet surfaces. As before, no bulk penetration of the sulfur and chloride was noticed.

2.4.4 Corrosive Effects of HCl and H_2S

As mentioned above, there was no noticeable enhanced corrosion or stress corrosion cracking seen in the hardware of either fuel side or oxidant side hardware of any cell examined in this program. Even after 3000+ hours of exposure to HCl and H_2S, only normal "hot corrosion" is in evidence. Corrosion rates are plotted in Figure 2.12 for this cell and for the HCl addition cell along with those from a number of other ERC cells and stacks. Both cells meet the goal for 40,000-hour life.

Carbonate cells are able to withstand fuel side sulfur and oxidant halide exposures at levels expected to be present as trace residue from gasifier clean-up streams. There is no evidence to show that operation is affected, although water-gas shift equilibrium is affected somewhat. There is no evidence of enhanced corrosive attack by any contaminant species.

2.5 REFERENCES

2-1. "Catalytic Steam Reforming", J.R. Rostrup-Neilson, Springer-Verlag, Berlin, 1984.

2-2. Pigeaud, A. and Klinger, J. "Study of the Effects of Soot, Particulate, and Other Contaminants on Molten Carbonate Fuel Cells Fuel by Coal Gas", Final Report, DOE Contract No. DE-AC21-84MC21154, Aug. 1987.

2-3. Cairns, E.J. et. al., J. Electrochem. Soc. 110, No. 10, 1025 (1963).

2-4. Weaver, D. and Winnick, J., J. Electrochem. Soc. 136, 1679 (1989).

2-5. Kunz, H.R., et. al., "The Effect of Halides on the Performance of Coal Gas-Fueled Molten Carbonate Fuel Cell", Final Report, DOE Contract No. DE-AC21-83MC20212, Oct. 1987.

2-6. Remick, R., "Effects of H_2S on Molten Carbonate Fuel Cells", Final Report, DOE Contract No. DE-AC21-83MC20212, May 1986.

2-7. Kunz, H.R. et. al., "Development of Molten Carbonate Fuel Cell Technology", Final Report, Vol. I, DOE Contract No. DE-AC21-79ET15440, Feb. 1988.

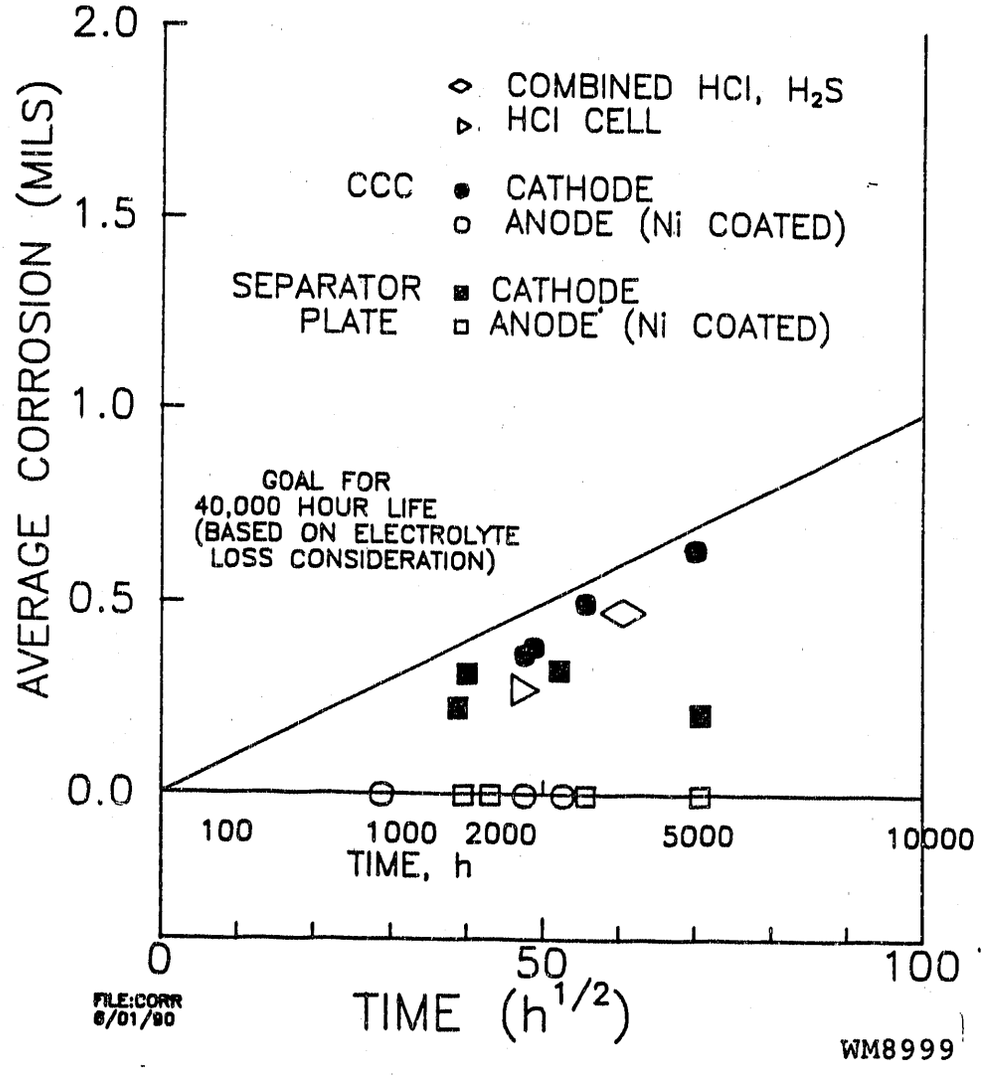

FIGURE 2.12 CORROSION RATES OF ERC CELLS:

Addition of HCl and/or H_2S does not Affect Corrosion Rate

3.0 CELL AND STACK TECHNOLOGY IMPROVEMENT

Significant advancement of the cell and stack technology was achieved. An improved matrix was successfully evaluated in single cells and then in multicell stacks, showing approximately 40mΩ-cm² (∿10%) reduction in cell resistance and at least 50% improvement in matrix gas seal efficiency.

Several manifold gasket designs were identified. These designs are expected to meet the seal efficiency goal of 0.2% fuel leak at 15 inches of water pressure. An advanced gasket, which has also been evaluated in a stack, provides adequate manifold seal as well as projects reduction of the electrolyte migration rate by an order of magnitude. This gasket design, as well as a parallel end-cell electrolyte source and sink approach (which was successfully verified in single cells), may provide adequate electrolyte management to ensure 40,000-hour useful life for a full-size stack. These approaches for electrolyte management are being evaluated in a short stack. An approach for achieving a two-fold improvement in cathode stability has also been demonstrated in single-cell accelerated tests.

These improvements together project better performance, higher fuel utilization, longer stack life, and provide a sound basis for a full-size stack design for demonstration of system integrated operation.

3.1 INTRODUCTION

A stack is the major power producing component in a carbonate fuel cell power plant. Its performance and longevity can have a major impact on system efficiency and overall economics. To be competitive with other emerging power plant systems (e.g., gas turbine combined cycles), a stack useful life over 40,000 hours is desired.

During the past decade, significant progress was achieved in terms of stack component development (e.g., creep-resistant anode, matrix tape-cast methods, and corrosion-resistant hardware materials and coatings); therefore, stable stack performance over an operating period of several thousand hours was demonstrated. However, several stack technology areas still needed further improvement for achieving the goal of a 40,000-hour life. The following four areas were targeted in this effort for concentrated research: electrolyte migration mitigation, decreasing matrix gas cross-over, improving cathode stability, and reducing ohmic resistance. Significant progress was achieved in all these areas. The results are discussed in detail in the following sections.

3.2 ELECTROLYTE MIGRATION MITIGATION

An electrolyte redistribution, caused by electrolyte migration through porous manifold gasket, may reduce stack end cell life to several thousand hours as opposed to the desired life goal of 40,000 hours. This phenomenon does not affect the central cell electrolyte balance. An electrolyte redistribution model, described in Section 4.4, shows that increasing gasket resistance, in combination with the end cell electrolyte inventory

adjustments, has the potential to reduce the electrolyte redistribution rate to achieve the desired 40,000-hour end cell life. In this development effort, several candidate gasket designs were first recommended, based on the modeling and stack results. Promising candidate gaskets were then selected based on out-of-cell migration and gas leakage experimental results. The inventory adjustment approach was also verified in single-cell tests. The selected designs are now being evaluated in short stacks.

3.2.1 Gasket Development

ERC's prior baseline gasket is powder impregnated zirconia felt. Due to its high porosity, it becomes filled with carbonate during stack operation. The filled gasket then serves as an ideal path for electrolyte migration, caused by the high voltage gradient ($\sim$3 V per inch) along the gasket. Reduction of gasket width and thickness (using less gasket layers) - although it can increase gasket resistance is projected to increase gasket resistance by two to four times. Also, the porosity can be reduced by inert ZrO_2 powder filling or with high manifold clamping pressure. However, stack tests revealed that the above improvements are not adequate to fully mitigate the problem. Therefore, alternate gasket designs were explored for achieving a desired gasket resistance, without affecting its mechanical properties and gas sealing efficiency.

Two advanced gasket designs (AG-1 and AG-2) were evaluated. In the AG-1 design the baseline gasket has been modified to disrupt the continuous migration path. The AG-2 design is basically a densified baseline gasket that reduces the available pore volume for carbonate pickup (hence a lower migration rate).

Candidate gaskets were evaluated in an out-of-cell test rig, similar to that reported in the literature [3.1]. Voltage was applied between the positive and negative electrodes; the resulting current (shunt current) was recorded as a function of time. The test duration was between 20 to 90 hours.

Figure 3.1 illustrates a significantly lower (approximately one order of magnitude) shunt current in the AG-1 design than in the baseline design. Post-test electrolyte inventory and composition also revealed no indication of electrolyte migration (see Figure 3.2) using the AG-1 design. The AG-1 gasket is now being evaluated in both a 7in. x 7in. (five-cell) bench-scale and a 24in. x 24in. short (five-cell) stack test. The 7in. x 7in. cell has a BOL inventory $\sim$10% of the 24in. x 24in. cell. Therefore, this bench-scale test can be considered an evaluation of the gasket under an accelerated migration condition. After $\sim$1400 hours, no effect of electrolyte migration was observed (see results presented in Section 5.0).

An AG-2 gasket design was also evaluated, in parallel to the AG-1 design, in out-of-cell migration testing. The migration rate was found to be from 50% to 60% of the baseline (see Figure 3.3), indicating a beneficial effect of the densification procedure in reducing migration rate.

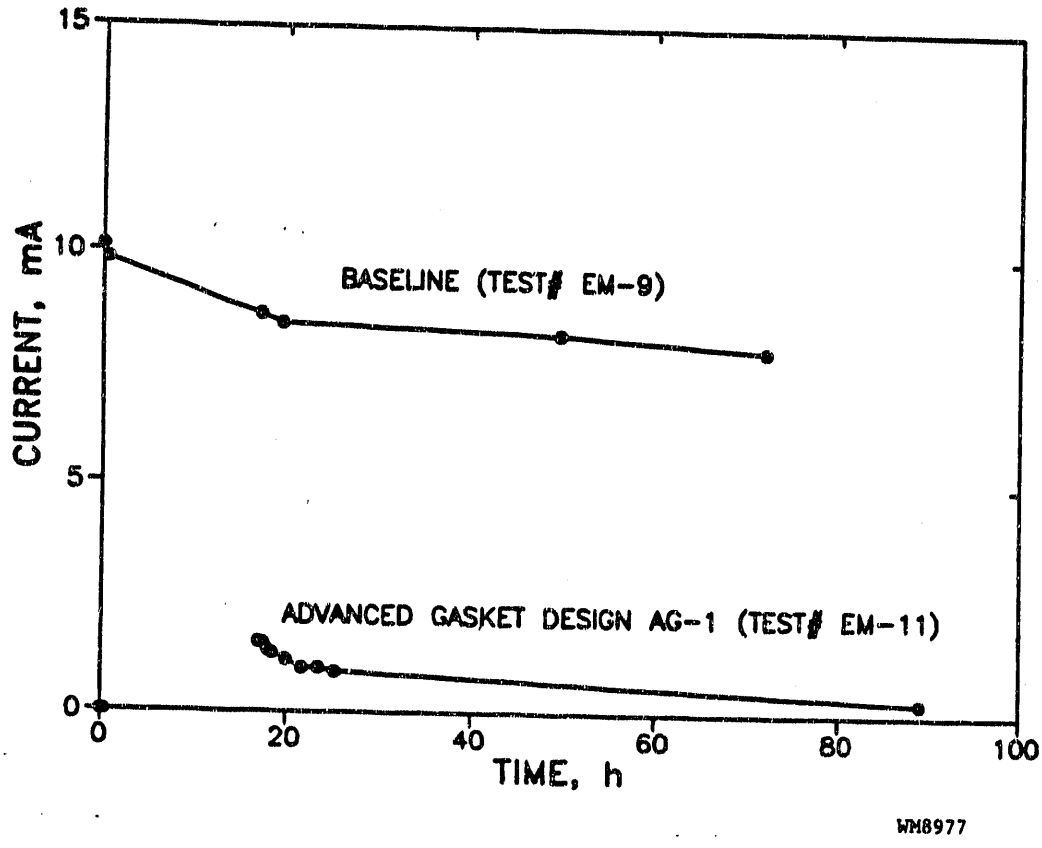

FIGURE 3.1 **ELECTROLYTE MIGRATION POTENTIAL FOR GASKETS (OCT RESULTS):**

Approximately an Order of Magnitude Improvement in Migration Rate can be Projected for the AG-1 Gasket

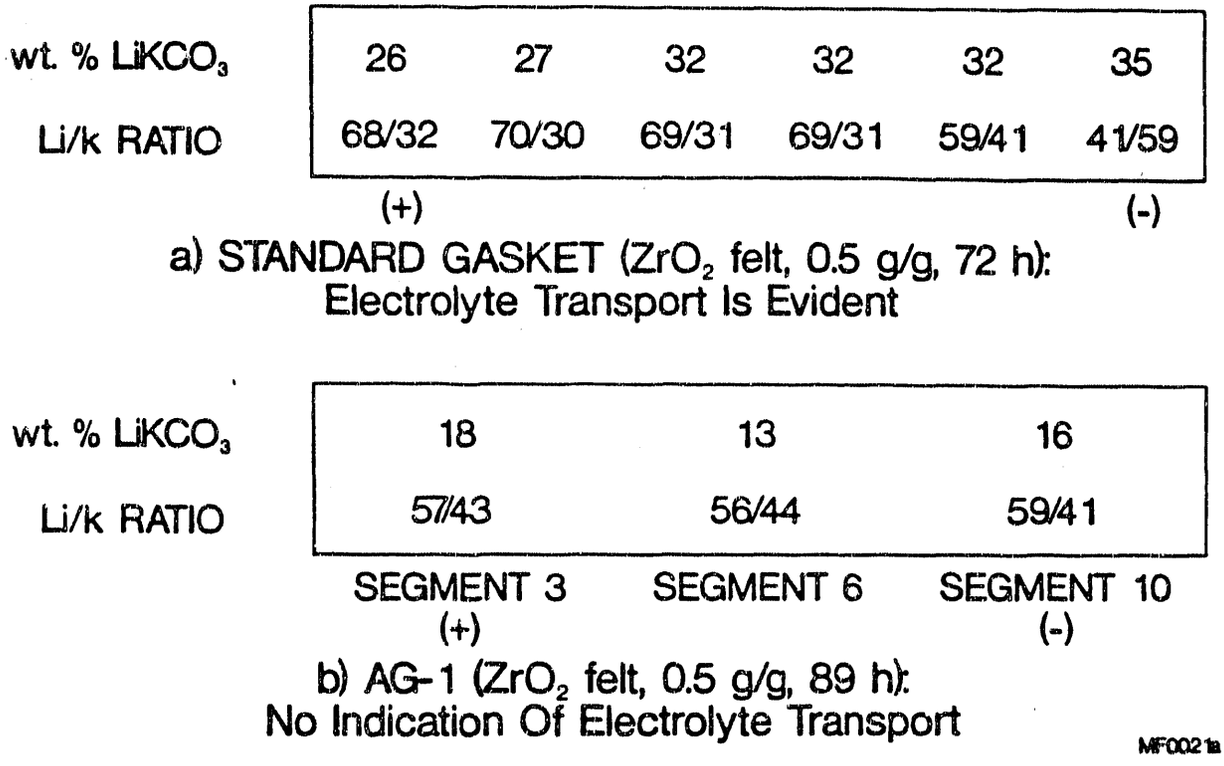

FIGURE 3.2 POST-TEST ELECTROLYTE CONCENTRATION IN GASKETS:

Significant Reduction of Electrolyte Migration
Using AG-1 Design has been Achieved

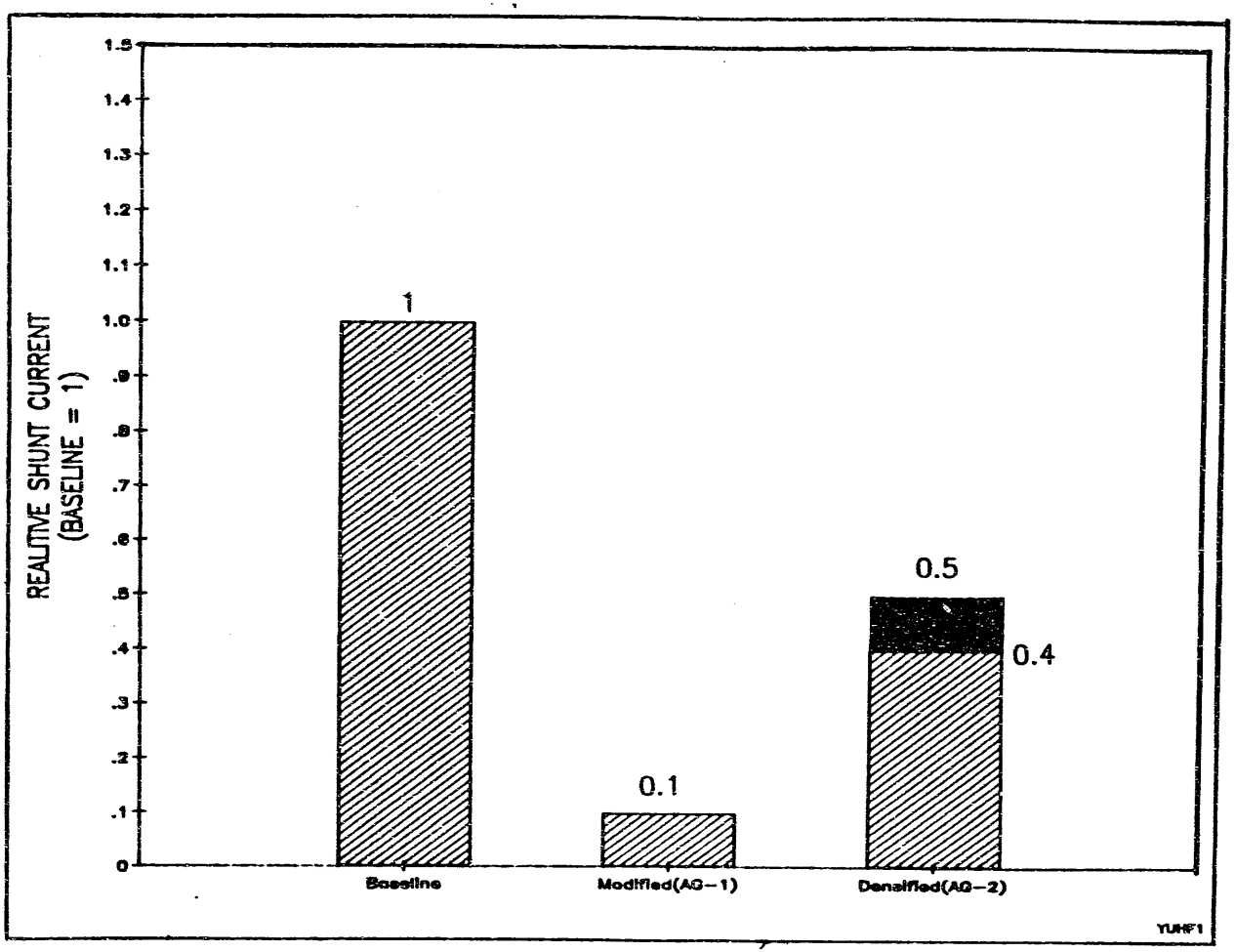

FIGURE 3.3 SHUNT CURRENT COMPARISON:

Lower Shunt Current Observed with Advanced Gasket Designs (AG-1 and AG-2)

The electrolyte redistribution model discussed in Section 4.4 was utilized to project full-size stack life, incorporating AG-1 gasket in combination with end cell inventory adjustment approach. The calculation showed that an end-cell life of 40,000 hours is a well achievable goal (see Figure 3.4).

The selected gaskets should also be able to provide an adequate manifold gas sealing, affected by the gasket mechanical properties. The candidate gaskets were first evaluated for their mechanical (compressive stress vs. strain) property. Figure 3.5 shows that these candidate gaskets have only slight compliance in use. The compliance is in the range of approximately 1 mil per 100 psi. A gasketing procedure was developed to maintain an adequate gas sealing, even with such a low gasket compliance and a thermally distorted stack surface. The sealing efficiencies for several gasket designs obtained in bench scale tests are compared in Figure 3.6. The results indicate that all candidate designs met gas sealing criteria. The criteria for manifold sealing is 0.2% leak for SRNG fuel under 15 inches of H_2O back pressure at operation. The AG-1 gasket design which provided significant reduction in migration rate also provided acceptable gas sealing. The gas sealing efficiency of this gasket was further verified in subscale out-of-cell tests. Evaluation of the design in stacks has been initiated.

3.2.2 End Cell Inventory Adjustments

According to the electrolyte redistribution model results (Section 4.4), the AG-1 or AG-2 gasket alone may not be adequate to the reduce migration rate to achieve 40,000-hour life for the end cells, with a baseline electrolyte inventory. Therefore, biased electrolyte storage in end cells may be needed. In order to increase the BOL electrolyte inventory for positive end cells to accommodate high electrolyte loss (source) and allow more room for negative end cells to receive electrolyte (sink), a thick-electrode approach together with higher or lower than normal BOL electrode fill levels were also adopted. A thick anode and cathode were fabricated, with pore structures similar to those of the normal-thickness electrodes. The electrodes were evaluated in 7in. X 7in. single cells and then verified in a 2kW 24in. X 24in. stack. The results (shown in Table 3.1) show that there is no performance penalty associated with the thick electrodes. The long-term stability of thick-electrode end cells is expected to be improved over the baselines. The evaluation of the endurance of the thick-electrode cells is in progress.

3.3 MATRIX IMPROVEMENT

The tape matrix, sandwiched between the anode and cathode, stores electrolyte and prevents direct chemical reaction of fuel and oxidant. The state-of-the-art matrix is fabricated by a tape casting method, allowing fabrication of a thin tape matrix of low mean pore size. The "green" tape, consisting of ceramic powder, organic binder, plasticizer and other organics; all the organics are burnt off during cell start-up, leaving a fine-pored ceramic powder bed to be completely filled with carbonate after electrolyte melting. The matrix should be completely filled with carbonate, and have adequate flexural strength to prevent matrix cracking; both are needed to provide adequate bubble pressure, and to prevent excessive direct combustion of fuel with oxidant.

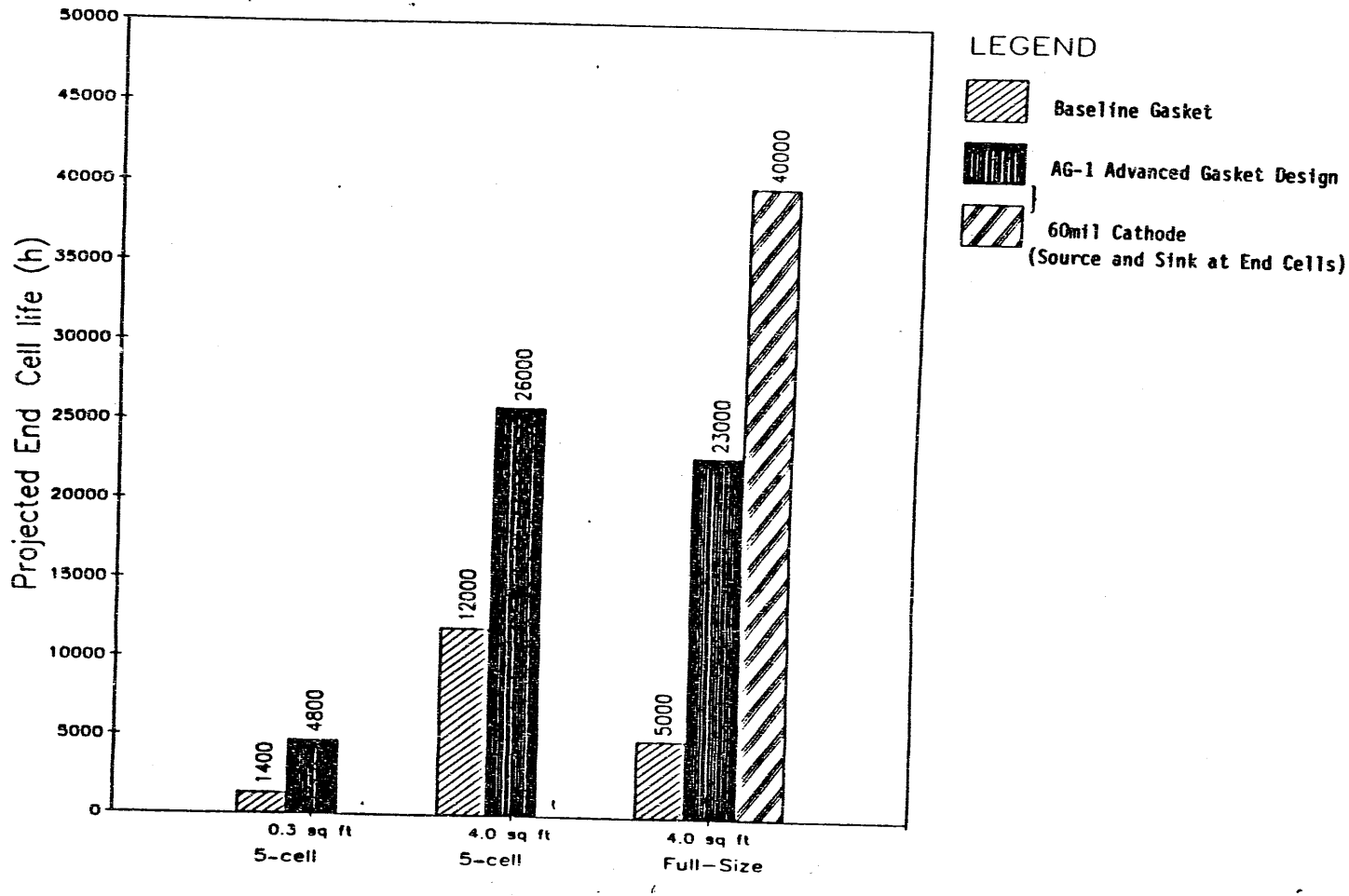

FIGURE 3.4 MODEL PROJECTED END CELL LIFE (R_W/R_C = 30, 50% ELECTRODE FILL LEVEL):

40,000-Hour Life Can Be Projected Using 50% BOL Fill Level of Electrodes, Advanced Gasket, and Source and Sink at End Cells

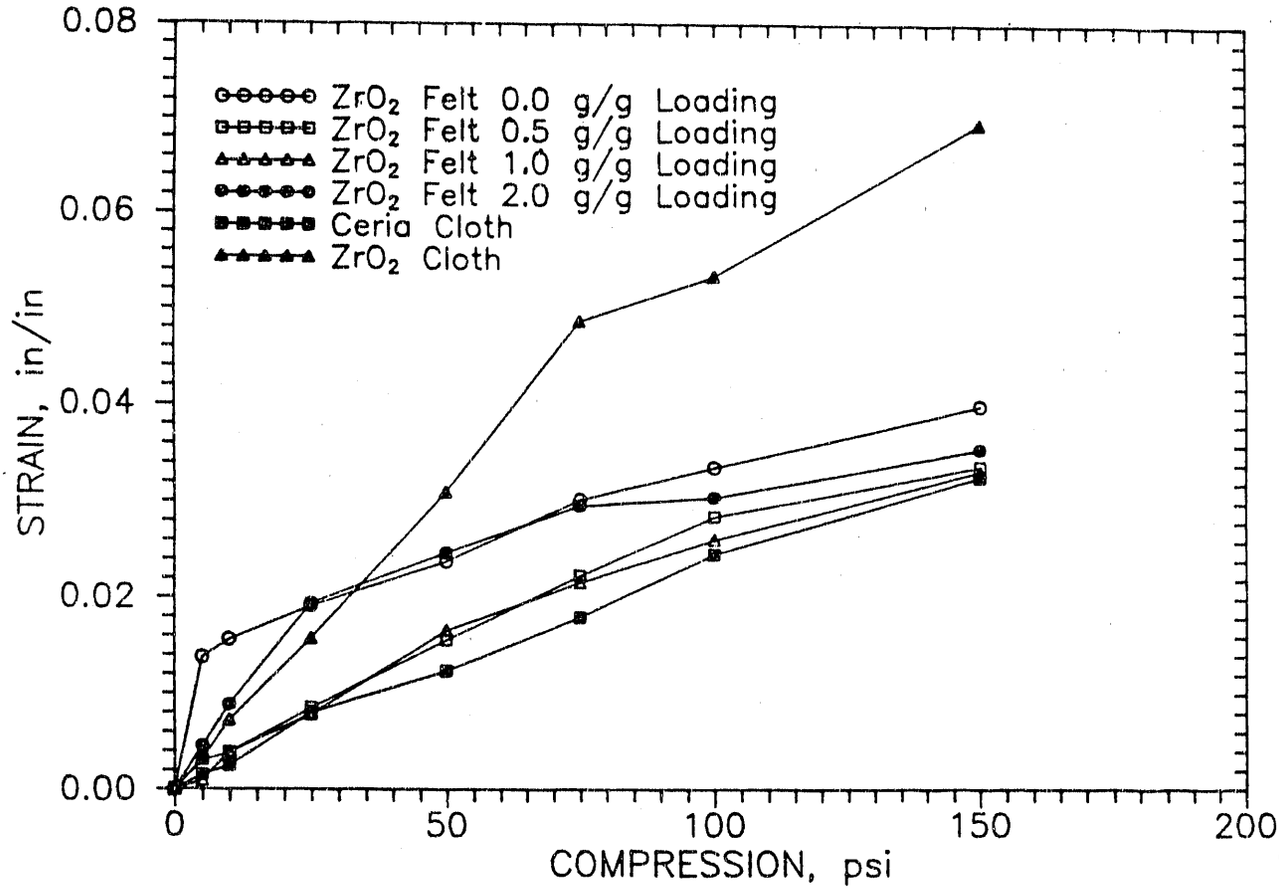

FIGURE 3.5 GASKET COMPLIANCE (STRESS-STRAIN FOR GASKETS AFTER PRE-COMPRESSION):

Lack of Gasket Compliance After Pre-Compression to 175 psi, Compliance is only ∿1 mil/100 psi

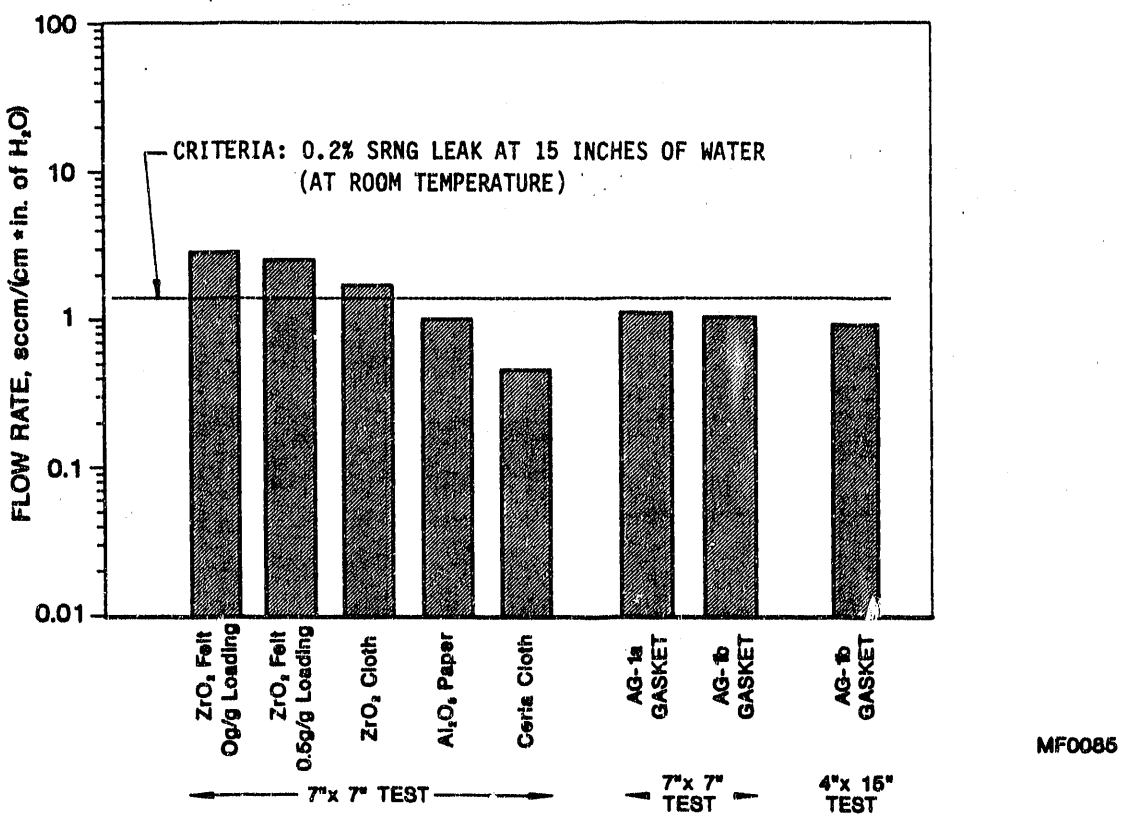

FIGURE 3.6 SEAL EFFICIENCY CHARACTERIZATION OF CANDIDATE GASKETS:

Most of the Candidate Gaskets Meet Minimal Allowable Leakage Rate, at Flat Surface and Under Uniform Compression

TABLE 3.1

EVALUATION OF INVENTORY ADJUSTMENTS APPROACH:

The End-Cell Source and Sink Design was Successfully Verified.

TEST VEHICLE		PERFORMANCE @ 160 mA/cm^2	RESISTANCE ($m\Omega \cdot cm^2$)	BOL INVENTORY %
Stack AF-2-9B	Cell #1 (Sink)	702	390	84
	Cell #2-4	725	305	100
	Cell #5 (Source)	711	460	132
Single Cell 7-256	--------	700	290	120

WM8995a

To improve gas cross-over resistance of the matrix, an improved matrix formulation providing lower temperature burn-out was developed. An out-of-cell binder burn-out experiment verified the lower temperature complete burning of this matrix, using precision carbon residue analysis. Furthermore, it was also found that the cell components (anode, cathode, CCCs) did not interfere with the burn-off of the improved matrix.

Cell testing of the improved matrix showed that a significant reduction of BOL N_2 cross-over is achieved (see Figure 3.7). The N_2 cross-over is frequently lower than 1%, well below the 2% allowable limit. The stack testing (AF-2-9B), incorporating the advanced matrix, also revealed low BOL N_2 cross-over, further verifying the benefit of using the advanced binder system (see Figure 3.8).

To evaluate the bubble pressure of the advanced matrix, a single cell was tested under a variety of high cathode gas pressures relative to the anode. Pressure difference up to 12in. H_2O was applied to the cell; the recorded cross-over results are shown in Figure 3.9. It is evident that a <1% cross-over is achievable for up to 12in. H_2O pressure difference. Some decrease of matrix bubble pressure occurred after cell thermal cycles, indicating a need to further improve its flexural strength. A strengthening method, such as the use of ceramic fibers, is expected to produce a more durable composite material than the baseline matrix. Its usefulness will be evaluated in the future.

3.4 OHMIC RESISTANCE REDUCTION

High and increasing cell ohmic loss can limit carbonate fuel cell endurance. Cell ohmic resistance is mainly attributed to tape matrix, oxide formed at the contact (current transmitting) area, and poor contact due to component warpage or non-uniform pressure distribution. Nevertheless, there is still no clear understanding of the resistance increase mechanisms and the relative contribution of the various resistance-contributing elements described above. In this effort, an out-of-cell testing facility for simultaneous corrosion and ohmic resistance measurements was designed. Various cell components (electrode, matrix, CCC, bipolar plate) were laminated together into a miniature cell package where each of the resistance contributions were measured using an AC impedance technique (see Figure 3.10). The tests were carried out at 650°C in the presence of Li/K eutectic melt under an ERC system oxidant atmosphere. The objectives of this study were to determine major resistance-contributing elements and to evaluate several cathode-side current collector designs in terms of ohmic resistance contributions. The results are also reported in Reference 3.2.

Several resistance experiments were carried out with 310S and 316L baseline current collector designs. Figure 3.11 shows the range of the ohmic resistance measured between CCC and matrix. This resistance value includes resistance attributions of cathode as well as the oxide formed at cathode-CCC interface. The resistance was found to vary between 50 to 250 $m\Omega\text{-}cm^2$. 316L baseline CCC had an initially low BOL resistance ($\sim$50 $m\Omega\text{-}cm^2$) but increased over time to $\sim$160 $m\Omega\text{-}cm^2$ after 1300 hours. The 310S baseline CCC had an initially higher resistance ($\sim$130 $m\Omega\text{-}cm^2$) but gradually increased to 200 $m\Omega\text{-}cm^2$ after 2150 hours. In order to discern the relative

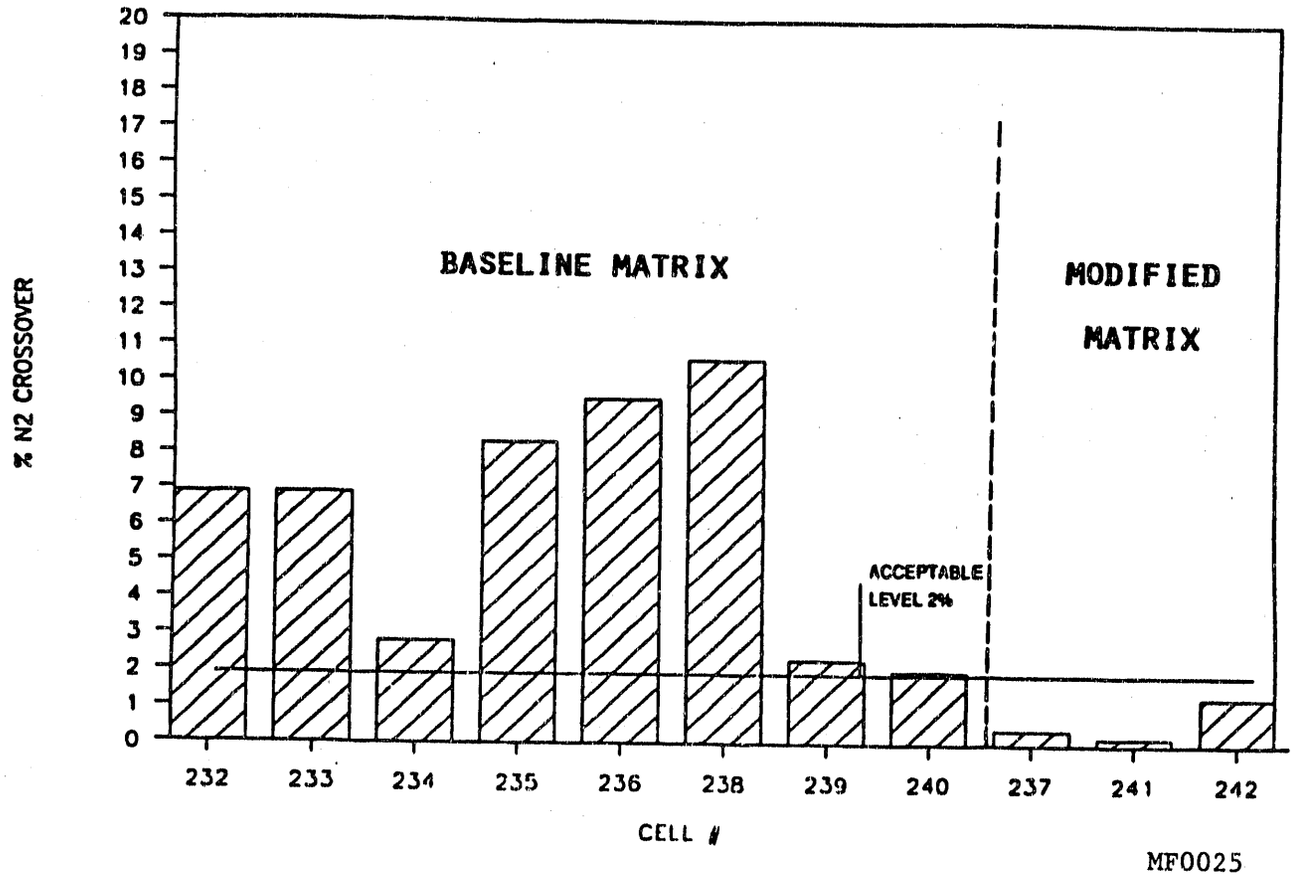

FIGURE 3.7 CHARACTERIZATION OF MODIFIED MATRIX IN SINGLE CELLS:

Low BOL Gas Cross-Over (<1%) is Achieved with Modified Matrix

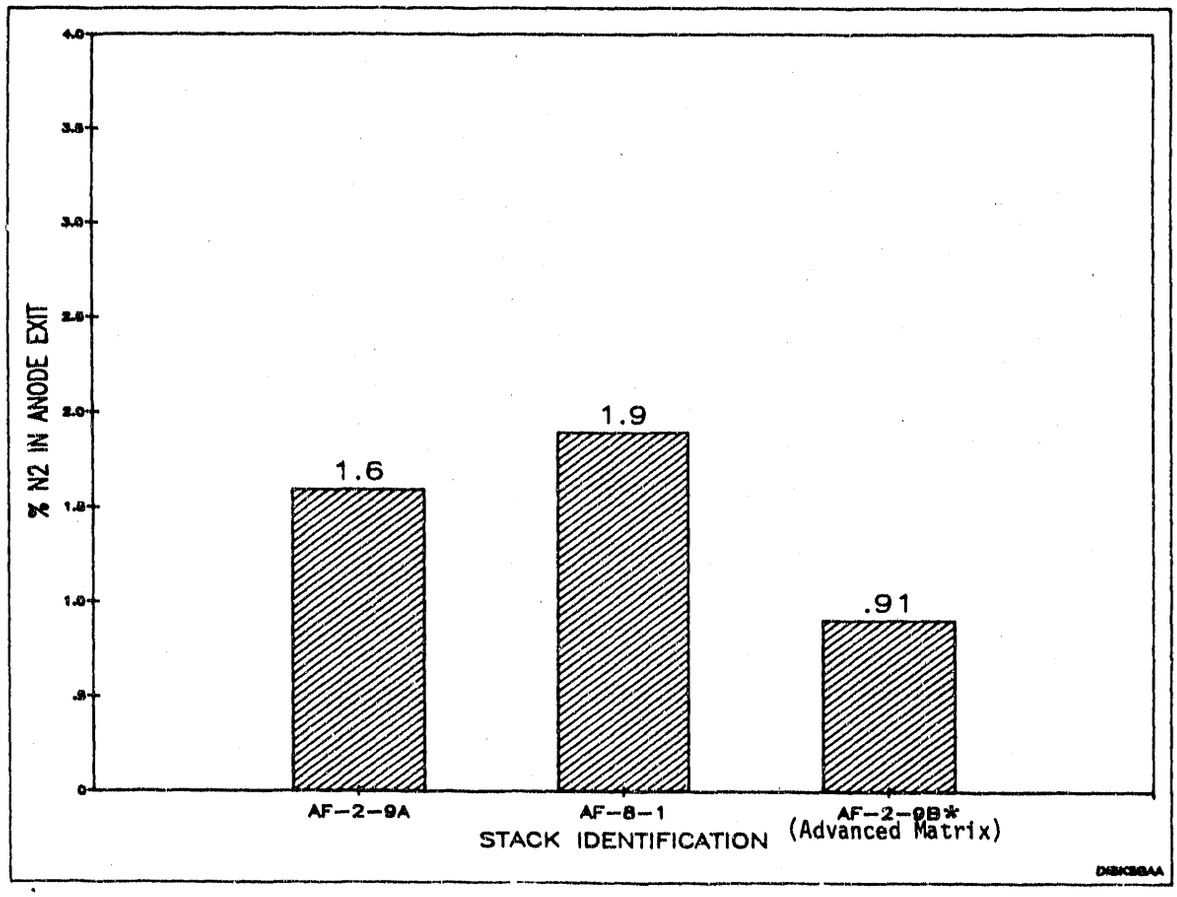

FIGURE 3.8 STACK EVALUATION OF MODIFIED MATRIX:

Use of an Improved Matrix Resulted in Significant Reduction of Reactants Cross-Leak

* Represents Cost-Share Stack

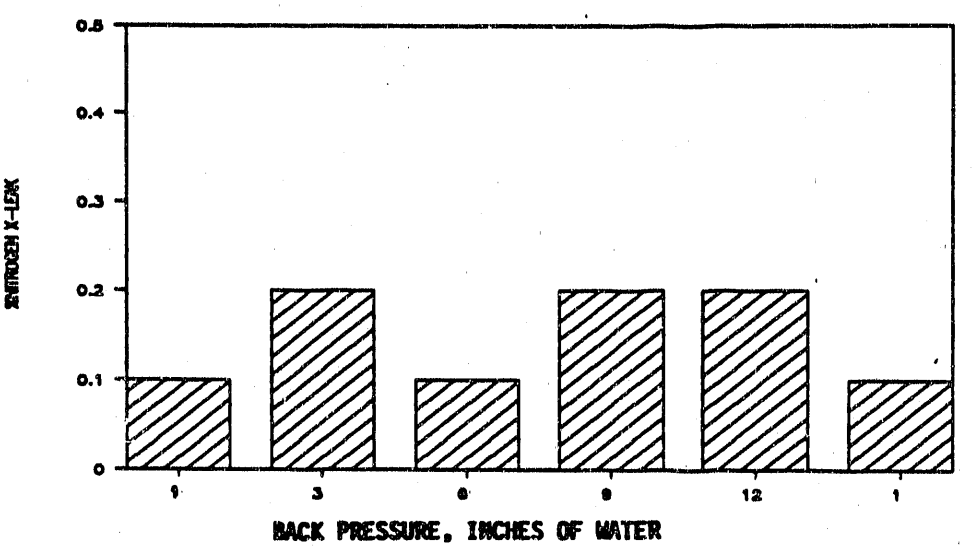

FIGURE 3.9 HIGH BACK PRESSURE TESTS (CELL 258):

Cell <1% Crossover with 12 Inches of Water Backpressure Demonstrated

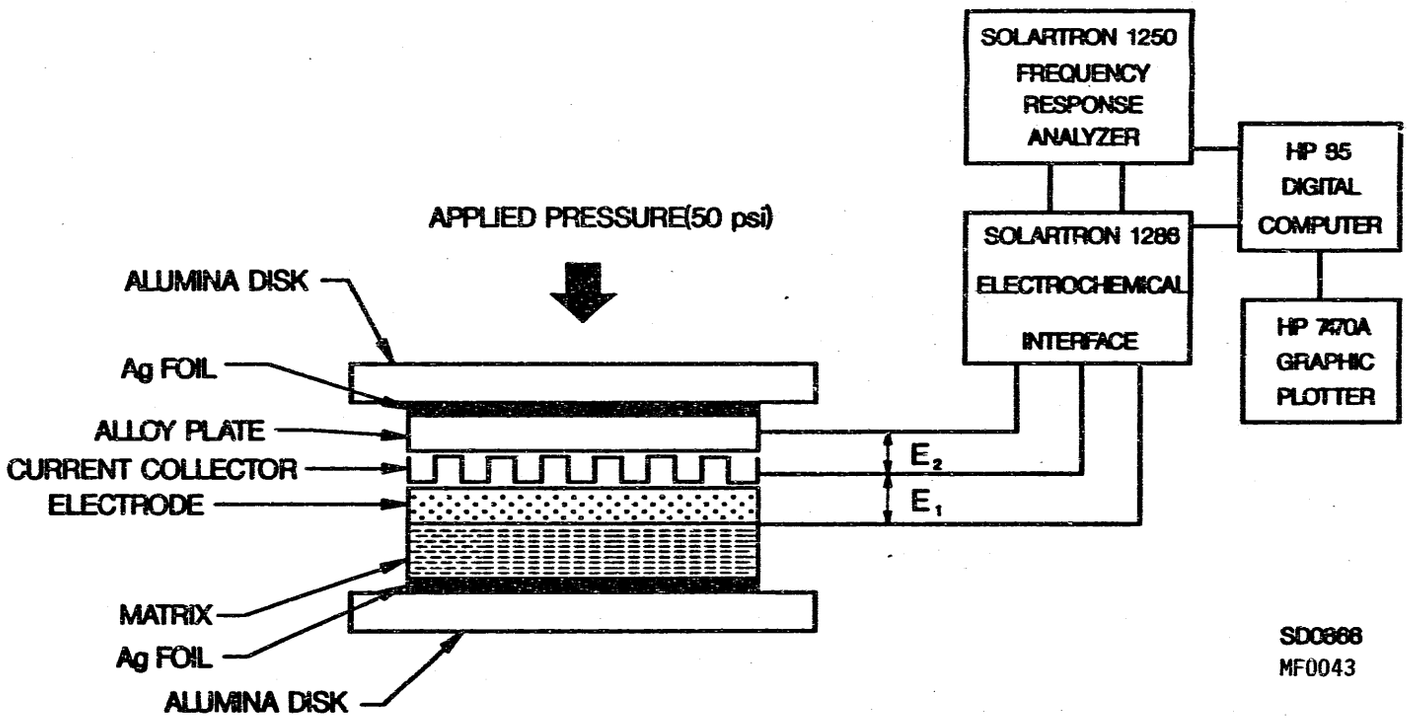

FIGURE 3.10 SCHEMATIC DIAGRAM OF OHMIC RESISTANCE EXPERIMENTAL FACILITY:

Simultaneous Hot Corrosion/Ohmic Resistance Measurement Can Be Performed

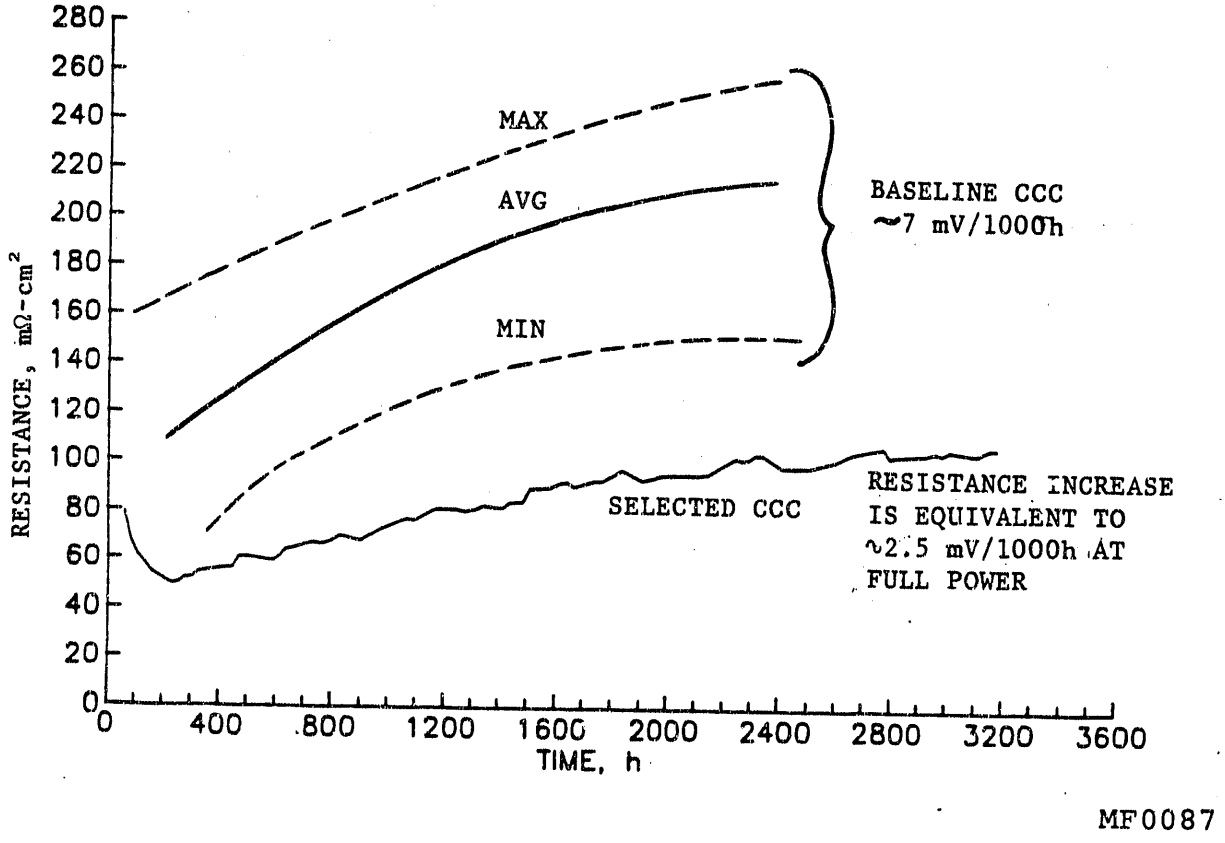

FIGURE 3.11 RESISTANCE INCREASE WITH TIME (OCT):

Cathode CCC to Cathode Contact Resistance Appears to be Dependent on Choice of Geometry

resistance contribution by cathode and oxide, a test with a silver (Ag) current collector was performed. The silver is much more stable than a stainless steel current collector; therefore, no resistance contribution due to oxide scale is included in the measurement. The resistance of NiO cathode could then be measured directly. It was found that the ohmic resistance of the baseline NiO cathode was <10 $m\Omega\text{-}cm^2$, a small fraction of the total cathode-side resistance. Therefore, the major contributor is the oxide scale formed at the CCC-cathode interface. The 310S materials appears to cause a higher beginning-of-life (BOL) resistance, likely due to its more resistive (although thinner) oxide formation; a more corrosion resistant material (e.g., 310S) in general forms a more resistive surface oxide. Although 316L is not as corrosion resistant as 310S, its oxide conductivity is better, causing a somewhat lower oxide ohmic loss.

The ohmic resistance attributed to the CCC-bipolar plate interface was found to be small (<10 $m\Omega\text{-}cm^2$) and stable over 2500 hours. This suggests that a good metal-metal contact is achieved where accessibility of carbonate to the contact area for corrosion attack is restricted. Therefore, the corrosion of the metal to metal contact area is expected to be minimal.

The resistance of the matrix material was also measured. The standard matrix ($\sim$20 mil) was found to contribute $\sim 200 m\Omega\text{-}cm^2$ resistivity. Based on the above information, it can be concluded that the major cell resistance contributor is the tape matrix, followed by the oxide scale formed at the cathode-CCC interface. The NiO cathode and the CCC-bipolar plate contact together contribute to $<20 m\Omega\text{-}cm^2$ resistivity. The resistance breakdown in ERC's carbonate fuel cell is shown in Figure 3.12. Future efforts will be concentrated on reducing matrix and oxide resistivity.

Matrix resistivity can be reduced by using an alternative, more conductive electrolyte (e.g., Li/Na carbonate). It is projected that a $40 m\Omega\text{-}cm^2$ reduction in ohmic resistance can be achieved using Li/Na eutectic melt. Further reduction of ohmic resistance is also likely, using the advanced matrix, discussed in Section 3.3. The above two approaches to reduce matrix ohmic loss have been verified in out-of-cell testing (for Li/Na case) and in stack (DOE-8 and AF-2-9B) testing (for advanced matrix).

The selected CCC (one-piece design) was also evaluated in the resistance experimental facility. The cathode side resistance (shown in Figure 3.11) was found to be lower and more stable than the baseline, equal to a $40 m\Omega\text{-}cm^2$ reduction in the BOL resistance value. Although a 2.5mV/1000h performance decay at full power may be projected from the resistance lifegraph data, it appears that a lower increase rate may be likely in a long-term test, due to a parabolic oxide growth rate. Note the slow decreasing of the resistance increase rate for the selected CCC case (in Figure 3.11), indicating a likely lower rate of increase than 2.5mV/1000h in the long run.

An advanced CCC (also one-piece but more compliant than the selected CCC) was also evaluated and showed an even lower resistance than the selected CCC. An additional $30 m\Omega\text{-}cm^2$ reduction may be achieved using this design. This CCC needs to be further evaluated in longer-term tests.

In conclusion, the BOL resistance of 320 $m\Omega\text{-}cm^2$ with baseline CCC design can be reduced by 150 $m\Omega\text{-}cm^2$, using all the approaches described above (see Figure 3.12). However, it should be cautioned that the analysis is based on the assumption of uniform component contact, which may not be entirely true for a large area stack. Component fabrication variation and thermal distortion can contribute to poor contact and higher ohmic loss than estimated here. Therefore, a good component-to-component contact should be maintained through proper design and fabrication of full-area stack components.

The results of this study are only valid with a NiO cathode. An alternate cathode material (i.e., $LiFeO_2$) may contribute to a much higher contact ohmic resistance, due to its own high specific resistivity or alteration of oxide scale structure formed at the cathode-CCC interface.

Improving CCC corrosion resistance without introducing high oxide ohmic loss is desirable for low and stable resistance. Lower corrosion resistance also reduces corrosion and creepage electrolyte losses, thereby reducing matrix resistance increase. Surface modifications are the recommended approach to achieve the goal. Several surface modification schemes will be evaluated in the future.

3.5 CATHODE STABILITY IMPROVEMENT

The dissolution of NiO into carbonate and subsequent deposition of metallic Ni in tape matrix have been identified as a major life-limiting factor. Although a loss of 30-40% of the baseline NiO cathode was projected to occur after 40,000-hour stack operation (with a cathode gas containing $\sim$13% CO_2), long-term cell testing (7000 to 10,000 hours) at ERC showed that such a loss is tolerable from the cathode performance point of view. However, the cell internal shorting caused by the deposited metallic Ni may shorten the projected cell life. Therefore, the major target here is to develop methods to increase the time before shorting.

One recommended approach is to change the melt chemistry to reduce the NiO dissolution rate, achievable by using additives or alternate electrolyte (e.g., Li/Na). Their primary mechanism is to increase melt basicity to reduce NiO acidic solubility. Another approach is to increase the matrix thickness for increasing Ni^{++} diffusion path (hence lowering Ni^{++} transport rate) and for shifting Ni deposition zone away from the anode. Both approaches were evaluated in 7in. X 7in. single-cell tests. The results are summarized in Table 3.2. It can be concluded that about a two-fold improvement in the time-to-short can be achieved using a 60% thicker matrix (than the baseline) and additive $CaCO_3$. $CaCO_3$ has a higher solubility in carbonate melt than the previously evaluated additives. Therefore, a larger quantity of the additive $CaCO_3$ can be included in the melt for long-term suppressing of Ni solubility. However, it should be cautioned that an increase of matrix ionic loss ($\sim$20 mV at 160 mA/cm^2) will result from such a thicker matrix.

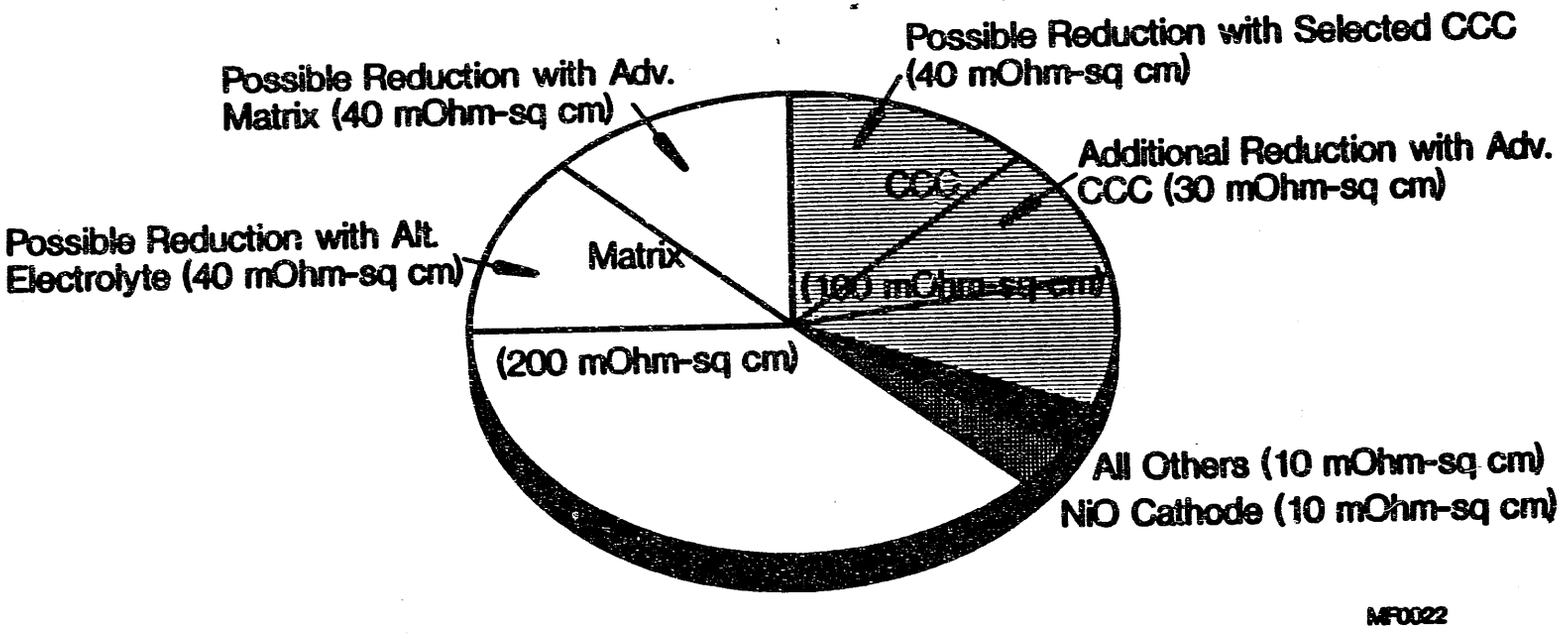

FIGURE 3.12 RESISTANCE BREAKDOWN OF ERC'S CFC CELL:

The Standard Design Projects to a BOL Resistance of 320 mOhm-sq cm. Use of Alternate Matrix, Electrolyte and CCC may Reduce Cell Resistance by 150 mOhm-sq cm

TABLE 3.2

IMPROVEMENT IN TIME-TO-SHORT AT ACCELERATED CONDITIONS:

About Two-Fold Improvement in Time-to-Short Has Been Observed
Using a 60% Thicker Matrix and an Alternate Additive

CELL NO.	ADDITIVE	MATRIX THICKNESS RELATIVE TO STANDARD	INCREASE IN TIME TO SHORT (RELATIVE TO BASELINE)
7-234	Standard	1.0	1.00
7-210	Standard	1.30	1.14
7-237	MgO	1.20	1.28
7-242	$CaCO_3$	1.60	1.90

WM8979a

3.6 CONCLUSIONS

Four technology areas were selected for a concentrated research effort to improve carbonate fuel cell performance and endurance. Significant progress was achieved in all these areas. In terms of electrolyte migration mitigation, a gasket design (AG-1) was identified to reduce theelectrolyte migration rate by an order of magnitude, as well as to meet the seal efficiency goal. The gasket design as well as a parallel end-cell electrolyte inventory adjustment approach is expected to provide adequate electrolyte management to ensure a 40,000-hour useful life for a full-size stack. In terms of decreasing matrix gas cross-over, an improved matrix that shows a 50% improvement in matrix gas seal efficiency over the baseline matrix was successfully developed. In terms of cathode stability improvement, an approach for achieving a two-fold improvement has been demonstrated in single-cell accelerated tests. The major ohmic resistance contributors were identified. The selected CCC design was shown to contribute to a lower and more stable ohmic resistance than the baseline CCC.

These improvements together project better performance, higher fuel utilization, longer stack life and provide a sound basis for a full-size stack design for demonstration.

3.7 REFERENCES

[3.1] H.R. Kunz, "Transport of Electrolyte in Molten Carbonate Fuel Cells", J. Electrochem. Soc., 134(1), 105, 1987.

[3.2] C.Y. Yuh, "Hot Corrosion and Oxide Ohmic Resistivity in CFC Cathode Environment", Proc. Symp. Molten Carbonate Fuel Cell Technology, PV 90-16, The Electrochemical Society, NJ, 368, 1990.

4.0 CARBONATE FUEL CELL STACK DESIGN DEVELOPMENT

ERC has selected a fuel-flexible internal reforming carbonate fuel cell stack design to allow operation on both pipeline natural gas and various coal-gases using a common stack design. The basic design includes external manifolding, rectangular cell size, and internal reforming. The initial design was selected based on prior test experience and input from mechanistic modeling. The stack design was subsequently updated through iterative stack tests. The 2ft X 2ft size stacks were used for the stack design evaluation testing in this program.

The thermo-mechanical behavior of the carbonate fuel cell stack was modeled and the impact of key design variables was analyzed. The results were utilized to select a mechanically sound stack design. The electrolyte loss mechanisms were investigated and quantified. An electrolyte management strategy was recommended based on the model.

As a final product, the components design as well as the assembly approach for the stack scale-up were recommended; and the areas for further improvement, which would allow attainment of performance and cost goals, were identified.

4.1 INTRODUCTION

A carbonate fuel cell (CFC) stack is the primary power producing component in a power plant system. Its performance and longevity can have a significant impact on the overall power plant efficiency and economics. In this stack development effort, the carbonate fuel cell design was developed with input from prior experience, mathematical modeling, and iterative test evaluations.

The main emphasis of stack design was meeting performance, endurance and cost goals. The power plant system study results, presented in Section 9.0, provided a guideline in setting up these goals, as listed in Table 4.1. ERC has selected a fuel-flexible stack design approach which allows operation on both natural gas and various types of coal-gases without requiring design changes. This feature lends itself to cost effective stacks and many highly sought-after system benefits.

The stack requirements were identified based on prior experience. The conceptual design was defined, and the key component detailed design was selected and verified in short stack tests. The short stack test results are discussed in Section 5.0. Several stack models were also developed to aid the stack design development effort. The stack mechanical behavior was analyzed to select the most suitable design. The electrolyte loss mechanisms were investigated and modeled. This was used to select the electrolyte management strategy. The component designs as well as the models were updated with input from test results. Details of these activities are discussed next.

TABLE 4.1

REFERENCE OPERATING CONDITIONS FOR DUAL-FUEL STACKS:

Performance Achievable in Near Term was Assumed

	COAL SYSTEM O_2-Blown Fluidized Bed Gasifier	**NATURAL GAS SYSTEM** MW-Class Simplified
Fuel:	20% H_2, 27% CO, 11% CO_2, 37% H_2O, 4% CH_4, 1% N_2, 85% Utilization	67% H_2O, 33% CH_4
Oxidant:	9% O_2, 17% CO_2, 17% H_2, 57% N_2 40% Utilization	16% H_2O, 16% CO_2, 12% O_2 Bal. N_2
Current Density (mA/cm^2)	150-200	140
Average Temperature (°C)	650	650
Temperature Gradient (°C) (*Gas Phase*)	110	90
Operating Pressure	Atmospheric	Atmospheric
Cell Voltage	~700 mV at Design Point (190 mA/cm^2)	740 mV (140 mA/cm^2)
Power Density (W/cm^2)	0.133	0.096
Life (h)	40,000	25,000 - 40,000
Contaminants	H_2S: <1 ppmv; HCl: <0.1 ppmv; NH_3: <0.5% with fuel	H_2S: <1 ppmv

4.2 MAJOR DESIGN FEATURES

Stack features were selected first, as listed in Table 4.2. These features were selected based on performance, fabrication, cost, and system considerations.

4.2.1 Cell Size

Cell sizes of 4 to 16 ft^2 were considered and evaluated based on FOB cost and manufacturability. The cost details are discussed in Section 8.0. The cost associated with shipping and field installation was not considered in the cost analysis. It appears that there is not much economic incentive to increase the cell size much beyond the presently used $4ft^2$ size at a manufacturing rate of 400 MW/yr, a projected manufacturing rate for carbonate fuel cell market entry.

Use of substantially larger size cells, such as the $16ft^2$ size, provides a small, $\sim$5% cost benefit at production volumes approaching 1600 MW/yr and lowers the effect of electrolyte migration. But it also requires a substantial additional investment in equipment and adds a technology risk that can only be minimized with additional research efforts.

In consideration of the factors discussed above, the 2ft X 2ft size stack was selected as the initial design for performing component development activities in this task. It was concluded that should the need arise to increase the cell area to meet stack pallet engineering requirements, then the component length could be increased (e.g., to 3 ft). Thus, most of the existing component manufacturing equipment can be utilized. This would have minimum impact on the component designs developed in this task.

4.2.2 Flow Configuration, Cell Shape, and Manifolding

Rectangular shape, cross-flow, and external manifolding were selected for the component designs. The rectangular shape was selected mainly for its fabrication simplicity. Cross-flow and external manifolding were selected mainly because they allow simplicity in the design and fabrication of bipolar plate, matrix, and manifold. The counter and Co-flow configurations require development of complicated and high-cost bipolar plate designs. Although electrolyte migration is a concern with the external manifold design, results presented in Section 3.0 show that promising approaches are available which can reduce electrolyte migration in an externally manifolded stack to a reasonably low rate to assure a 40,000-hour life.

4.2.3 Fuel Flexibility and Operating Pressure

ERC has selected the fuel-flexible carbonate fuel cell stack design and atmospheric pressure operation for its CGCFC system application. A fuel-flexible stack will improve power plant availability, accelerate commercial entry through natural gas test experience and reduce stack cost through volume production. In terms of operating pressure, pressurized operation offers no economic gain and no energy conversion efficiency advantage. Results presented in Section 9.0 show that, even

TABLE 4.2

CONCEPTUAL FEATURES OF ERC CARBONATE FUEL CELL STACKS:

A Fuel Flexible Stack Design Feature has been Selected

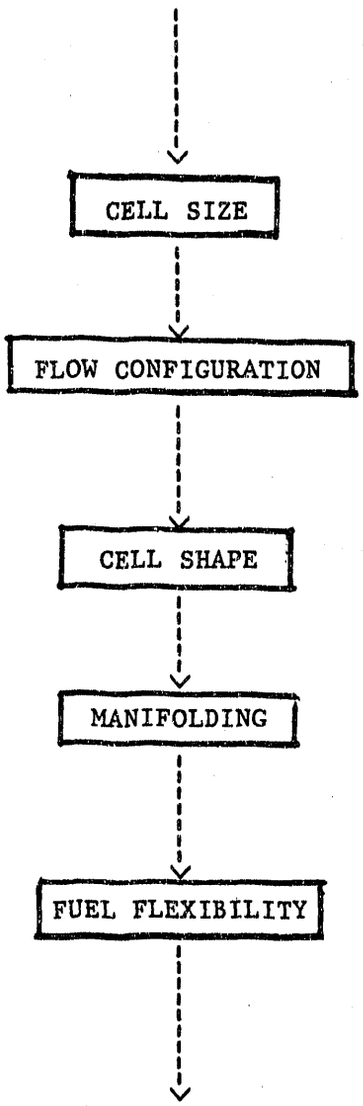

	PARAMETERS AFFECTING THE CHOICE	SELECTED FEATURES
CELL SIZE	FABRICABILITY, MARKET-SIZE COST	4 FT^2
FLOW CONFIGURATION	SIMPLICITY IN MANIFOLDING, BIPOLAR PLATE	CROSS-FLOW
CELL SHAPE	PRESSURE BALANCE, PERFORMANCE	RECTANGULAR
MANIFOLDING	SIMPLICITY IN MANIFOLD DESIGN, BIPOLAR PLATE & MATRIX DESIGN	EXTERNAL
FUEL FLEXIBILITY	FLEXIBILITY TO OPERATE ON COAL GASES AS WELL AS OTHER FUELS	IR

with a technology breakthrough leading to a constant fuel cell life (no pressure penalty on life), the near atmospheric operation (i.e., 3 atm) promises only a slight COE reduction ($\sim$1%), which may be within the accuracy of the estimating methods of the study. ERC recommended that stack design and testing be based on atmospheric pressure.

4.3 COMPONENT DESIGN DEVELOPMENT

The selected stack design is an improvement over ERC's previous short stack design. In this section, the stack design results, together with the associated modeling information, are described.

The stack components are categorized into repeating and non-repeating components. The repeating components include anode, cathode, matrix, and bipolar plate. These are the actual power generating components. The non-repeating components include end plate, stack compression system, manifolding system, piping, instrumentation, busbar, and insulation. These are the auxiliary components for gas sealing, load distribution, and thermal insulation. Figure 4.1 represents a schematic of ERC's stack components and their assembly. The development of each component will be discussed in the following sections.

4.3.1 Repeating Components

A schematic diagram of the repeating components and their assembly is shown in Figure 4.2. The design was already verified in short stack testing. The selected anode uses an Ni-Al alloy. Aluminum content and anode porosity were determined based on the improved high-temperature creep strength. The strengthening mechanism is suggested to be due to a dispersed $LiAlO_2$ phase in the bulk Ni phase. A 5,000-hour $4ft^2$ stack test (AF-5-1) did not reveal noticeable creep (<1%) in ERC's Ni-Al anode, indicating its satisfactory high-temperature strength for CFC application. However, due to its relatively high cost, thickness reduction for ultimate power plant application is contemplated. No risk in terms of its strength, electrochemical performance or fabrication is expected by reducing anode thickness.

The cathode is porous NiO, in-situ oxidized and lithiated from a porous metallic Ni structure. Porous NiO cathode is so far the best cathode material in terms of its electrochemical performance and cost. However, cathode dissolution and subsequent deposition in the matrix may cause electrical shorting and shorten stack life, particularly under pressurized conditions. Development work to alleviate this problem, by reducing the NiO dissolution rate or by using alternate cathode materials, is under way; some results are discussed in Section 3.0. Another area that needs further development effort for the cathode is its intrinsic low strength, particularly as porous Ni metal before in-situ oxidation during stack start-up. Even after in-situ oxidation to form NiO, this component is weak mainly due to its high porosity ($\sim$60%). A 5,000-hour stack testing showed cathode creep of more than 2 mils. Its low strength can be further aggravated by the loss of NiO material due to dissolution. Reducing NiO dissolution can partially slow its decrease in strength. Using reinforcement or alternate higher strength cathode materials are the approaches that require development effort.

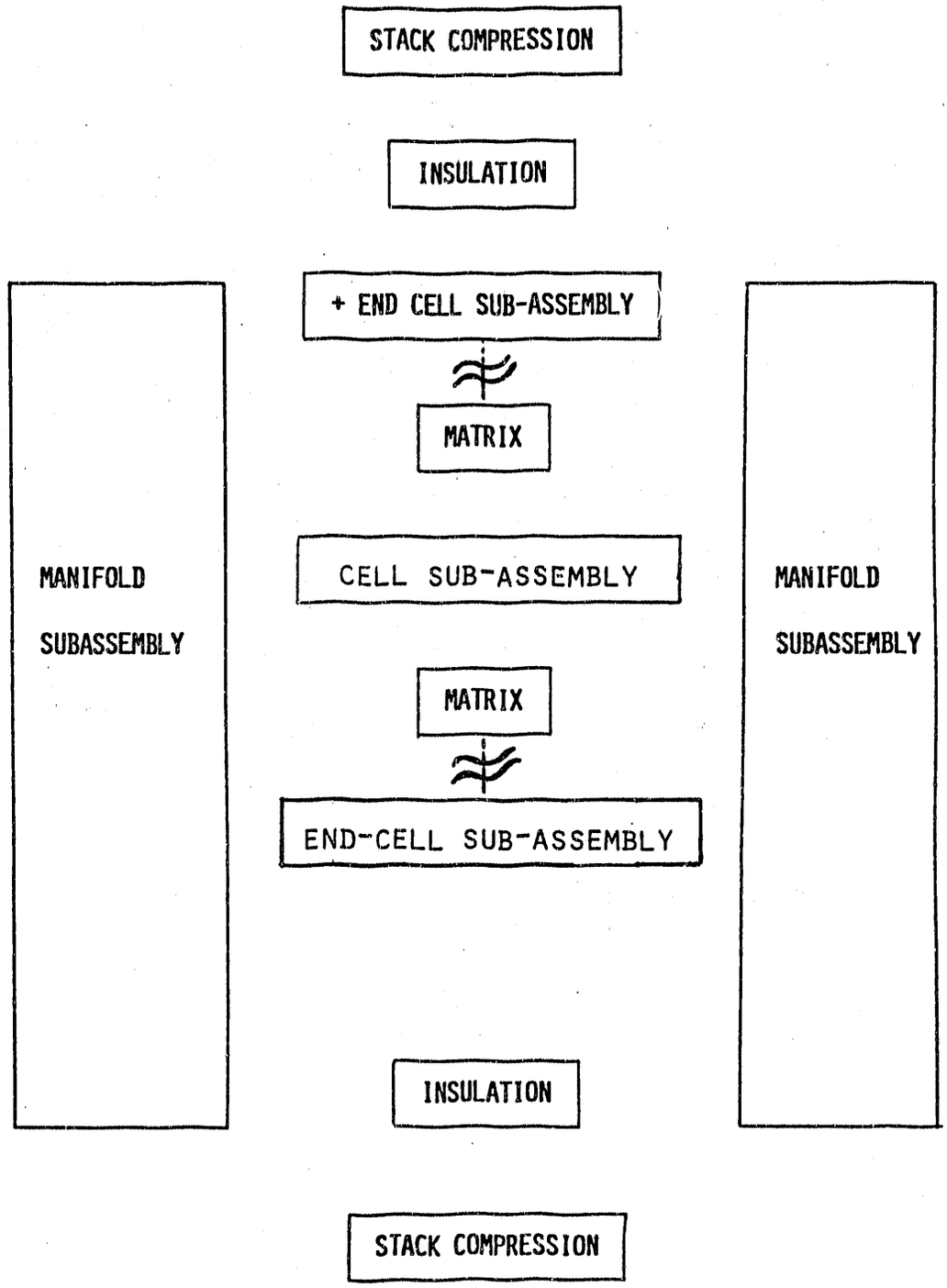

FIGURE 4.1 SCHEMATIC OF STACK ASSEMBLY:

The Stack Components and Their Assembly are Identified

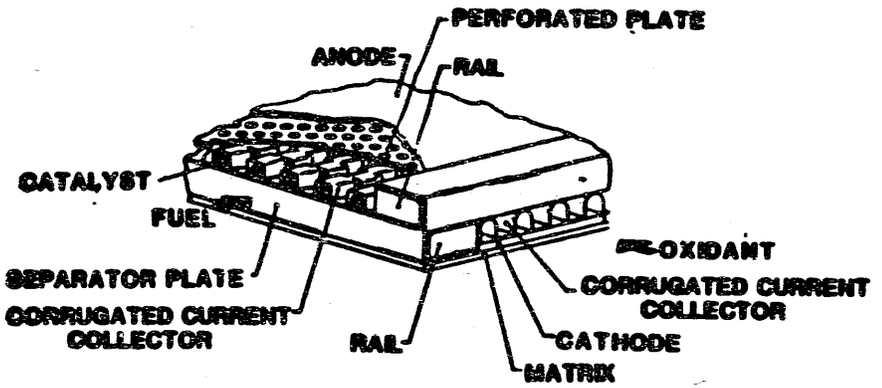

a. SINGLE CELL

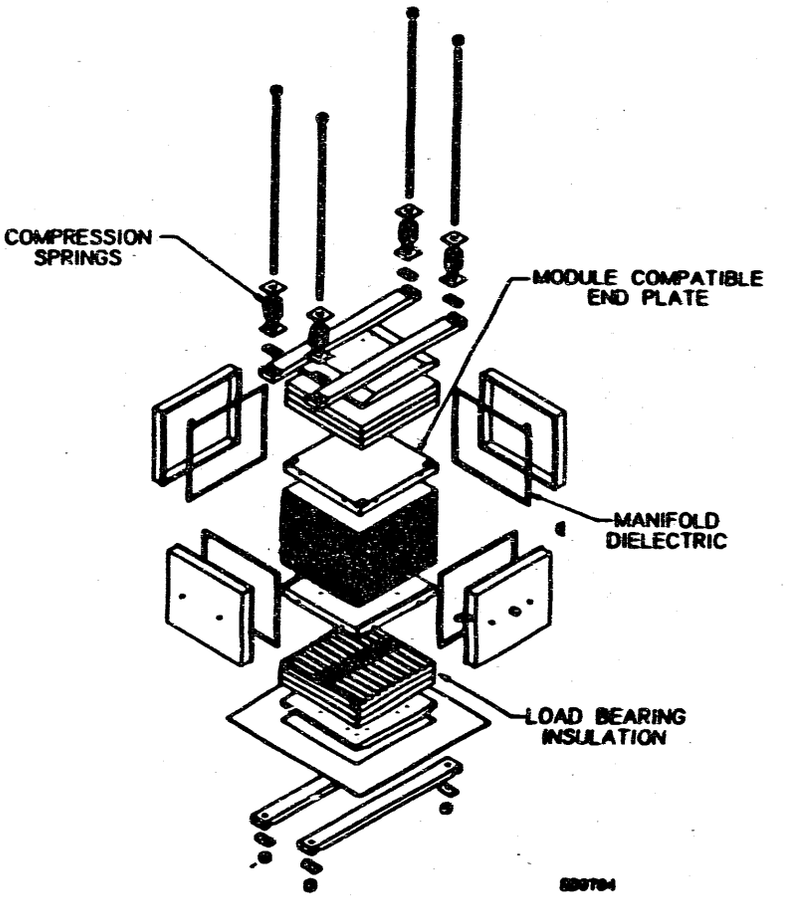

b. FULL SIZE STACK

FIGURE 4.2 SCHEMATIC DIAGRAMS OF SELECTED REPRATING COMPONENT AND FULL SIZE STACK:

The Basic Stack Components are Defined; Performance Verified

Electrolyte matrix fabricated by a tape-casting process is selected. Fine γ-$LiAlO_2$ powder is used as the main electrolyte support material. Reinforcements are also used to improve its flexural strength. Stack test results identified the need for improvement in the baseline matrix with respect to gas-sealing efficiency and loss of gas-sealing efficiency with thermal cycle.

The selected electrolyte composition for near-term stack application is a $(62Li/38K)CO_3$ eutectic mixture, with an additive to suppress NiO dissolution. This electrolyte composition was used in stack and single-cell testing for up to ~5,000 and ~10,000 hours, respectively. Some electrolyte composition changes were observed due to corrosion, creepage losses, and migration, although no stack failure can be attributed to this. Selected approaches (discussed in Section 4.4) to reduce corrosion and creepage losses and migration effects will help maintain an EOL electrolyte composition that does not deviate significantly from the BOL composition. Alternate electrolyte and additives were also evaluated; the results are discussed in Section 3.0. Biased electrolyte fill levels are selected for end cells to lessen the effect of electrolyte migration. Additional discussions are presented later.

Supported Ni catalyst was selected for internal reforming. A packed-bed loading approach is selected for simplicity and economics. Flow maldistribution due to non-uniform catalyst loading can be reduced by selecting proper loading methods. ERC has evaluated both DIR (direct internal reforming) and IIR (indirect internal reforming) concepts for its fuel-flexible stack operation. The DIR concept has catalyst loaded inside the anode chamber, right next to the anode, whereas the IIR concept requires a separate reforming unit (RU). Theoretically, higher efficiency is attainable in the DIR design as compared with the IIR design, because of a better heat and mass transfer. The drawback of the DIR is its shortened IR catalyst life (<10,000 hours) caused by carbonate contamination. On the other hand, the life of the IIR catalyst is projected to be more than 40,000 hours. Presently, ERC has adopted a stack design including both IIR and DIR, to ensure adequate reforming throughout the required stack operating life.

The selected bipolar plate has a protected coating for anode-side stainless steel current collector. The cathode-side CCC (corrugated current collector) is a one-piece, low electrolyte loss, and low-cost design. A solid rail design is selected to minimize stack dimensional change. Wet seal area is aluminized to improve the seal corrosion resistance, to combat the severe wet seal corrosion environment. In producing the aluminized coating, the wet seal surface is first coated with an aluminum-rich layer and then diffusion heat-treated in a protective gas environment to form an iron-aluminide protective coating [3.1]. The test results of the selected bipolar plate are discussed in Section 5.0.

The mechanical behavior of a repeating component package (consisting of anode, cathode, matrix, and bipolar plate) can have a very strong effect on its performance. Improper design of the repeating component package can result in undesirable load force distribution, poor component-to-component contact (hence high contact ohmic loss), component cracking (particularly the weak tape matrix) and even stack failure. The compressive force at the wet seal area needs to be adequately maintained

to prevent leakage of reactant gases. A proper repeating component single-cell package design should maintain adequate contact at both active and wet seal areas without inducing high stresses on weak components.

A finite-element computer analysis of the repeating component package was performed to evaluate various design options. A three-dimensional modeling was first performed for ERC's baseline CCCs. Reasonable agreements between the calculated and measured values for stress - strain characterisitcs and stress distribution were achieved. The results revealed significant impact of the corrugation build variables (i.e., angle and fins per inch) on the mechanical properties. The CCC mechanical properties calculated were then used in the cell finite-element analysis.

The modeling results for the baseline DOE-5 (AF-2-3) type cell design showed that a uniform pressure throughout the cell, except near the cell boundaries where the effect of the open horizontal gaps (between rail and active components), influences the stress contours. Figure 4.3 illustrates the open horizontal gaps and the displacement near the wet seal area while under compression at 650°C. The wet seal gap widths at room temperature are both 25 mils. The displacement plot shows the gap width at 650°C. Differences in anode side and cathode side gap width was caused by different material Poisson ratio and thermal expansion coefficient. It is noted that more elements were placed near the high stress, unsupported area to calculate the stress level more accurately. In this region the stresses are highest since the load present over the cell edge is transferred to the inner portion of the cell. The higher stresses may be undesirable, causing over-stress, cracking, and leakage. The horizontal gap width should therefore be controlled both to minimize the stress level at the matrix and to allow thermal expansion at operation under compression and during thermal expansion.

Various design options were analyzed using the model to study their effects on the stress levels and the maximum shear stress levels on the matrix, the most brittle and crack-prone component in a carbonate fuel cell, are compiled in Table 4.3 The effect of stack design can be ascertained from the calculated maximum stress intensity (Si). The major conclusions are listed in Table 4.4. The above results may explain the higher gas cross-leakage observed in single cells, particularly with a soft CCC design. The selected bipolar plate design and electrolyte wet seal gap are mechanically sound and are expected to minimize stress on the unsupported matrix area.

The pressure drop of the selected bipolar plate package was estimated using Darcy's equation. The selected bipolar plate was predicted to cause <5in. H_2O pressure drop, satisfying the stack operating requirements. Table 4.5 shows a comparison of calculated and measured ΔP for typical fuel and oxidant compositions. The results have been verified in both out-of-cell and stack testing. However, out-of-cell pressure drop testing revealed cell-to-cell flow variation (at the same pressure drop) due to an uneven catalyst loading and variations in wet seal gap width, causing channeling. Significant cell-to-cell flow variation can result in significant cell performance variation. Therefore, uniform catalyst loading and will-controlled wet seal gap width should be maintained during manufacturing.

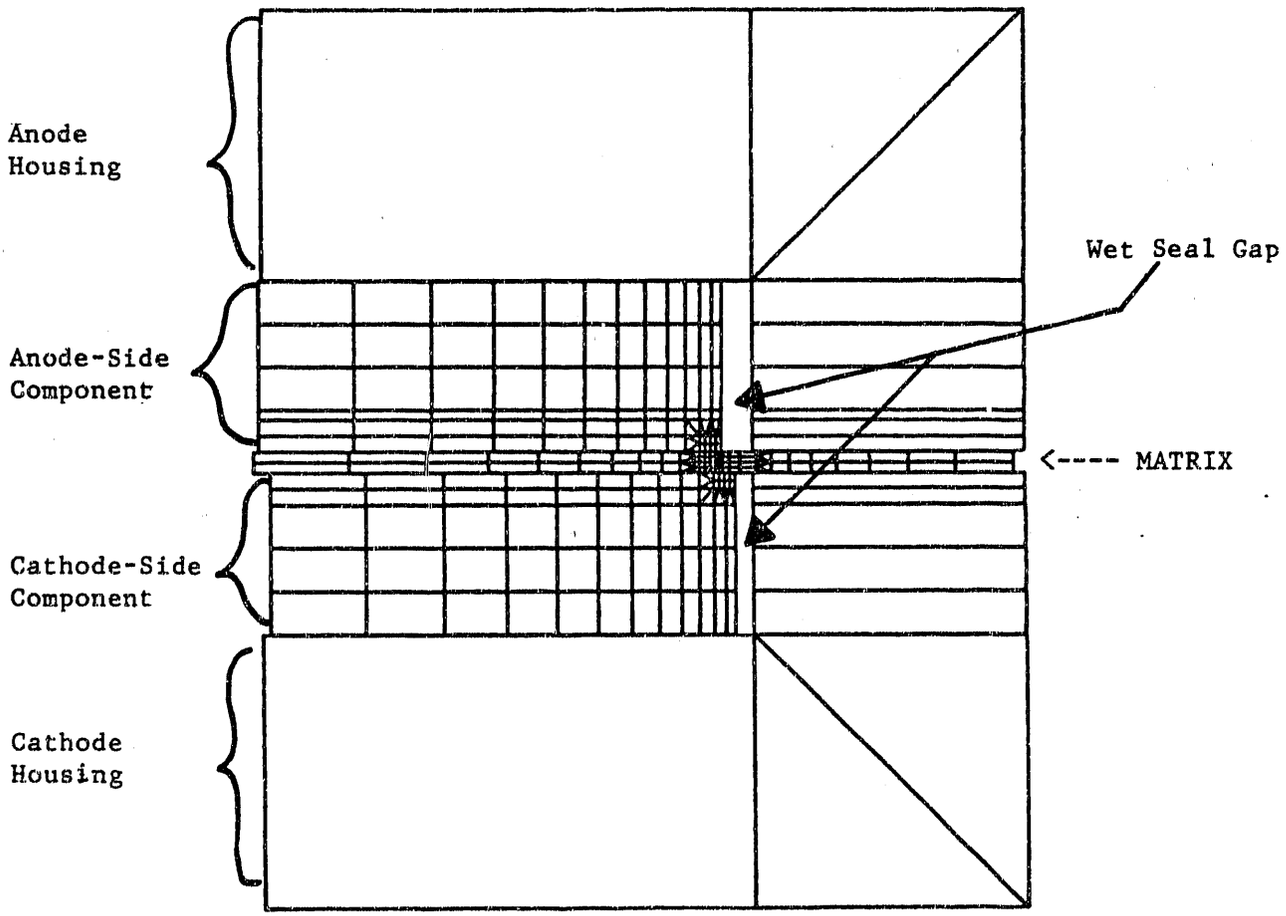

FIGURE 4.3 A DISPLACEMENT PLOT OF A SINGLE CELL AT 650°C AND 50 PSI AVERAGE PRESSURE:

Gap is Needed for Component Expansion due to Temperature and Pressure (Each Block Represents an Element in Finite-Element Analysis; Element number not Shown here for Clarity)

TABLE 4.3

STRESS LZVELS ON TAPE MATRIX FOR VARIOUS DESIGN CONFIGURATIONS (CONCLUSIONS IN TABLE 4.4):

Stress Intensity is used for Evaluating
Various Cell Designs

DESIGN CONFIGURATION	STRESS LEVEL	MAXIMUM SHEAR STRESS (psi)	MAXIMUM STRESS INTENSITY (psi)
SINGLE-CELL	BASELINE	31.3	260.8
STACK CELL	BASELINE	40.4	130.4
	310 ANODE CCC	40.1	129
	SELECTED CATHODE CCC	41	132.5
	SOFTER CATHODE CCC	66.7	221.6
	TUBULAR RAIL	40.3	129.7
	120mil SELECTED CCC	42.7	139.8
	62.5mil WET SEAL GAP	31.1	112.6
	125mil WET SEAL GAP	31.4	146.8

TABLE 4.4

PARAMETRIC EVALUATION BY MECHANICAL MODELING:

Selected Bipolar Plate and Cell Design Appears Mechanically Sound.

Comparison	Stress Level On Matrix
Single Cell VS. Stack Cell Design*	- Higher for Single Cell
Selected Corrugation	- Roughly Same as the Baseline
Softer Corrugation	- Higher Stress
Tubular Rail	- Similar to Solid Rail
Corrugation Height (75 mil VS. 120 mil)	- Not much Different
Unsupported Matrix Span	- There Exists an Optimum Span Width for a Lowest Stress on Matrix
316L VS. In600	- No Significant Effect

* Different Wet Seal Configurations

4.3.2 Non-Repeating Components

A discussion of the stack non-repeating components is presented below:

4.3.2.1 End Plate

The major function of an end plate is to transmit current and load uniformly from external system to active components. It should also provide smooth horizontal surface for manifold sealing. Easy assembly, modular handleability, light weight, and low cost are also the desired features.

ERC's prior end plate (EP-1) was machined from a thick solid stainless steel block. This end plate was, therefore, heavy and had high fabrication and material costs associated with it. Thermal distortion due to temperature gradient tended to warp the plate and cause high ohmic resistance and low performance of end cells. A compliant and flexible end plate (or with such properties near the active components) are therefore recommended.

Three subsequent designs (EP-2 through 4) have been evaluated in stack testing and the results as well as conclusions are discussed in Section 5.0. The latest design, EP-4, appears to have met both the mechanical and functional requirements. However, refinements in the end plate design may be desired to incorporate more compliance to accommodate manufacturing tolerance of this component. This design was made available and awaiting stack evaluation.

TABLE 4.5

COMPARISON OF CALCULATED AND MEASURED PRESSURE DROPS IN SELECTED BIPOLAR PLATE:

A Reasonably Good Agreement is Attained

	Anode Δ P, Inches of Water			Cathode Δ P, Inches of Water		
	SRNG	System 6C	Fluidized Bed (O_2-Blown) CFC System	6C	MW-CLASS Type B	Fluidized Bed (O_2-Blown) CFC System
Calculated	0.35	0.28	0.36	3.0	1.2	4.6
Measured	0.4	0.35	0.6	3.1	1.4	3.4

4.3.2.2 Manifold Retention System

The major function of a manifold retention system is to provide adequate sealing pressure to the manifold sealing area. Because a stack experiences thermal distortion during stack operation, the retention system should minimize thermo-mechanical interactions between the stack and the manifolds. The manifold retention system should also allow accommodations for stack height change. ERC has selected a clamp-type retention system in replacing the prior leaf-spring retention system.

The test results and the conclusions on the prior and selected clamp-type retention system are discussed in the stack tests section (Section 5.0). The clamp-type system, consisting of manifold horizontal clamp (MHC) and manifold vertical clamp (MVC), is expected to achieve the desired sealing efficiency in taller stacks, based on results from short stacks. Design improvements, to reduce material and fabrication costs, are still desirable for further reducing stack cost.

4.3.2.3 Stack Compression System

The primary function of the stack compression system is to provide a steady and uniform compressive load pressure to the stack even with a continuous change in stack height during stack operation. The prior design includes external compression plate, load bar, tie rod, and load-bearing insulation.

The selected design is basically the same as the prior design, but has disc springs attached to the load bar and tie rod to improve the compliance of the whole compression system. Figure 4.4 shows that by using disc springs, the stack compression variation with time due to height decrease during stack operations is essentially eliminated.

The prior load-bearing insulation design used a low-density-type calcium silicate insulation that creeps and cracks easily during use. A combination of strong, high-density insulation materials were selected to replace the low-density one. Stack testing of this selected design showed less creepage, less cracking, as well as acceptable heat insulation.

4.3.2.4 Manifold Dielectric

The function of the dielectric insulator is to electrically isolate the stack from the manifold, to avoid electric shorting. The previous design was an expensive one-piece alumina dielectric picture frame. Due to the brittleness of the alumina material, cracking of the picture frames was observed in stack tests, probably due to the combined effect of wet seal fabrication irregularities, stack face thermal distortion, and clamping force applied by the manifold retention system. Cracking of dielectric can cause gas leakage and poor stack efficiency.

Two different designs, multi-piece design and coating, were evaluated to replace the one-piece design. Their benefits and drawbacks are described in Table 4.6. For the multi-piece design, several joint geometries and adhesives (to seal the joint) were evaluated in out-of-cell manifold leakage tests. The tests showed that cracking and separation

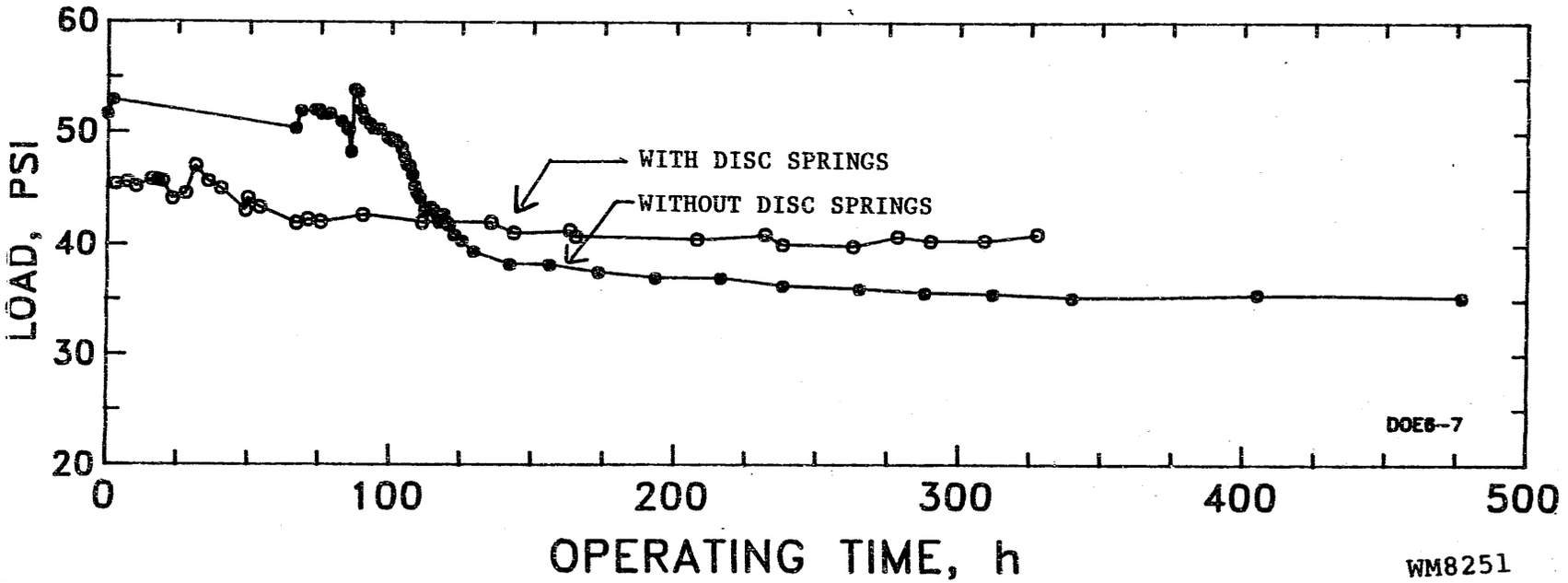

FIGURE 4.4 VERIFICATION OF EXTERNAL COMPRESSION SYSTEM DESIGN:

Less Clamping Pressure Change due to use of Disc Springs in External Compression System is Evident

TABLE 4.6

DESIGN OF DIELECTRIC FOR MANIFOLD APPLICATION:

The Multi-Piece Design has been Selected

DESIGN OPTION	BENEFITS AND CONSIDERATIONS
1. BASELINE DESIGN (ONE PIECE)	• EXPENSIVE • PRESENT TEST VEHCILE • SCALE-UP MAY RESULT IN INCREASED STRESS CRACKING • POOR AVAILABILITY
2. MULTI-PIECE DESIGN	• GOOD FABRICABILITY IN LARGE SIZES • REACTANT GAS LEAKAGE PATH MAY INCREASE • LESS PRONE TO CRACKING • LOWER COST
3. COATING	• GAS LEAKAGE INTERFACES MINIMIZED • STABILITY IN MCFC ENVIRONMENT NOT RESOLVED (POROSITY AND ELECTROLYTE EFFECT)

of the joint with associated high gas leakage had occurred for several types of joint. The cracking occurred mostly at the areas with a stress-raising tendency (i.e., sharp corners). Nevertheless, an improved joint design was found to be crack-free. Futhermore, this type of joint can still provide adequate sealing even with some joint cracking (due to a special joint design), ideal for accommodating height change due to stack temperature change. The selected multi-piece design was evaluated in an out-of-cell test. The measured gas leakage rate was found to be similar to that for the one-piece design. The measured electrical resistivity of the multi-piece dielectric frame is also the same as that of the one-piece frame (Figure 4.5).

Another option is to replace the picture frame by the dielectric coating. However, due to the hot corrosion environment encountered in the carbonate fuel cell environment, and the large thermal expansion mismatch normally existing between the ceramic coating and the stainless steel substitute, cracking and delamination of the coating is very likely to occur. This development effort is currently being performed in the cost-shared EPRI program. This development effort, if successful, will eliminate the leakage caused by the cracking and the expensive fabrication cost of the picture frame.

4.3.2.5 Thermal Insulation

Large heat loss can reduce overall power plant efficiency. It can also reduce stack performance if it results in stack non-uniform temperature distribution. The selected stack thermal (not for load-bearing) insulation material is a low-density calcium silicate type material. This material is low-cost and has excellent heat insulation characteristics. A thermal balance model was developed to predict stack heat loss (to guide the insulation design) and size the insulation.

The model was first applied to the 2kW stacks (DOE-3 and DOE-5). The calculated heat loss was found to be within 10% of the loss estimated by the natural convection calculation. Using the thermal balance model, heat loss for a 300-cell stack ($\sim$100kW output) is projected to be $\sim$3.6 kW. The selected thickness of the insulation material, based on heat loss and cost considerations, is $\sim$6 in.

4.4 ELECTROLYTE MANAGEMENT

Electrolyte management has been recognized as one of the key issues in stack technology improvement. Electrolyte loss from the stack active components, mainly due to corrosion and creepage losses, and electrolyte redistribution, due to electrolyte migration, has been projected to shorten stack life significantly.

To quantify electrolyte loss and to recommend design correction, mathematical models were developed, taking into account all the known mechanisms contributing to electrolyte loss. The model consists of two parts: (1) electrolyte loss model, and (2) electrolyte redistribution model (migration).

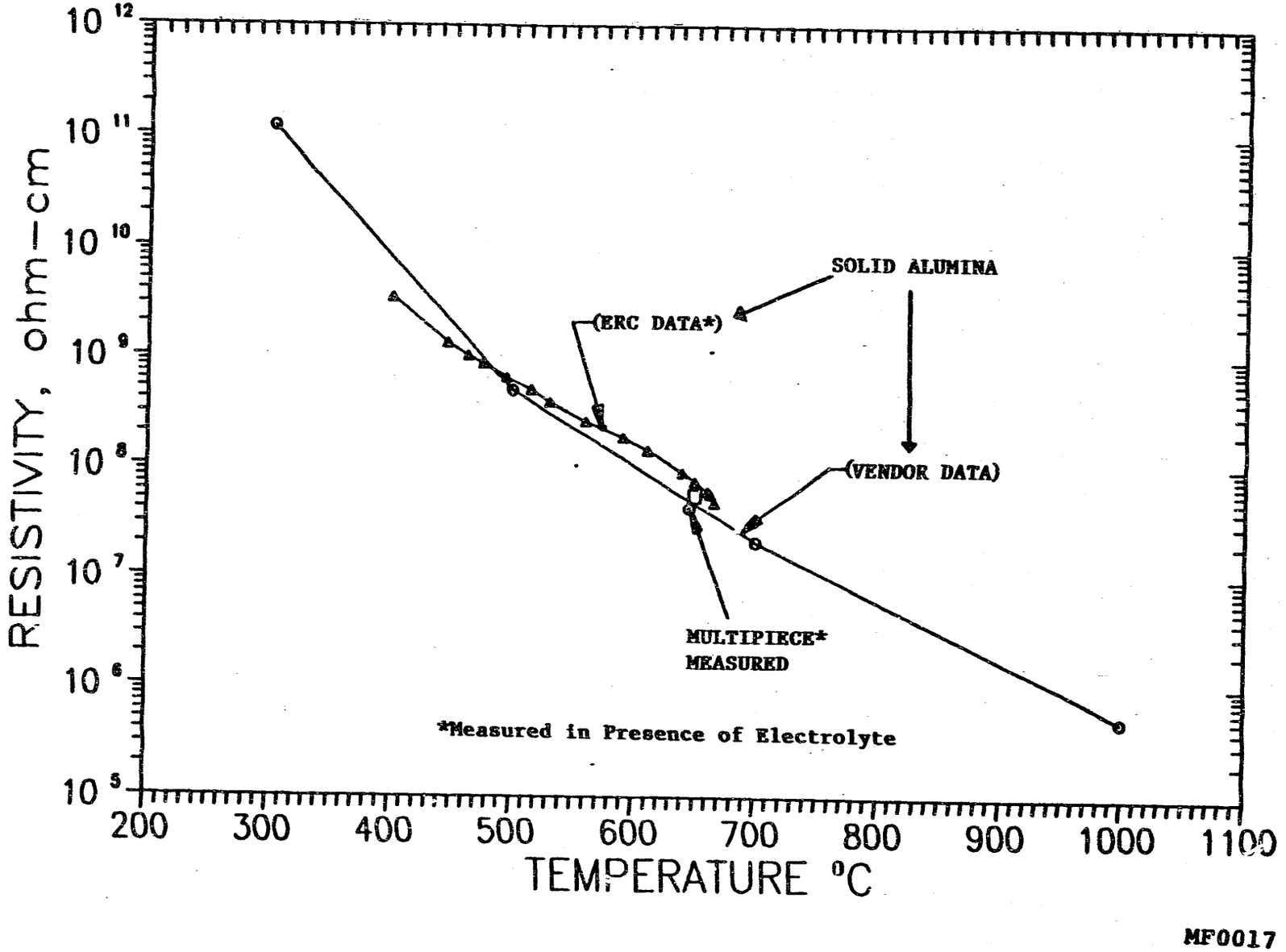

FIGURE 4.5 RESISTIVITY OF DIELECTRIC FRAME:

The Multi-Piece Dielectric Resistivity
is the same as that of the One Piece Frame

4.4.1 Average Electrolyte Loss

The developed electrolyte loss model is summarized in Figure 4.6 which classifies all losses as fixed and continuous losses. The fixed loss, occurring early in stack life, includes lithiation of cathode, gasket and matrix alumina materials and electrolyte absorption by porous gasket as well as internal reforming catalyst. This loss accounts for ∿10% of BOL inventory for a $1ft^2$ and ∿5% for a $4ft^2$ stack. This projection is based on post-test results of several short stacks. The continuous loss is mainly contributed by corrosion, creepage, and evaporation. For an 11-cell stack (BP-5), this corrosion and creepage was estimated to be ∿35% of BOL inventory after 2,700-hour operation (as well as verified by post-test results). This is significantly more than the fixed loss. The evaporation loss over 40,000 hours can also contribute to ∿10% of the BOL inventory (projected from 10,000-hour cell test data). Therefore, stack design to minimize continuous loss should be an important focus.

The electrolyte loss model was verified by comparing it with the end-of-life (EOL) inventories of the several short stacks tested earlier (see Figure 4.7). A reasonably good agreement between the calculated and measured losses is achieved. The model can then be utilized to screen stack design for lowering the average loss.

According to the average loss model, corrosion and creepage electrolyte losses are the major loss contributors and should be reduced in order to have a major impact on extending stack life. Using more corrosion-resistant hardware materials and reducing the hardware corroding surface area are the recommended approaches. An anode-side protective coating can virtually eliminate anode-side corrosion as well as electrolyte losses by creepage. Using more corrosion-resistant stainless steel on the cathode side can greatly reduce the total average electrolyte loss since a large proportion of it is caused by the corrosion of the cathode-side hardware. Reducing the number of CCC components and using a lower surface area CCC are the options for reducing the corroding surface area. The selected cathode-side CCC has a much smaller surface area than the baseline CCC; therefore, the average electrolyte loss is expected to be significantly reduced. Figure 4.8 illustrates the effect of the above recommended approaches in reducing the average electrolyte loss. The selected bipolar plate design is expected to easily satisfy the CGCFC life requirement (40,000-hour life) in terms of average electrolyte loss.

4.4.2 Electrolyte Migration

Electrolyte migration occurred in externally manifolded carbonate fuel cell stacks due to unequal mobilities of cations and anions in carbonate and the continuous path provided by the porous gasket. The potential gradient in a carbonate fuel cell stack leads to the transport of carbonate from the positive end cells to the negative end cells, due to larger cation (Li^+, K^+) mobilities than the anion's (CO_3^{-2}). The porous manifold caulking and gasket are filled with carbonate; thus, they serve as ideal paths for migration. ERC's stack testing revealed shorter end cell life than the central cells mainly due to electrolyte migration. The objectives of electrolyte migration modeling are to estimate the electrolyte migration rate of ERC's stacks and to provide input to stack design to counter the electrolyte migration effect.

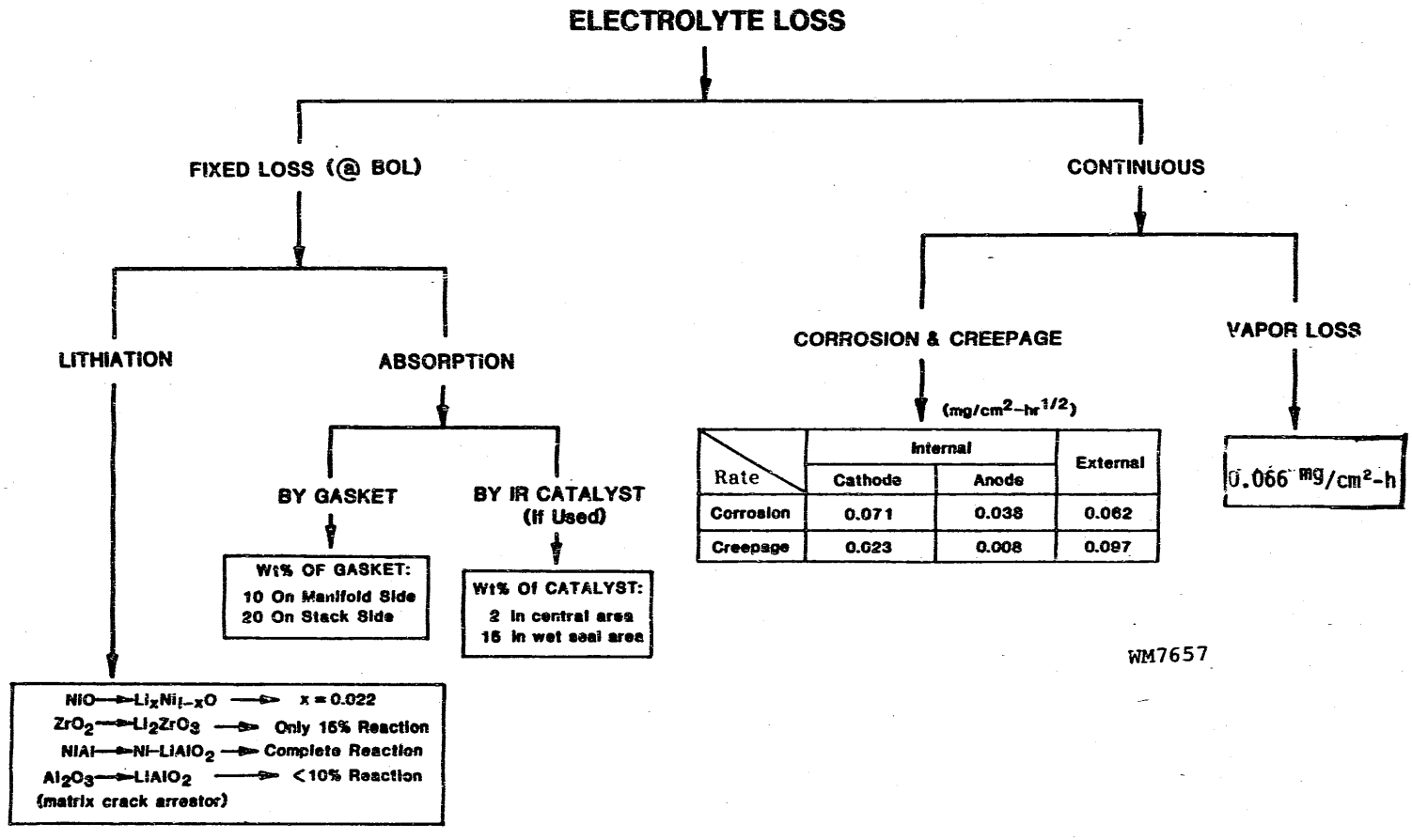

FIGURE 4.6 ELECTROLYTE LOSS MODEL:

Corrosion and Creepage Losses Could be Quite Significant and Need to be Controlled

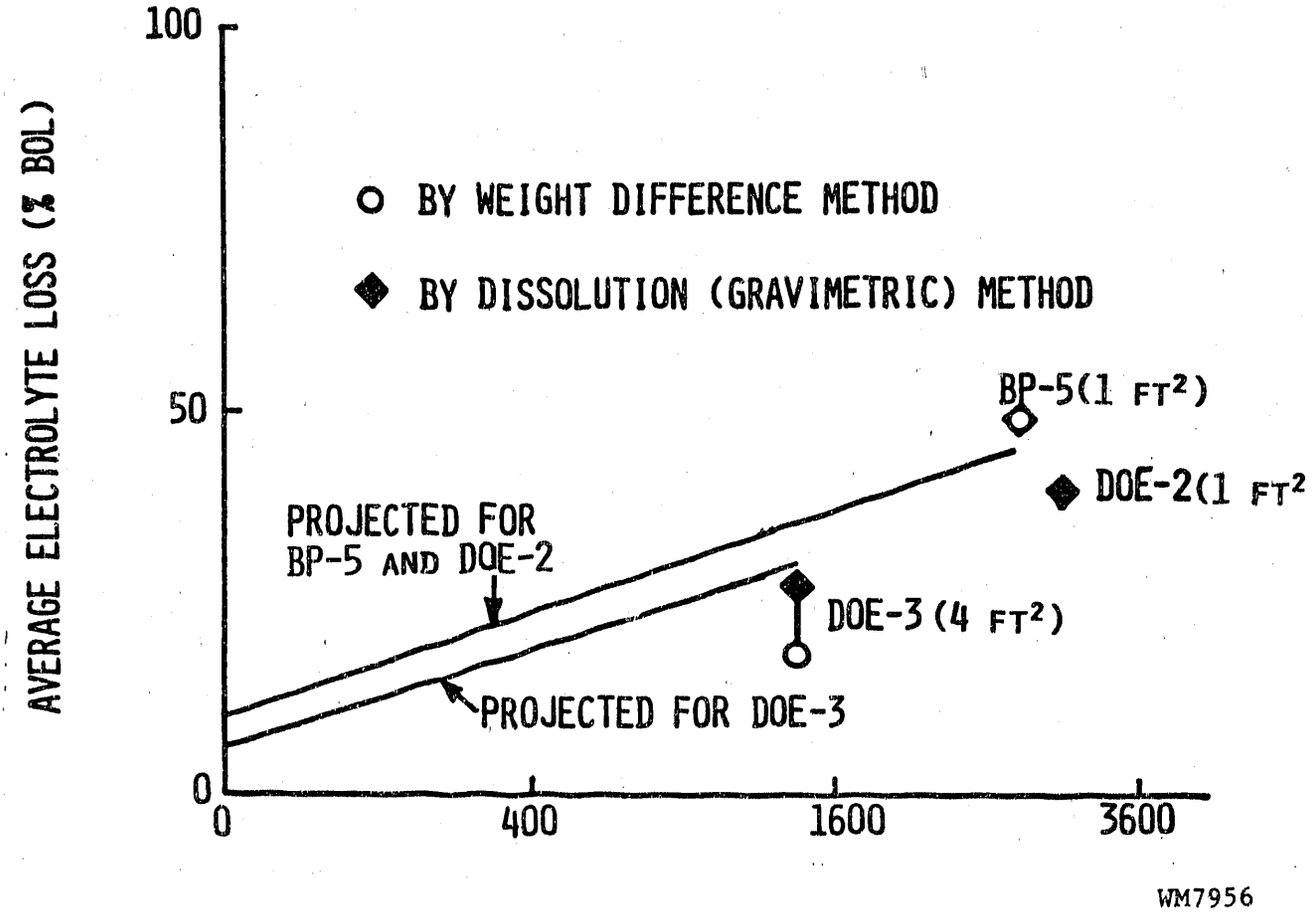

FIGURE 4.7 LOSS MODEL VERIFICATION:

Reasonable Agreement Between the Calculated and Measured Losses is Evident

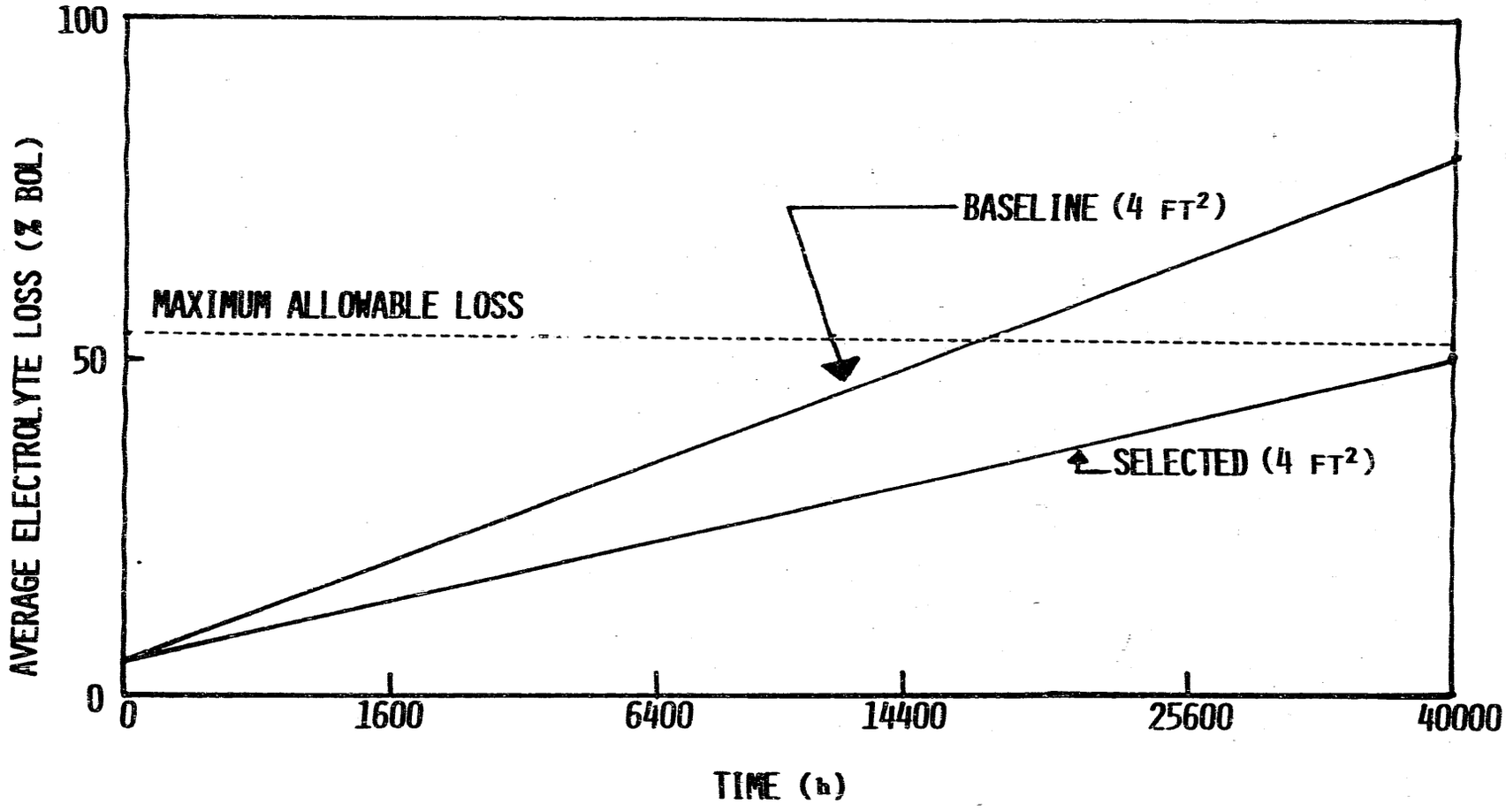

FIGURE 4.8 EFFECT OF BIPOLAR PLATE DESIGN ON AVERAGE ELECTROLYTE LOSS:

The Selected Bipolar Plate is Expected to Provide ∿35% Reduction in Electrolyte Loss Rate

To accurately estimate electrolyte migration rate (total and individual cell migration rates), an electric analog model, as illustrated in Figure 4.9, was developed. R_G denotes gasket resistance, which accounts for the ionic resistance of the carbonate melt in manifold caulk and gasket. R_W denotes wet seal resistance, which accounts for the polarization resistance of the manifold wet seal area. Note that the capillary effect was not considered here. Capillary effect tends to counter the effect of electrolyte migration; it tends toward uniform electrolyte distribution.

R_G has been shown by Kunz [3-2] as:

$$R_G = \frac{\rho_E}{\Theta^{1.81} S T} \int_0^L \frac{dx}{[f(x)]^{1.81}}$$

Θ = Porosity

S = Thickness

T = Width

L = Length

ρ_E = Intrinsic Electrolyte Conductivity

f(x) = Fraction of Filled Pore Volume

Parametric exercise of the electric analog model (shown in Figure 4.9) provided the following important insight on electrolyte migration:

- Increasing R_G decreases overall migration rate substantially. Increasing R_W alone also decreases overall migration rate, although to a much smaller extent than increasing R_G; its effect becomes substantial only when $R_W/R_G > 10$. However, increasing R_W tends to distribute the electrolyte migration effect more uniformly and therefore less on the end cells, which extends end cell life.

- The rate of migration increases with the number of cells in a stack, becoming constant after the number of cells in the stack reaches an critical value. This critical value depends on R_W/R_G ratio and is ~15 cells for the R_W/R_G value of 2.0.

The electrolyte migration model has been verified using ERC's EOL electrolyte inventory data from several stacks (DOE-3, PG&E-2, and AS-5-1). The fitting of the data is illustrated in Figure 4.10. The R_G values were estimated from the post-test gasket electrolyte fill level. The (R_W/R_G) values were determined from the fitting and were found to be ~30-40. With these R_W/R_G values, it was found that a significant number of cells were affected by migration (as shown in Figure 4.10). Therefore, the approaches of increasing R_G and R_W are considered essential to lessen migration effect.

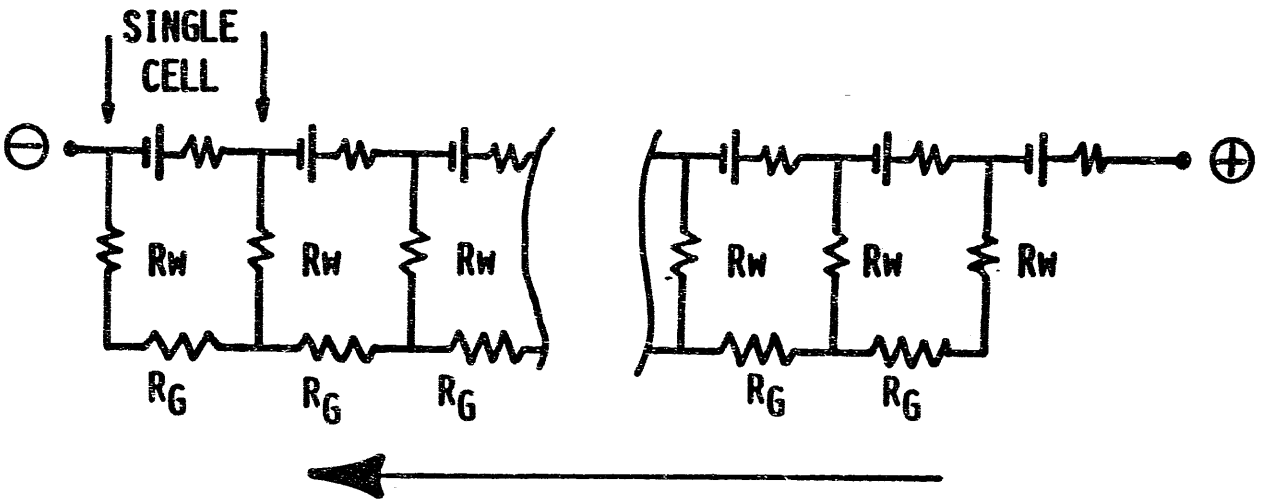

FIGURE 4.9 MIGRATION MODEL (ELECTRIC ANALOG MODEL):

Wet Seal and Gasket Resistances are Controlling Factors

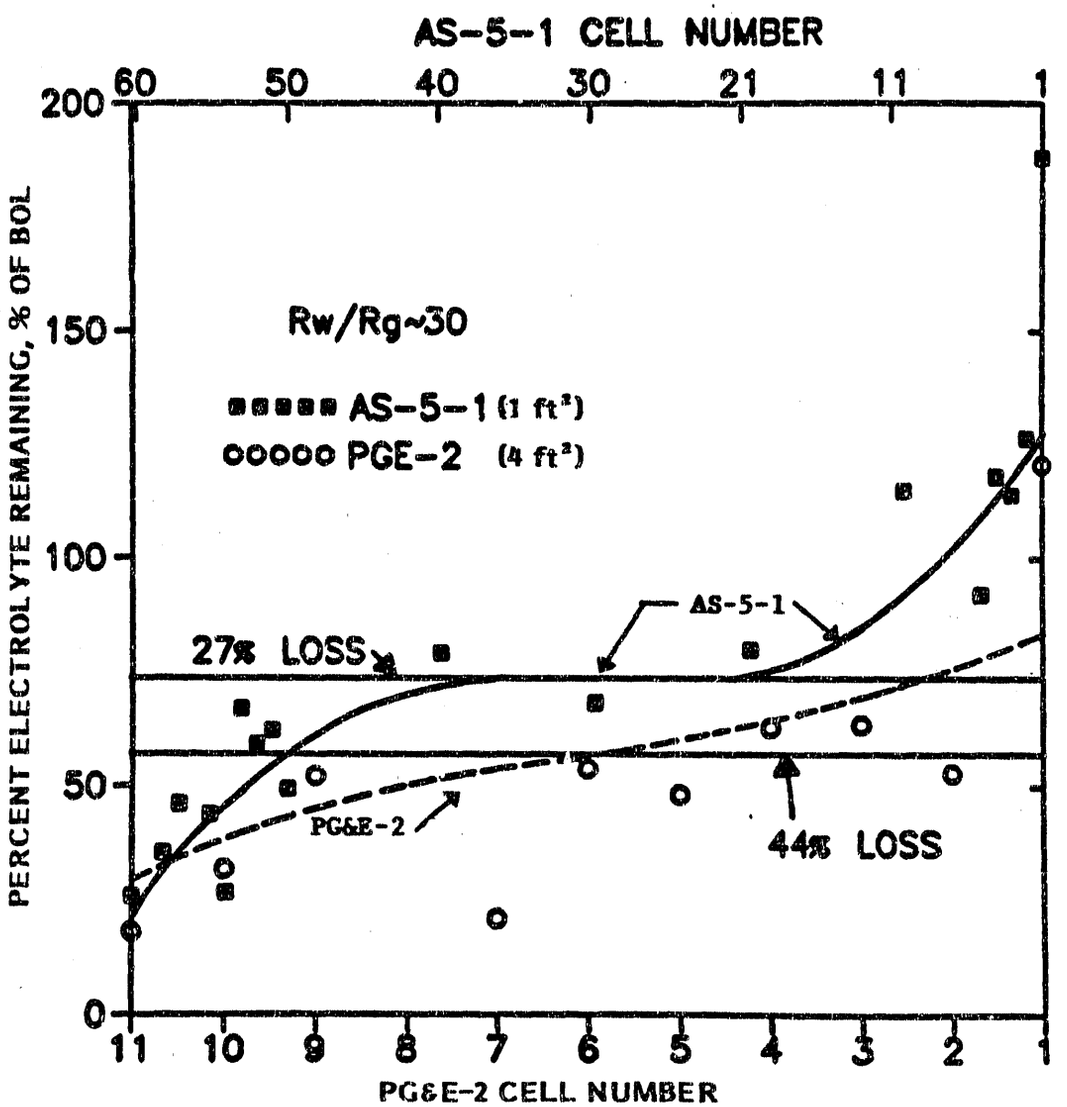

FIGURE 4.10 EOL ELECTROLYTE INVENTORY OF AS-5-1 AND PG&E-2 STACKS:

Reasonable Fit Achieved Using Developed Model

4.5 RECOMMENDED ELECTROLYTE MANAGEMENT STRATEGY

All the electrolyte required for the stack's operating life is stored in the stack. The relative magnitudes of electrolyte loss/gain projections for a 60-cell full-area stack (after 40,000 hours) are given in Figure 4.11. The electrolyte loss/gain caused by each of the contributing factors is identified and expressed relative to metallic component corrosion and creepage loss. The corrosion and creepage loss used in this comparison is derived from stacks tested at ERC (including the 5000-hour stack). The fixed electrolyte loss contributed by cathode lithiation and gasket adsorption is only 14% of the corrosion and creepage loss. Evaporation loss, estimated based on ERC's single-cell results, is only 25% of the corrosion and creepage loss. The relative contributions of the above-mentioned losses are shown in Figure 4.12 (from BOL to 40,000 hours). The migrational loss/gain affects a group of cells at the positive and negative ends. The positive-most end cell looses the maximum amount and the negative-most end cell gains an approximately equal amount of electrolyte. Using the present gasket design, gasket resistance R_G 12 ohm/cell as used in Stack DOE-7, the migrational loss of the positive-most cell (in a 60-cell stack) over 40,000 hours will be high, roughly six times the corrosion and creepage loss. It has been estimated that a three-fold increase in gasket resistance (achievable by optimizing gasket design) over the Stack DOE-7 gakset will be required to assure 40,000-hour life. This will reduce the migrational loss of the positive-most end cell to only $\sim$100% of the corrosion and creepage loss. ERC plans to provide extra electrolyte to the positive-most end cell to make up for this migrational loss and assure the required amount of electrolyte at the end-of-life. Further reduction of gasket resistance can be achieved using advanced gaskets recommended in Section 3.0. Discussions on the follow-up activities in this area are presented in Section 3.0.

Based on the above results, the following design recommendations were recommended:

(1) Increase gasket resistance R_G:

--> Reduce gasket width, thickness, and porosity without sacrificing manifold sealing efficiency.

--> Reduce electrolyte migration by using an advanced gasket design (i.e., AG-1).

(2) Increase wet seal resistance R_W:

--> Dielectrically coated wet seal area.

(3) Biased electrolyte inventory:

--> Increase BOL inventory in positive end cells.

--> Decrease BOL inventory in negative end cells.

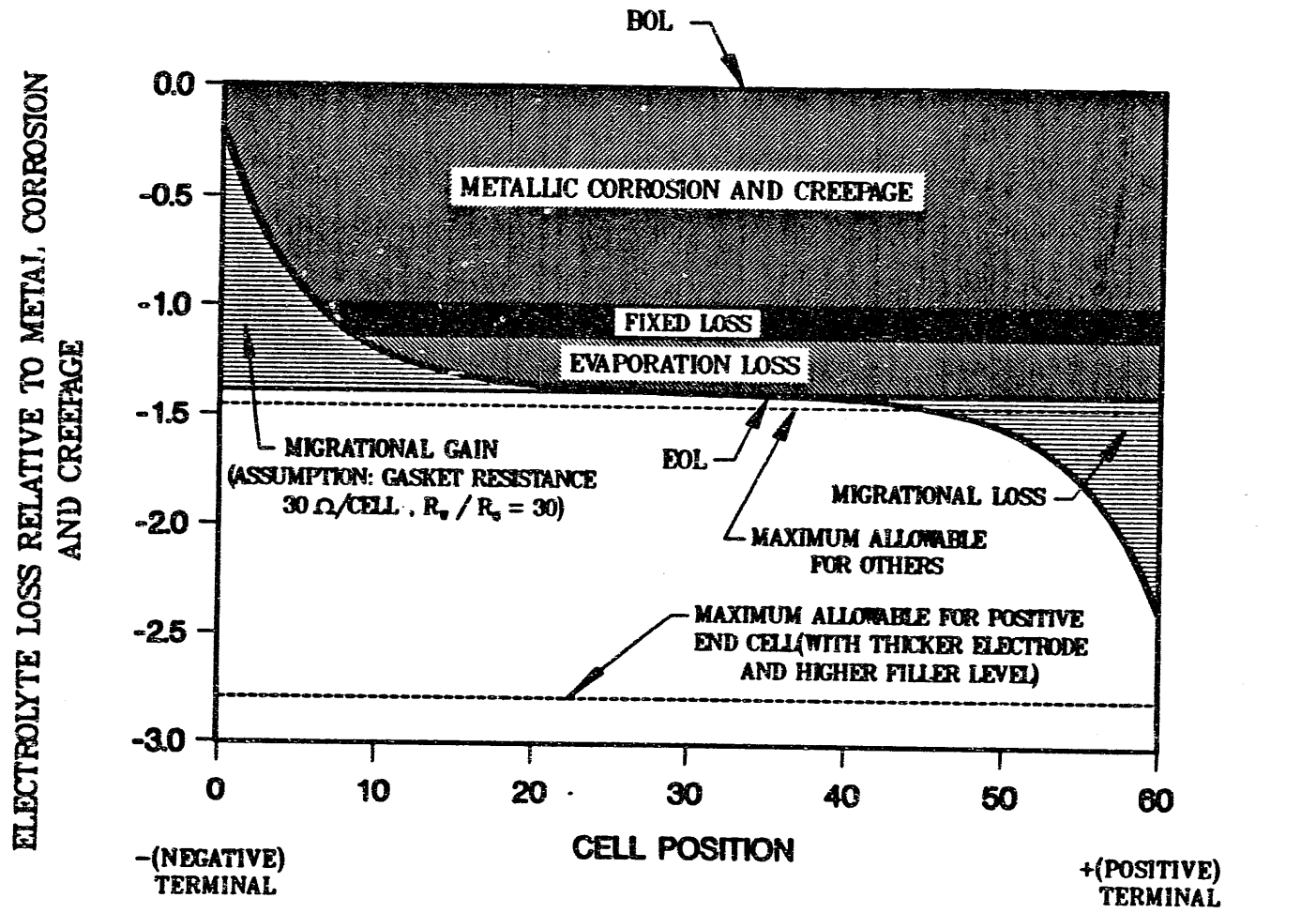

FIGURE 4.11 ELECTROLYTE LOSS PROJECTION OF ERC STACK:

Electrolyte Management for 40,000h Appears Achievable

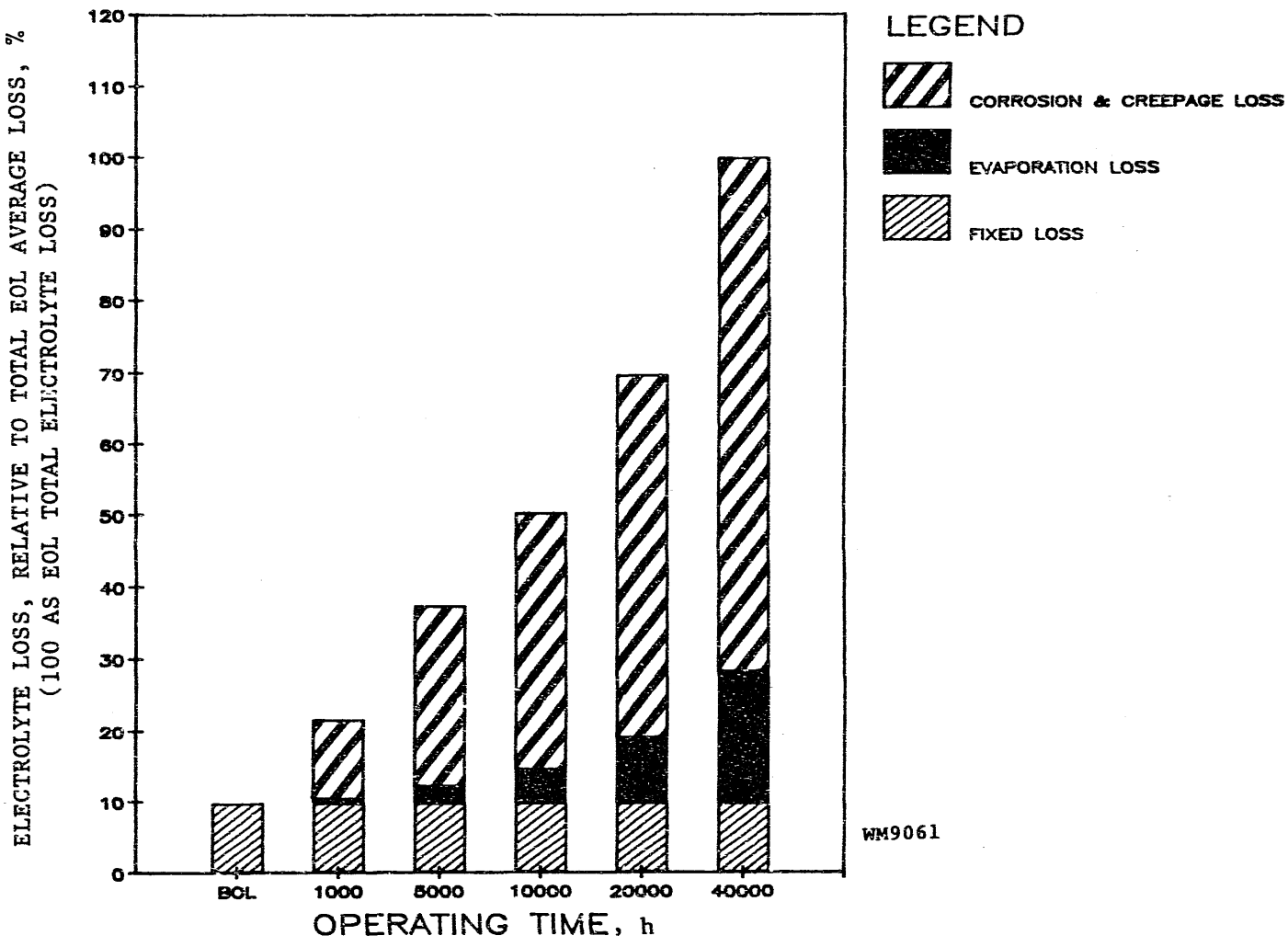

EL LOSS

FIGURE 4.12 RELATIVE ELECTROLYTE LOSS CONTRIBUTIONS BY LITHIATION AND ABSORPTION, EVAPORATION, CORROSION, AND CREEPAGE:

Corrosion and Creepage Loss are the Major Contributors

The above approaches were all evaluated in another task and the detailed results are described in Section 3.0.

4.6 REFERENCES

3-1. C.Y. Yuh, P. Singh, L. Paetsch, and H.C. Maru, "Development of Aluminized Coatings for MCFC Wet Seal Applications", Paper 276, Corrosion/87, Annual Meeting of NACE, 1987.

3-2. H.R. Kunz, "Transport of Electrolyte in Molten Carbonate Fuel Cells", J. Electrochem. Soc., 134(1), 105, 1987.

5.0 STACK TESTS FOR DESIGN VERIFICATION

In this program ERC tested seven, 4ft² stacks (of which five were five-cell, 2kW size) and one, 60-cell 1ft² stack. Over 14,000 hours of stack test experience was accumulated in the process. Most of these tests were at system operating conditions, providing useful operating experience with representative fuel and oxidant at high utilizations.

The stack testing activities emphasized the development of stack repeat and non-repeat hardware. The end plate, bipolar plate, and manifold retention designs were refined through several design iterations and made available for tall stacks. The stack component design developed in this program, except the manifold dielectric, are mass-producible. Some cost reduction of stack components at a future time will be desired to attain the overall cost goal. This manifold dielectric frame will require future development focus for cost effectiveness.

In 1988-89 ERC tested an 11-cell internal reforming stack at the MW-Class power plant (natural gas) system condition for 5000 hours. During the same time, ERC tested a 60-cell, 1ft² size stack, the tallest IRCFC stack tested to date, to investigate the stack height scale-up issues. ERC also tested a 20-cell, 8kW stack at coal-gas system conditions. In addition, a 54-cell, full-size stack intended for natural gas system condition testing was assembled. Attainment of performance within 50 mV (7%) of the coal-gas as well as natural gas applications was demonstrated. Attainment of 3mV/1000h (0.5%/1000h) decay rate was demonstrated in an 11-cell, 4ft² stack operated at natural gas conditions for 5000 h.

5.1 INTRODUCTION

Stack development activities were initiated at ERC in early 1980. The early stacks were 1 ft^2 or smaller and were used mostly for verifying cell active components, internal reforming catalyst and reformer designs. The internal reformer design was found to be quite versatile in the choice of fuels and therefore remained an integral design concept in ERC's stack development programs. During the 1985-86 time period, emphasis was on development of component specifications and fabrication of components meeting these specifications. Test verification of these components culminated in a successful 3000h, four-cell, 1ft^2 size stack test.

The present program was initiated in 1987 and the cell components were scaled to commercial size (4 ft^2) by 1988. In the 1988-89 time frame, the focus was on stack hardware development and scale-up. The stack tests conducted during this period are reported here. Short (five-cell), 2kW, 4ft^2 stacks were used as a cost-effective test vehicle for component evaluations. Five stacks of this type were tested on the program in support of the component selection process. In the final portion of the program (1989-1990), effort was directed at scaling up the stack height and extending the operating life. The program culminated in a 20-cell, 8kW stack test which showed good and stable performance at coal-gas system conditions with the selected components.

This program was cost shared by the Electric Power Research Institute, Pacific Gas and Electric Company, and ERC's corporate funds. Several stacks were tested on a cost-share basis in support of the height scale-up and operating life issues. These tests included an EPRI 60-cell, 1ft^2 stack tested to investigate height issues, and a 4ft^2 PG&E-2 stack test at natural gas system conditions for 5000 hours. The PG&E stack evaluated an indirect internal reforming approach. An overall summary of ERC's stack tests in this program is presented in Table 5.1. Over 14,000 hours of stack test experience was accumulated and most of this was at system operating conditions. Thus considerable experience was gained in stack operation on representative dilute fuel and oxidant gases at high utilizations. The results of the stack testing were divided into four major areas: Performance and Coal-Gas Experience, Component Development, Operating Life, and Scale-up. Progress made in each of these areas is discussed below.

5.2 PERFORMANCE AND COAL-GAS EXPERIENCE

Stack performance was tracked at realistic test conditions throughout the development process. Good and reproducible performance was achieved at natural gas system conditions with each class and size of stack tested. Consistent test results enabled meaningful component and hardware design evaluations to be made. The performance of representative stacks of each size tested is shown in Figure 5.1. The average performance of these stacks with simulated reformed natural gas fuel at 75% fuel utilization and with dilute oxidant gas (9% O_2, 13% CO_2) at 50% oxygen utilization was 710 mV ± 20 mV. Performance and design goals were set for both coal and natural gas systems and are shown in Table 5.2. These goals were used to define test conditions and ensure meaningful results. Current performance status with respect to these goals, performance shortfall, and the current approach to achieve the required improvement is outlined below.

TABLE 5.2

CFC STACK GOALS FOR COMMERCIAL ENTRY:

Realistic Design and Performance Goals Have Been Set To Ensure Early Market Entry

FUEL:	Dual (Coal-Gas/Natural Gas)	
CONTAMINANTS:	H_2S: <1 ppmv; HCl: <0.1 ppmv; NH_3:	<0.5%
COOLING:	Process Gas Cooling With 200°F ΔT	
MANIFOLDING:	External	
PERFORMANCE:	MW-Class Type A	100MW-Class KRW/O_2/HGC
MID-LIFE, ASF @ 0.7 V:	150	175
LIFE, h	40,000	40,000

TABLE 5.1

SUMMARY OF ERC'S PROGRAM STACK TESTS:

Over 14,000 Hours of Stack Test Experience Accumulated,
Mostly at System Operating Conditions

STACK DESCRIPTION	TEST OBJECTIVE	LIFE	PERFORMANCE		OPERATING CONDITION**	
		Hours	mV	$m\Omega \cdot cm^2$		
2kW-CLASS (5 CELLS)						
- DOE-5 (AF-2-3)	DUAL-FUEL	2100	640	690	100MW-CLASS COAL	75% FUEL UTIL.
- DOE-6 (AF-2-4)	BIPOLAR PLATE	2100	750	380	100MW-CLASS COAL	55% F, 40% O UTIL., 120ma/cm^2
- DOE-7 (AF-2-5)	MODULE COMPATIBILITY	800	725	490	100MW-CLASS COAL	55% F, 40% O UTIL., 120ma/cm^2
- DOE-10 (AF-2-6)	MANIFOLD SYSTEM DESIGN	200	672	390	100MW-CLASS COAL	72% FUEL UTIL.
- AF-2-S (STACKABILITY TEST)	RAIL DESIGN	200	720	530	100MW-CLASS COAL	CENTRAL CELLS
5kW-CLASS (11 CELLS)						
- PG&E-2 (AF-5-1)*	IIR SCALE-UP	5000	765	410	MW-CLASS TYPE-B	
5kW-CLASS (60 CELLS, 1ft^2)						
- EPRI-60 (AS-5-1)*	DIR HEIGHT SCALE-UP	2000	690	350	MW-CLASS TYPE-A	CENTRAL 40 CELLS
8kW-CLASS (20 CELLS)						
- DOE-8 (AF-8-1)	HEIGHT SCALE-UP	1600 (cont'd)	735	460	100MW-CLASS COAL	

*SYSTEM DESIGNATION	CURRENT mA/cm^2	FUEL COMPOSITION %							OXIDANT %				
		H_2	CO_2	CO	CH_4	N_2	H_2O	UTIL	O_2	CO_2	N_2	H_2	UTIL CO_2
LABORATORY TEST CONDITION	AS SPECIFIED	73	18				9		16	25	59		50
MW-CLASS TYPE-A	160	32			27		41	75	9	13	73	5	50
MW-CLASS TYPE-B	140				40		60	75	13	16	55	16	75
100MW-CLASS COAL	160	50	35		5	1	9	85	13	12	63	12	25

WM8960a

* Represents cost share stacks

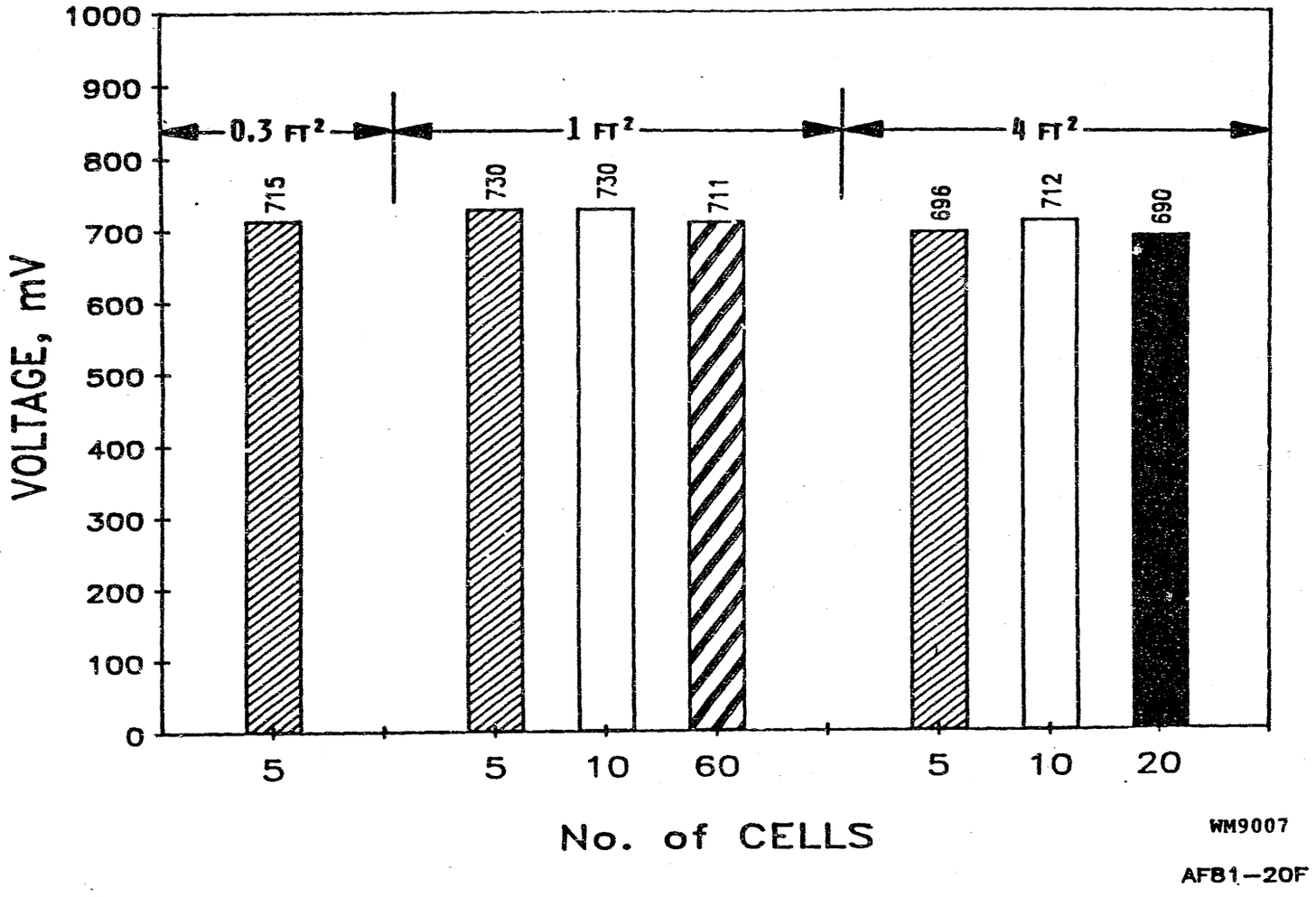

FIGURE 5.1 STACK PERFORMANCE COMPARISON AT 160 mA/cm²:

Reproducible Performance Achieved

The central cell performance observed at coal and natural gas system conditions in a 1989-90, 4ft^2, five-cell stack test is shown in Figure 5.2. The performance goals are defined at middle-of-life (MOL), which is 20,000 hours of operation, so a projection of performance decay is used for comparison to the design goal. Using a 2mV/1000h decay rate, the goal set by ERC, the performance decay at 20,000 hours would be 40 mV. As shown (Figure 5.2), an approximately 10mV gap is seen between the stack performance and goal, which translates to a 50mV (7%) shortfall from the coal-system goal. A similar analysis for a 5kW (11-cell, 4 ft^2) stack tested in 1988 at natural gas system conditions shows an approximately 50mV shortfall at BOL for the natural gas system.

The approach for gaining the required 50mV performance improvement was to reduce ohmic resistance and improve cathode performance and fuel flow uniformity. Activities were initiated to attain the performance goal (Section 3.0 for additional discussion).

ERC to date has operated four 2kW stacks and one 8kW stack on coal-gases. One of the stacks was operated on a coal-gas representative of the oxygen-blown fluidized bed gasifier product for approximately 1000 hours continuously, including a thermal cycle. As shown in Figure 5.3, a very stable performance was observed. Also included in this test-run was a 600h operation with the oxidant composition representative of the coal power plant operation. As expected, a slight improvement in performance, resulting from coal oxidant, was noticed (see pertinent discussion in Section 2.0). The stacks were also operated on coal-gases representative of oxygen-blown entrained bed, fluidized bed, and air-blown fluidized bed gasifiers. No operating problem was encountered with any of the coal fuels. The performance variations were as expected from single-cell tests (discussed in Section 2.0).

The 20-cell, 8kW stack was tested on coal-gas for 1000 hours. This stack is undergoing a thermal cycle at this time and will be restarted soon.

5.3 COMPONENT DEVELOPMENT

In the 1988-1989 time frame, the program testing activities focused on verification of improved stack hardware designs which met the manufacturing and cost goals. The five-cell, 2kW stack test vehicle was used for these evaluations. The bipolar plate, end plates and manifold retention system each underwent several design and testing iterations.

The bipolar plate was identified as a key component for improvement due to its performance and cost impact. The plate hardware consists of a folded separator sheet with edge rails and an anode and cathode current collector. The current collectors act as gas flow fields as well as current collectors. The separator sheet and edge rails prevent mixing of reactant gases.

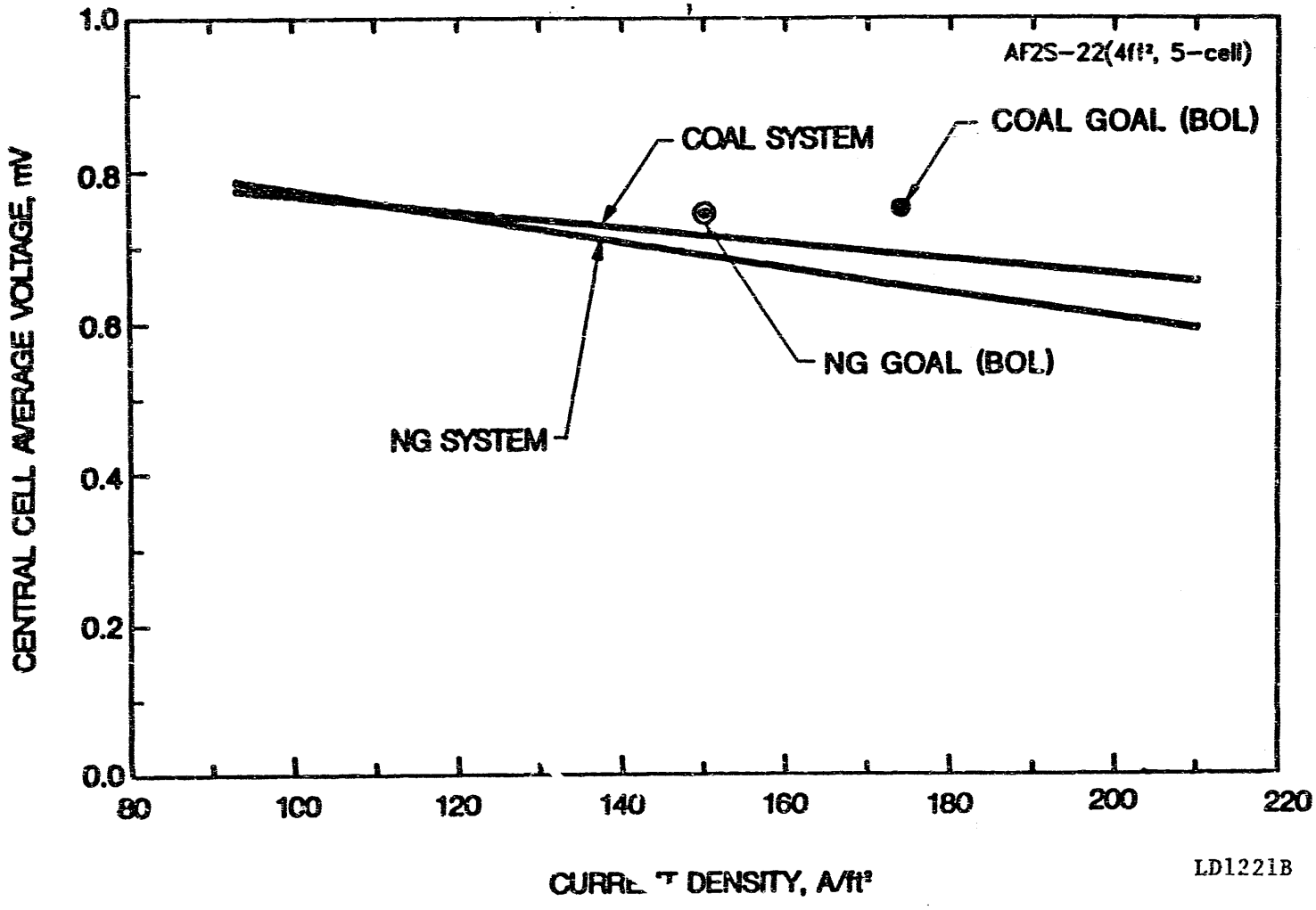

FIGURE 5.2 AVERAGE BOL PERFORMANCE OF SUBSCALE STACK (2 kw, 4 ft²) ON DUAL-FUEL:

The BOL Cell Voltage is Within 7% of the System Goal

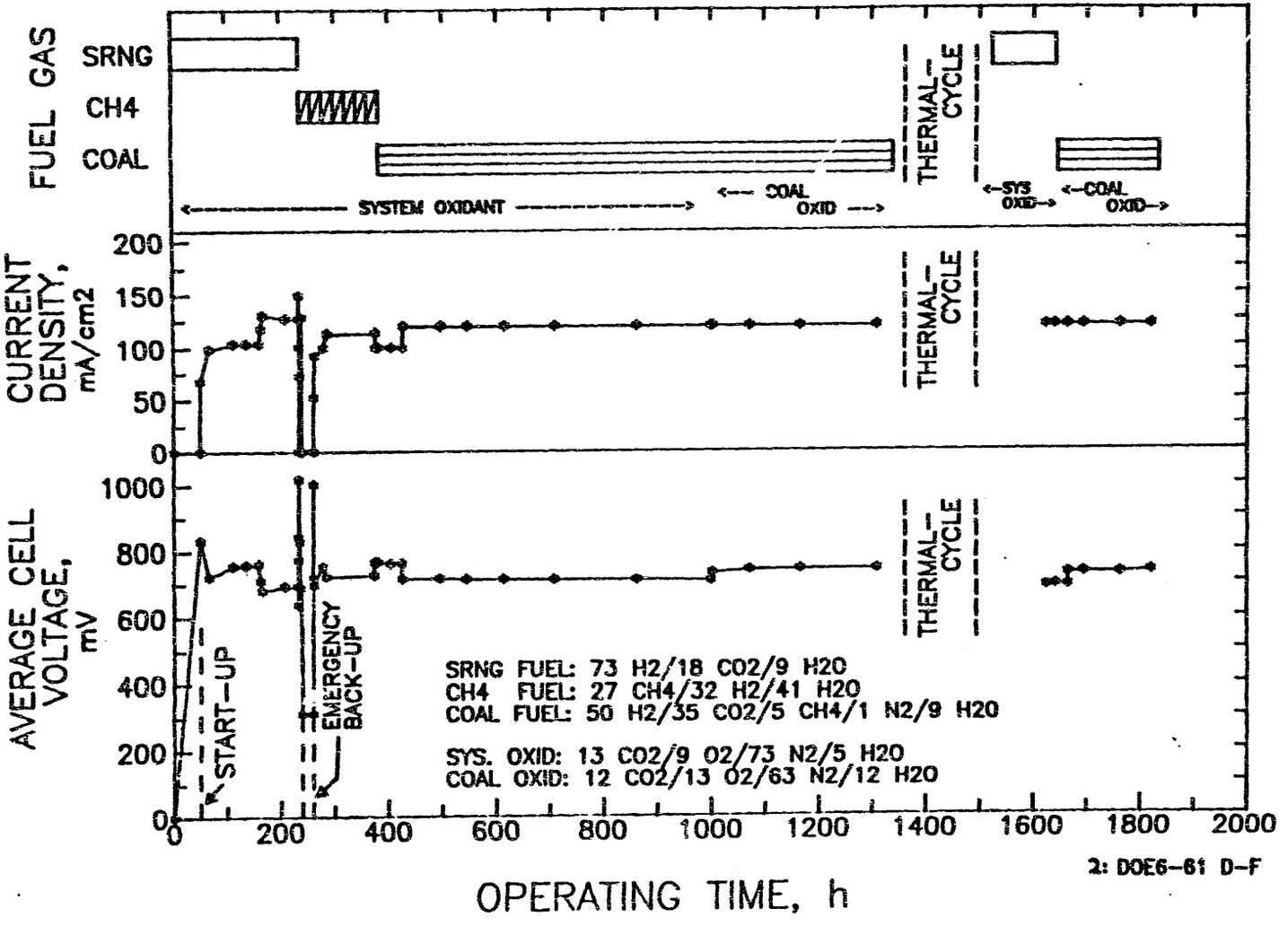

FIGURE 5.3 OPERATION ON COAL-GAS:

Stable Operation on Coal-Gas Demonstrated

To improve manufacturing and reduce cost, a cathode current collector with a simplified geometrical pattern was developed and tested. The new pattern eliminated a perforated support plate in the baseline design, resulting in reduced ohmic losses. The reduced surface area of the selected design also minimizes electrolyte losses due to corrosion. Corrosion protection on the anode current collector was improved by the use of a protective coating. Protection of the current collector enabled cheaper substrate materials to be used while virtually eliminating electrolyte loss due to corrosion of this component.

The standard performance curves for the stacks tested with the improved cathode current collector are shown in Figure 5.4. The figure illustrates that significant but incremental progress was made with each stack tested over the course of the program. Performance improvement from the first (DOE-6) to the last stack tested was ∿75 mV at 160 mA/cm^2.

A 4ft^2 stack test with the selected bipolar plate improvements demonstrated low and stable resistance when compared to the baseline design as illustrated in Figure 5.5. Initial lower resistance as well as a lower rate of resistance increase was observed with the selected cathode current collector design.

The stack end plates are responsible for uniformly distributing the compressive force, collecting electrical current, maintaining end cell temperature and providing manifold gas sealing surfaces. To accomplish these functional requirements, the end plates must be mechanically stable during thermal changes and have minimal heat loss. End cell resistance is an important parameter in assessing end cell functionality because it is a good measure of mechanical stability and component contact.

Four end plate design iterations (EP-1 through EP-4) were fabricated and tested in 4ft^2 stacks in this program. The first three designs satisfied some, but not all, of the requirements. A major problem was maintaining the strength required to distribute the compressive force while reducing the mass and simplifying the manufacturing process. The end cell resistance obtained for each of these designs is shown in Figure 5.6. The latest design meets the resistance goal while satisfying the functional requirements. Some cost improvement of the end plate may be desirable in the future.

ERC has selected an externally manifolded stack design. The manifold assembly includes four gas manifolds, gas seal assembly with dielectric insulator and a retention system. While progress was made with each of these components, the major effort focused on redesign of the manifold retention system. The functional requirements of the manifold system are simply to deliver the fuel and oxidant gas to the cells without a performance loss. Gas seal efficiency goals were set based on COE as well as safety considerations. The fuel manifolds have the most stringent requirements. The acceptable fuel leakage rate is set at 0.2% of the fuel feed at 15in. H_2O pressure at 650°C. Manifold performance is most easily monitored by measuring seal leakage at room temperature. This

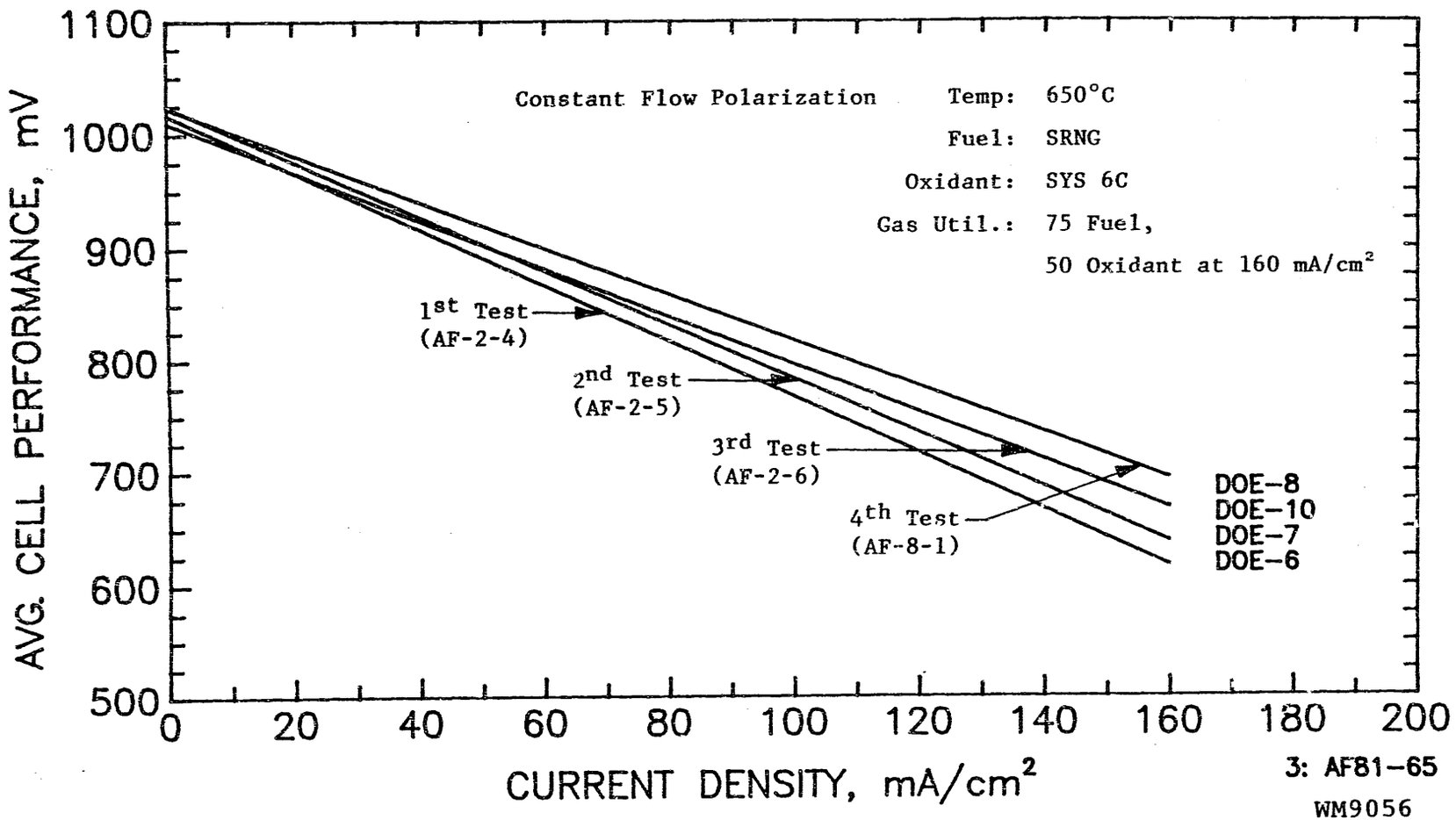

FIGURE 5.4 PERFORMANCE IMPROVEMENT ACHIEVED IN STACKS WITH THE SELECTED CATHODE CURRENT COLLECTOR:

Incremented Progress was made with each Stack Tested

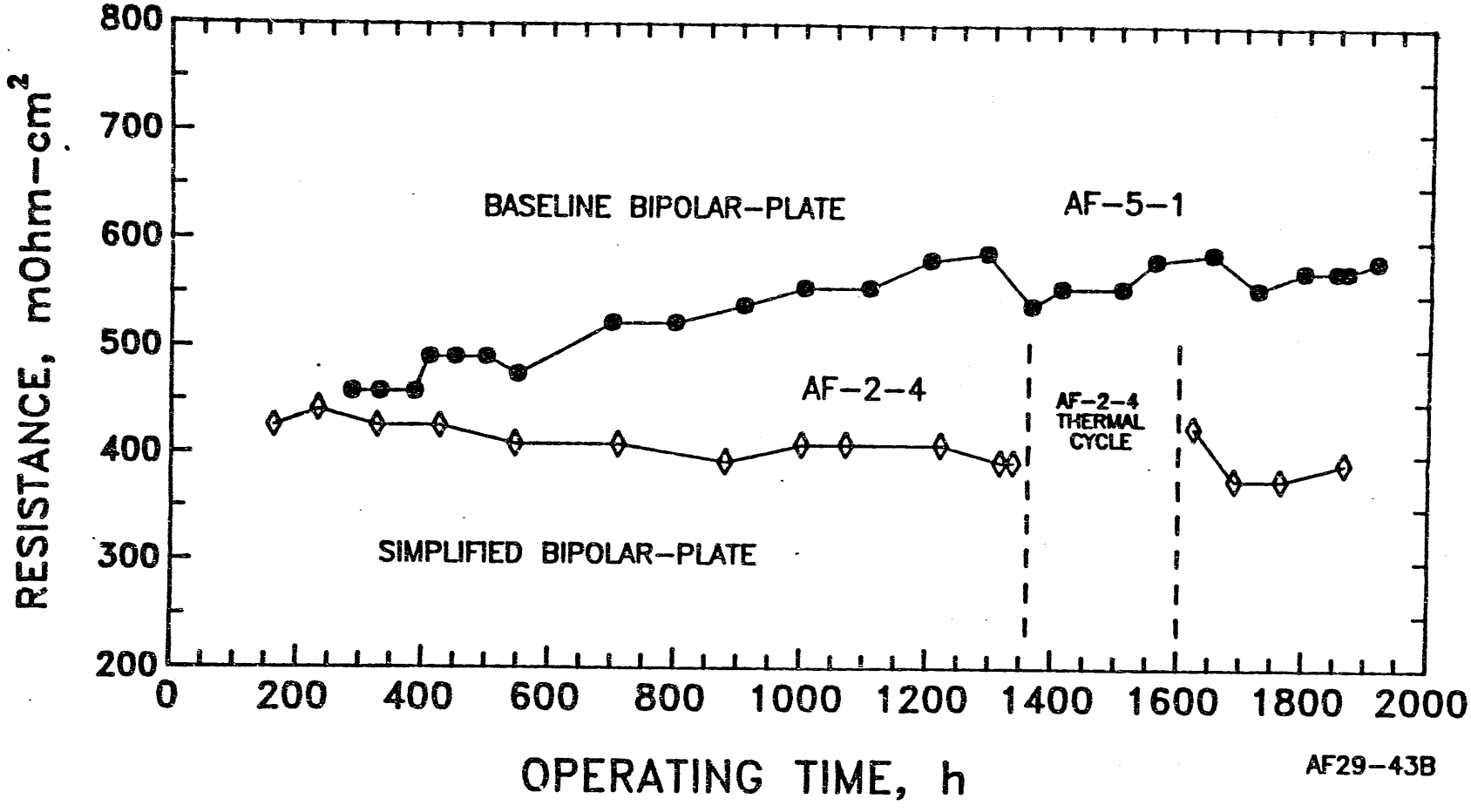

FIGURE 5.5 COMPARISON OF CENTRAL CELL RESISTANCE FOR STACKS AF-5-1 AND AF-2-4:

The Selected C-CC Provided a Lower BOL Resistance as well as a Lower Rate of Increase

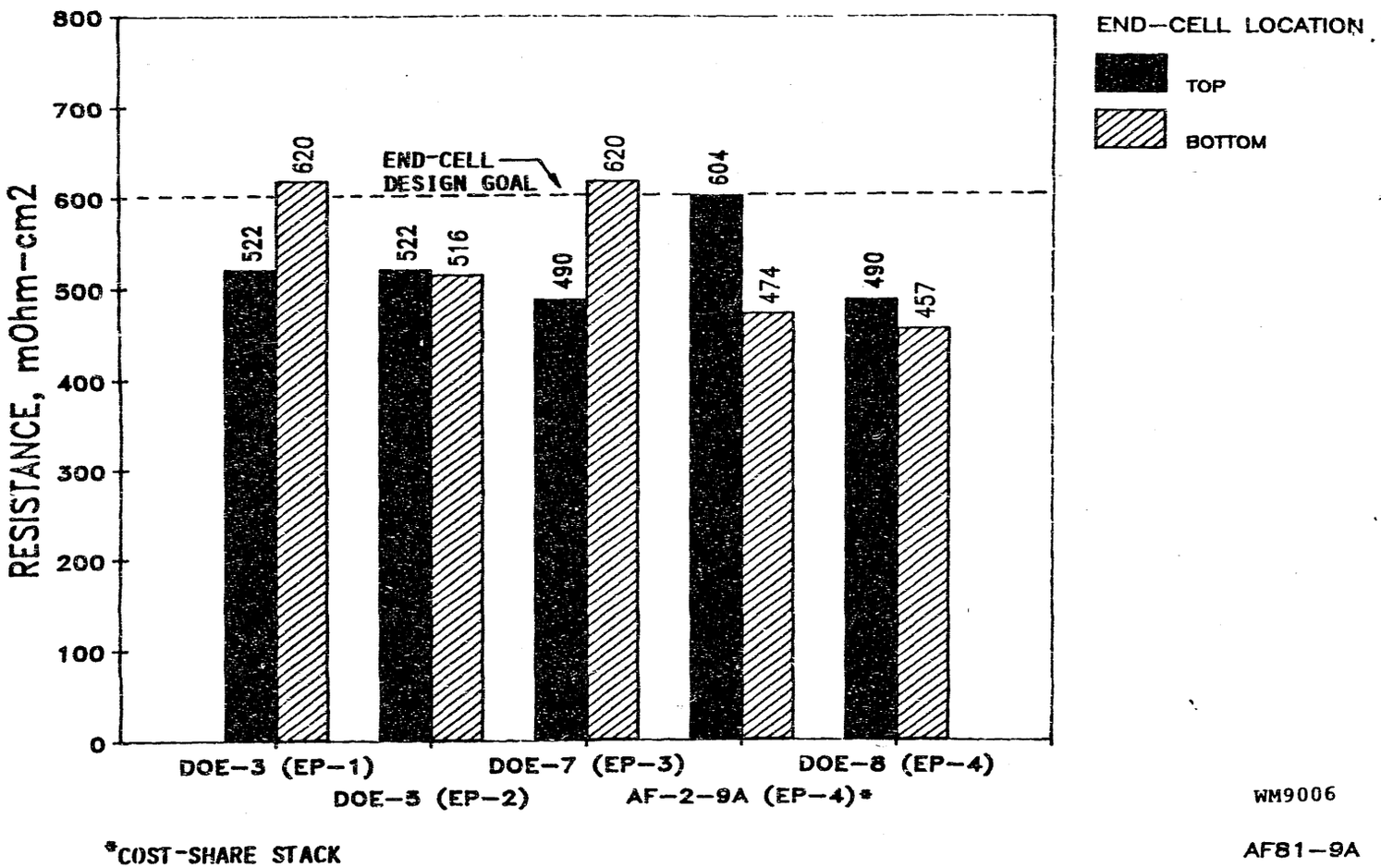

FIGURE 5.6 COMPARISON OF END CELL RESISTANCE IN STACKS WITH DIFFERENT END PLATE DESIGNS:

End Plate Design Meets Functional Requirements and Provides Low End Cell Resistance

simple and direct measurement may be done both before and after testing. The leakage goals when translated to room temperature by correcting for viscosity, temperature and pressure as well as being normalized on a seal perimeter basis is 1 cc of air per minute per in. of water per cm of seal.

The technique for the manifold body fabrication was changed from welding to a stamped construction. This process is more amenable to commercial scale manufacturing. No impact on performance was observed as a result of this improvement.

The manifold seal subassembly was modified to inhibit electrolyte transport along the seal edges. Most of this development effort was conducted in out-of-cell tests and is discussed in Section 3.0. Stack test evaluation is currently in progress as part of the ongoing effort.

The manifold retention system was redesigned. The baseline "leaf spring" design was functionally deficient, cumbersome, difficult to scale up and physically connected to the stack end plates. Decoupling the manifold retention system from the end plates allows the design/redesign process to proceed independently while also reducing the function requirements of each component. The design selected by ERC for development is comprised of a horizontal clamp (MHC) and a vertical clamp (MVC). The MHC is completely independent of the stack and consists of a hoop which when tightened exerts a force on a series of springs which apply pressure to the horizontal sealing surface. The MVC is a series of clamps running along the vertical edges of the stack. The vertical clamps connect manifold-to-manifold and when tightened exert pressure on the vertical seal surface. By utilizing small springs the compressive force is applied uniformly during both transient and steady state operation.

These clamping designs were qualified in five-cell, 2kW stack tests. Two design iterations on the MHC design (MHC-1 and MHC-2) were performed. The room temperature seal characterization results shown in Figure 5.7 indicate that the seal efficiency goal of 0.2% fuel leak at 15in. of water pressure, as characterized by 1.0 cc per min air leakage per cm of seal per in. of water pressure, was met. Based on these results the MHC-2 and MVC compression system was selected for use in taller stacks.

The dielectric component of the seal subassembly is a ceramic. Ceramics are brittle and have a low coefficient of thermal expansion when compared to metals. Cracking of the dielectric can, therefore, easily occur during heat-up, cool-down and transient operation. Refinement of both the design and assembly procedures virtually eliminated ceramic cracking in the short stacks. The incidence of dielectric failure for the various designs is summarized, (Table 5.3) showing the progress achieved with the latest design.

The current status of the baseline stack components is presented in Table 5.4. It can be noted that further performance improvement of the cathode, matrix, and the gasket efficiency will be desired. This may require some design improvement of the cathode in terms of optimizing

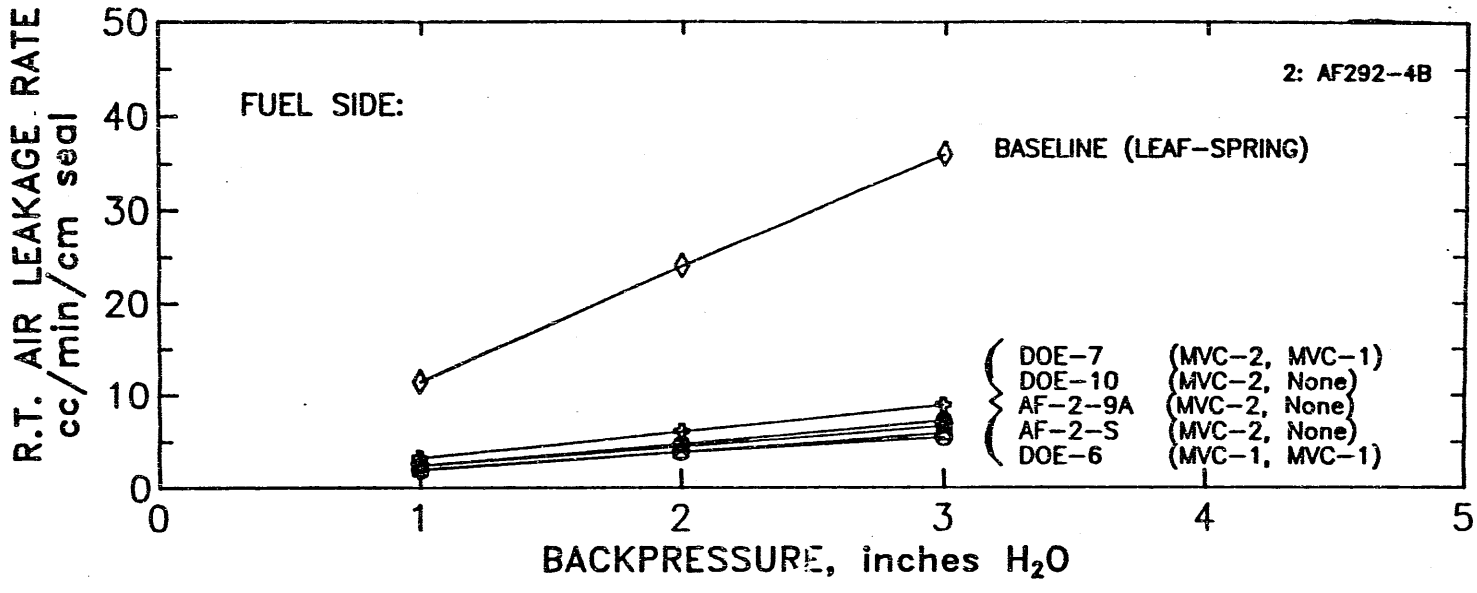

FIGURE 5.7 EFFECT OF MANIFOLD COMPRESSION SYSTEM DESIGN IMPROVEMENTS ON SEAL EFFICIENCY:

The Desired Seal Efficiency (<1.0cc/min per cm Seal per in. of Water at Room Temperature) has been Achieved

TABLE 5.4

PRESENT STATUS OF STACK COMPONENTS:

Cost Reduction of Stack Hardware and Development of Manifold Dielectric Separator are Recommended

BASELINE STACK COMPONENT	PRESENT STATUS								
	FUNCTIONALITY			MANUFACTURABILITY			COST		
	ACCEPTABLE	IMPROVEMENT DESIRED	IMPROVEMENT NEEDED	MASS PRODUCTION PROCESS IDENTIFIED	SCALEUP NEEDED	PROCESS IMPROVEMENT NEEDED	ACCEPTABLE	REDUCTION DESIRED	REDUCTION NECESSARY
REPEAT HAEDWARE									
ANODE	X			X				X	
CATHODE		X		X			X		
MATRIX		X		X			X		
BIPOLAR PLATE									
SEPARATOR PLATE	X			X				X	
CATHODE CURRENT COLLECTOR	X			X			X		
ANODE CURRENT COLLECTOR	X			X				X	
EDGE SEAL	X			X				X	
REFORMING UNIT	X			X				X	
REFORMING CATALYST		X		X			X		
NON REPEAT HARDWARE									
COMPRESSION SYSTEM	X			X			X		
LOAD BEARING DIELECTRIC	X			X			X		
END PLATE	X			X				X	
MANIFOLD SYSTEM									
- MANIFOLD	X			X			X		
- DIELECTRIC			X			X			X
- GASKET		X		X			X		
- CLAMPING	X			X				X	
CURRENT TAKE-OFF	X			X			X		
STACK INSULATION	X			X			X		

LD1210R

the structure, matrix in terms of mechanical strength, and gasket in terms of seal efficiency. Cost reduction of several components such as anode, end plate, manifold clamping system, and manifold dielectric will be necessary to meet stack cost goals. It may be pointed out that the cost for none of these components individually, except for the manifold dielectric, is very high. Only some reductions in all of the areas identified will have sufficient impact on stack cost.

TABLE 5.3

SUMMARY OF DIELECTRIC CRACKING IN 2kW STACKS:

Dielectric Cracking Minimized With Latest Design and Procedure

Stack	Hours	Retention System	FUEL IN	FUEL OUT	OXIDANT IN	OXIDANT OUT
DOE-5	1400	Leaf Spring	0	0	0	0
DOE-5	2000	Leaf Spring	0	0	0	0
DOE-5	2200	Leaf Spring	0	0	0	0
DOE-6	1400	MHC-1, MVC-1	0	1	2	0
DOE-6	2200	MHC-1, MVC-1	0	1	0	0
DOE-7	800	MHC-2, MVC-1	3	1	2	2
DOE-10	200	MHC-2, NONE	0	0	0	0
AF-2-S	260	MHC-2, NONE	0	0	0	0
AF-2-9A	400	MHC-2, NONE	0	0	0	0
AF-2-9A	1200	MHC-2, NONE	0	1	0	0

5.4 SCALE-UP

Technical issues were examined during both area and height scale-up. The stack area was increased from 1 to 4 ft^2 in the 1987-1988 time frame. Problems encountered and resolved included manufacturing of components to close dimensional tolerance, mechanical deflection and thermal distortion of auxiliary hardware during transients and large thermal gradients. Manufacturing issues were resolved by appropriate selection of fabrication techniques such as tape casting for cell active components. Thermal distortion was overcome by reducing mass and thermal conductivity in large area auxiliary components. Special attention to mechanical strength was found to be critical in handling force concentration and providing uniformly distributed loads. Increased thermal gradients are a direct consequence of area scale-up; however with an internal reforming stack design, the endothermic reforming reaction can be utilized to absorb part of the stack heat generation. Design of the flow configuration in inter-cell reforming units was particularly successful in uniformly distributing heat and electrical current.

Height scale-up results in the accumulation of voltage, since the cells are electrically connected in series. Dielectric isolation of auxiliary components such as external manifolds and voltage-driven electrolyte migration are the current focus of development efforts. A 1ft^2, 60-cell stack shown in Figure 5.8 was tested for over 2000 hours. This stack was operated at natural gas system conditions, meeting BOL performance goal. Post-test electrolyte inventory was measured, migrational effects were quantified, and the need for a high-resistance manifold gasket was identified.

Porous gaskets are currently used to form the gas seal between the rough surface of the stack and the gas manifold. Off-the-shelf ceramic products exhibit good gas sealing properties but provide a low resistance path through which the electrolyte can migrate to the negative end of the stack. A variety of promising approaches were identified to increase the resistance. A detailed discussion on this topic is provided in Section 3.0. A gasket design that may provide an order of magnitude improvement in reducing the rate of migration through the gasket has been identified in out-of-cell evaluation. This gasket is currently being evaluated in a five-cell laboratory scale (250 cm^2) stack. This test represents an accelerated electrolyte migration condition due to high edge/active area ratios of a subscale stack. The end cells and central cell performance lifegraph shown in Figure 5.9 indicate no evidence of migrational effects in approximately 1000 hours, demonstrating significant progress over previous experience with baseline gasket design. A 54-cell internal reforming stack using large area plates (4 ft^2) was assembled under a cost-shared program; an assembled stack photograph is shown in Figure 5.10. Evaluation of the improved gasket in this stack is also planned.

High-voltage dielectric isolation between metallic manifold and stack face is accomplished with dense non-conductive ceramics. These ceramics are typically brittle and possess lower coefficients of thermal expansion than the surrounding metallic components. Scale-up of the stack height imposes fabrication and functional requirements which include: dielectric isolation to >200 V in the operating environment, flexibility to conform to the thermally distorted shape of the operating stack and sufficient mechanical strength to avoid cracking caused by differential thermal expansion during heat-up, cool-down and transient operation. Progress was made in this area by refinement of assembly procedures and adjustment of clamping pressure as discussed in the manifold retention system section.

In the stack height scale-up, average performance remained unchanged (Figure 5.1). Also, excellent cell-to-cell performance uniformity was maintained. The individual cell data of a 20-cell stack obtained at coal system conditions, shown in Figure 5.11, indicate good performance as well as resistance uniformity. The cell temperature profile (in the coolant flow direction) is shown in Figure 5.12. The 20-cell stack operated at coal-gas condition with a cell temperature differential of 90°C and maintained complete thermal balance. As expected, the internal reforming 11-cell stack was operated with a 40°C lower temperature differential than the coal-gas stack.

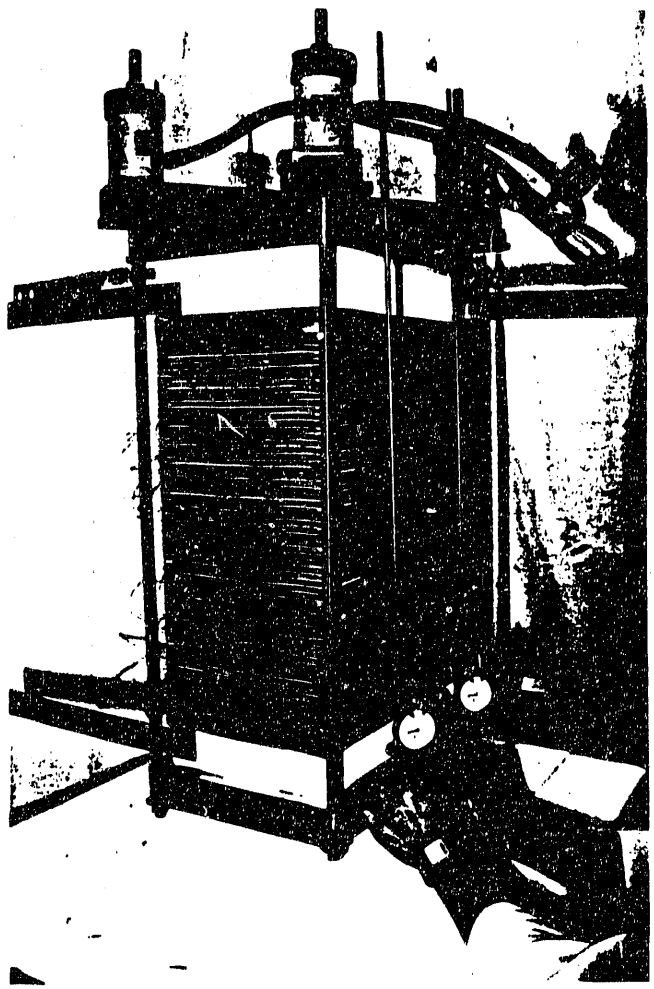

PO722

FIGURE 5.8 SUBSCALE 5kW STACK (AS-5-1)* (1FT², 60-CELL, INTERNAL REFORMING):

This Stack Provided Design Information on Height and Electrolyte Management

* Cost-Shared Stack

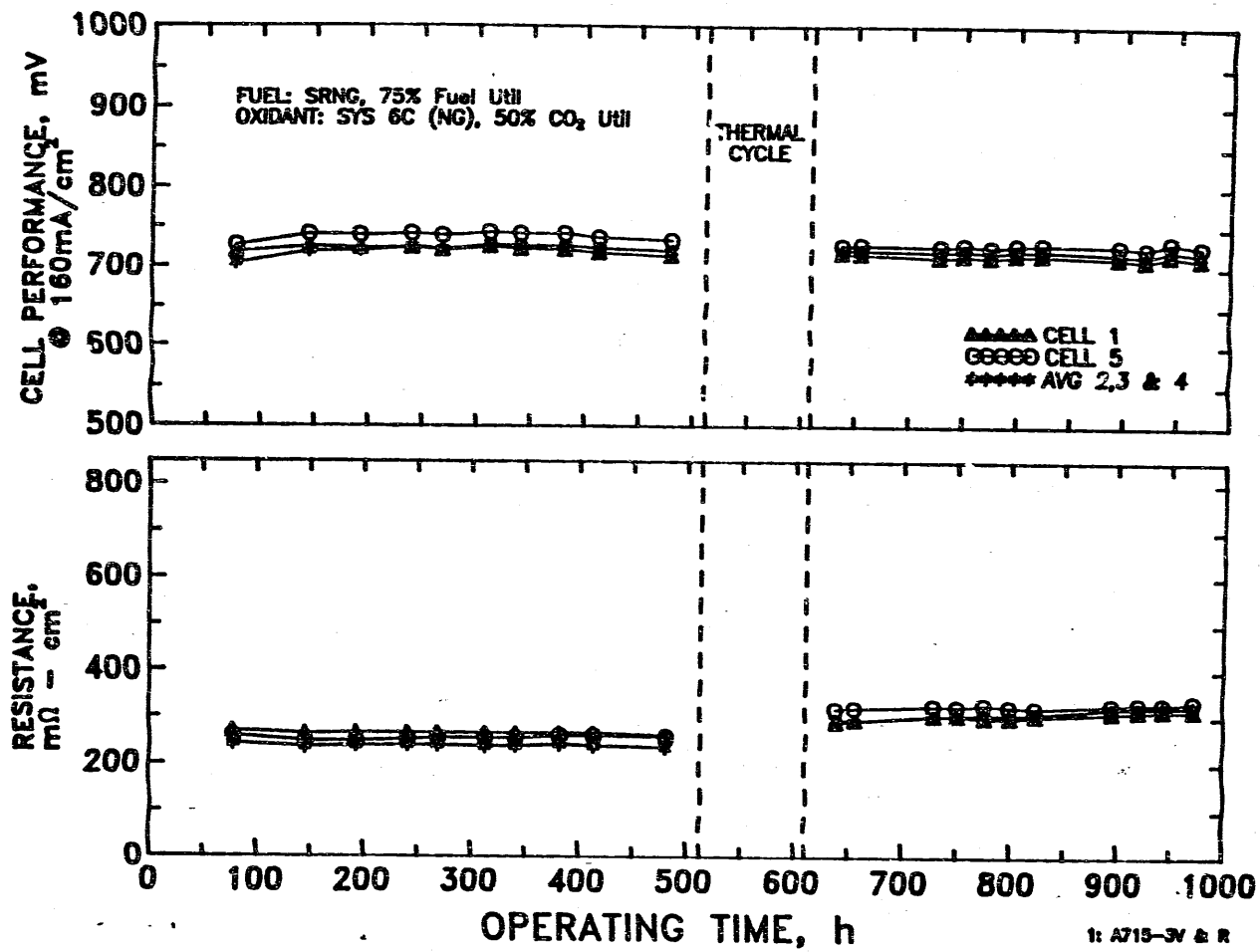

FIGURE 5.9 LIFEGRAPH OF END CELL AND CENTRAL CELL PERFORMANCE IN A LAB-SCALE (250 cm²) STACK:

No Evidence of Migrational Effects in 1000h

FIGURE 5.10 ASSEMBLY PHOTOGRAPH OF A 20kW*, 4FT² AREA, DUAL-FUEL STACK:

Tallest 4ft² Area Stack Built at ERC to Date; Evaluation of Electrolyte Migration Mitigation Approaches Planned

* Cost-Shared Stack

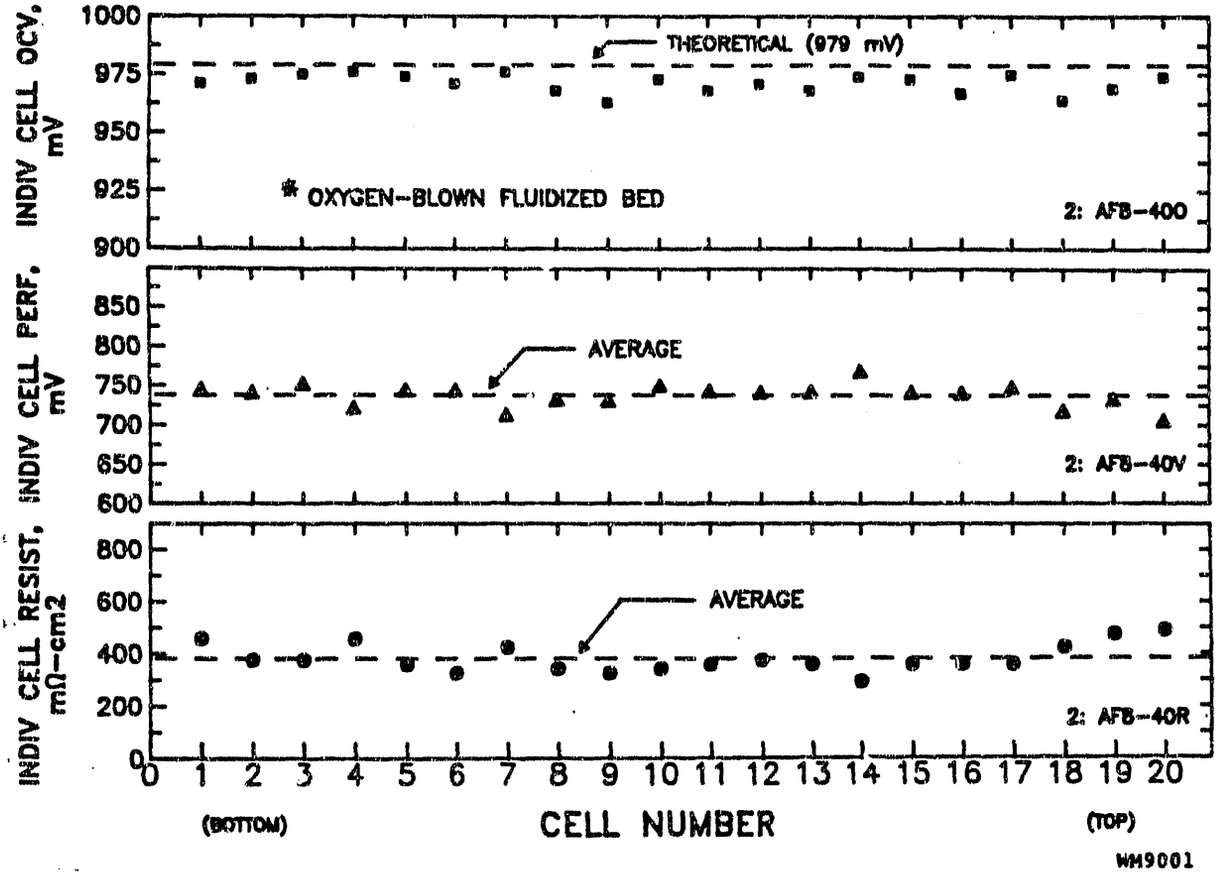

FIGURE 5.11 CELL PERFORMANCE UNIFORMITY AT 140 mA/cm^2 (COAL FUEL AND OXIDANT):

A Narrow Performance and Resistance Spread Between Cells is evident

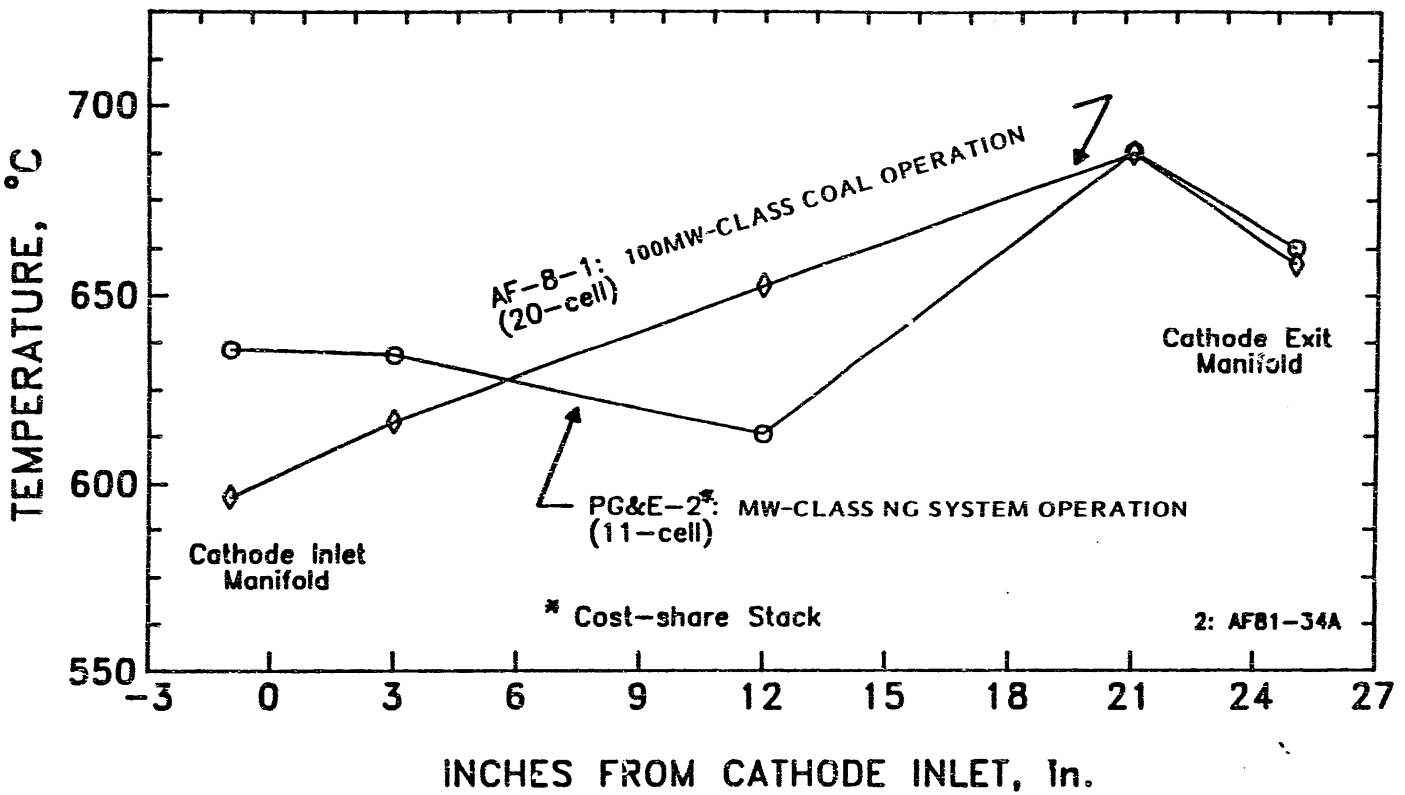

FIGURE 5.12 HORIZONTAL TEMPERATURE PROFILES:

Maintained Thermal Balance and
Operated Normally

5.5 CELL AND STACK STABILITY

Carbonate fuel cell stacks are being designed for a five-year useful life and a 2mV/1000h (i.e. 0.3%/1000h) decay rate in order to be competitive in the power generation market. The current issues limiting attainment of the life goal can be summarized as follows:

- Resistance increase
- Electrolyte loss
  - migrational loss
  - other losses
- Gas seal integrity
  - gas seal formation
  - thermal cycle
- Material stability
  - hardware corrosion
  - cathode dissolution

In short stacks, ERC demonstrated attainment of 3mV/1000h decay rate (i.e., 0.5%/1000h), (Table 5.5). The 11-cell, 4ft^2 stack has been operated at natural gas system conditions for 5000 hours, demonstrating a decay rate of 3 mV/1000h. An increase in cell resistance is partly responsible for observed decay rate. Reduction of the cell resistance increase with time will be sought in future stacks; this issue is being investigated (see Section 3.0 for additional discussion). A Lifegraph for the 5000h stack is shown in Figure 5.12.

TABLE 5.5

DEMONSTRATED CFC DECAY RATE:

ERC has Demonstrated a Decay Rate
of 0.5%/1000h in an 11-Cell Stack

TEST VEHICLE	HOUR	DECAY RATE mV/1000h
Single Cell	10,000	≤
Stack w/1ft^2 Cells (DOE-2, 4-Cell, 1 ft^2)	3,000	3
Stack w/4ft^2 Cells (PG&E-2, 11-Cell, 4 ft^2)	5,000	3

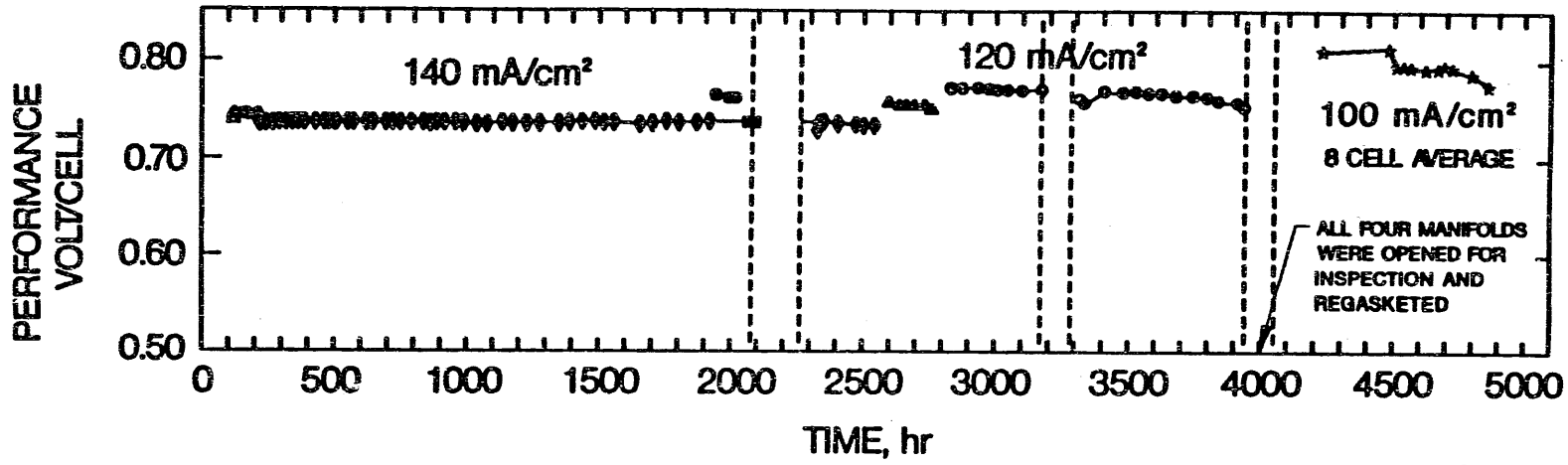

FIGURE 5.13 STACK ENDURANCE; STACK PG&E-2*:

5000h of Operations with Three Planned Room Temperature Thermal Cycles and Several Standby Operations were Demonstrated

* Cost-Shared Stack

Electrolyte loss causes increased resistance and eventually mixing of reactant gases resulting in fuel loss and accelerated corrosion. An electrolyte management strategy was developed to reduce losses to an acceptable level. Further discussion of this issue is provided in Section 4.0.

Gas seal integrity is required for long life. The electrolyte matrix is the component which forms the internal gas seals and separates the fuel from the oxidant. Gas cross-leakage results in combustion, causing high local temperatures and accelerated decay. One of the most significant accomplishments of this program was improvement of the matrix. Refinement of the matrix formulation has resulted in a more compliant component. This enables the matrix to form a continuous wet seal at the cell perimeter, despite variations in bipolar plate dimensional tolerances. Leakage in the cell active area was also reduced due to more complete removal of the organic binders during the initial conditioning process. Results of one evaluation of this component are discussed in Section 3.0.

Thermal cycling of the stack is necessary for plant operation and maintenance. Cracking of the matrix on thermal cycle may occur and was observed on occasion. Such effects were minimized by procedural modifications. Further strengthening of the matrix shear and tensile strength is recommended.

Material stability in the environment of the CFC stack for five years is important. Improvements in hardware stability were accomplished by a corrosion protective coating on the anode current collector and a low surface area cathode current collector fabricated from a corrosion-resistant stainless steel alloy.

Mechanical stability of stack components is required for successful endurance operation. Component stability can be monitored by the measurement of dimensional changes which occur during stack operation. A summary of the height changes during operation for the stacks tested in this program is given in Table 5.6. The table shows that those stacks with acceptable hard rail wet seal designs produced an average height change of 2.2 mils/cell which is well within the design range.

The average corrosion rates of ERC stack metallic components (separator plate, cathode current collector, and anode current collector) observed in several recent stacks operated between 1000 to 5000 hours are presented in Figure 5.14. The solid line represents average corrosion penetration of 2 mils in 40,000 hours of life. This goal is set based on electrolyte loss consideration. It should be noted that a higher corrosion rate could have been tolerated from mechanical strength and gas-sealing limitation considerations. These results demonstrate that the anode side hardware is very stable and the cathode side corrosion is well within the tolerable range.

TABLE 5.6

SUMMARY OF STACK HEIGHT CHANGE DURING OPERATION:

For Hard Rail Stacks the Cell Compaction is Limited
to the Designed-In Active Component Protrusion

STACK ID # (ID #)	OPERATING TIME (H)	HEIGHT CHANGE (mils/cell)	HEIGHT CHANGE GOAL (mils/cell)	COMMENTS
DOE-3	1400	1.2	3	Baseline Design (Hard Rail Wet Seal)
DOE-5	2100	0.8	3	Not Including End Cell Assemblies (Hard Rail Wet Seal)
DOE-6	2100	17**	3	Insufficient End Cell Strength
DOE-7	800	3**	3	Insufficient Edge Rail Strength
DOE-10	200	6**	3	Insufficient Edge Rail Strength
PG&E-2*	5000	4.4	3	Baseline Design (Hard Rail Wet Seal)
AS-5-1*	2000	2.3	3	60-Cells (Hard Rail Wet Seal)

* Represents Cost-Share Stacks

** Designs Rejected

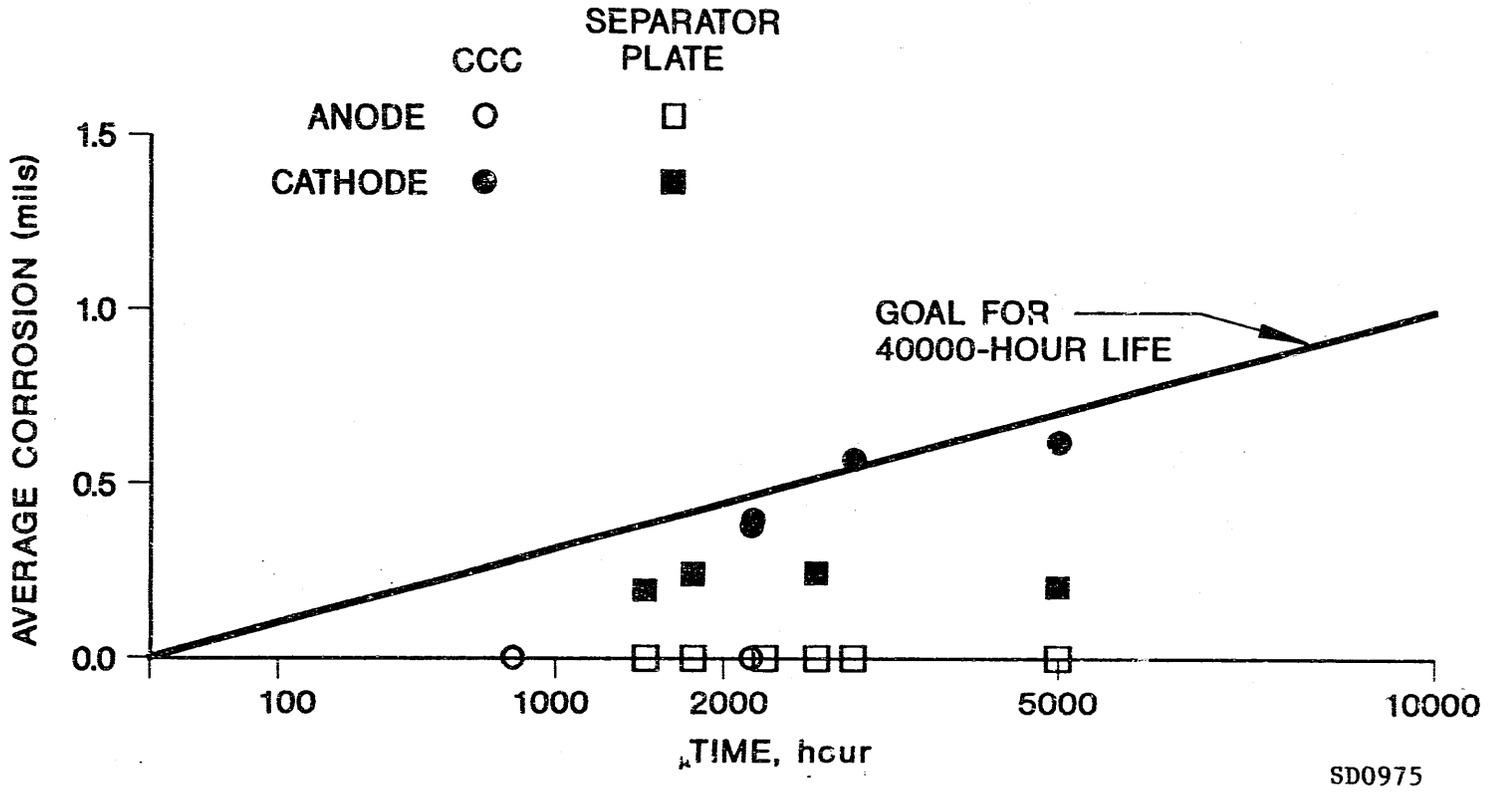

FIGURE 5.14 BIPOLAR PLATE HARDWARE CORROSION IN STACKS:

Selected Materials Meet Corrosion Requirements

5.6 CONCLUSIONS

Excellent progress was demonstrated in resolving stack research issues. No major manufacturing and assembly issues exist at this time. Approximately 7% improvement in cell electrochemical performance, resolution of two key stability issues (cathode stability improvement and electrolyte migration mitigation), development of a cost-effective dielectric separator, and cost refinement of several repeat components remain to be achieved. Successful attainment of these goals will result in a market-responsive stack design.

An 11-cell, 5kW stack has been tested at the natural gas system condition to 5000 hours. A 20-cell, 8kW stack has been operated for 1600 hours, most of which was at coal-gas system condition. A 20kW (54-cell) stack was assembled and made ready for testing. The full-size stack is the next logical step and a demonstration is planned.

6.0 FULL-SIZE STACK DESIGN

The stack to be used in a pilot demonstration of the simplified natural gas power plant design (MW-Class Type B system) has been designed. Both the direct and the indirect internal reforming features (DIR/IIR) have been incorporated to allow stable operation on pipeline natural gas. A 232-cell single stack using 4ft²-area cells with a reforming unit every six cells has been selected.

The power plant demonstration site is at Pacific Gas and Electric Company's Research and Development Facility in San Ramon, California. The stack will be manufactured and pretested at Energy Research Corporation's Danbury facility. The stack will be truck transported from Energy Research Corporation to the customer's San Ramon test site. The carbonate fuel cell transportation logistics related to packaging, environmental, and shock and vibration controls have been established. The cell design and the auxiliary hardware designs already qualified in multiple short stack tests have been incorporated in the stack design. The indirect internal reformer selected has also been prequalified in two short stacks.

6.1 INTRODUCTION

Energy Research Corporation (ERC) is developing MW-Class natural gas fueled (NGCFC) and 100MW-Class coal-gas fueled (CGCFC) carbonate fuel cell power plants. The natural gas power plant designs are significantly less integrated than the coal-gas based plants, as such are expected to be commercialized first. ERC has a plan to demonstrate a 2MW-size NGCFC power plant in the 1993-94 time period. A one-twentieth size NGCFC pilot plant operation has been planned in 1991 at a utility test site. The carbonate fuel cell stack to be used in this pilot plant demonstration has been designed under this activity.

ERC has selected a fuel flexible carbonate fuel cell stack design for the power plant use. A common stack design is employed for various fuel applications. The stack incorporates internal reforming, and therefore, is capable of operation on natural gas as well as various types of coal-gases containing various amounts of methane.

In the ERC power plant conceptual designs (for natural gas as well as coal-gas fuels), the fuel cell power block consists of factory built truck transportable pallets. The pallet is a power block repeat unit and is assembled with full-size stacks on a skid, which provides structural support during transportation and during operation in the field. Each of the pallets will have a power capacity of 1 MW. The repeat element in the pallet is the full-size carbonate fuel cell stack. The overall power block assembly steps are shown in Figure 6.1. The repeating cell package is stacked together with the non-repeating hardware and assembled as a full-size stack. Then several full-size stacks are placed on a skid to provide a truck transportable pallet. The cell design and performance have been verified in several short stacks. The full-size stack has been designed in this task and demonstration is planned for 1991. The pallet demonstration is planned for the 1993-94 time frame. A discussion of the considerations leading to full-size stack design is presented next.

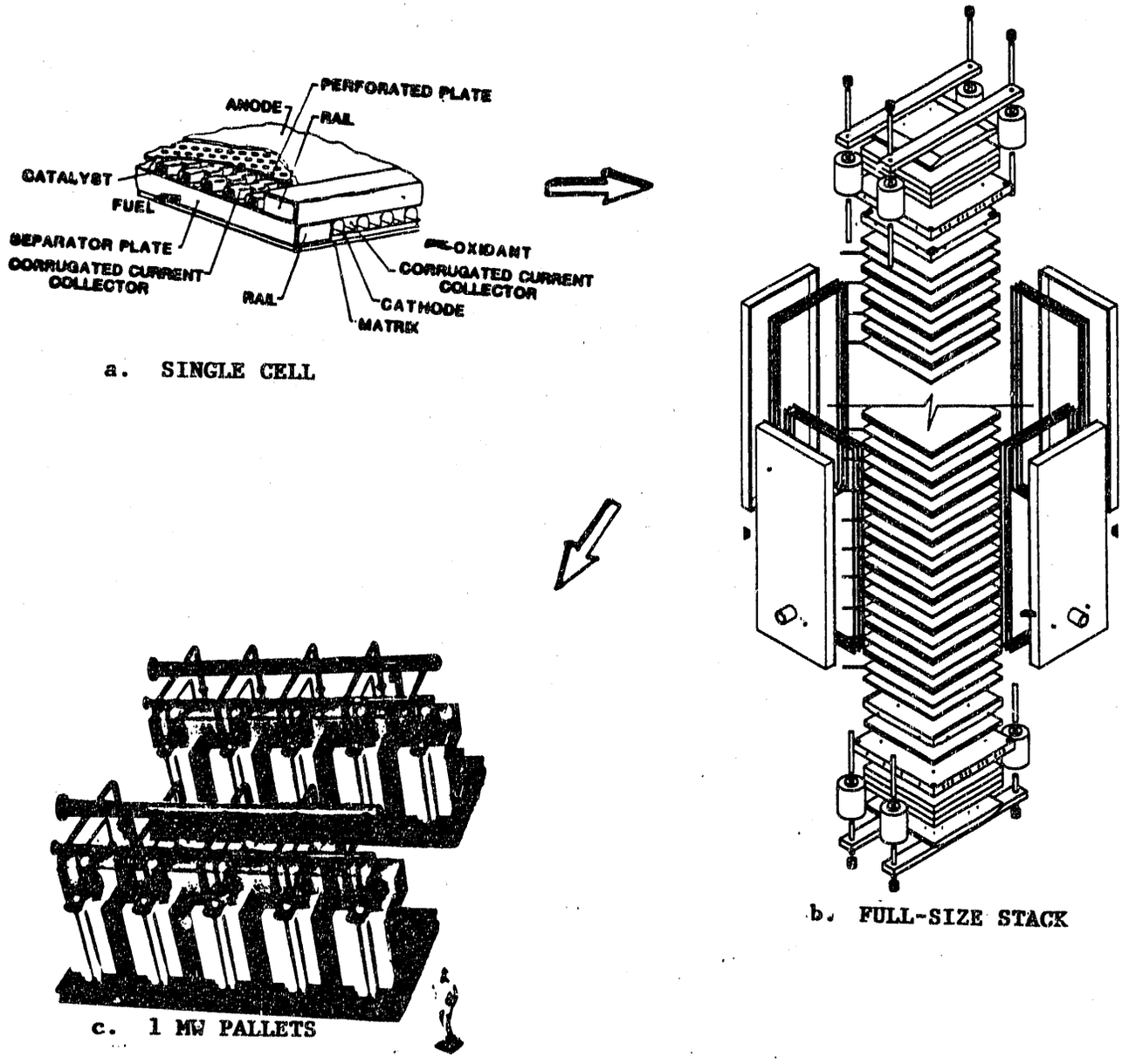

FIGURE 6.1 POWER BLOCK ASSEMBLY STEPS:

Components Defined; Performance Verified; Remaining Important Milestones are Full-Size Stack Tests (1991); Pallet Demonstration (1993-94)

6.2 FULL-SIZE STACK CONCEPT

The full-size stack designed in this activity will be fabricated at ERC and tested at the PG&E San Ramon, CA test site. The field support logistics require that the stack be built and preconditioned at ERC and then transported to the test site. This stack can be built using: (a) a building block unit (BBU) or (b) a single-stack approach. The difference between these approaches are identified in Figure 6.2. In the building block approach, the BBU is a repeat block in a stack. The BBUs are stacked one on top of another to provide a full-size stack. The BBU consists of approximately 60 cells and is manifolded separately. The transportation and field support logistics require that the BBU be factory built and pretested; then transported separately to the field and field-assembled. For the single-stack approach, the stack can be built and pretested at the factory and then transported to the site. For this approach, no field assembly is required. The relative merits and demerits of the two approaches are identified in Table 6.1. Although the BBU approach carries lower technical risk, it has several handicaps. A discussion of these is presented next.

The BBU approach carries lower technical risk because the manifold dielectric can be obtained in one piece from the vendor; the stack contains a smaller number of cells, approximately 60. The stack shrinkage per manifold is only one-fourth that of a single tall stack. The cost impact of the BBU approach is small. On a manufactured cost basis, the BBU approach is slightly more expensive (see cost comparison in Figure 6.3) than the single-stack approach. However, the BBU approach requires the use of two heavy end plates (3-in. thick each) per module, resulting in a total of eight extra end plates for a five-BBU stack. The weight of these end plates approximately doubles the stack weight. The impact of stack weight on cell compression is shown in Figure 6.4. It is evident that the heavy end plates increase the compression on the bottom cells of a 300-cell, five-BBU stack (with respect to the top cells) by $\sim$12 psi. Also, these heavy end plates, because of high heat capacity as well as specific mass content, have significant impact on the stack heat-up rate.

The BBU approach requires each BBU to have its own compression system during preconditioning and transportation; then in the field the compression can be transferred to the tall stack compression system. This load transfer process needs to be accomplished without significant loss of compression. An approach developed to accomplish this is illustrated in Figure 6.5. Here, the module end plate is used as the load transfer plate and load bars inserted inside the end plate hold the module compressive load via tie rods and specially designed bellville washer packs. The compressive load for each BBU can be easily released in the field after assembling the five BBUs to a full-size stack and installing the stack external compression system.

Furthermore, the BBU approach requires extra plumbing for connections to individual BBU manifolds. The packaging and shipping logistics for a multi-BBU stack are also more involved than they are for a single stack.

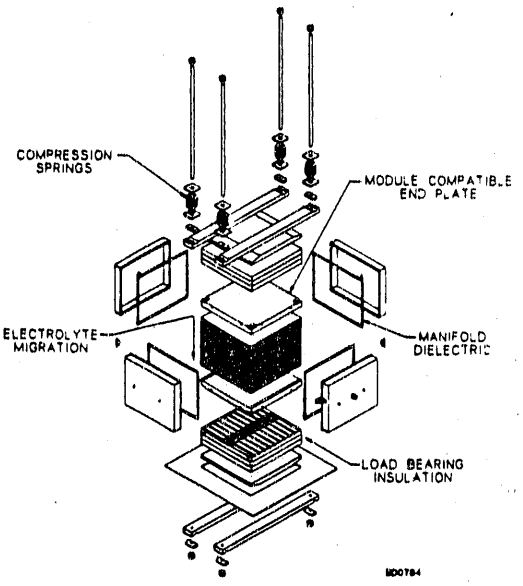

60 CELL MODULE

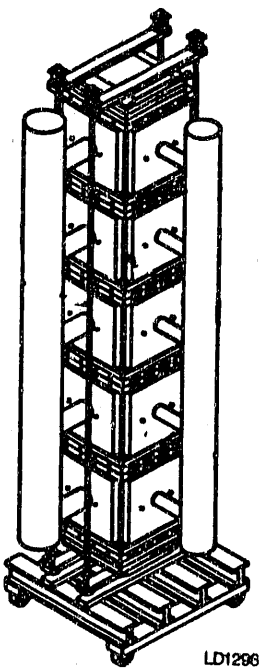

FULL-SIZE STACK

a. BBU APPROACH

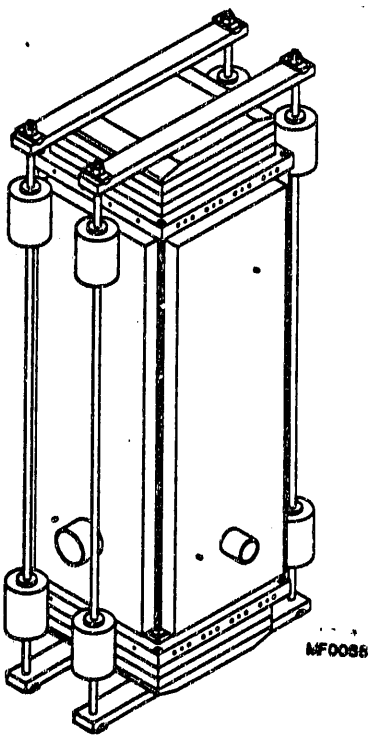

FULL-SIZE STACK

b. SINGLE STACK APPROACH

FIGURE 6.2 STACKING CONCEPTS:

For Simplicity, a Single Stack Approach has been Recommended

TABLE 6.1

COMPARISON OF STACK ASSEMBLY APPROACHES:

A Single Stack Appears to be the Logical Choice

APPROACH	ADVANTAGE	DISADVANTAGE
BBU-STACK	- LOWER TECHNICAL RISK - LOWER INITIAL DEVELOPMENT COST	- HEAVY (EXTRA 8 END-PLATES) - REQUIRES LOAD TRANSFER - EXTRA FIELD ASSEMBLY - EXTRA PACKAGING AND SHIPPING - EXTRA PLUMBING - HIGHER COST OVERALL - LOWER POWER OUTPUT FROM SAME HEIGHT - HIGHER COMPRESSION AT BOTTOM CELLS - LONGER START-UP TIME
SINGLE-STACK	- MORE CELLS PER TRUCK TRANSPORTABLE UNIT - NO FIELD ASSEMBLY - LESS WEIGHT - LESS MANIFOLDS - LOWER COST OVERALL	- STACK SHRINKAGE MANAGEMENT - LARGE SIZE DIELECTRIC AND MANIFOLD ISSUES - FLOW DISTRIBUTION ISSUES - THERMAL EXPANSION MISMATCH MANAGEMENT

MF0014A

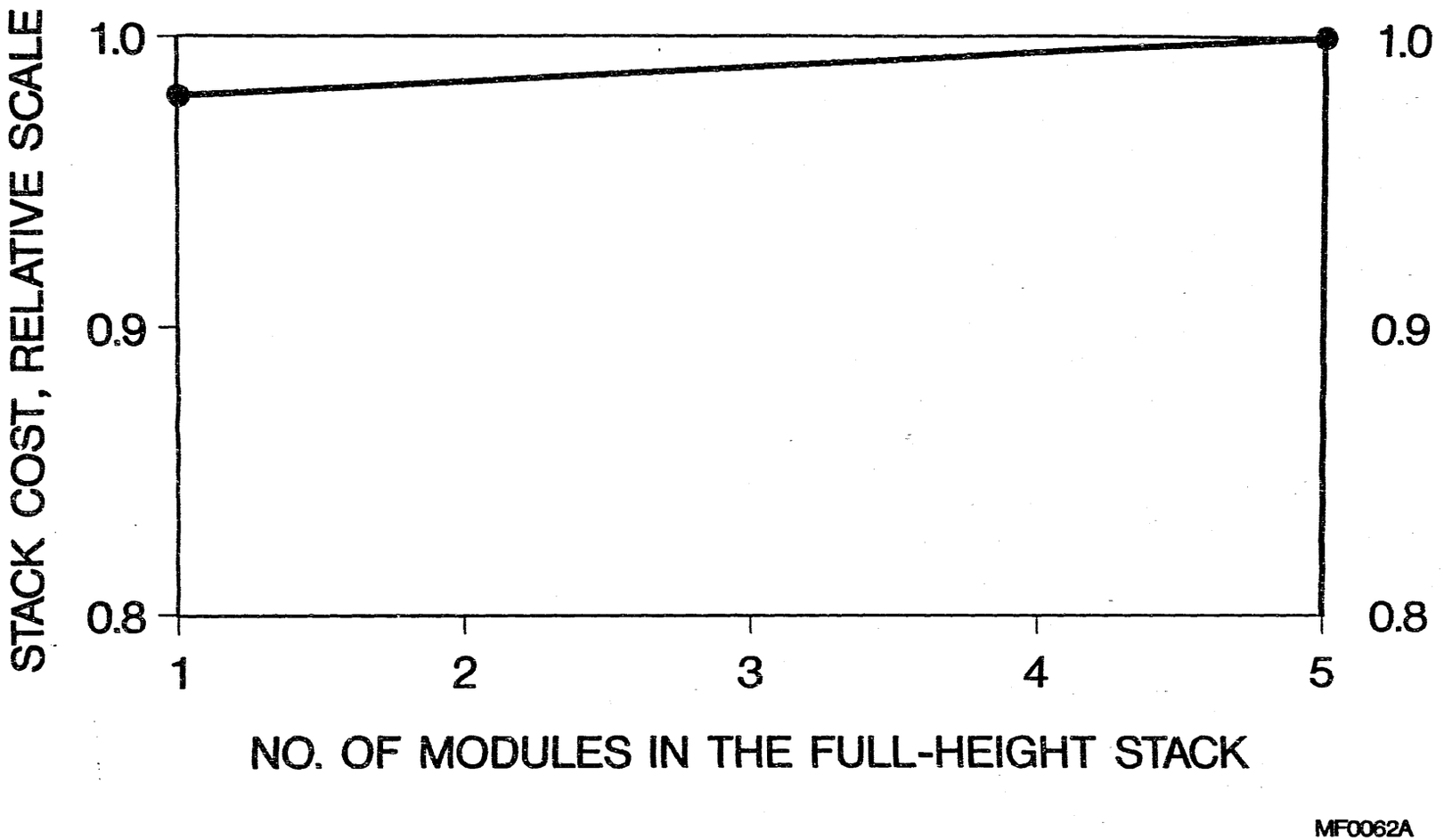

FIGURE 6.3 EFFECT OF NUMBER OF MODULES PER STACK:

A Slight Cost Benefit is Projected for Single-Stack Design

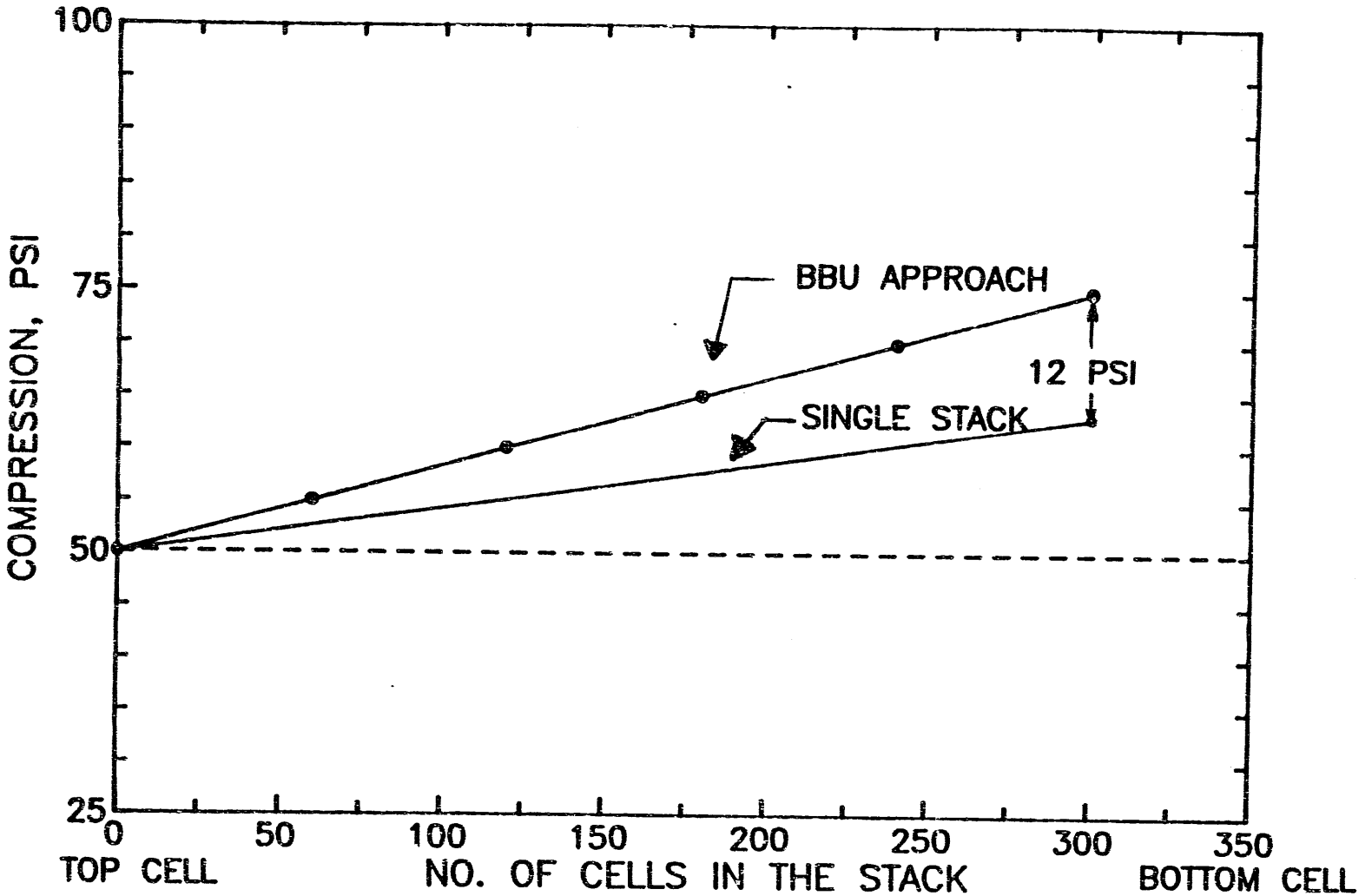

MF0090

FIGURE 6.4 EFFECT OF CELL SIZE ON BOTTOM CELL COMPRESSION:

Use of BBU Approach Results in an Additional 12 psi of Compression to the Bottom Cell of the Full-Size Stack

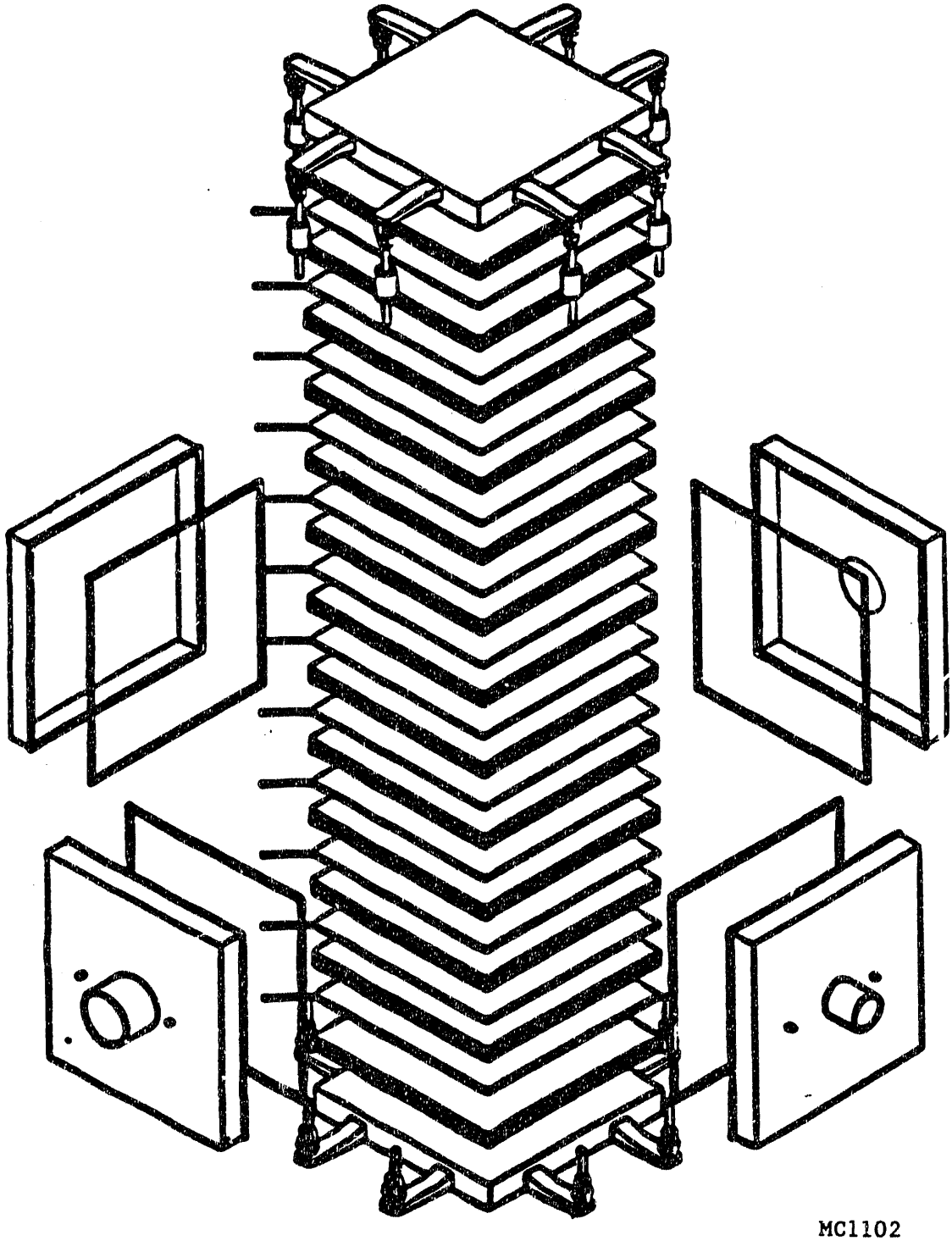

MC1102

FIGURE 6.5 LOAD TRANSFER FIXTURE FOR MULTI-MODULE STACK:

Module End Plate is Used by the Load Transfer Plate

On the other hand, the single-stack approach reduces compression on the bottom cell, requires no load transfer, minimizes field operations, and involves less plumbing. Most importantly, the height saved by eliminating eight thick end plates in a five-BBU stack allows packing of 65 additional cells in a truck transportable full-size stack. These considerations suggest the single-stack approach to be most logical. However, some uncertainties relating to stack height shrinkage management, manifold dielectric design, and flow distribution in the manifold need to be resolved. Discussion on these areas is presented next.

6.3 SINGLE-STACK ISSUES

The single-stack design issues include: stack shrinkage management, dielectric design, flow distribution design, and thermal expansion mismatch management. ERC's design approach for resolution of these issues is discussed next.

6.3.1 Stack Shrinkage Management

Due to the use of unique hard rails in ERC's stack design, the electrode compaction is limited to the designed-in active component protrusion, which is ∿3 mils per cell. The component creep is independent of the number of cells in the stack. Nonetheless, the total height shrinkage of a stack is equal to the sum total of individual cells, and therefore is dependent on the number of cells in a stack. The projected stack height dynamics for a full-size stack are presented in Figure 6.6. A tall stack would undergo a height shrinkage of ∿0.70 in. (3 X 232 = ∿700 mils), ∿30% of it during the first start-up.

For ERC's stack design, the manifolds and stack compression system are completely thermo-mechanically decoupled. Thus, a slip plane exists at the manifold/stack contact surface. When a tall stack shrinks, the resulting sliding force may become approximately two orders of magnitude greater than the opposing friction force offered by manifold compression pressure. Therefore, it is quite likely that the stack and the manifold interface would slide to adjust to their relative height change. During this relative sliding, the gasket on the stack face gets compressed rather than stretched. Therefore, no reduction in gas-sealing efficiency is anticipated from this event. For the 60-cell stack tested at ERC, the stack shrinkage was approximately one-fourth that of a full-size stack, i.e., ∿0.18 inch. This stack maintained proper gas sealing and no tearing of the manifold gasket was observed in post-test analysis. Further verification of this in another 20kW stack is in progress.

6.3.2 Manifold Dielectric

A ceramic window frame is required to electrically isolate the metallic manifolds from the stack voltage. The developmental status of this component is summarized in Section 4.3.2. A single-piece window frame is availabe at the sizes required for a 60-cell BBU stack, but not for a single full-size stack. Nonetheless, a multi-piece design has shown adequate gas sealing and electrical isolation in out-of-cell tests; stack

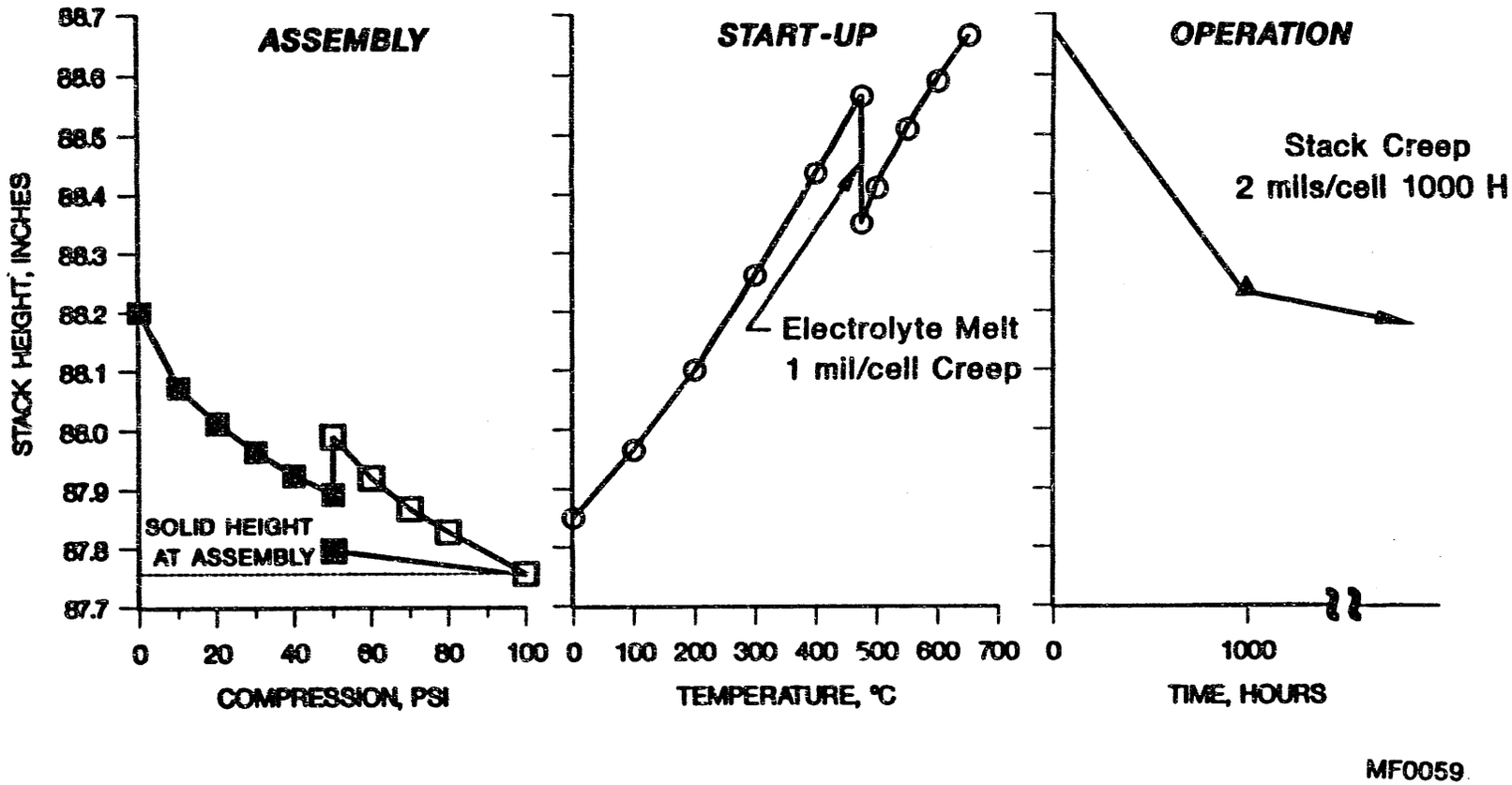

FIGURE 6.6 FULL-SIZE STACK HEIGHT PROJECTION (ACTIVE COMPONENTS ONLY):

A Total Height Shrinkage of ∿0.7 Inch Over Lifetime is Projected Based on the Results of 60-Cell Test

verifications have been planned. This multi-piece design also accommodates thermal expanison mismatch of the stack and the dielelctric. In parallel, a dielectric coating process is being optimized to provide stable dielectric coating of the manifold. The successes with multi-piece design and the coatings will provide the basis for the single-stack dielectric separation approach.

A multi-piece dielectric frame incorporating an expansion joint together with a dielectric coating of the manifold have been defined for the full-size stack use.

6.3.3 Thermal Expansion Mismatch Management

The vertical thermal expansion of the stack body, the dielectric separator, and the manifold are different due to their different thermal properties. During the initial start-up, prior to the electrolyte melting point, the maximum thermal expansion difference between the stack and the dielectric is around 400 mils. After the electrolyte melting point and the inital operating period (650°C), the thermal expansion difference between the stack and the dielectric reduces to the 0-200 mils range because of cell creepage. But, in subsequent thermal cycles, the thermal expansion difference will be in the range of 600 mils. Also, at the operating temperature (650°C), the vertical thermal expansion between the manifold and the dielectric will be ∿600 mils. The corresponding thermal expansion difference in the horizontal plane will be ∿250 mils. To accommodate this thermal mismatch, expansion joints are incorporated in the multi-piece dielectric frame. The thermal expansion mismatch in the vertical and horizontal planes will be accommodated separately by the joints provided in the horizontal and vertical areas of the dielectric, respectively. Each joint in the dielectric is capable of accommodating the appropriate amount of differential thermal expansion without exceeding maximum allowable leakage. To insure proper alignment of the dielectric pieces, the dielectric frame will be captivated inside the manifold sealing lip.

6.3.4 Gas Maldistribution

The causes of flow maldistribution in a fuel cell stack may be due to: (1) cell-to-cell build variables, (2) uneven kinetic head of the gases in the manifold, and (3) variation in hydrostatic head of the gas within the manifolds. The impact of the first two causes are the same for both tall and short stacks. These issues have been studied in short stacks, and a flow distributor design has been developed. This flow distributor design will be employed in the cathode inlet manifold to provide uniform kinetic head. The fuel inlet manifold does not require the use of a flow distributor because of the use of indirect internal reformers (which distributes the reformed gas uniformly to the anode inlet manifold). The cell build tolerances have been controlled through the use of production process improvements and appropriate quality control. The combined effect of these two variables on cell-to-cell flow variation is expected to be less than $\pm 5\%$. This projection is based on the latest stack results. Additional improvements are anticipated in the future as the components are manufactured reproducibly in the pilot manufacturing facility.

The effect of hydrostatic head is a consideration for tall stacks only. The impact of hydrostatic head on flow maldistribution for anode and cathode flows were analyzed and are presented in Table 6.2. The results indicate that only the fuel side is affected because of large density variations between the inlet and exit manifold gases. The resulting flow variations for a 2ft X 2ft tall stack is $\sim\pm$1.6%, which is assumed to be acceptable.

Therefore, for the 2ft X 2ft tall stack, the projected total flow variations are $\pm$6.6%; which translate to performance variations of only $\pm$13 mV.

6.4 SHIPPING LOGISTICS

The full-size stack will be transported to the test site in California. The transportation considerations include size contstraints, vibration and impact control, environment control, and permit requirements. These issues were investigated in detail.

The truck transportation constraints within the USA are identified in Table 6.3. A standard shipping package requiring no special permit is the goal for full-size stack transport. The maximum clearance for the United States road surface is 13.5 feet. The maximum allowable stack height (including the skid and environmental enclosure), assuming use of a double drop low-bed truck, is therefore 11.5 feet. This basically defines the maximum height of a transportable single full-size stack.

The maximum number of cells in a stack is thus set by this 11.5ft limit and the desire to transport a stack in the vertical position. Horizontal transportation is possible and would allow for an increased number of cells per stack, beyond the allowable limit for a vertically transported stack. However, the horizontal shipping approach is more risky, and does not quite solve the issue of the stack pallet transportation which is an important system requirement. Allowing some margin of safety for handling and uncertainties of implementation, the height available for active components stacking is only 88 inches (Figure 6.7). The number of cells that can be accomodated in this space have been estimated to be 232 (considering one reforming unit per six cells).

Since transportation of a preconditioned stack is planned, control of humidity, impact, and vibration ("G" force) is very important. A shipping crate has been designed to implement these controls. Snubbers will be provided to limit impact and vibration loads to a maximum of 3 "G's", and shipping crate relative humidity will be limited to 15%.

A shipping experiment using a 2kW stack was conducted to verify the logistics of handling, transportation, and most importantly verification of "G" force control. A schematic of the shipping crate is shown in Figure 6.8. The crate is completely instrumented to record "G" forces, temperature, and humidity. The stack was transported to Chicago and back using both plane and truck. The "G" force was maintained in all directions around the 1 to 3 range, even during plane landing. Stack leak tests after this transportation experiment did not expose any deleterious effects on manifold or matrix seal efficiencies.

TABLE 6.2

EFFECT OF HYDROSTATIC HEAD ON FLOW VARIATIONS:

The Resulting Effect is Only a ±1.6% Flow Variation

REACTANT	STACK SIZE	PROJECTED PRESSURE DROP AT PG&E DEMONSTRATION CONDITION; INCHES OF WATER	HYDROSTATIC HEAD, INCHES OF WATER		PROJECTED FLOW VARIATION DUE TO HYDROSTATIC HEAD, %
			INLET MANIFOLD	EXIT MANIFOLD	
ANODE	2ft X 2ft	0.55	0.013	0.031	±1.6
CATHODE	2ft X 2ft	1.30	0.034	0.028	±0.25

TABLE 6.3

TRANSPORTATION CONSTRAINTS:

Standard Size Requiring no Permits is Desired; with this Goal the Maximum Allowable Stack Height is 11.5 Feet

1.	Height	13' 6"	(Over this, individual bridges underpasses, etc., have to be considered)
2.	Width	8' 6"	No Permit
		10'	Permit required, no escort required
		>10'	Permit and escort required
3.	Length	22'	Normal
		>22'	Trailer design has to be special
4.	Weight	80,000 lb	Including the tractor
		>80,000 lb	Trailer & tractor design consideration, No escort required

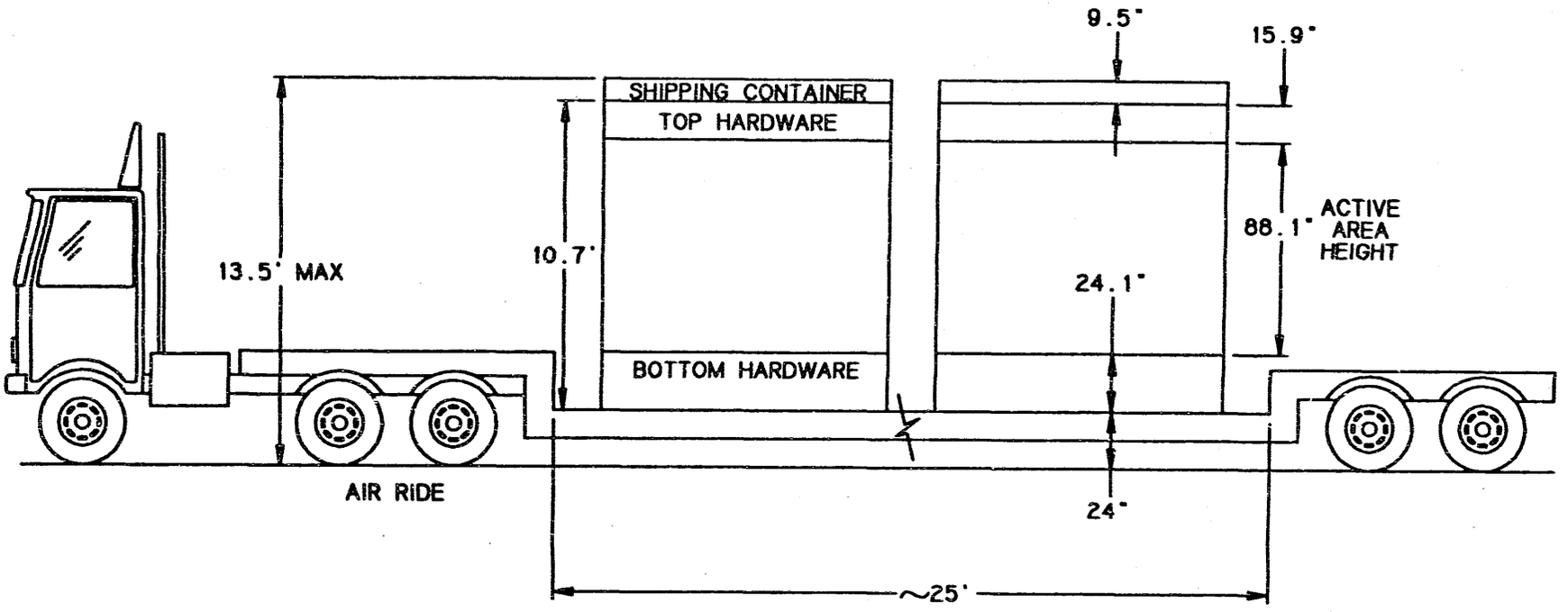

⇨ THE MAX. SHIPPING CONTAINER HT IN A DOUBLE DROP LOW-BED TRUCK IS 11.5 ft

MAX. CLEARANCE: 13.5'
LOWBED: - 2.0'
ALLOWABLE: 11.5'

MF0011c

FIGURE 6.7 TRANSPORTABILITY CONSTRAINTS:

Available Shipping Container Height in a Double Drop Low-Bed Truck is 11.5 Ft

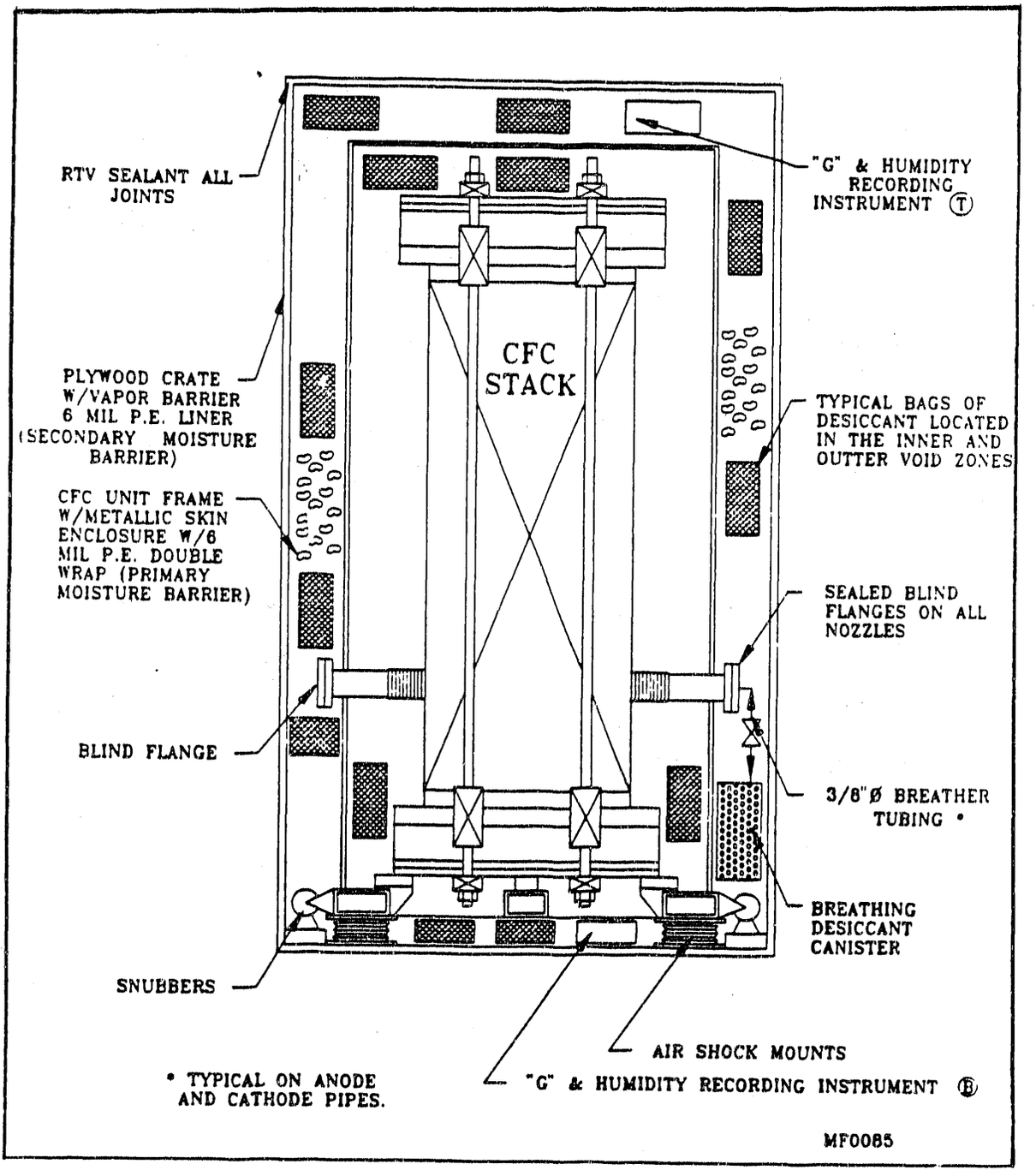

FIGURE 6.8 SHIPPING ENCLOSURE:

"G" Forces and Environment Controls Implemented

The carbonate fuel cell does not require EPA and/or OSHA permits for transportation. Also, no permits are required for international transportation.

6.5 FULL-SIZE STACK COMPONENTS

An exploded view of the full-size stack selected in this effort is shown in Figure 6.9 and the design highlights are provided in Table 6.4. The stack contains 232 cells. The stack includes the IIR/DIR internal reforming approach (this concept is illustrated in Figure 6.10). The stack uses a total of 39 reforming units, one placed every six cells to provide indirect internal reforming of the pipeline natural gas. The internal reformer design has been qualified in subscale stack tests. The stack projects a middle-of-life performance of 75 kW at 140 mA/cm^2.

The detailed design descriptions of the repeating and non-repeating components such as anode, cathode, matrix, bipolar plates, manifold, manifold compression system, end plate, compression plate, and electrolyte management were presented in Section 4.0. These designs have been verified in several short stack tests. Pressure drop characteristics of the anode and cathode side are shown in Figures 6.11 and 6.12, respectively. The stack start-up requires much higher flow than for normal steady state operation; therefore, it results in greater pressure drop. For the steady state on-load operation, the cathode side pressure drop is only 1.3 inches of water. The projected anode side pressure drop is also very small, ~0.5 inches of water. Therefore, the matrix will be subjected to a differential pressure considerably lower than the design goal of 5 inches of water. The reformer unit pressure drop is 10 to 15 inches. This has no impact on cell design since the supply pressure is available at a much higher value.

6.6 CONCLUSION

The full-size stack to be used for the 100kW pilot plant demonstration of the MW-Class power plant design has been designed. The stack consists of 232 single cells with $4ft^2$ cell area and 39 internal reformers (using one reformer unit for every six cells). The stack incorporates an IIR/DIR capability and generates approximately 75kW DC power at middle-of-life at the MW-Class simplified (Type B) system condition. The repeating and non-repeating components of this full-size stack are all proven technology, verified in short stack tests. The stack height will be 11.5 ft, including the skid and environmental enclosure, which is truck transportable on United States highways without requiring any permits.

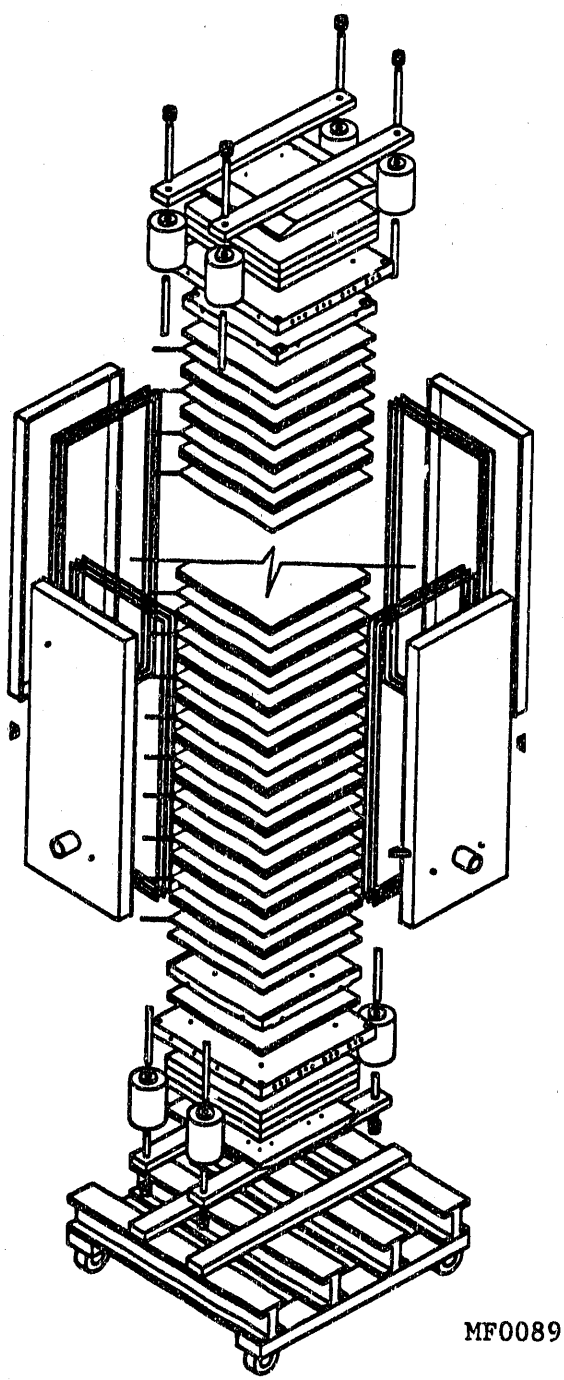

FIGURE 6.9 EXPLODED VIEW OF FULL-SIZE STACK ASSEMBLY:

This 232-Cell ($4ft^2$ Cell Area; 39 Reforming Units) Stack will be Operated at MW-Class (Type B) System Integrated Mode

TABLE 6.4

FULL-SIZE STACK DESIGN FOR FIRST PG&E DEMONSTRATION:

A Truck Transportable Single Stack Containing 232 Cells and 39 Refroming Units has been Designed

CELL SIZE: 2'x 2' (4 ft^2 NOMINAL)
NO. OF CELL: 232
NO. OF RU: 39
NO. OF CELL/RU: 6
TYPE: IIR/DIR
MANIFOLD: EXTERNAL
TOTAL STACK HEIGHT: 11.5 ft.
DIELECTRIC: MULTIPIECE WITH COATING ON MANIFOLDS
STACK NOMINAL POWER: 75 kW DC (at 140 mA/cm^2, 700 mV/cell)

MF0012

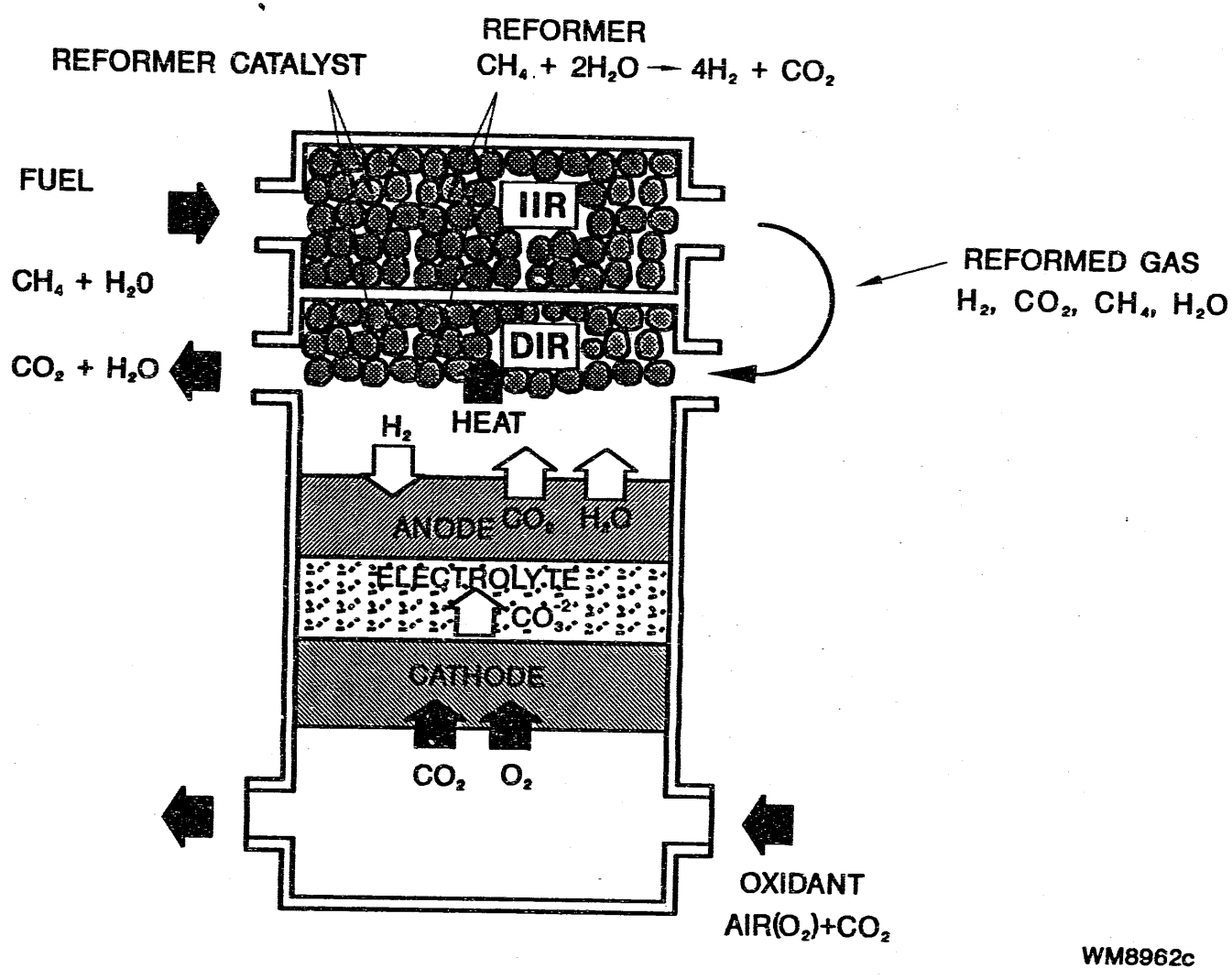

FIGURE 6.10 OPERATING CONCEPT FOR THE IIR/DIR CFC DESIGN:

The IIR/DIR CFC Design has been Incorporated allowing Operation on Pipeline Natural Gas as well as Coal-Gas

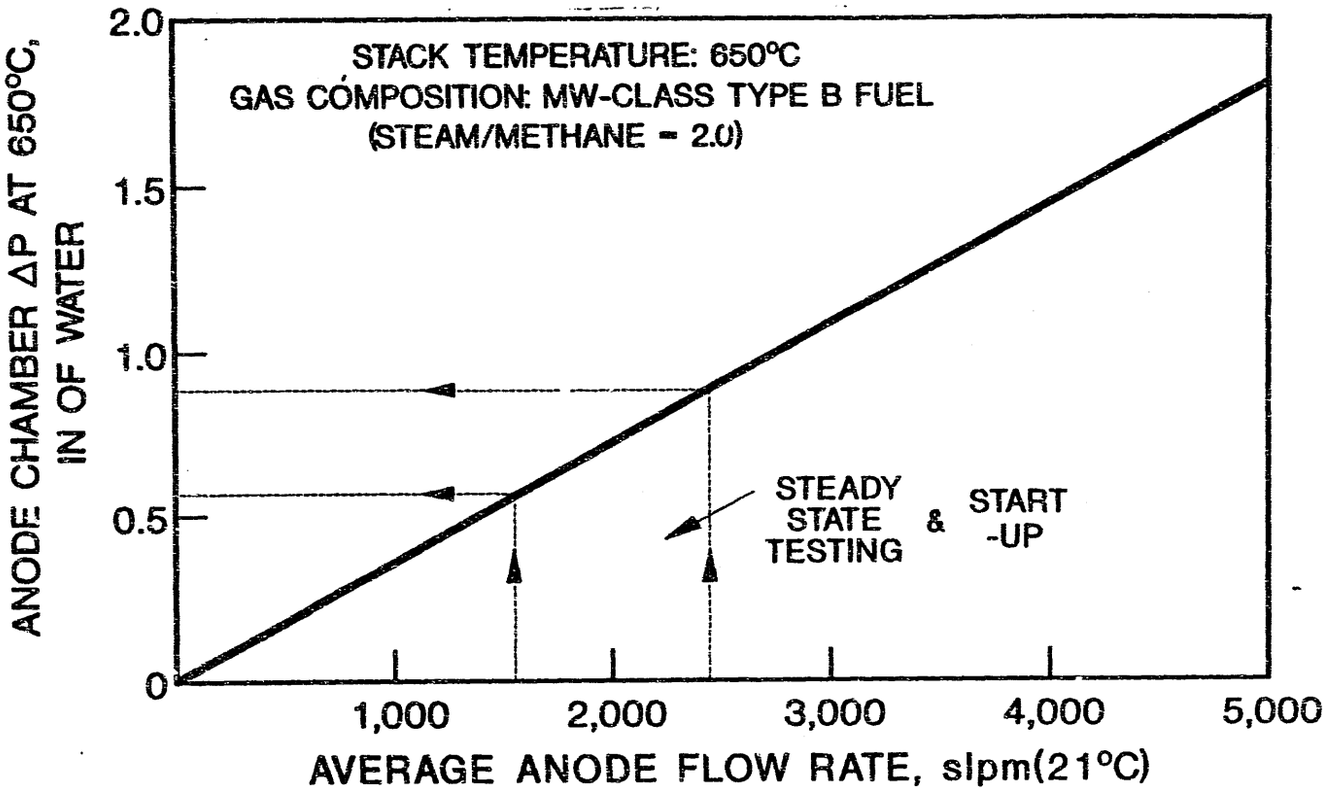

FIGURE 6.11 PROJECTED PRESSURE DROP CHARACTERISTICS FOR FULL-SIZE STACK (4 ft²):

Pressure Drop Through the Anode Chamber does not Include the Reformer Unit; A 10-15 Inch H_2O Pressure Drop is Expected for the RU. The Start-up Flow Rate is Almost Similar to the Steady State Operating Range (140-160 mA/cm²)

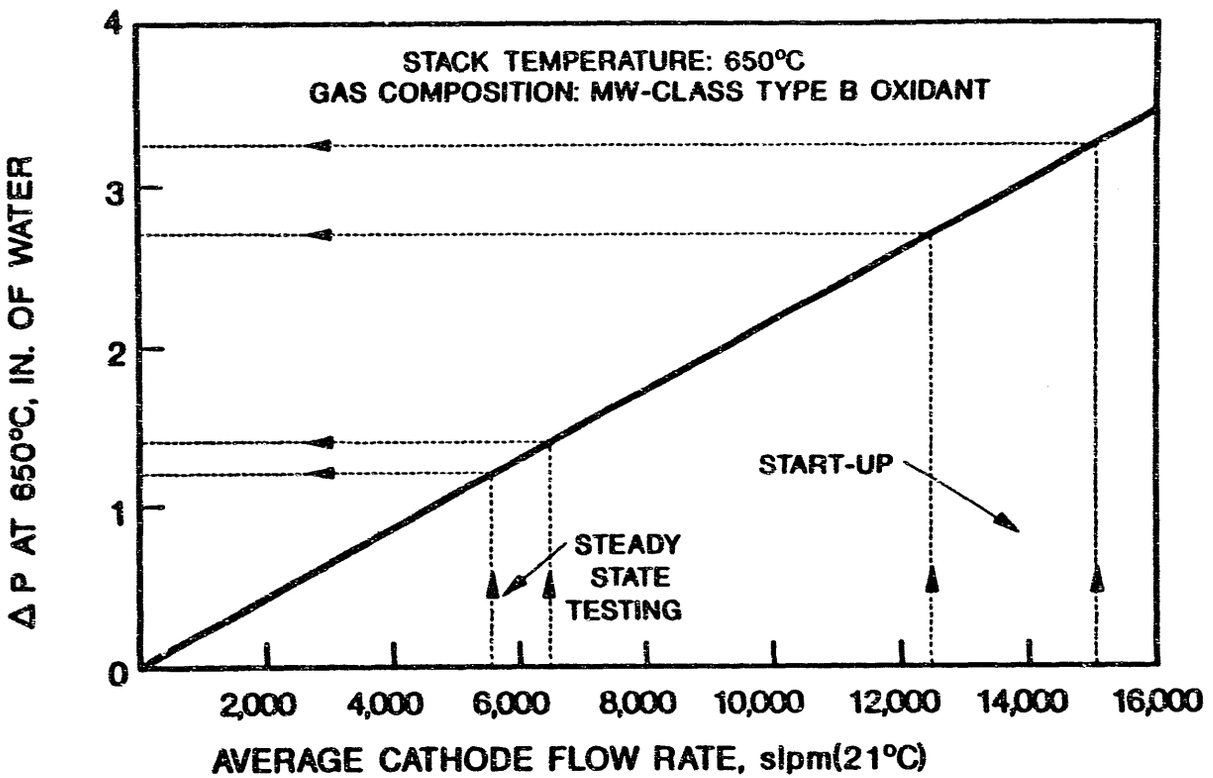

WM9030

FIGURE 6.12 PROJECTED PRESSURE DROP CHARACTERISTICS FOR FULL-SIZE STACK (4 FT²):

Pressure Drop Through the Cathode is Higher than Anode Due to the Higher Flow Rate and the Different Current Collector Design

7.0 TEST FACILITY DEVELOPMENT

The capability and reliability of existing test facilities have been greatly improved. A new flexible facility was designed and fabricated to test taller stacks in the size range of 8 to 32 kW. This facility can simulate gas compositions for different type natural gas as well as coal-gas power plants. Capability for future pressurization was also incorporated. Provision is made for recirculation of cathode gases and regenerative heat exchangers, thus providing experience towards power plant system operation.

7.1 INTRODUCTION

The objective of this topical area was to supply the necessary test facilities, maintenance and support required for the carbonate fuel cell testing effort of the program. This testing included lab-scale (7in. X 7in.), 2kW size stacks, and 8-32kW size stacks. Also, ERC has developed capabilities for reliable addition and detection of coal-gas contaminants. Operation of these facilities has been demonstrated and their reliability and flexibility have been progressively improved via cumulative experience of 26,000 stack operating hours.

7.2 LAB-SCALE (7in. X 7in.) FACILITIES

The capabilities of the existing lab-scale test facilities were expanded to allow operation on various coal-gasification carbonate fuel cell (CGCFC) system conditions. The reliability of the test panels was also improved through design revisions and implementation of a preventive maintenance program. Four of the stations were modified for operation with various coal-gas contaminants. The capabilities required to measure, inject, and quantify these contaminants were also developed. This upgrading process was completed with minimal impact on the lab-scale testing schedule by staged addition of features. The lab-scale test stations now have the following major capabilities:

- Flexible fuel compositions for simulating desired system conditions:
  - centralized gas blending for cost effectiveness
  - special compositions simulated at individual stations
- Flexible oxidant composition (simulation of different system compositions is possible)
- Unattended round-the-clock operation (fail-safe safety circuit)
- Manual data collection
- Four of the stations are equipped with systems for introducing contaminants and safety and alarm systems necessary for handling the contaminants.

7.3 2kW-SIZE STACK TEST FACILITIES

An existing 2kW stack test facility was modified to allow flexible operation on various CGCFC system conditions. Operational reliability was significantly improved. The capabilities were installed to add coal-gas contaminants and unstable (carbon-containing) gases to the facility. An exhaust gas management system was added due to the toxic nature of some of the coal-gas contaminants. The implementation of these features was carried out with a minimum impact on the testing schedule. In fact, the 2kW stack facility has been used quite extensively for the last two years. Two photographs of this facility are shown in Figure 7.1. In total, ten stacks have been tested in this facility. Last year alone, the facility was utilized for well over 60% of the time and provided a very high reliability: no facility related failure was experienced. The key features of this facility include:

- Flexible fuel and oxidant compositions to simulate natural gas and coal-gas CFC systems
- Fail-safe shutdown
- Automatic process monitoring (PM) and data acquisition (DAS) (with redundant operator control)
- Once-through cathode flow
- Highly reliable (redundant features) and easily maintainable

7.4 5kW SIZE STACK TEST FACILITY

A flexible 5kW stack test facility, shown in Figure 7.2, was provided for some DOE stack testing by a cost shared EPRI/ERC/PG&E effort. The facility can test stacks up to the 8kW size (5kW nominal design) at ambient pressure. The facility has single pass process streams and regenerative gas heating. This facility was available at the beginning of the program and allowed stack testing to start prior to completion of the 8-32 kW facility (see Section 7.5).

7.5 8 TO 32kW SIZE TEST FACILITY

Under this program, a flexible test facility capable of operating an 8 to 32kW size stack was designed, fabricated, checked out, and qualified. A flow schematic of this facility is shown in Figure 7.3. Various views of the completed facility are shown in Figure 7.4.

A major design goal of this facility was high reliability. This was accomplished by careful design and by the use of redundant critical components where practical. Standby power was provided to minimize unscheduled stack thermal cycles. The facility has the flexibility for easy upgrading to higher capacities or design conditions. It also has

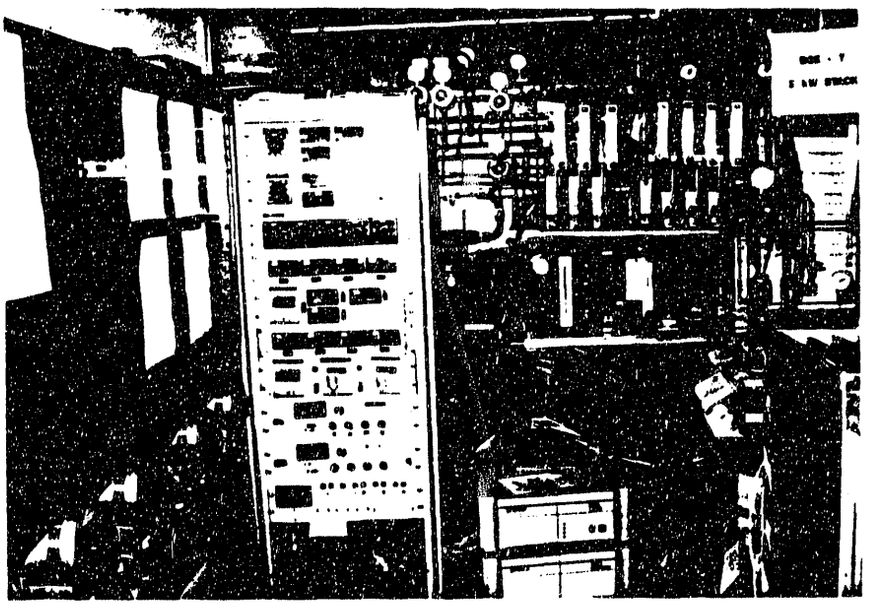

PM0562

a Test Panel and Instrumentation

PM0563

b DOE Stack (DOE-7) on Test

FIGURE 7.1 THE 2kW FACILITY CAPABLE OF TESTING AT CGCFC SYSTEM CONDITIONS:

The System was Used Extensively Under this Program

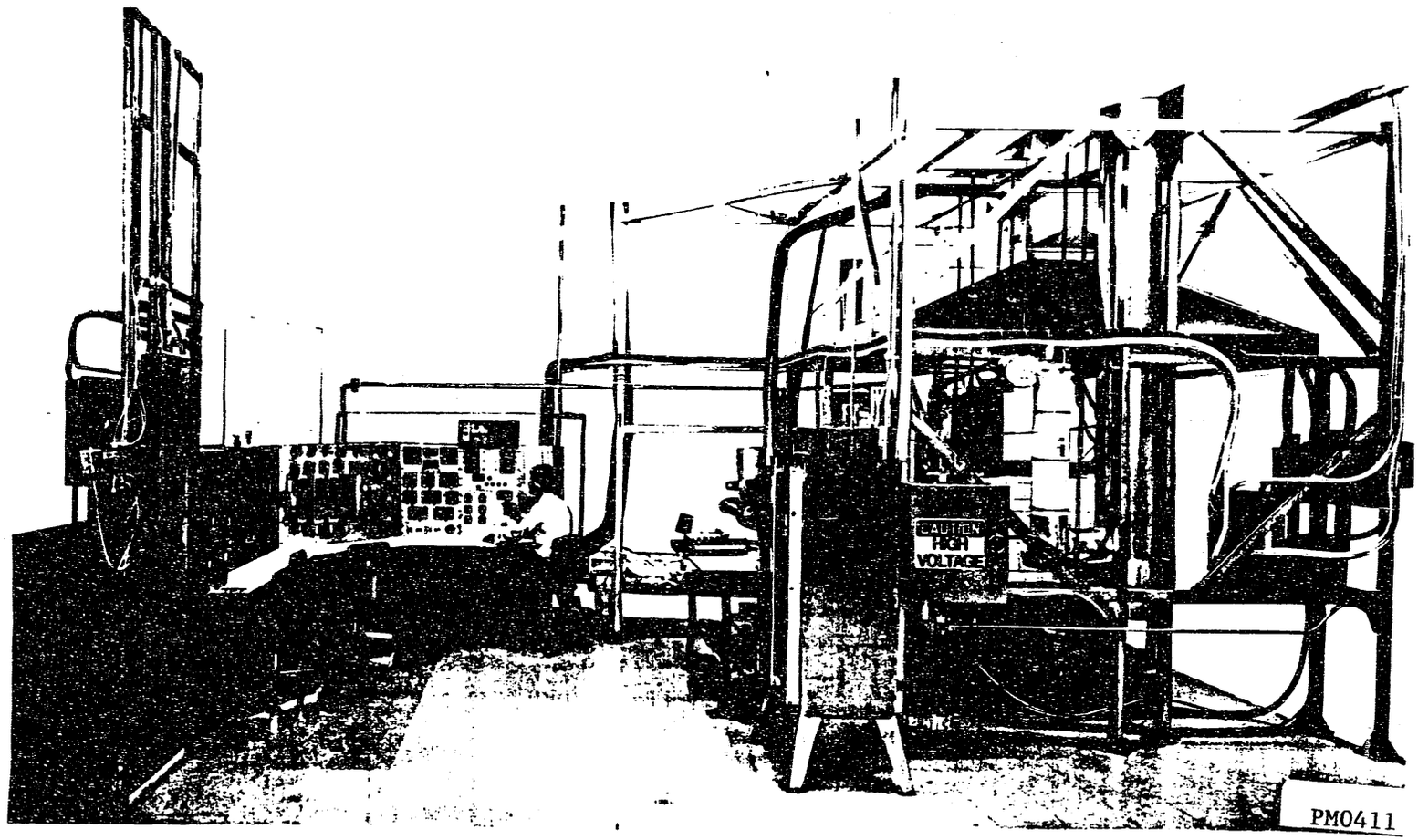

FIGURE 7.2 A FLEXIBLE 5kW TEST FACILITY:

This Facility was Available at the Beginning of the Program to Allow Early Stack Testing

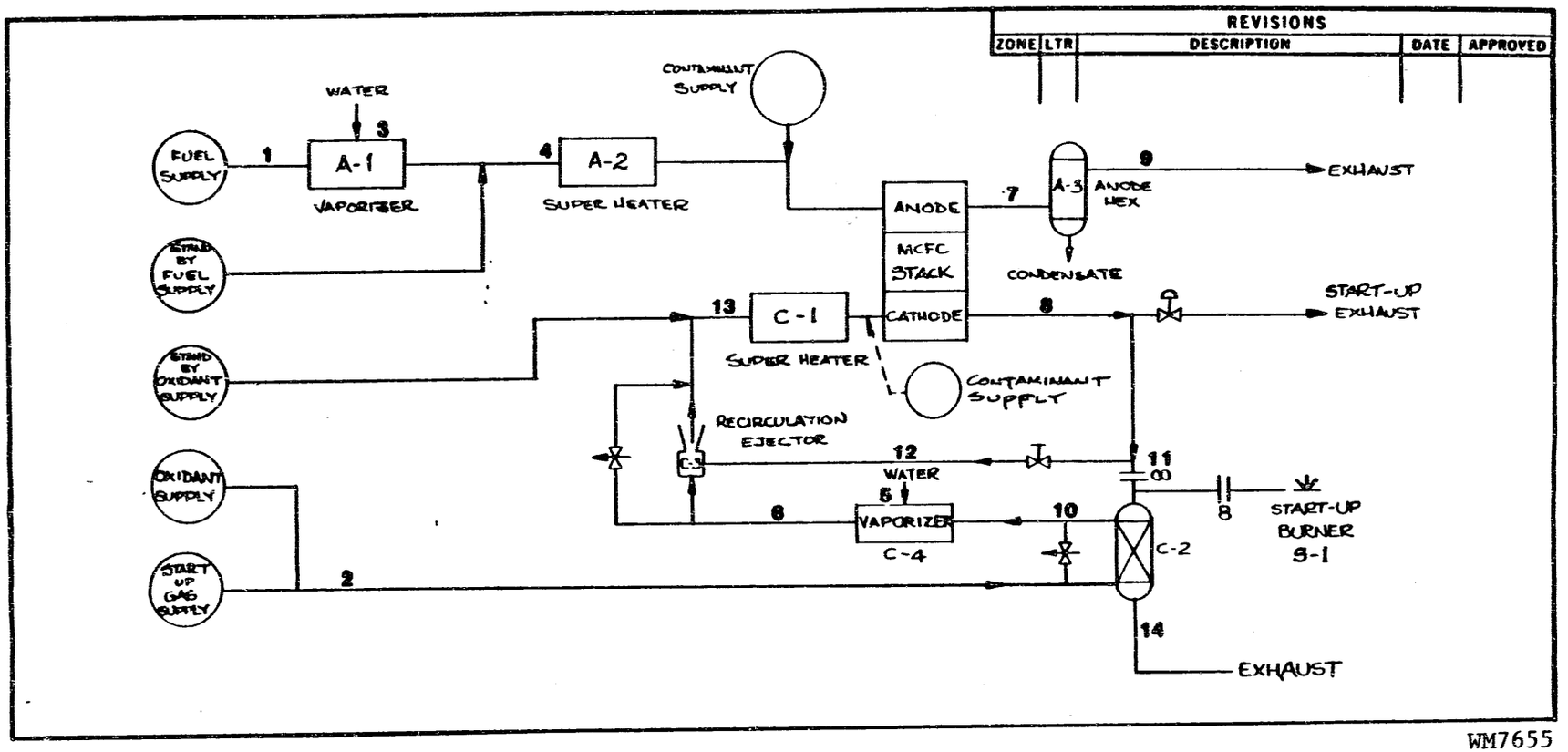

FIGURE 7.3 FLOW SCHEMATIC FOR 8 TO 32kW FACILITY:

Cathode Recirculation and Regenerative Heat Exchangers are Provided to Gain Experience Towards Power Plant Development

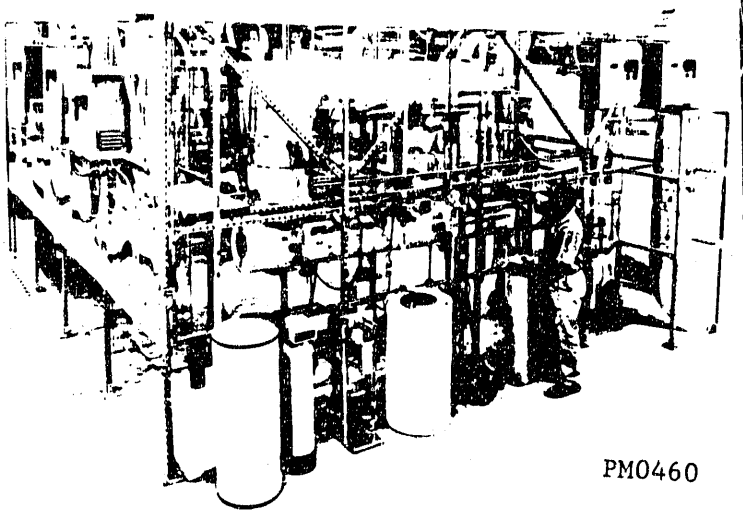

PM0460

Facility Includes All
Required Process Equipment

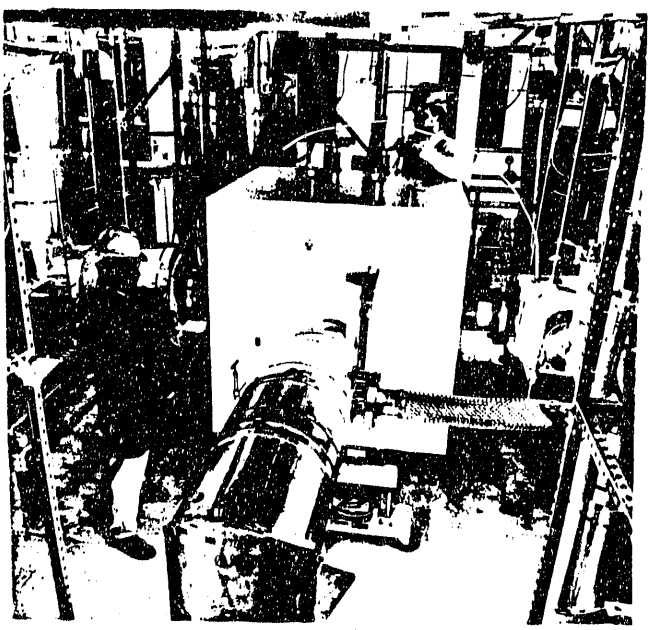

PM0470

Facility Operation Check-out In
Progress Using a 60-Cell Stack
Simulator

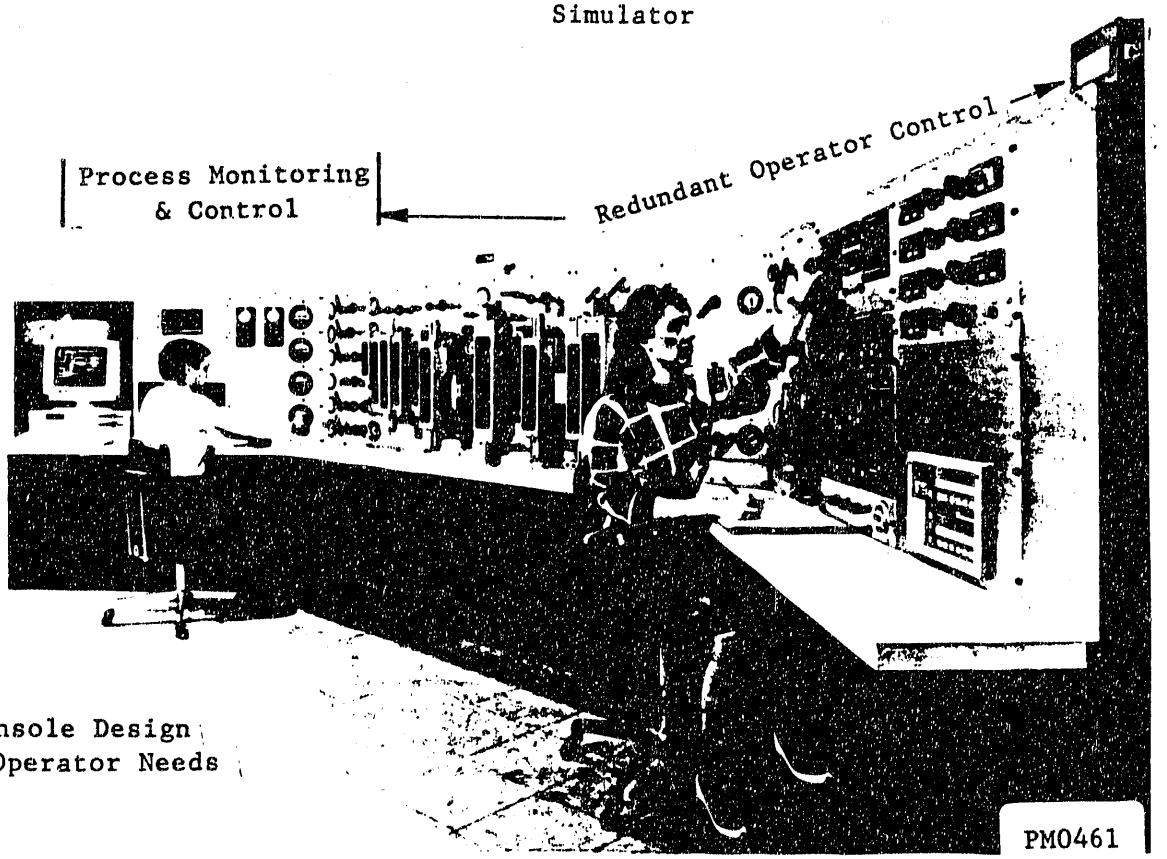

Control Console Design
Minimizes Operator Needs

PM0461

FIGURE 7.4 ERC'S 8 TO 32kW STACK TEST FACILITY:

This Facility Provides Cathode Recycle

the capability to simulate the conditions anticipated for the CGCFC systems. Several design approaches were used to minimize operating costs. The facility was designed for unattended operation to reduce the labor cost for long-term operation. As shown in Figure 7.3, recirculated cathode flow and regenerative heat exchangers were used to conserve process fluids and heat. A failure mode control system was incorporated to minimize undesirable stack upsets due to system malfunctions or upsets during unattended operation. The major facility capabilities are:

- Atmospheric operation (plumbing retrofittable for pressurized operation)
- Flexible fuel and oxidant compositions for simulating natural gas and coal-gas operating conditions
- Hot cathode recycle, start-up burner, regenerative heat exchangers
- Fail-safe shutdown
- Automatic process monitoring (user-friendly on-line), control and data collection (with redundant features for operator control)
- Carbonate Fuel Cell power conversion for AC use.

The facility was designed with flexible operation as a goal. It can simulate various system process gas compositions. It can also accommodate various size stacks. These flexible operating ranges are presented in Table 7.1.

The facility is complete and operationally qualified. The testing operators have been trained in the facilities operation. A preventive maintenance program was established and initiated. This facility will continue to be used to qualify and test the tall stacks.

TABLE 7.1

8 TO 32kW TEST FACILITY OPERATING RANGES

This Facility Has Very Flexible Operating Ranges

PARAMETERS	
Electrical	
Power Output (kW)	Up to 35
Total Voltage (V)	13-63
Cell Voltage (mV)	658-787
Stack Current (A)	163-652
Temperature	
Stack Operating (°C)	625-675
Oxidant Inlet (°C)	700 Max.
Fuel Inlet (°C)	700 Max.
Pressure and Flow	
Operating Pressure (atm)	1*
Stack Back Pressure (inches of water)	<0.5
Oxidant Flow Rate (SCFM)	44-345
Oxidant Pressure Drop (inches of water)	<5
Fuel Flow Rate (SCFM)	3-28
Fuel Pressure Drop (inches of water)	<5
Other	
Number of Data Points Monitored	200
Stack Height (feet)	<8'6"
Stack Weight (lbs.)	20,000

*Retrofittable to 3.4 atm operation.

8.0 CARBONATE FUEL CELL STACK COST ASSESSMENT

Energy Research Corporation, utilizing the services of a manufacturing consultant (Fluor-Daniel,Inc.), has developed a detailed materials and manufacturing cost estimate of the carbonate fuel cell stack. The cost estimate has been arrived at through defining components manufacturing processes, establishing a conceptual design for a fully equipped and staffed manufacturing plant, and obtaining materials cost quotes from vendors. A computer cost model was developed and utilized to evaluate various design concepts. Stack cost sensitivities to cell size (4 ft² to 16 ft²) production volume scenarios (400, 800, and 1600 MW per year) and production parameters were investigated.

The findings of this study showed that the carbonate fuel cell costs are sensitive to production volume, manufacturing equipment capacity, especially the Ni-plating line speeds and widths, and to cell size only at the larger production volume (1600 MW) only. The carbonate fuel cell cost appears to be materials driven, contributing over 60% of the final cost. The bipolar plate material alone contributes 45% of the material cost, and thus provides the best opportunity for cost reduction. A significant materials credit, over 20% of the initial stack cost, appears to be feasible by recovering material contents of a used carbonate fuel cell stack in the form of specialty steel.

8.1 INTRODUCTION

The stack is the heart of a carbonate fuel cell (CFC) based power plant. In most system designs depending on the applications, the fuel cell provides 50 to 100% of the output power. As an example, in a coal gasification based plant design (design and performance of several cases are discussed in Section 2 of this report), roughly two-thirds of the power is produced by the fuel cell. Therefore, a systematic study was undertaken to investigate manufacturing and cost feasibilities of this key component of the carbonate fuel cell power plant. The services of several manufacturing consultants, including that of Fluor-Daniel, Inc., who provided a leading role in establishing the plant design and the manufacturing cost model, were utilized.

The major objectives of this CFC stack cost study were:

- Develop plant layout concept for carbonate fuel cell manufacture and assembly.
- Determine manufacturing cost of carbonate fuel cell (CFC) based on proven manufacturable design in production volume of hundreds of MW per year.
- Identify design refinements that would improve the manufacturability and reduce cost of fuel cells.

8.2 STUDY APPROACH

8.2.1 Stack Design Basis

An approach outlined in Figure 8.1 was followed to define the stack manufacturing plant design and stack cost estimate. First, a stack design was defined to provide guidelines for selection of component designs in terms of mechanical specifications and choice of materials. The initial stack design, derived from ERC's most current experience, included proven component designs. Next, the basic ERC stack design was reviewed to identify improvements that would facilitate component mass-manufacture, and volume assembly, and therefore, cost savings. The major improvements identified were:

- Replace Inconel components with Ni-plated ones.
- Use Ni-plated in place of Ni-clad stainless steel.
- Reduce thickness of manifold skins and some of the repeat components.
- Replace ion vapor deposition (IVD) aluminizing with cost-effective alternatives (aluminum tape or painting).
- Use lightweight end cell design in place of the presently used solid end plate design.
- Replace solid alumina frame with ceramic coated material for manifold dielectric use.

Research and development activities have already been initiated to attain these cost improvements.

The fuel cell stack design utilized in this cost study assumes these improvements and consists of 300 cells, external compression plates and hardware, electrical insulating plates, and thermal insulation. Each fuel cell module consists of sixty 24in. X 24in. fuel cells with one manifold on each face, and two end cells. Each fuel cell consists of a bipolar plate that contains an anode current collector and electrode on one side and a cathode current collector and electrode on the other side. Each fuel cell is separated by a tape matrix.

8.2.2 Component Manufacturing

Next, the manufacturing process and production lines for all key components were established. First, the specifications for each component as defined by the stack design were assessed to evaluate the ERC used processes as well as fabrication specification. Alternate processes for component manufacture were cataloged and reviewed in terms of processing time required, mass-producibility, environmental impact, and most importantly, cost of production. Based on this analysis the production system concept for components fabrication and assembly (using already proven processing) were established. The tape casting method was selected for anode and matrix manufacture. A dry doctoring process was selected for cathode manufacture.

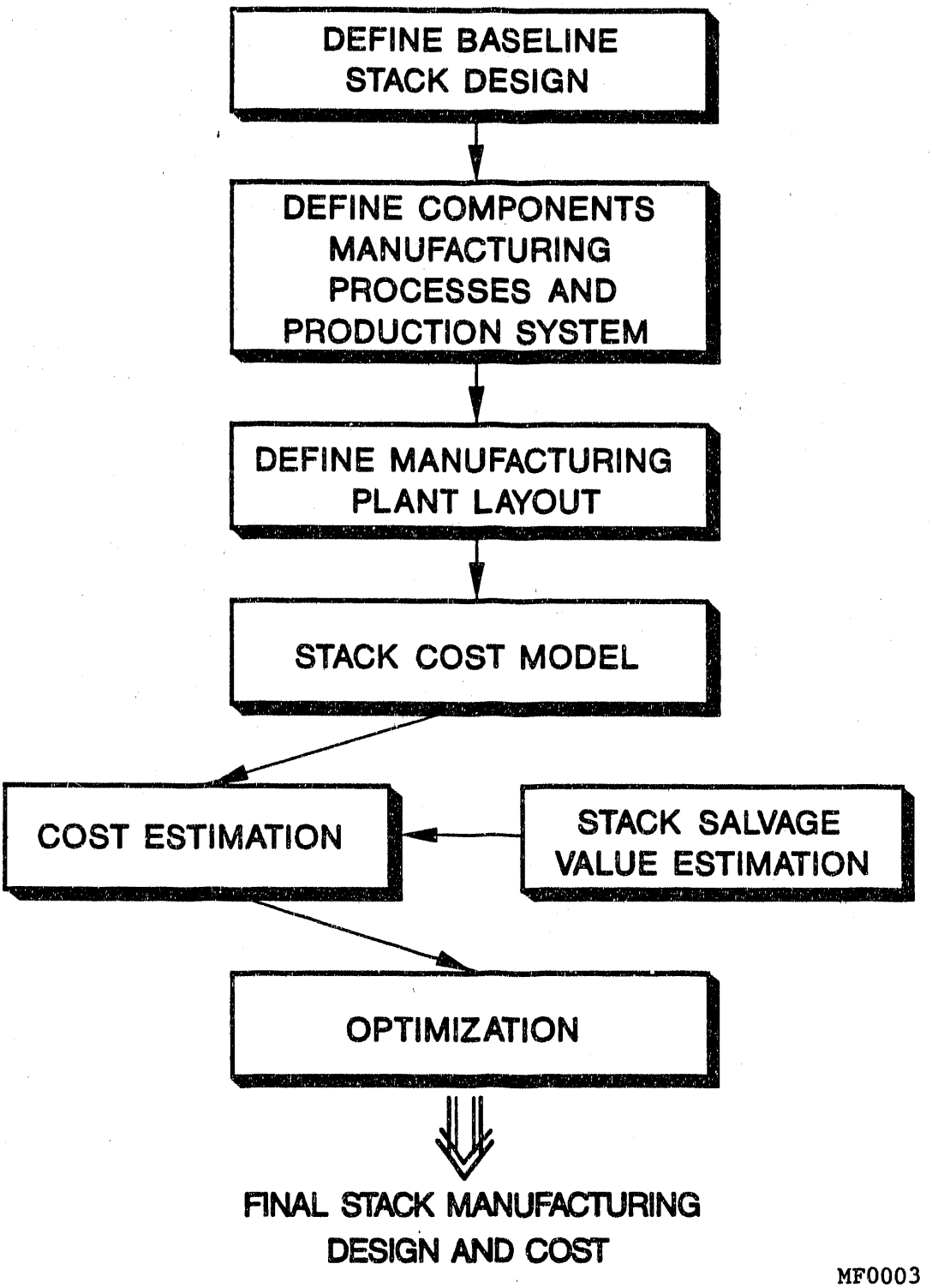

FIGURE 8.1 CARBONATE FUEL CELL STACK MANUFACTURING FEASIBILITY STUDY STEPS:

A Systematic Approach Consisting of Stack Design Definition, Stack Components Manufacturing Process Layout, Equipment Screening, Cost Modeling, and Parametric Optimization was Followed Resulting in Final Design and Cost of Stack Manufacturing Facility

The services of a commercial supplier of tape casting process equipment were utilized to define the tape casting process layout and the optimum equipment sizes for anode and matrix production. As an example, the layout of the anode production system and the processing equipment information is provided in Figure 8.2 and Table 8.1, respectively. The operating labor as well as cost information on each and every equipment in Table 8.1 was obtained for the 24in. wide as well as the 48in. wide production lines. The 48in. wide tape requires two processing lines, as opposed to three for the 24in. anode tape manufacture, requiring less labor, but 8% higher capital investment. Note that the 24in. wide tapes can be produced from the 48 in.wide tapes by splitting. Cost sensitivity analyses show that this approach is economically attractive at production volumes approaching 1600 MW/yr.

Similarly, a sheet metal processing equipment supplier was consulted for designing the bipolar plate manufacturing and assembly system. The equipment and labor requirements were also established by the consultant. The plating option was selected as the cost-effective means for applying the protective layer on the anode side of the separator plate. The plating speed was found to be an important process variable in terms of cost and was investigated to establish the optimum cost. Thus all key component production lines were laid out and staffed with input from suppliers of the appropriate technologies. Three stack assembly concepts such as the Progressive Assembly, Stationary Assembly, and Rotary Assembly were evaluated. The Progressive Assembly approach outlined in Figure 8.3, which requires less capital investment and somewhat more labor and would be easier to automate at a later date, was selected.

TABLE 8.1

ANODE MANUFACTURE PROCESSING EQUIPMENT LIST (400MW/YR):

By Producing a 48in. Wide Tape and Splitting it into two 24in. Strips, the Number of Processing Lines can be Reduced from 3 to 2

Equipment	Processing Line 24in. Width	Processing Line 48in. Width
500 gal. Tank and Mixer	2	2
2000 gal Tank and Mixer	1	1
Ball Mill - 165cu. ft.	1	1
Tube Pump 25gpm., 5hp.	2	2
Tape Caster/Dryer	3	2
Slitter	3	2
Shear	3	2
Automatic Stacker	12	8
Powder Spreader	3	2
Reduction Furnace	3	2
Electrolyte Furnace	3	2
Total Cost, Relative	1.00	1.08

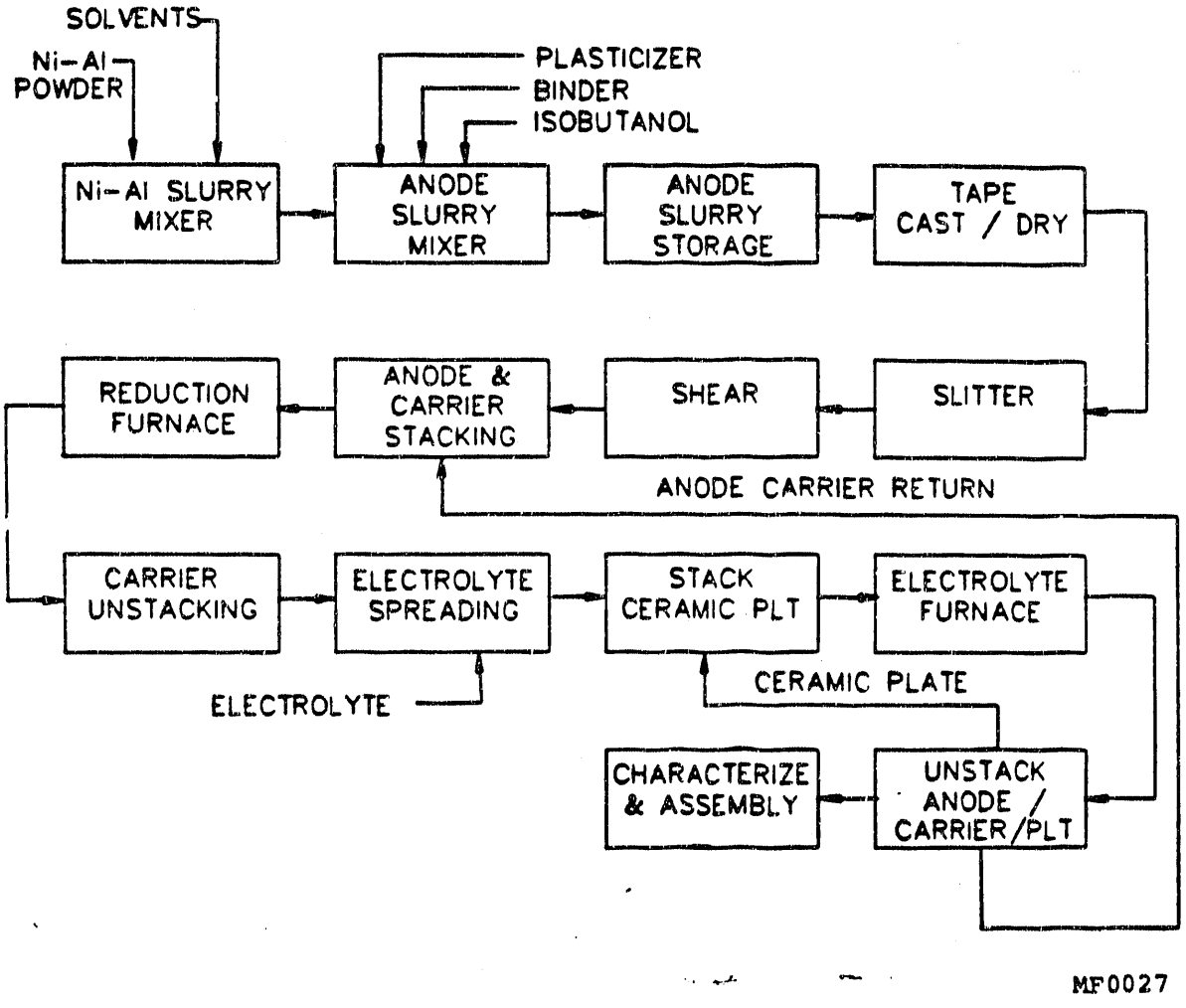

FIGURE 8.2 ANODE MANUFACTURE PROCESS STEPS:

The Processing Steps for Anode Manufacture by Tape Casting, as Identified here, are Commercially Available

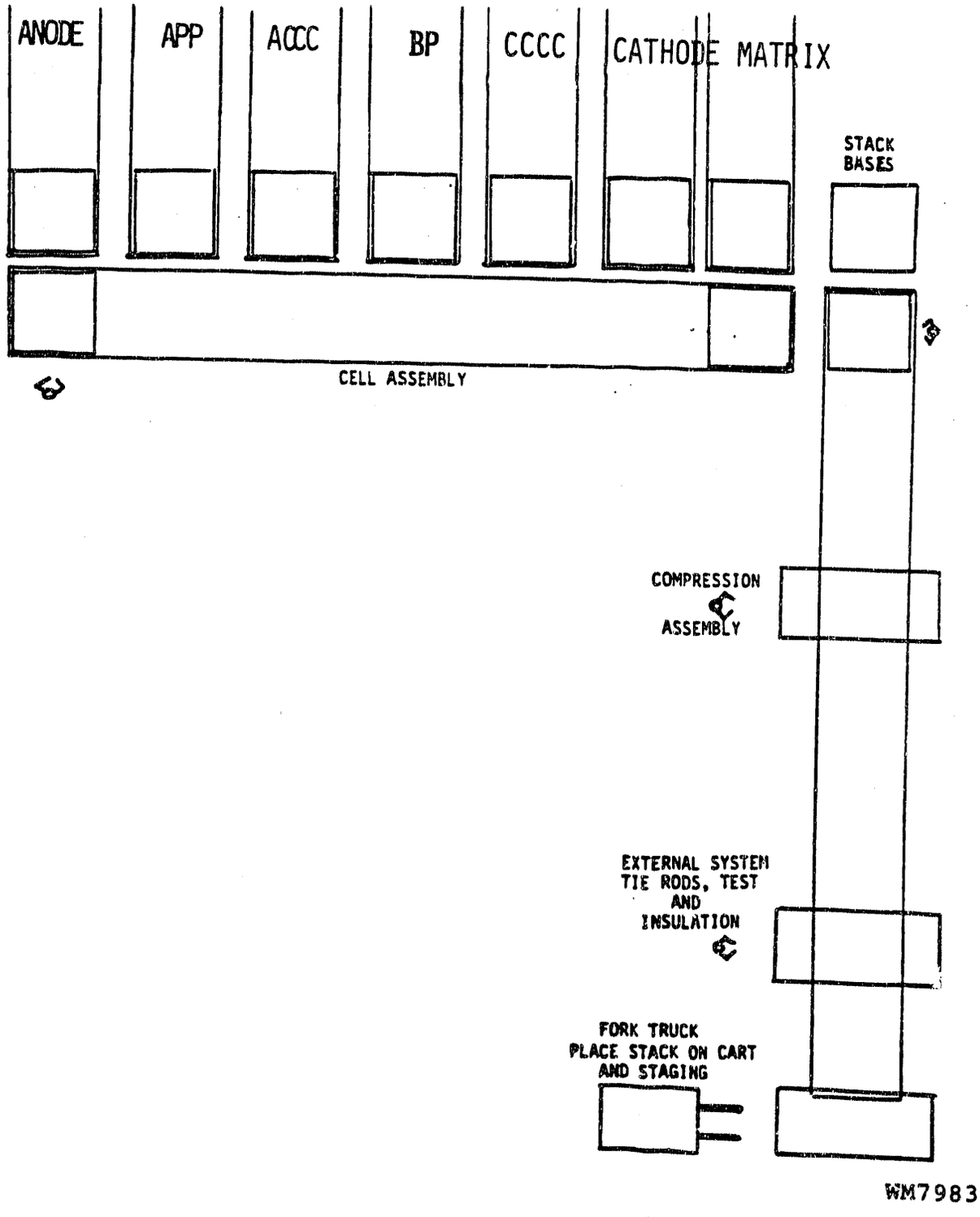

FIGURE 8.3 SELECTED STACK ASSEMBLY APPROACH:

This Progressive Cell Assembly Approach Appears most Attractive

8.2.3 Manufacturing Plant Conceptual Design

Next, a conceptual stack manufacturing plant layout was developed which incorporated mostly automatic operation for component manufacture and assembly, whereas stacking was assumed as a manual operation. The manufacturing plant's design, developed in this study, is based on several considerations and assumptions such as: overall material flow optimized to minimize in-process inventories; built-in flexibility to increase plant capacity at minimal cost without disrupting existing production facilities; component manufacturing lines arranged so that components can be automatically fed to the assembly area without delay or inventory accumulation; final assembly area; insulation, packaging, and shipping located in one area so that handling is minimized; receiving docks located close to where materials are needed and where storage and handling methods can be consolidated; process/assembly, engineering, and maintenance located in an area that is central to all manufacturing activities; administration offices are located in an area close to the assembly and feeder areas so that visitors can be given brief tours of the main functions of the plant.

The equipment arrangement within production lines were established individually. The overall plant layout is based on the collective layouts of each of the production lines and the aforementioned considerations. Plant layouts with production capacities of 400 MW/yr, 800 MW/yr, and 1600 MW/yr were developed (an example of the plant layout is provided in Figure 8.4).

The plant staffing requirements were established under the direct labor, indirect labor, and administration categories. The staffing needs change with each plant layout or model scenario in order to match the changes in production volumes and available equipment capacity. As an example, the staffing needs for the 400MW/yr plant were estimated to be:

Category	Total Staff	1st Shift	2nd Shift	3rd Shift	4th Shift
Mfg'ing Direct	145	58	45	25	17
Mfg'ing Indirect	37	11	10	9	7
Maintenance	31	9	9	8	5
Salary	59	32	11	9	7
Total	272	110	75	51	36

This plant is designed to operate on three shifts with a fourth shift needed to provide 17 percent of the total capacity. The fourth shift would require a seven-day work week of 20 work shifts and one down shift for equipment maintenance. This latter situation is not uncommon among other manufacturers. It is particularly cost-effective in a capital intensive facility like the fuel cell manufacturing plant.

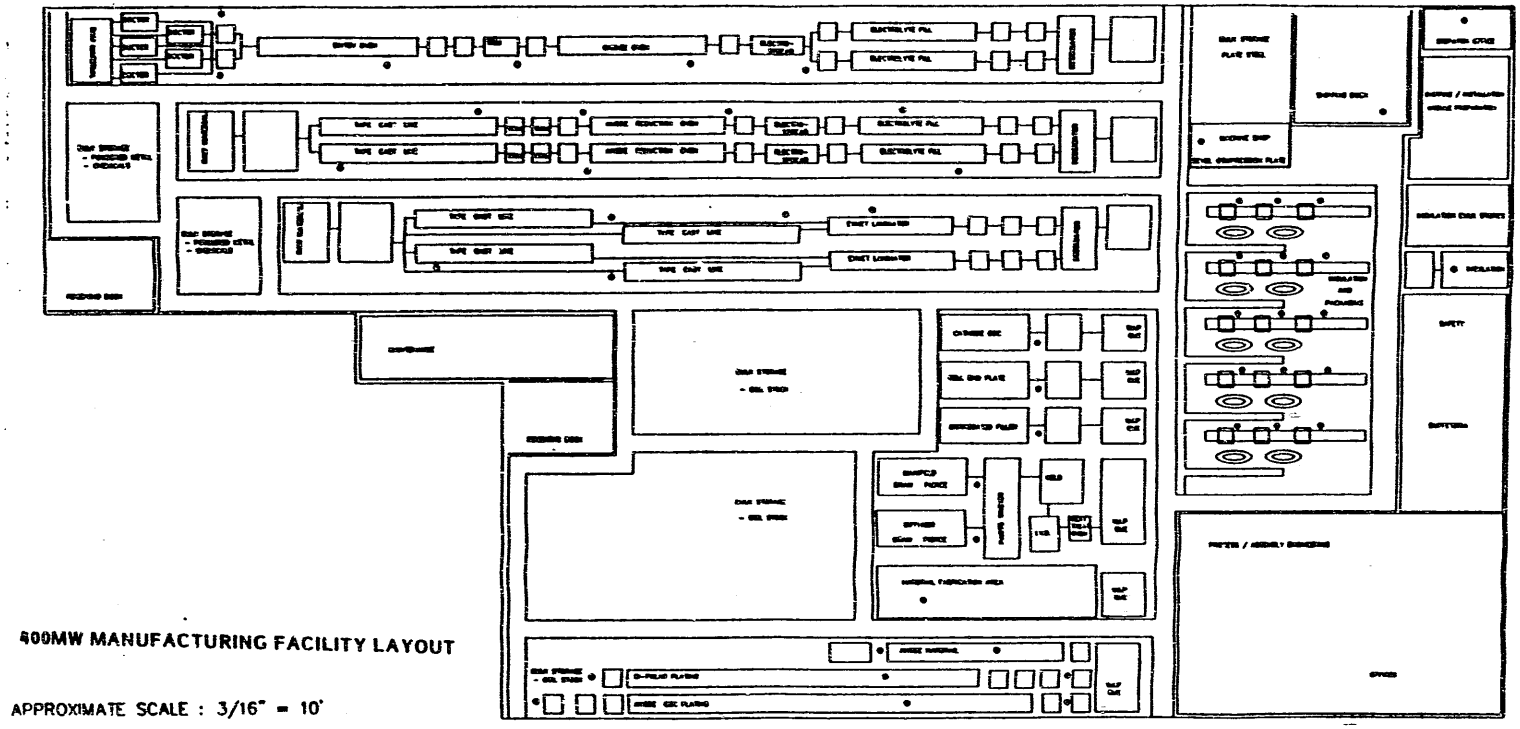

FIGURE 8.4 FULLY EQUIPPED AND STAFFED PLANT CONCEPTUAL DESIGN:

This Plant Layout is made Flexible for Future Expansion, Considering Potential for Exponential Growth of Fuel Cell Production

8.2.4 Salvage Value Estimate

A detailed study was conducted with the support of a scrap recycle vendor to establish carbonate fuel cell stack salvage value. An experiment conducted in support of this study indicated that used carbonate fuel cell stacks could be melted and converted to a very useful specialty steel containing ∿43% nickel. The cost credit of this alloy is roughly the same as the price of Ni content in the alloy. The Ni content in carbonate fuel cell represents approximately 34% of the stack cost, most of which could be salvaged as specialty steel. It has been estimated that a credit for this special alloy is equivalent to 20% of the stack initial cost on a present-worth cost basis (10% cost of money for the time in use was assumed).

8.2.5 Cost Model

A cost model was utilized to estimate the fuel cell stack cost on an annualized basis. The Lotus 1-2-3 spreadsheet analysis package was used on an IBM PC to exercise the model. The important economic assumptions in this model included:

- 1988 constant dollar analysis
- Just-in-time manufacturing
- 10% cost on capital
- Straight line depreciation
- South Carolina plant location

In selecting the plant location factors such as closeness to critical material suppliers, manufacturing permitting advantages, low labor costs, closeness to customer base, and tax and insurance burdens were considered. The State of South Carolina provided a good match on these selection criteria.

8.2.6 Cost Estimate

Utilizing the plant concept, the plant capital investment, labor costs, working capital, and raw material costs were estimated. Using these for input along with the above-described cost model the carbonate fuel cell cost was estimated for three volume scenarios, three cell sizes, and methods of manufacturing. The CFC stack cost was developed for production rates from 400 MW/yr to 1600 MW/yr and for stack sizes of 4 ft^2 and 16 ft^2. These are compared in Figure 8.5 on a relative cost basis. The results indicate that at a production rate of 400 MW/yr, the cost of a 4 ft^2 stack is quite similar to the larger size stack (16 ft^2). At higher production scenarios, the 16ft^2 size stack becomes slightly cheaper. At this production level, the increase in cost for capital equipment for the larger size plates is offset by the reduction in materials and labor costs. But, the cost of 4ft^2 stacks can be lowered

at higher production rates by modifying the plating line (Curves C and D in Figure 8.5). If a plating line speed of 12 feet per minute is assumed, the cost of a $4ft^2$ is only 5% higher than the $16ft^2$ stack at the 1600 MW/yr production scenario (assuming no tolerance penalty for the larger size cells). The analysis also shows that if a wider Ni plating line (48 in.) is designed for the $4ft^2$ stack where the 24 in. X 24 in. plates are produced by splitting the 48 in. bipolar plate, a slight cost benefit is realized only at high production level (Curve C in Figure 8.5).

A close review of the stack cost (Figure 8.6) indicates that it is materials driven, contributing over 60% at a 400MW/yr production case, where approximately 30% is contributed by the bipolar plate alone. Also, the bipolar plate manufacturing equipment contributes 37% of the plant capital cost. Thus, bipolar plate design improvement offers an opportunity for stack cost reduction.

8.3 CONCLUSION

This study shows that the carbonate fuel cells can be mass produced cost-effectively for $4ft^2$ size and at a production volume of 400 MW/yr. Since fuel cells are replaced in a power plant every five years, the demand for stacks is expected to be significantly higher in later years. In such a scenario, larger size fuel cells such as 16 ft^2 and higher volume production plants are expected to be more cost competitive.

One major advantage with the carbonate fuel cell identified in this study is that the material content in used stack can be essentially salvaged as a specialty alloy with significant cost credit (over 20% of the stack initial cost).

The fuel cell cost at all sizes is mainly materials driven. The bipolar plate contributes a major portion of the materials as well as plant capital costs. Therefore, the bipolar plate provides the best opportunity for cost reduction. Nevertheless, cost savings in other areas are also likely. An in-depth design-to-manufacture analyses is recommended to identify cost saving designs and manufacturing process changes.

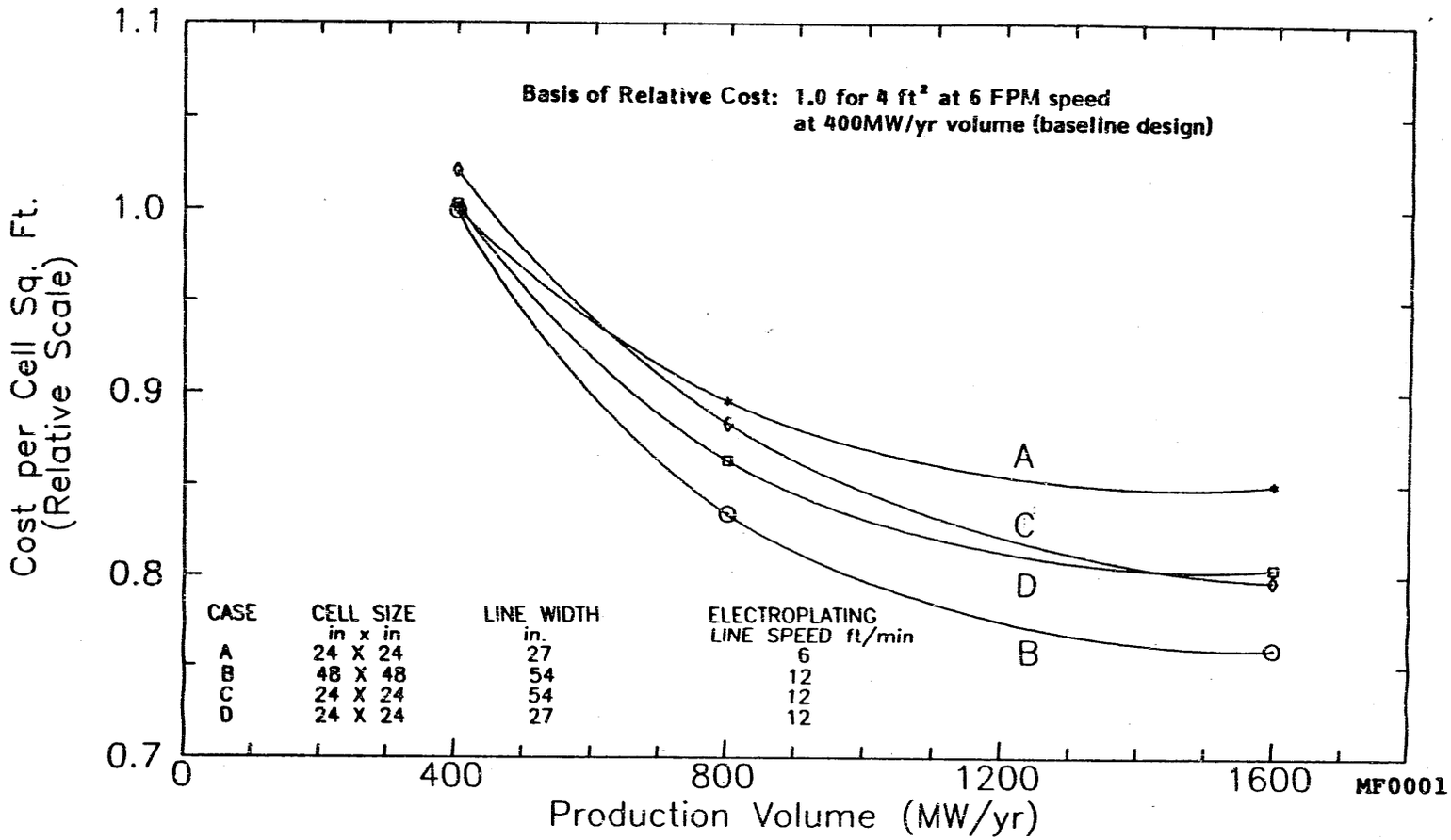

FIGURE 8.5 EFFECT OF VARIABLES ON STACK COST:

At 400Mw/yr Rate, the 4ft² Stack Cost is Quite Similar to the Larger Size Stacks (16 ft²)

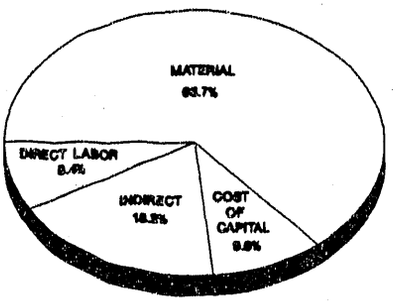

MANUFACTURING COST SUMMARY

(a) Material Cost Accounts for over 60% of the Stack Cost

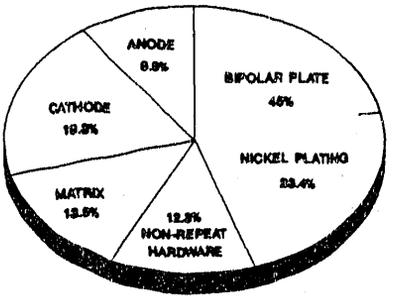

MATERIAL COST

(b) Bipolar Plate Contributes Nearly Half of the Material Cost

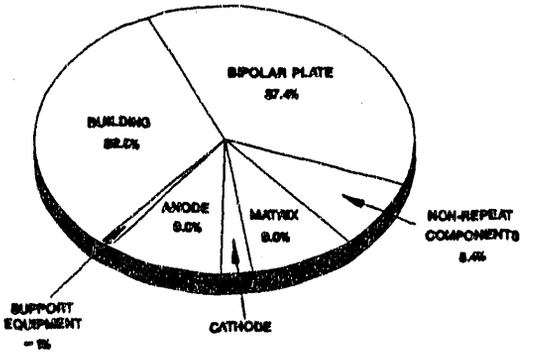

MF0005

PLANT COST

(c) The Building and the Bipolar Plate Equipment

FIGURE 8.6 STACK COST ANALYSIS (400MW/YR, 4FT^2 CASE):

Bipolar Plate Provides an Opportunity for Stack Cost Reduction

9.0 COAL-FUELED CARBONATE FUEL CELL (CGCFC) POWER PLANT DESIGNS AND COMPARATIVE ASSESSMENT

ERC, in close collaboration with Fluor-Daniel (providing engineering design and costing), conducted a detailed system study to develop a market-responsive coal carbonate fuel cell power plant (CGCFC) configuration for baseload utility application. Also, as a part of this investigation, the present-day as well as the emerging alternate coal-based power plant technologies were compared with the CGCFC using anidentical design basis to assess their competitive position. A 200MW-size plant located in Chicago, started in 1998, and operating on Illinois #6 coal was used as the study basis.

The results of this study indicated that highly efficient and cost-effective carbonate system configurations can be designed from a broad range of gasifiers, representing entrained bed, fluidized bed, and moving bed gasifiers, and utilizing both hot and cold cleanup systems. Site specific issues and other considerations may guide the plant choice.

The market competitiveness of the CGCFC power plants with respect to three competing technologies: pulverized coal (PC) boiler, atmospheric fluidized bed (AFBC), and an advanced integrated gasification combined cycle (IGCC) were assessed. The CGCFC systems provide heat rates of 7246-7604 Btu/kWh (efficiencies of 45-47%) while the competing systems have heat rates of 8420-10780 Btu/kWh (efficiencies of 30-40%). The capital costs of the competing systems are 3-15% lower than the lowest cost CGCFC system, but the COE's for the competing systems are 2-32% higher than the lowest cost CGCFC system. Environmental emissions for CGCFC power plants are well below stringent standards anticipated in the 1990's and are significantly lower than the estimated emissions for any of the competing technologies evaluated in this study. In addition, carbon dioxide emissions and water usage are lower due to the higher efficiency.

The results of this study indicate that CGCFC systems are significantly superior to present-day and emerging technologies in terms of efficiency and emissions, yet are economically competitive.

9.1 INTRODUCTION

ERC, in close collaboration with Fluor-Daniel (providing engineering design and costing), conducted a detailed system study under a Department of Energy, Morgantown Energy Technology Center sponsored effort [9-1] to develop a market-responsive coal-gasification carbonate fuel cell (CGCFC) power plant configuration for baseload utility application. Also, as a part of this investigation, the present-day as well as the emerging alternate coal-based power plant technologies, were compared with the CGCFC using an identical design basis to assess its competitive position.

A systematic approach, consistent design and economic basis, and utility user input were used for establishing the preferred configurations, identifying competing alternate coal systems, and conducting a comparative analyses of all these power conversion options.

The study approach consisted of a prescreening step where the potential process options were first identified followed by a screening step where 13 complete systems, representing different cross-combinations of the selected processes, were configured and analyzed to identify potential system configurations as well as to select of the best subsystems. Subsequently, four best cases identified from the results of this screening step were configured and analyzed in detail to identify the most preferred configurations. Some limited optimization of the preferred cases and key system parameter sensitivity analyses followed to gauge the full potential of the coal-gas carbonate fuel cell plants. In parallel, three alternate coal technologies representing the presently used Pulverized Coal (PC) and Atmospheric Fluidized Bed (AFBC) and advanced IGCC (Integrated Coal-Gasification Combined Cycle) systems were analyzed to the same level of detail as the CGCFC systems using the same design and economic basis and then compared with CGCFC.

A Utility Advisory Group (UAG) consisting of Electric Power Research Institute (EPRI), Pacific Gas and Electric (PG&E), and Virginia Electric Power Company provided input to the study basis and periodic review of results. The study methodology and results are presented in a separate Topical Report [9-1] and are summarized in the following discussion.

9.2 SYSTEM SELECTION ASSUMPTIONS AND ECONOMIC BASIS

To provide an unbiased comparative evaluation, this study used a consistent design and economic basis for all the CGCFC systems as well as the alternate coal systems. The key economic and design assumptions used are outlined in Table 9.1. The major ground rule of this study was that the technology should be ready for commercialization in the late 1990's. A 200MW plant, to be built in the Chicago area and started in 1998, was the design basis. The coal was an Illinois No. 6 bituminous (composition based on EPRI Technical Assessment Guide Manual [9-2]). The economic evaluation was also based on the EPRI TAG Manual in 1988 U.S. dollars with no inflation.

The fuel cell power block consisting of 2.5MW rail transportable modules was based on the ERC 4ft^2 internal reforming stack design. A reliable cost estimate of ERC's stack was developed by a manufacturing consultant for use in this study. This cost has been arrived at by defining a 1600MW/yr manufacturing plant conceptual design, developing component processing designs, and obtaining material cost quotes from vendors.

The fuel cell size requirement for each system was determined by calculating operating current density assuming constant efficiency cell operation at 0.7 V using a performance model. This simplistic performance model was calibrated against ERC's single-cell performance and represents near-term achievable cell performance.

In the screening study, for all 13 cases, a 30% moisturization level was maintained to prevent carbon deposition. However, in the detailed study of the four cases, each individual case was evaluated with respect to the stability of the gas composition generated and only the required

TABLE 9.1
SUMMARY OF PLANT DESIGN BASIS, CFC PARAMETERS, AND ECONOMIC FACTORS:

A Consistent Set of Assumptions Have Been Utilized To Obtain Reliable One-to-One Comparison

PLANT DESIGN BASIS

- 200MW Plant Size
- Baseload Operation
- Illinois #6 Coal
- Chicago Location
- Stringent Environmental Standards
- Contingencies
  - TAG I: (Screening Study) 20%
  - TAG II: (Detailed Study)
  - 18-20%, per Risk Analysis

CELL/STACK PARAMETERS

- Atmospheric Pressure Operation
- $4ft^2$ Stack
- 0.7 V per Cell
- 40,000-Hour Life
- Stack Replacement
  - 20% a Year - Starting Year 4 until year 27
- Moisture Content
  - TAG I: (Screening Study) 30%
  - TAG II: (Detailed Study)
  - Consistent with Soot Suppression

ECONOMIC FACTORS

- 1988 Constant Dollars
- Capacity Factor
  CGCFC: 85%
  IGCC: 80%
  PC, AFBC: 65%
- Fuel Price $\$1.60/10^6$ Btu (0.8% Escalation/yr)
- 1998 Commercial Operation
- 4-Year Construction
- Federal Tax Rate: 34%
- State Tax Rate: 6%
- Book Life: 30 Years
- Tax Life: 20 Years
- COE According to EPRI TAG Investor-Owned Utilities Approach Specified in Terms of 30-Year Levelized Cost

the required level of moisturization needed to ensure stability was used. This resulted in varying moisture levels at the cell inlet for the various cases. The carbon deposition issue appeared to be aggravated by the zinc-ferrite sorbent in the hot cleanup cases due to the catalytic effect of the sorbent on carbon formation, and therefore required a higher moisturization level than the other cases.

9.3 SYSTEM CONFIGURATION SELECTION

Prescreening

The most promising subsystems were selected first from a detailed list of gasifiers, cleanup systems, and oxidant systems in a prescreening step. Also, the stack operating pressure was defined and the stack reforming type was selected. The candidate gasifier list was narrowed

down to two entrained beds, one fluid bed, two moving beds, and one catalytic methane producing gasifier from a list of 38 gasifiers which were preselected from an original list of 80 gasifiers. The cryogenic oxygen, the Air Product's Moltox process [9-3], and air were selected options for supplying gasifier oxidant. Similarly, the cold-gas cleanup involving both Rectisol as well as Selexol and hot-gas cleanup involving in-bed as well as total external sulfur capture were identified as candidate choices from a review of 22 different cleanup systems. ERC's internal reforming (dual-fuel operation) stack design and atmospheric operation of the stack was identified as the best choice.

The stack operating pressure impacts system performance, capital cost, as well as stack life. An independent trade-off study was undertaken to define the optimum fuel cell operating pressure [9-4]. For this study, a CGCFC system was configured with an oxygen-blown Texaco gasifier (530psia operation), Selexol acid gas removal, fuel cell stacks, a flue expander where applicable, and a steam bottoming cycle. Four stack operating pressure cases (1, 2, 3, and 10 atm) were analyzed using EPRI TAG-I level of details and compared on a COE and efficiency basis. The net effects of stack operating pressure on COE is shown in Figure 9.1. The results indicate that when the pressure penalty on fuel cell life is considered, the COE is lowest for atmospheric operation. On the other hand, if a technology breakthrough leading to constant fuel cell life (no pressure penalty on life from high CO_2 activity) is assumed, the near atmospheric operation, i.e. 3 atm, promises a slight COE reduction of only 1%, which may be within the accuracy of the estimating methods of this study. Since pressurization offers no overall economic gain, ERC selected atmospheric operation for the stack. Pressurized operation also provides no energy conversion efficiency advantage.

Electrochemical utilization of coal-gas borne methane in the carbonate fuel cell is highly desired for high efficiency operation. Internal reforming offers the most attractive approach to methane utilization in a CFC system. When an internal reforming CFC (IRCFC) stack is used, natural gas can be utilized as a backup fuel increasing power plant availability and the CGCFC plant can be built using a "phased construction" approach. CGCFC plants introduced through "phased" construction--in which smaller capacity modules operating on natural gas may be installed as the demand grows and a coal-gasifier may be added when the economics of natural gas versus coal prices and economy of scale are justified--could provide significant economic advantages. Therefore, IRCFC provides the most logical selection for the CGCFC system.

Screening

After identifying promising subsystems, 13 complete system configurations using cross-combinations of these promising processes were identified. The basic ERC system concept identifying the key subsystems is presented in Figure 9.2. The different subsystem cases and the cross-combinations used are identified in Table 9.2. A methane producing gasification case was included to study its overall impact on the system. In addition to air and cryogenic oxygen cases, a thermally regenerative oxygen generation process (Moltox) was included to investigate its integration with the heat producing CGCFC system. The 13 systems were analyzed

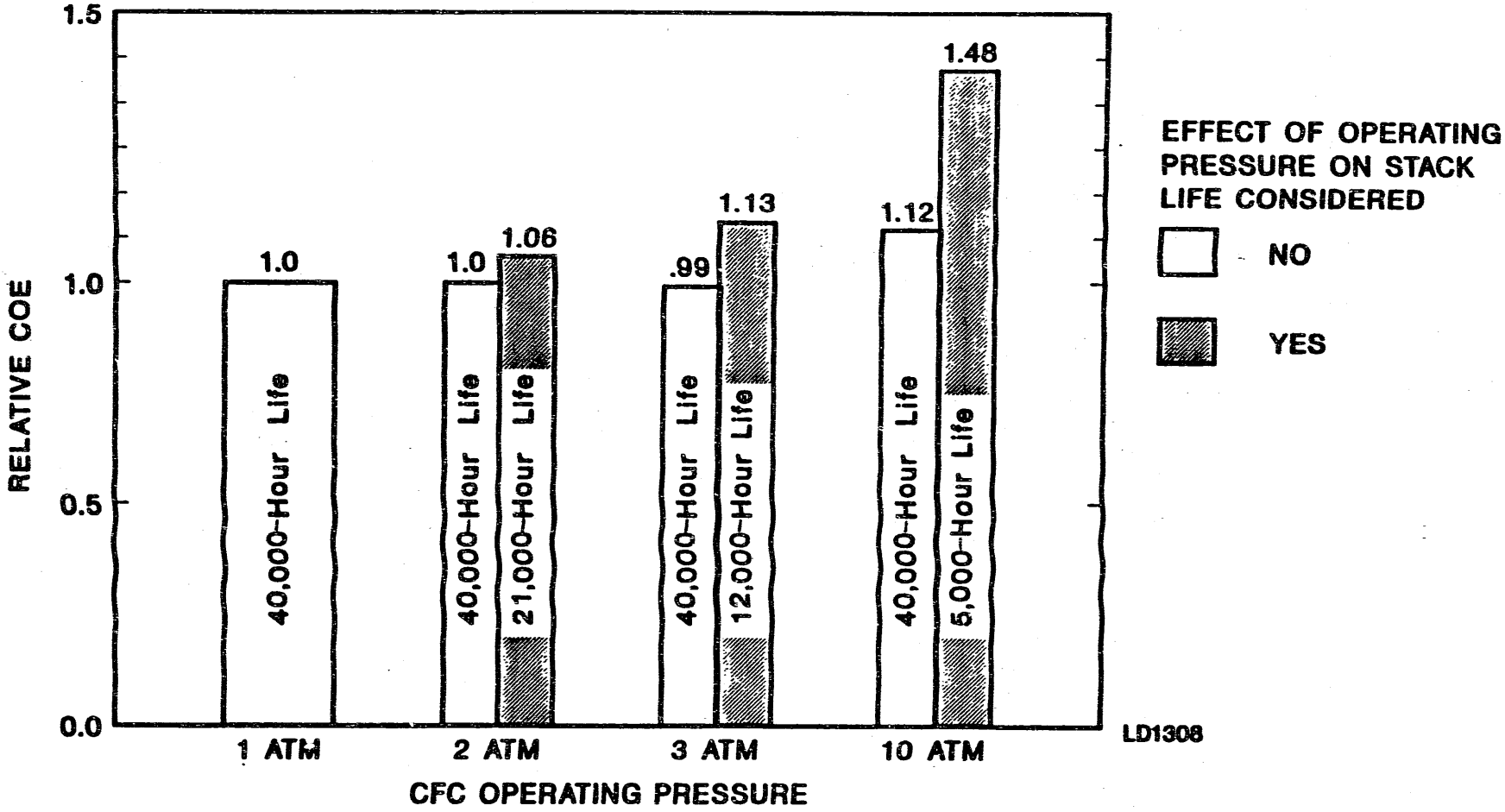

FIGURE 9.1 EFFECT OF STACK OPERATING PRESSURE ON CFC COE:

There Appears to be no Economic Incentive for Operating the CFC STacks at Pressures Higher Than 1 Atm

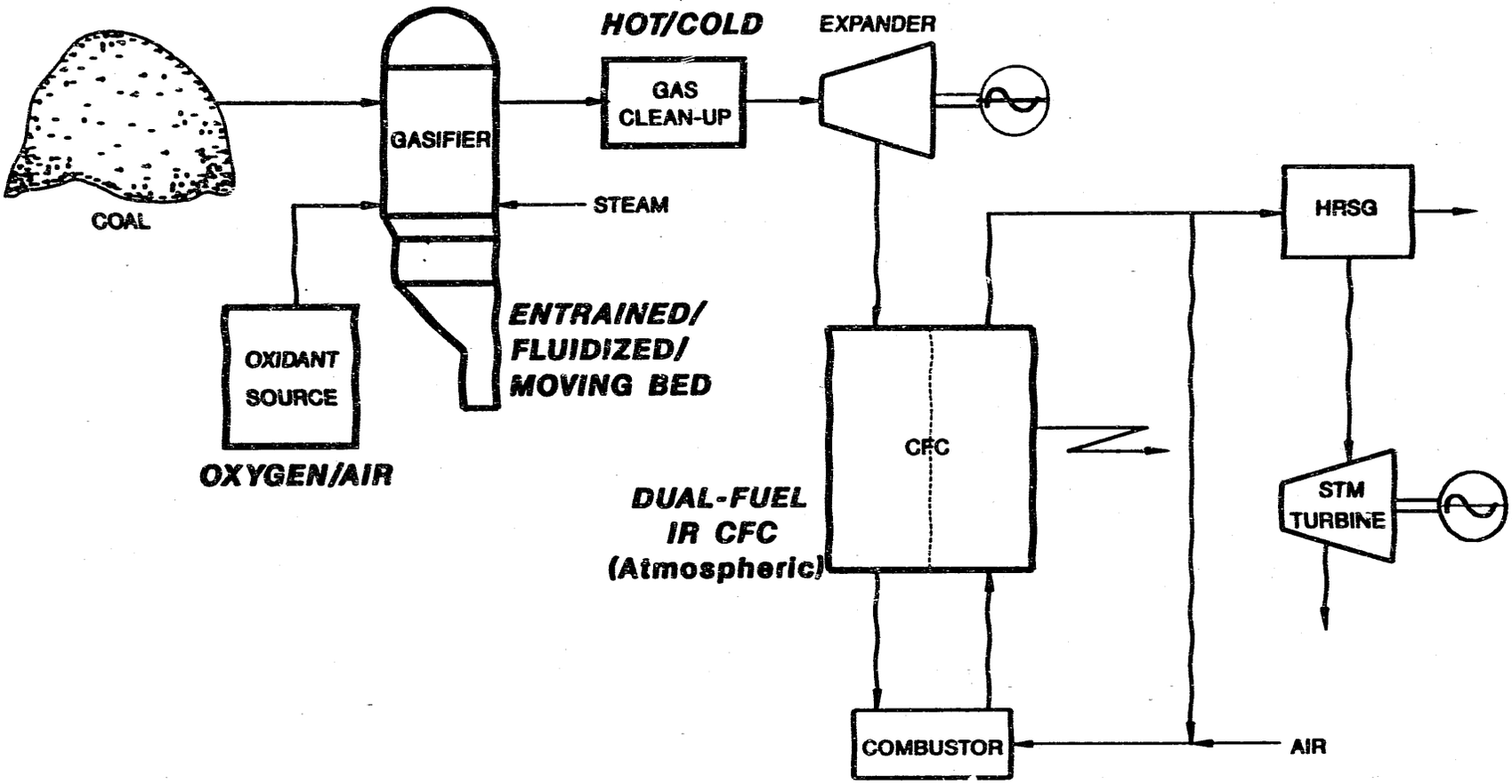

FIGURE 9.2 ERC'S CGCFC SYSTEM DEFINED:

Attractive Power Plants Designed with Available Gasifier and Cleanup System

TABLE 9.2

CROSS-COMBINATIONS OF SUBSYSTEMS WERE EVALUATED:

Thirteen CGCFC Systems were Analyzed to Identify Preferred Gasifier Type, Cleanup, Oxidant Systems and Their Best Combinations

SUBSYSTEM		STUDY CASE NUMBER												
		1	2	3	4	5	6	7	8	9	10	11	12	13
GASIFIER	ENTRAINED BED — TEXACO		X			X				X				X
	ENTRAINED BED — SHELL												X	
	MOVING BED — BGL	X			X									
	MOVING BED — LURGI													
	FLUID BED — KRW			X			X	X	X		X			
	METHANE PRODUCING — EXXON											X		
CLEANUP	COLD — SELEXOL	X	X	X	X	X	X					X	X	X
	COLD — RECTISOL													
	HOT — IN BED SULFUR							X	X	X	X			
	HOT — EXTERNAL SULFUR													
OXIDANT	AIR	X	X	X	X	X	X	X	X	X	X		X	X
	CRYOGENIC OXYGEN													
	MOLTOX													

SD0779

using EPRI TAG-I level of details. All units were sized and costed. Although a nominal 200MW size was used as the overall design basis, the actual plant size was controlled by the size of the gasifier (in all cases full discrete gasifier units were used). This, plus the system efficiency difference, resulted in a power plant net power output difference between the system evaluated. The overall performance and COE projection of 12 of these 13 cases are compared in Table 9.3. These results plus comparison of individual subsystem cost contributions and performances provided interesting insights:

- **Hot cleanup with in-bed sulfur capture appears to be preferable.**

  Hot-gas cleanup improves efficiency and lowers cleanup cost (comparison of Case #3 with Case #4). This conclusion only applies to where in-bed sulfur capture is used. The Texaco hot cleanup case (#9) with external sulfur recovery did not fare as well when compared to the cold cleanup (Case #2).

- **Cryogenic oxygen is more advantageous over air and Moltox.**

  Oxygen-blown systems offer slightly lower COE and significant efficiency advantages over the air-blown cases (comparison of Cases #7 and #10). The air-blown CGCFC system of 200MW size appears to be slightly more expensive than the oxygen-blown system. Savings in the oxygen plant are compensated by an increased cost in other areas (gasifier, gas treating, power block, and support facilities).

- **No clean demarkation within gasifier types.**

  All three major types of gasifier, entrained bed, fixed bed, and fluid bed appear competitive and cannot be ruled out as a class at this level of detail.

  - Dry versus slurry feed in an entrained bed does not make significant difference. (The dry feed Shell system did not pose any COE advantage over the slurry feed Texaco system, although a slight efficiency advantage was noticed).

  - Dry bottom Lurgi is not favored for bituminous coal. (High steam usage and inability to use fines penalize system COE.)

- **High methane producing gasifier poses a significant CGCFC efficiency advantage.**

  The Exxon-based CGCFC system posed 10 percentage points efficiency advantage over other CGCFC systems compared in this study.

After ranking the TAG I systems by heat rate, capital cost, and COE, the four most promising of these systems were chosen in discussion with UAG members for detailed analysis to pick the preferred systems. These systems are: (i) Texaco, O_2, cold cleanup; (ii) BGL, O_2, cold cleanup; (iii) KRW, O_2, hot cleanup; and (iv) KRW, air, hot cleanup.

TABLE 9.3

SCREENING STUDY RESULTS:

Cryogenic Oxygen and Hot Gas Cleanup with In Bed Sulfur Capture Appears to be Attractive

CASE	1	2	3	4	5	6	7	8	9	10	11	12
Process Data:												
Gasifier	Lurgi	Texaco	KRW	Lurgi	Texaco	KRW	KRW	KRW	Texaco	KRW	Exxon	BGL
Oxidant	Cryogenic Oxygen	Cryogenic Oxygen	Cryogenic Oxygen	Air Blown	Air Blown	Air Blown	Cryogenic Oxygen	Moltox Oxygen	Cryogenic Oxygen	Air Blown	Catalytic Steam	Cryogenic Oxygen
Gas Cleanup	Cold	Cold	Cold	Cold	Cold	Cold	Hot	Hot	Hot	Hot	Cold	Cold
Gas Cleanup Process	Rectisol	Selexol	Selexol	Rectisol	Selexol	Selexol	Zn Ferrite	Zn Ferrite	Zn Ferrite	Zn Ferrite	Selexol	Rectisol
Gasification												
Operation Data:												
Cold Feed, ST/SD	1,806	1,576	1,312	1,798	1,500	1,680	1,833	1,833	1,576	2,581	1,366	1,800
Cold Gas Efficiency,%	82.0	81.0	83.5	73.7	50.2	73.4	83.0	83.0	79.1	72.8	95.3	82.9
Heat Rate, Btu/kWh	8,816	7,694	7,830	9,774	11,412	8,424	7,456	7,889	8,558	8,372	6,013	7,770
CH_4 in Gas, Vol.%	9.4	0.08	7.2	3.8	0.02	1.5	6.1	6.1	0.08	0.93	26.7	4.8
Overall Efficiency,%	38.7	44.4	43.6	34.9	29.9	40.5	45.8	43.3	39.9	40.8	56.8	43.9
Oxygen Feed, ST/D	750	1075	633	---	---	---	1013	1013	1149	---	---	910
Carbon Utilization,%	97.4	99.0	94.9	97.4	97.0	92.8	94.6	94.6	99.0	92.8	(2) 90.0	96.9
Power Data, MW:												
Production:												
• Expander	14.7	18.0	13.5	24.0	43.5	40.8	19.9	19.9	31.8	58.2	9.6	12.6
• MCFC	141.3	115.8	107.2	122.5	67.6	126.0	155.2	155.2	117.2	179.6	151.9	138.6
• Bottoming	38.3	70.7	43.0	35.6	45.6	50.6	63.2	44.7	34.3	90.6	(3) 41.2	74.2
• Total Production	194.3	204.5	163.6	182.2	156.6	217.4	238.2	219.7	183.3	328.4	202.7	225.4
Internal Use:												
• O_2 Plant or Air Comp.	11.3	17.1	11.2	16.6	38.2	27.2	16.0	9.7	18.4	39.1	0.0	14.5
• MCFC Blowers	5.2	7.8	6.1	4.9	4.0	7.3	8.7	8.7	6.8	10.7	4.8	10.4
• Other	5.4	7.2	5.3	5.9	3.8	15.0	6.5	5.6	3.2	19.1	6.7	5.8
• Total Internal Use	21.9	32.1	22.6	27.4	45.9	49.5	31.2	24.1	28.3	68.9	11.5	30.4
Net Power Production	172.4	172.4	141.0	154.9	110.7	167.9	207.0	195.6	155.0	259.5	191.2	195.0
Relative Economic Data:												
Capital Cost, $MM	1.19	0.99	0.77	1.17	Not	1.07	1.00	1.01	0.96	1.28	1.06	1.00
Capital Cost, $/kW	1.43	1.19	1.14	1.56	Calculated	1.32	1.00	1.07	1.28	1.02	1.15	1.06
COE, Mills/kWh (1)	1.26	1.07	1.07	1.38		1.17	1.00	1.07	1.22	1.03	0.98	1.03

(1) The base case levelized COE is based on a fuel cell life of 40,000 hours and 0.8% fuel cost escalation.
(2) Remaining 10% carbon is combusted externally to heat recycle gas and produce HP steam.
(3) Includes addition of reheat in bottoming cycle.

Selection of Preferred Configurations

Detailed TAG-II level design and economic evaluation of the four systems identified in the screening step were carried out to identify possible economic difference between these systems. In this detailed analysis, for each of the CGCFC cases, detailed block diagrams of the entire process were developed to identify the key process units. Next, separate process flow diagrams were developed for each of the key process units for mechanical equipment specifications. Several process refinements were incorporated in the TAC-II study. The cost-effective dual reboiler concept was incorporated to provide cryogenic oxygen (95% purity). The DOW Spec process was used to replace the Selexol process in the Texaco-gasification based power plant system.

For each case, detailed mass and energy balance and steam integration were carried out, all equipment were sized, the plant plot plan was laid out, and a one-line electrical diagram was prepared to provide complete system definition. The fuel cell power block consists of 10MW clusters. Each cluster has a common inverter and fuel cell air system. The fuel cell power block in the 10MW cluster consists of four identical rail transportable stack pallets. This modular arrangement of stacks and distributed inverter design makes the CGCFC power plant highly reliable. Therefore, a power plant availability of 85% has been assumed in the COE calculation.

The plant material costs were developed with mostly licensee and vendor quotes. Direct field cost and plant investment costs were generated using factors from Fluor experience in actual construction projects. Operating and maintenance costs were generated similarly. Finally, year-by-year and 30-year levelized cost-of-electricity was calculated using the EPRI TAG Investor-Owned Utilities cost code.

The performance and economics of the four selected cases are compared in Table 9.4. The CGCFC systems provided an efficiency range of 45 to 47% with the best efficiency provided by the KRW/O_2/Hot cleanup case. These results point to the same trend observed in the screening step that the hot-gas cleanup and cryogenic oxygen, and to some extent the gasifier operating temperature (cold-gas efficiency) has a positive impact on overall system efficiency. The BGL case has a cold-gas efficiency (85.6% as opposed to 81.2% for the KRW/O_2 case), however it did not offer a winning heat rate because this system configuration employed a cold-gas cleanup subsystem.

The BGL system projects higher emissions of SO_x and NO_x compared to other cases. This results from combustion of sulfur containing tar and oil byproducts for heat recovery. The power block cost is higher for the KRW hot-gas cleanup cases. This is a result of lower fuel cell performance penalty resulting from higher moisturization requirements. Within the hot gas cleanup cases, the air-blown system projects a lower fuel cell cost, but a slightly higher power block cost results from increase in balance of power block equipment cost due mainly to higher fuel gas throughput with the air-blown system. The hot-gas case projects high O&M costs which are mainly due to higher catalyst and chemical costs contributed by dolomite and zinc-ferrite it consumes.

TABLE 9.4
PERFORMANCE AND ECONOMIC COMPARISON OF THE FOUR SELECTED CGCFC CASES:

CGCFC Cases Indicate High Efficiency, Close Ranking in Terms of COE and Excellent Emission Characteristics

	TEXACO O_2-Cold Cleanup	KRW O_2-Hot Cleanup	KRW Air-Hot Cleanup	BGL O_2-Cold Cleanup
Coal Feed T/D	2139	1800	1800	1800
MW Net	238	209	199	205
Heat Rate	7565	7246	7604	7379
Efficiency	45.1	47.1	44.9	46.3
Capital Cost, $/kW (Relative to Texaco-$O_2$-Cold Cleanup)	1.00	0.93	0.99	1.02
COE, Mills/kWh (Relative to Texaco-O_2-Cold Cleanup)	1.00	1.07	1.11	1.05
Emissions:				
SO_2, lb/MWh	0.03	0.003	0.003	0.25
NO_x, lb/MWh	Trace	0.10	0.10	0.18
CO_2, lb/MWh	1578	1598	1661	1540

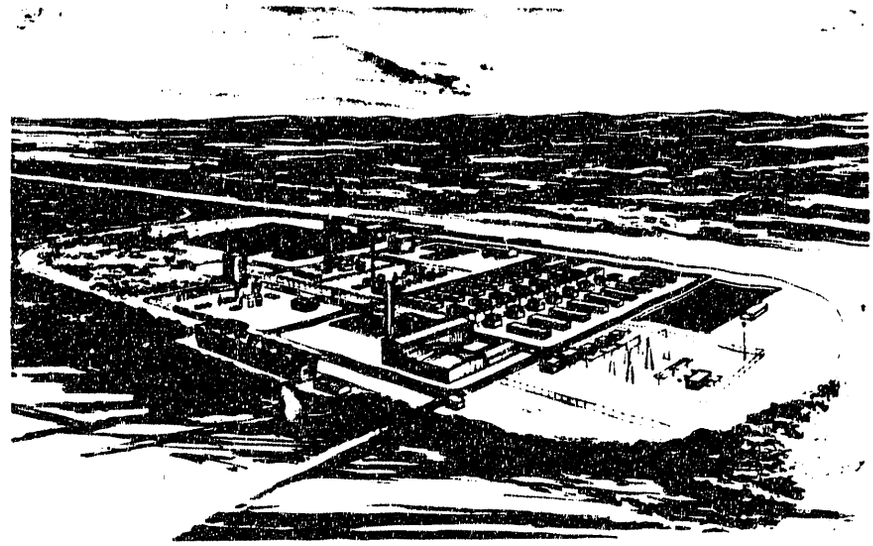

PM0538

FIGURE 9.3 ARTIST'S RENDERING OF A TYPICAL 200MW CGCFC POWER PLANT:

Offering High Efficiency and Low Emissions at Competitive COE

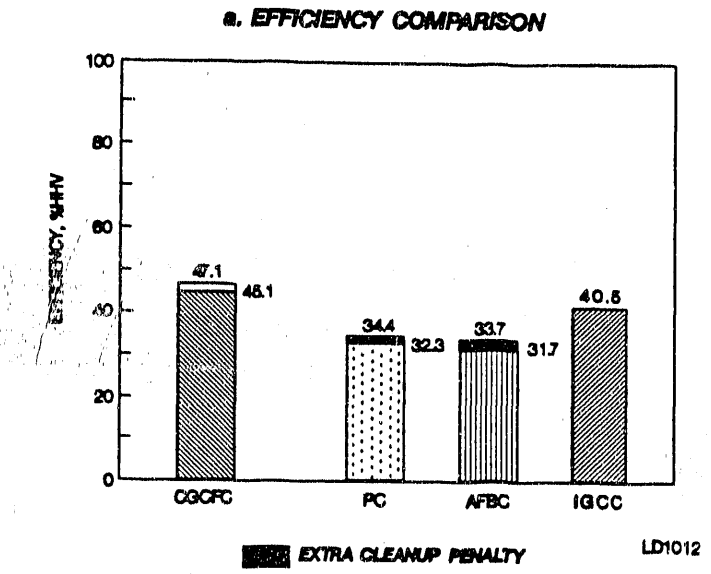

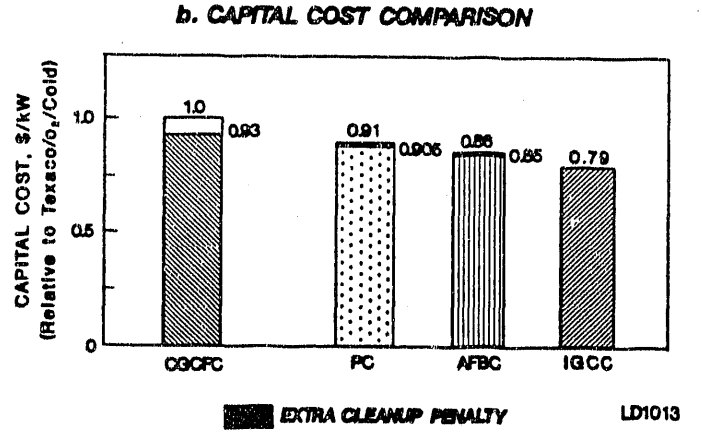

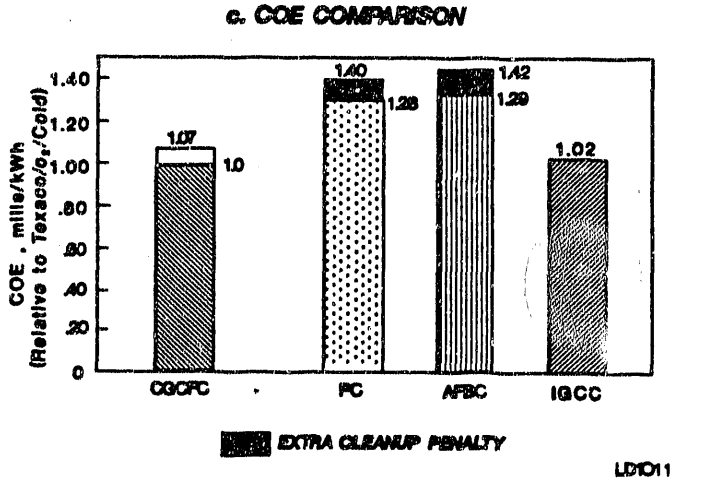

LD1037B

FIGURE 9.4 CGCFC FIGURES-OF-MERITS COMPARED TO AVAILABLE SYSTEMS: Superior CFC Advantages are Evident.

The PC and AFBC designs were selected from literature and normalized to the current study standards as follows:

The baseline PC with wet flue gas desulfurization and AFBC with in-bed sulfur capture, respectively, permitted 90% sulfur recovery, not meeting the stringent NSPS standard of 95%. Therefore an alternate design incorporating coal cleanup was considered, and a sulfur removal of 96% and 98% for PC and AFBC was achieved, respectively. A catalytic Denox unit was added to the PC system to conform to the NSPS requirement for NO_x emissions of 0.1 to 0.2 lb/MM Btu.

The results establish that the present-day technologies, such as PC and AFBC, are inferior both environmentally and economically to the advanced IGCC system. The results also point out that coal cleaning, which improved the sulfur emission characteristics of PC and AFBC, increases capital cost and reduces the heat rate by 6%.

The efficiency, capital cost, and COE, comparisons are shown in Figure 9.4; environmental emissions are compared in Table 9.5. By each and every figure-of-merit, the CGCFC systems are significantly superior to PC and AFBC systems. Even the modified PC and AFBC systems with additional cleanup equipment would result in orders of magnitude greater SO_x and NO_x emissions.

The toughest competition to CGCFC is expected to come from advanced IGCC systems. Again, in terms of efficiency and environmental emissions, the CGCFC systems offer superior characteristics. Even the CO_2 release and makeup water requirements are 15% and 40%, respectively, lower for the CGCFC system. The CGCFC capital is slightly higher, but the COE is slightly lower because of efficiency and availability advantages. A fuel price escalation of only 0.8% per year was assessed in this study. At a higher fuel price, even greater economical advantage will be projected for the CGCFC systems. The CGCFC projects excellent part load efficiencies as shown in Figure 9.5. At 50% of design load, for the CGCFC the heat rate increases only 6%, as compared with a 25% increase in heat rate for an IGCC system. In addition, the CGCFC power plants offer a host of benefits which has not been quantified in this study but are quite valuable to utility planners. These include:

- Compatibility with Phased Construction
- Multifuel Capability
  - Wide Range of Coal-Gas Compositions
  - Natural Gas
  - Methanol
- Modular Size
- Unique Electric Power Characteristics
- High Efficiency and Low Cost Over a Broad Range of Sizes
- Common Stack Design Compatible with Natural Gas as well as Coal-Gas Power Plants (mass producibility)

TABLE 9.5 PROJECTED EMISSIONS OF COMPETING TECHNOLOGIES:

The CGCFC Projects Much Superior Emission Characteristics

POWER PLANT SYSTEM	ACID RAIN PRECURSOR EMISSIONS		CO_2	MAKE-UP WATER	SOLID WASTE
	AS SULFUR	NO_x			
	lb/MWh	lb/MWh	lb/MWh	lb/MWh	lb/MWh
CGCFC					
TEXACO/O2/CGC	0.03	TRACE	1580	3000	90
KRW/O2/HGC	0.003	0.10	1600	3700	280
PC					
WET FGD	3.9	6.1	2070	5800	440
COAL CLEANUP, DENOX, AND WET FGD	0.79	1.06	2070	6000	
AFBC					
IN-BED DESULFURIZATION	4	0.81	2107	5000	350
COAL CLEANUP, IN-BED DESULFURIZATION	1.6	0.86	2107	5000	
ADVANCED IGCC O2-BLOWN GASIFICATION IN-BED DESULFURIZATION, EXTERNAL ZINC-FERRITE	0.08	1.01	1860	4800	320

SD0936k

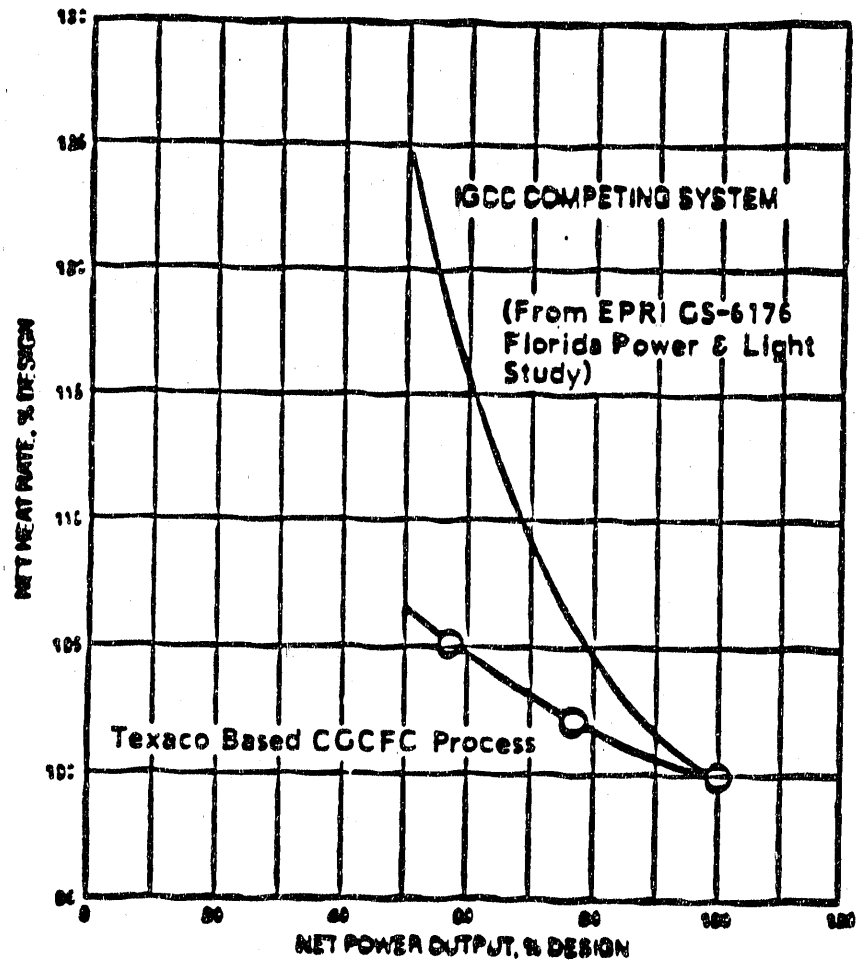

FIGURE 9.5 COMPARISON OF PART-LOAD EFFICIENCIES:

The CGCFC Heat Rate is Practically Invariant with Load, Contrary to IGCC which Loses Efficiency Significantly at Part-Load.

The modular size of CFC and multifuel compatibility of ERC design make the CFC an excellent candidate for phased construction. The CGCFC provides higher availability. The CGCFC, because of the inverters, provides unique reactive power control.

9.5 PARAMETRIC SENSITIVITY AND OPTIMIZATION

Sensitivity to a number of operating, sizing, and location parameters were evaluated for the Texaco case and to a limited extent KRW based CGCFC systems. These included the following:

- plant size (100 - 400MW)
- location (Houston vs. Chicago baseline)
- plant construction period (3 yr versus 4 yr)
- alternate design for the expander
- CFC operating parameters (cell voltage, fuel and oxidant utilizations)
- CFC performance improvement (50 ASF & 100 ASF increases)
- stack area (6 ft^2 vs. 4 ft^2)
- stack life (5yr baseline versus 7 yr and 10 yr)

The results showed that the largest impact on cost were made by the plant size (increasing from 200 to 400 MW), and the plant location (Houston instead of Chicago). A 27% reduction in capital cost of the plant, and correspondingly a 17-20% reduction in cost of electricity, was estimated for the cumulative effect of increasing the plant size to 400 MW and locating the plant in Houston instead of Chicago. The increased plant size provides economy of scale of the coal handling, gasification, oxygen plant, and other plant equipment. The Houston location offers a substantially lower labor rate than the Chicago location. The results also indicated that the cumulative effect of improved expander design, 0.75V fuel cell operation and higher overall air utilization (60% overall) on the baseline Texaco/O_2/CGC case represents 5.6% reduction of COE and 5.8% reductic in heat rates (from 7565 to 7129 Btu/kWh) in Figure 9.6. Similar impr vements in performance and economics from optimization are also expected for other coal-carbonate fuel cell cases studied in this study. The other parameters studied resulted in smaller improvements in cost-of-electricity in the range of 0.1 to 0.9 mills/kWh.

A comparison of the effect of capital cost, O&M cost, fuel cost, and fuel cell cost indicated that the largest impact on COE is made by changes in capital cost of the plant, and that the cost of the fuel cell is small by comparison to the rest of the plant, therefore, has small effect on COE.

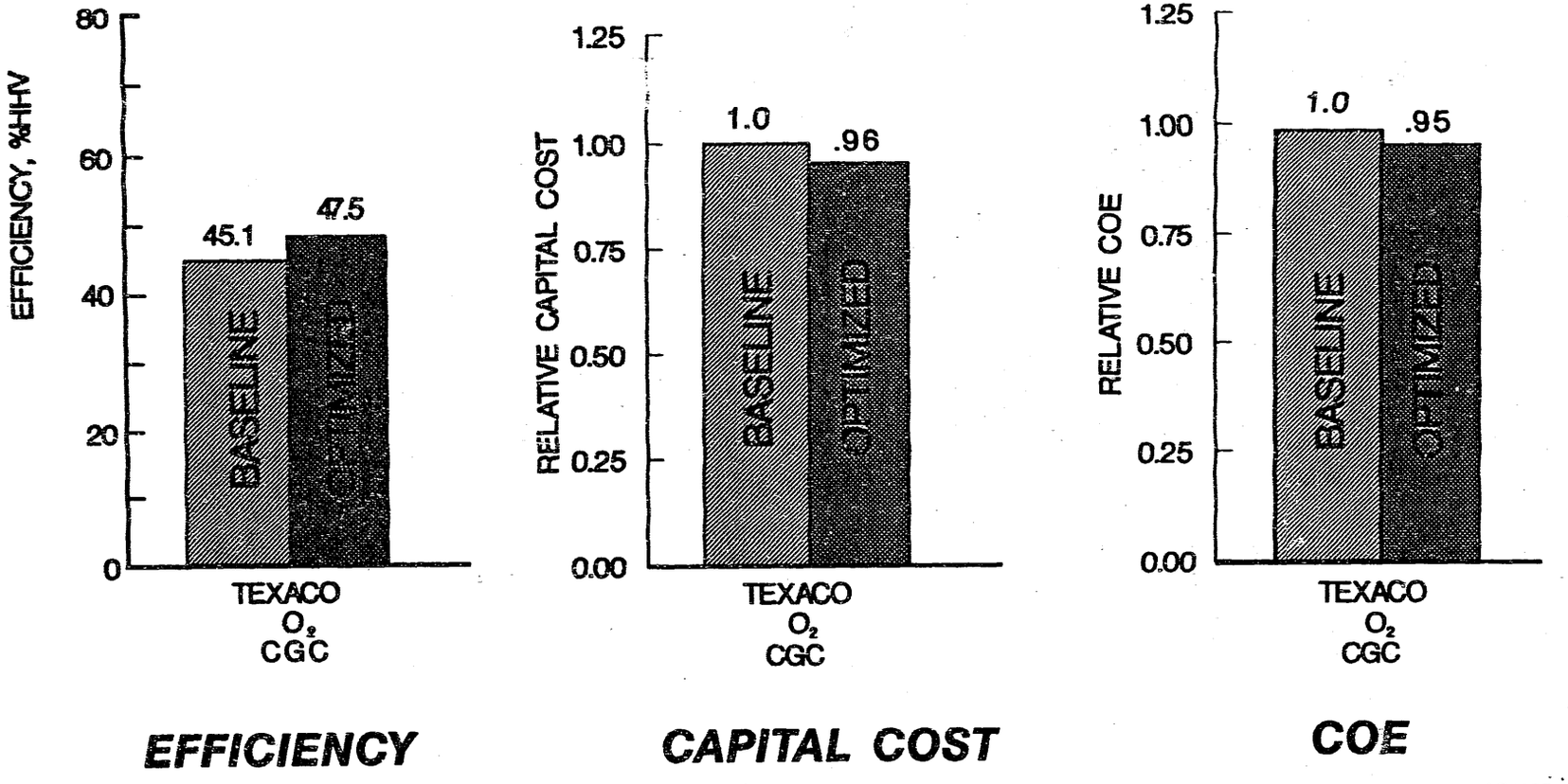

FIGURE 9.6 CGCFC SYSTEM OPTIMIZATION:

Improvement in Heat Rate and Economics of the Baseline CGCFC Systems can be Projected via Parametric Optimization.

9.6 CONCLUSIONS

Coal-gas fueled carbonate fuel cell power plant designs offering high efficiencies, very low environmental emissions and market responsive cost-of-electricity can be projected using available entrained bed, fluidized bed, and moving bed gasifiers. These CGCFC power plants are better than existing PC and AFBC power plants projecting lower COE and heat rate and better emission characteristics; competitive with IGCC - projecting comparable economics but better heat rates and emission characteristics. In addition, the CGCFCs provide excellent turndown capability and are suitable for phased construction. These advantages make the CGCFC an excellent choice for the power plant of the future.

Several interesting insights into the design of the CGCFC system obtained in this study include:

- There is no incentive for operating CFC stacks at higher than atmospheric pressure.

- High-methane content fuel may offer significant system efficiency advantages, although costs are uncertain at this time.

- Oxygen-blown gasification provided lower COE for 200MW size CGCFCs as compared with air-blown gasification.

- Cryogenic oxygen is economically preferred over alternate technologies for oxygen-blown gasifier use in a CGCFC plant.

- Recent improvements in cold-gas cleanup, as characterized by the Dow GAS/SPEC system, make them competitive with projected hot-gas cleanup for CGCFC application.

- High moisturization of coal-gas required to suppress soot in the zinc-ferrite hot-gas cleanup bed burdens CFCs.

9.7 REFERENCES

9-1. Energy Research Corporation and Fluor-Daniel, "Assessment of Coal Gasification/Carbonate Fuel Cell Power Plants," Topical Report submitted to DOE/METC (to be published) under Contract DE-AC21-87MC23274, June 1989.

9-2. EPRI Special Report "TAG Technical Assessment Guide", EPRI P-4463-SR, Volume 1, Dec. 1986.

9-3. Dunbobbin, B.R., Brown, W.R., "Air Separation by a High Temperature Molten Salt Process," Gas Separation and Purification 1987, Vol. 1, 23, Sept. 1987.

9-4. Energy Research Corporation, "Optimum MCFC Pressure Study," Topical Report submitted to DOE/METC (unpublished) under Contract DE-AC21-87MC23274, May 1988.

END

DATE FILMED

05 / 22 / 91